

UNCLASSIFIED

AD NUMBER
ADC018385
CLASSIFICATION CHANGES
TO: unclassified
FROM: confidential
LIMITATION CHANGES
TO: Approved for public release, distribution unlimited
FROM: Controlling DoD Organization... Director, Naval Research Laboratory, Washington, DC. 20375.
AUTHORITY
NRL ltr, 3 Mar 2004; NRL ltr, 3 Mar 2004

THIS PAGE IS UNCLASSIFIED

② LEVEL

CONFIDENTIAL

NRL Memorandum Report 3884
Volume 2 (Supplement)

Acoustic Fluctuation Workshop, Feb. 22-23, 1978 (U)
Technical Review, Editorial Summary, Synopsis and Papers
Volume 2

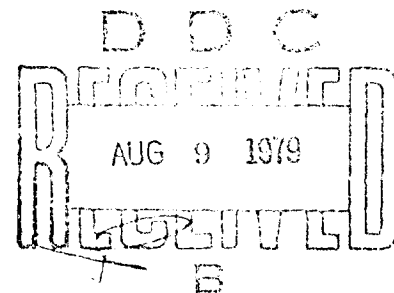
S. HANISH, C. R. ROLLINS, AND J. CYBULSKI

Acoustics Division

July 2, 1979

"NATIONAL SECURITY INFORMATION"

"Unauthorized Disclosure Subject to Criminal
Sanctions"



NAVAL RESEARCH LABORATORY
Washington, D.C.

CONFIDENTIAL - Unclassified
EXCLUDED FROM AUTOMATIC
DECLASSIFICATION

CONFIDENTIAL
Best Available Copy

AD C 018385

DDC FILE COPY

(This page is unclassified)

(19) NRI-MI 4-VOL

CONFIDENTIAL
UNCLASSIFIED

SECURITY CLASSIFICATION OF THIS PAGE (When Data Entered)

REPORT DOCUMENTATION PAGE		READ INSTRUCTIONS BEFORE COMPLETING FORM
1. REPORT NUMBER NRL Memorandum Report 3884 Volume 2 (Supplement)	2. GOVT ACCESSION NO.	3. RECIPIENT'S CATALOG NUMBER ⑨
4. TITLE (and Subtitle) Acoustic Fluctuation Workshop, Feb: 22-23 1978 "Technical Review, Editorial Summary, Synopsis and Papers" (U)		5. TYPE OF REPORT & PERIOD COVERED Final Report
7. AUTHOR(s) ⑩ S. Hanish, C. R. Rollins and J. Cybulski		6. PERFORMING ORG. REPORT NUMBER
9. PERFORMING ORGANIZATION NAME AND ADDRESS Naval Research Laboratory Washington, D. C. 20375		8. CONTRACT OR GRANT NUMBER(s) ⑪ F11121
11. CONTROLLING OFFICE NAME AND ADDRESS Naval Electronic Systems Command Washington, D. C. 20360 ⑫ L90A		10. PROGRAM ELEMENT, PROJECT, TASK AREA & WORK UNIT NUMBERS 81SO1-9 62711N XF11121-200
14. MONITORING AGENCY NAME & ADDRESS (if different from Controlling Office)		12. REPORT DATE July 2, 1979
		13. NUMBER OF PAGES 189
		15. SECURITY CLASS. (of this report) CONFIDENTIAL
		15a. DECLASSIFICATION/DOWNGRADING SCHEDULE Class by OPNAVINST S5510.72D Review on 22 Feb. 1998.
16. DISTRIBUTION STATEMENT Classification only ⑬ Acoustic Fluctuation Workshop Held at Naval Research Lab. on February 22-23 1978. Technical Review, Editorial Sum- mary, Synopsis and Papers. Volume II (U).		
17. DISTRIBUTION STATEMENT (of the abstract entered in Block 20, if different from report) ⑭		
18. SUPPLEMENTARY NOTES DDC RECEIVED AUG 9 1979 B		
19. KEY WORDS (Continue on reverse side if necessary and identify by block number) Acoustics Fluctuations in the Ocean Workshop Proceedings on Acoustic Fluctuations		
20. ABSTRACT (Continue on reverse side if necessary and identify by block number) (U) A Workshop on Acoustic Fluctuations in the Ocean, sponsored by NAVELEX 320 was held at the Naval Research Laboratory, Washington, D. C. on Feb. 22-23, 1978. The theme was (1) to highlight the relation between requirements of system performance models (APSURV, PSEUDO, APAIR, etc.) and current research on acoustic fluctuations conducted by Industry and the Navy (2) to find ways to establish closer cooperation between Researchers working in the field, and Users of research results (3) to recommend programs. — over (Abstract Continues)		

DD FORM 1 JAN 73 1473

EDITION OF 1 NOV 65 IS OBSOLETE
S/N 0102-014-6601

UNCLASSIFIED

SECURITY CLASSIFICATION OF THIS PAGE (When Data Entered)

CONFIDENTIAL

(This page is unclassified)

Best Available Copy

CONFIDENTIAL

UNCLASSIFIED

SECURITY CLASSIFICATION OF THIS PAGE (When Data Entered)

20. Abstract Continues

(U) This memorandum summarizes the agenda and key technical issues of the Workshop, and contains all papers presented. It also gives a brief history of previous Workshops on this subject, and a technical review of acoustic fluctuations in general.)

(U) Recommendations for programs are scheduled to be made available in a separate publication.

ACCESSION for	
NTIS	White Section <input type="checkbox"/>
DDC	Buff Section <input checked="" type="checkbox"/>
UNANNOUNCED	<input type="checkbox"/>
JUSTIFICATION	
BY	
DISTRIBUTION/AVAILABILITY CODES	
Dist. Avail. and/or SPECIAL	
9	

UNCLASSIFIED

11 SECURITY CLASSIFICATION OF THIS PAGE (When Data Entered)

CONFIDENTIAL

CONFIDENTIAL

CONTENTS (U)

I. INTRODUCTION (U)	1
II. BACKGROUND (U)	2
C. R. Rollins	
III. TECHNICAL REVIEW OF FLUCTUATION PHYSICS (U)	8
IV. FLUCTUATION WORKSHOP PAPERS — AN EDITORIAL SUMMARY (U) ..	9
V. SUMMARY OF RESEARCH RESULTS (U)	20
REFERENCES (U)	43
APPENDIX A — FLUCTUATION WORKSHOP PAPERS (U)	
KEY ISSUES IN THE APPLICATION OF STATISTICS OF ACOUSTIC FLUCTUATIONS TO SYSTEM PERFORMANCE MODELING (U)	44
S. Hanish	
THE APSURV DETECTION MODEL (U)	45
R. Larsen	
PSEUDO-SURVEILLANCE SYSTEM PERFORMANCE SIMULATOR (U) ...	55
L. Fretwell	
FLUCTUATIONS FOR THE APAIR, APSURF, APSUB MODELS (U)	62
R. Flum	
REVIEW OF BEAM NOISE FLUCTUATION MODELS (U)	68
R. C. Cavanagh	
THE EFFECT OF ACOUSTIC FLUCTUATIONS IN THE OCEAN UPON COHERENCE (U)	69
O. D. Grace	
THE EFFECTS OF FLUCTUATING SIGNALS AND NOISE ON DETECTION PERFORMANCE (U)	78
J. C. Heine and J. R. Nitsche	
WORKING FLUCTUATION MODELS WITH APPLICATION TO DETECTION PREDICTION (U)	79
R. J. Urick	
SIGNAL FLUCTUATIONS (U)	84
K. D. Flowers	

CONFIDENTIAL

NUMERICAL MODELS OF ACOUSTIC PROPAGATION THROUGH INTERNAL WAVES (U)	93
H. A. DeFerrari and R. Leung	
SINGLE PATH—PHASE AND AMPLITUDE FLUCTUATIONS (U)	94
(Abstract Only) T. E. Ewart	
PREDICTION OF DETECTION PERFORMANCE (U)	95
M. Moll	
ACOUSTIC FLUCTUATION MODELING FOR SYSTEM PERFORMANCE ESTIMATES (U)	96
R. C. Cavanagh	
BEAM OUTPUT FLUCTUATIONS ON TWO TOWED ARRAYS (U)	97
A. G. Fabula	
FLUCTUATIONS DUE TO RANGE RATE (U)	109
I. Dyer	
THE IMPORTANCE OF SOURCE MOTION RECEIVER ORIENTATION, AND THE OCEAN ENVIRONMENT (U)	110
(Abstract Only) W. Jobst	
IMPACT OF SOURCE MOTIONAL FLUCTUATIONS ON INTERARRAY SIGNAL COHERENCE (U)	111
A. A. Gerlach	
ACOUSTIC FLUCTUATIONS (U)	114
R. C. Spindel	
RANGE INDEPENDENT FLUCTUATIONS AND PATTERN RECOGNITION OF VERTICAL ANGLE OF ARRIVAL STRUCTURE (U)	115
F. H. Fisher	
OMNIDIRECTIONAL AMBIENT NOISE AS A FUNCTION OF DEPTH AND FREQUENCY IN THE DEEP NORTHEAST PACIFIC (U)	127
J. A. Shooter	
MEASUREMENT OF CHARACTERISTICS OF AN ACOUSTIC PROPAGATION CHANNEL BY INVERSE FILTER (U)	157
H. A. DeFerrari and R. F. Tusting	
MEASUREMENT TOOLS (U)	158
D. Keir	
APPENDIX B — SYNOPSIS OF THE FLUCTUATION WORKSHOP PAPERS NOT SUBMITTED FOR PUBLICATION (U)	173
APPENDIX C — A REVIEW OF SIGNIFICANT PAPERS ON FLUCTUATIONS AT THE 94th ASA MEETING (U)	177
S. Hanish	
APPENDIX D — BIBLIOGRAPHY (U)	178

CONFIDENTIAL

CONFIDENTIAL

I. INTRODUCTION

(See Volume 1 — Unclassified)

Manuscript submitted September 28, 1978.

CONFIDENTIAL
(THIS PAGE IS UNCLASSIFIED)

CONFIDENTIAL

II. BACKGROUND OF ACOUSTIC FLUCTUATION RESEARCH (U)

(C) About 10 years ago, several developments lead to an awareness of the lack of adequate knowledge about fluctuations in the signals and noise always present in acoustic detection systems. One of these developments was the interest in active undersea surveillance systems. A number of studies and analyses were undertaken to establish performance estimates as a function of source level, frequency, array gain, and other variables. It became clear that, due to the long ranges of acoustic transmission, the data rate would be low, and the fading, or fluctuation, of echo returns could seriously impair performance. In addition, it was recognized that the temporal correlation time was important in determining the effect of ping separation on statistical independence of pings. The frequencies of interest were in the few hundred hertz region, with temporal scales from about 1 to 30 minutes. At that time, very little data was available for use in system performance prediction models.

(C) A second factor which contributed to the interest in fluctuation was the development of a family of passive sonar prediction models, of which Anti-Submarine Warfare Program Surveillance (APSURV) is representative. This model was developed primarily by mathematically oriented operations research analysts. It was known that a fluctuating signal-to-noise ratio was characteristic of long range low frequency detection, and therefore a fluctuation was introduced into the model signal-to-noise ratio through use of a pseudo-normal process. One parameter

CONFIDENTIAL

CONFIDENTIAL

(C) τ established the correlation interval or "relaxation time" and a second parameter, σ established a normal distribution of signal excess values. Implementation in APSURV (model 1) was through an Ehrenfest random walk incorporated as part of a Monte-Carlo model. Developers and users of the model asked several questions which could not be adequately answered at that time:

1. (C) Can we isolate the signal, noise, and other fluctuations, or must we treat the net signal-to-noise ratio as one fluctuating process?
2. (C) What are the appropriate (correct) values of relaxation time τ and variance σ for the individual (signal, noise, array gain, etc) processes and for the resultant signal-to-noise ratio?
3. (C) Is the normal distribution an adequate representation of the statistical processes involved, or do we need something different?

(C) A third factor which contributed to interest in fluctuation research was the development of long line arrays with the attendant question of maximum coherence length. This motivated investigation of phase fluctuation as a function of spatial position and time, information needed by signal processors as well as array designers.

(C) The confluence of these questions and the importance for the Navy led to sponsor support and subsequently to several years of effective research into these various areas of fluctuations. In addition, closely related subjects such as target scintillation, ship traffic dynamics, source and receiver motion have been investigated. The result has been the production of a substantial body of information, both data and theory, which at this time appears to be unfocused. Answers to many of the original questions now exist, but in some cases the results have not been compiled and disseminated in a form suitable for the potential user. It must be remembered that for a user, *the most simple, uncomplicated result which is adequate for his use*, is what is needed. Thus, a detailed, mathematically elegant model which may provide great insight into causes and relationships may be completely inappropriate for a performance

CONFIDENTIAL

(C) prediction model or for a system designer. In other cases it may be necessary to carry a great amount of scientific sophistication into a production model in order to meet the requirements of the task. Some method must be found and implemented in which the results of fluctuation research can be organized, summarized, and in some cases simplified, in terms useful to the users. Who the users are, and what these requirements are, is discussed next.

Acoustic Fluctuation Research—Requirements (U)

1. Prediction of Submarine Detection (U)

(C) Developers and users of detection performance models are primarily interested in amplitude fluctuation of signal, noise, array gain, and in some cases, the variability of operator and hardware performance. Signal variability involves both source characteristics and transmission path characteristics. The performance prediction modeler would like to be able to separate the deterministic, predictable component from the nondeterministic component, and he would like a statistical description of the latter. The statistical description would include the parameters of the distribution and the temporal auto correlation function. With this information for each factor in the sonar equation, the modeler could accurately estimate the detection performance (in a threshold sense) of a submarine detection system.

(U) For many purposes combined statistics are adequate, such as combined source and transmission path fluctuation, array gain and noise fluctuation, and even total signal-excess fluctuations. The passive sonar equation may be written in several forms, combining terms differently to allow use of appropriate data or models. The fundamental form is as follows:

$$SE = SL - TL - N + SG - NG - RD \quad (1)$$

where

$SE \equiv$ signal excess

$SL \equiv$ source level

CONFIDENTIAL

- (U) $TL \equiv$ transmission loss
- $N \equiv$ omnidirectional noise level
- $SG \equiv$ signal gain for the receiving array
- $NG \equiv$ noise gain for the receiving array
- $RD \equiv$ recognition differential or detection threshold

(U) Ideally, the deterministic mean, the statistical variability, the correlation (or dependence) relative to other terms, and the temporal auto correlation coefficient of each term should be known. If the signal gain and noise gain terms are combined, the array performance, including fluctuation characteristics, can be characterized by array gain

$$SE = SL - TL - N + AG - RD \quad (2)$$

where

$$AG = SG - NG \equiv \text{array gain} \quad (3)$$

(U) Similarly, in many cases, it is convenient to model or measure noise level and fluctuations in noise on a beam. Thus:

$$SE = SL - TL + SG - BN - RD \quad (4)$$

where

$$BN = N + NG \equiv \text{beam noise} \quad (5)$$

(U) For engagement models which must be re-run repeatedly, where running time is a significant consideration, the complexity of the fluctuation processes must be reduced to simplest terms. The performance modeler would like to know the significance of the statistics of individual terms as compared to the statistics of signal excess, and whether a statistical description of signal excess is sufficient, or whether individual terms must be handled separately.

2. System Design (U)

(C) The system designer is interested in acoustic fluctuation processes as they affect the design of signal processors and receiving arrays. Temporal statistics of amplitude and phase indicate the length of integration times which may be utilized for coherent and non-coherent

CONFIDENTIAL

(C) processing. Frequency, bandwidth and type of acoustic path are important parameters. The "coherence length" of an acoustic field determines the maximum size array which will be effective. Coherence length has statistical properties associated with the fluctuation of phase across an array aperture. Thus phase fluctuation investigations contribute to the design of arrays and to an understanding of the variability of array gain. In addition, the development of inter-array processing (IAP), multi-array processing (MAP), and coherent multi-array processing (CMAP), requires information about the temporal and spatial fluctuations of both phase and amplitude for widely separated sites.

(U) In an effort to place these requirements in perspective and to identify users of the results of fluctuation research, Table 1, on fluctuation parameters has been prepared.

(U) The three major users of results selected are the performance detection modelers, the signal processing developers and the array designers. In a general sense, all the users are interested in all the results. However, the users indicated are those considered to be the primary and most important for the given fluctuation parameter.

CONFIDENTIAL

(U) Table 1 — Research in Acoustic Fluctuation Parameters and Potential Users (U)

Parameter of Research in Acoustic Fluctuations	detection performance modeling	signal processing development	receiving array design
Source Level SL (for given submarine)			
1. mean value as function of aspect (deterministic)	x		
2. statistical distribution (over all aspects)	x		
Transmission Loss TL			
1. mean value as function of frequency, range, source and receiver depth	x		
2. statistical distribution of temporal amplitude fluctuation	x	x	
3. statistical distribution of temporal phase fluctuations	x	x	
4. statistical distribution of spatial amplitude fluctuation	x	x	x
5. statistical distribution of spatial phase fluctuation		x	x
6. autocorrelation function of temporal amplitude fluctuation	x	x	
7. autocorrelation function of temporal phase fluctuation		x	
8. crosscorrelation function of spatial amplitude fluctuation		x	x
9. crosscorrelation function of spatial phase fluctuation		x	x
Ambient Noise N			
1. mean level of omnidirectional ambient noise	x		
2. statistical distribution of amplitude fluctuations	x	x	
3. temporal autocorrelation function	x		
4. spatial crosscorrelation function (spatial coherence)		x	x
5. statistical distribution of spatial amplitude fluctuation	x	x	x
Signal Gain SG (for array)			
1. mean value	x		x
2. statistical distribution of temporal fluctuations	x		x
Noise Gain NG (for array)			
1. mean value	x		x
2. statistical distribution of temporal fluctuations	x		x
Array Gain AG (= SG - NG)			
1. mean value	x		x
2. statistical distribution of temporal fluctuations	x		x
Beam Noise BN (= N + NG)			
1. mean value	x		x
2. statistical distribution of amplitude fluctuations	x	x	x
3. temporal autocorrelation function	x		
Signal Excess SE (= SL - TL - N + SG - NG - BN)			
1. mean as function of range	x		
2. statistical distribution of values	x		
3. temporal autocorrelation function (relaxation time)	x		

CONFIDENTIAL

III. TECHNICAL REVIEW OF FLUCTUATING ACOUSTIC CHANNELS

(See Volume 1 — Unclassified)

CONFIDENTIAL
(THIS PAGE IS UNCLASSIFIED)

CONFIDENTIAL

**IV. EDITORIAL SUMMARY AND SYNOPSIS OF PAPERS PRESENTED
AT THE ACOUSTIC FLUCTUATION WORKSHOP
[Unclassified Title]**

I. Editorial Summary (U)

(U) The editorial summary which follows is in order of the Workshop Agenda and is based upon material submitted by the author; with the Roman I and II after the name for those presenting more than one paper.

Index to Summary Contents

R. Cavanagh I
D. Grace
J. Heine
R. Urick
K. Flowers
De Ferrari I
M. Moll
R. Cavanagh II
A. Fabula
I. Dyer
A. Gerlach
R. Spindel/W. Munk
De Ferrari II
J. Shooter

CONFIDENTIAL

CONFIDENTIAL

Workshop Paper: "Beam Noise Fluctuation Models" (U)

Author: R. Cavanagh

Objective: (U) Review beam noise models, and recommend best features of each for specific applications.

Research Approach: (U) Review models in terms of treatment of ships, transmission loss, and receiver characteristics. Consider statistical quantities of each, and recommend types of ensembling.

Models Reviewed: (U) (1) Underwater Systems US1, (2) Bell Lab. BTL, (3) Bolt, Beranek and Neuman, BBN, (4) Wagner, (5) NABTAM, ORI, US1, NORDA, et al., (6) Science Applications DSBN, (7) NORDA (BEAMPL), (8) NRL, SIAM I, (9) NRL, SIAM II.

Chief Output: (U) Summary of each model's prediction of beam-noise statistics ensembled over some specific time (hour, day, week, etc.)

Chief Conclusion: (U) No single model satisfies all requirements.

Outstanding Problems: (U) (1) Need an approach to predict signal plus noise in one frequency bin, and noise in another.

(2) Need to treat a moving array.

(3) Source levels and locations of ships still not known accurately.

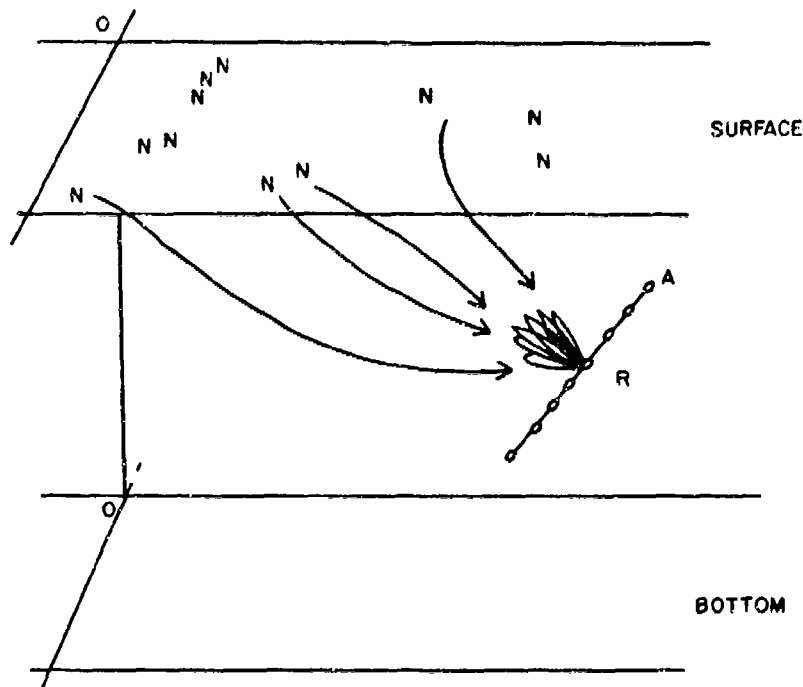
(4) Need evaluation of models, at least for mean values.

(5) Need to understand importance of weak generated noise.

A pictorial representation of this paper is shown next.

CONFIDENTIAL

Cavanagh*



(C) Comparative Review of Beam-Noise Models

Analytic	US1	NA9TAM	Brute Force
	BTL	DSBN	
	BBN	BEAMPL	
	WAGNER	SIAM I,II	

These are tabulated by how they model the noise $N(t)$.

$$N(t) = \sum_{u=1}^{J(t)} SL_u(t) \cdot T_u(t) \cdot AG_u(t)$$

intensity
transmission
array response

Good features of each model are selected and problems presented.

*This sketch is either (1) the editor's concept of the underlying experimental situation of the paper, presented for convenience of the reader or (2) an actual experiment conducted by others. In all cases the material boxed in heavy lines is the author's contribution as reported at the Workshop.

CONFIDENTIAL

Workshop Paper: "Signal Processor and Fluctuations" (U)

Author: D. Grace

Objective: (U) Review the problem of degradation of spatial coherence in multi-array processing with increasing integration time and processing bandwidth. Distinguish on a time difference-Doppler difference plot between peaks caused by platform motion and those caused by multipath.

Research Approach: (U) Review past experiments of Mohnkern, Sloat, Barbour and Grace.

Chief Parameters: (C) Plots of coherence between signals from one source arriving at two widely separated arrays versus time difference of arrival and Doppler difference. Plots of signal coherence versus time-bandwidth product (TW). Spectrum of phase fluctuations.

Chief Results: Mohnkern: (C)

- (1) increasing TW product decreases coherence.
- (2) increasing the integration time decreases the coherence more than increasing the bandwidths.
- (3) the power spectrum of random signal phase modulation falls off at -30 dB per octave as would be expected for internal waves.

Sloat: (C)

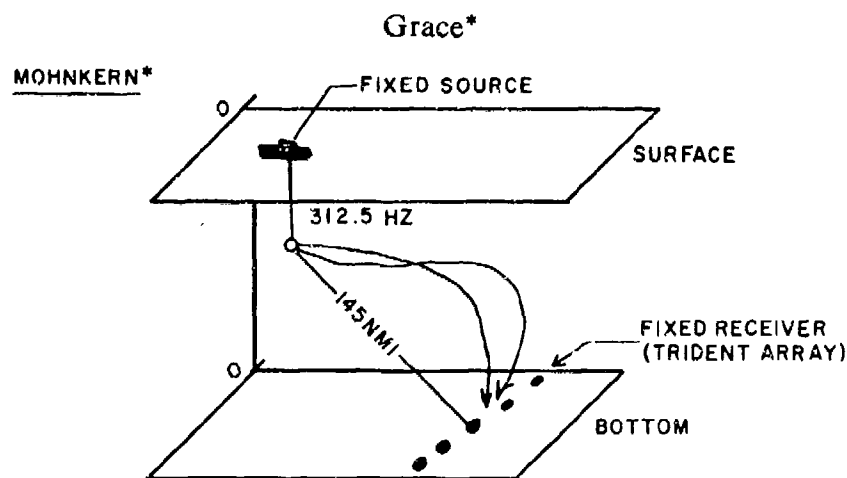
- (1) Random course and speed produce small effect on coherence.
- (2) Constant course and speed produce large effects.
- (3) Measured coherence lower than predicted.

Barbour: (C) Standard deviation of fluctuations in peak location on coherence surfaces is greater than expected.

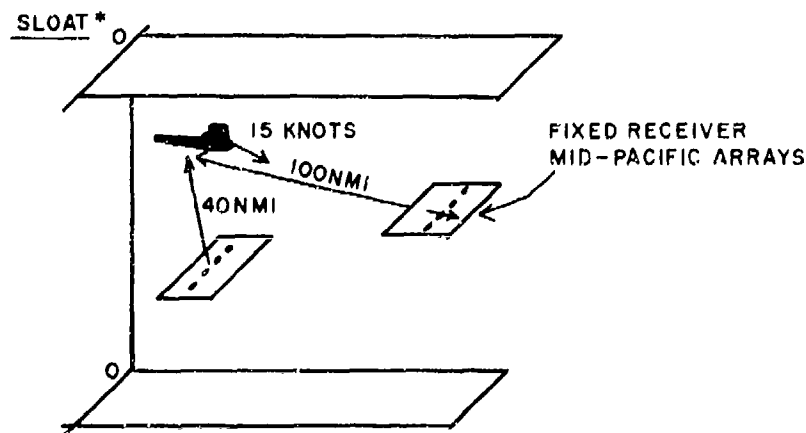
Grace: (C) If platform and medium indicate fluctuations are slow, and if differential Doppler between multipath components is great then coherence peaks due to multipath and due to platform motion can be separated.

Pictorial representations of the work of Mohnkern, Sloat, and Barbour are shown next.

CONFIDENTIAL



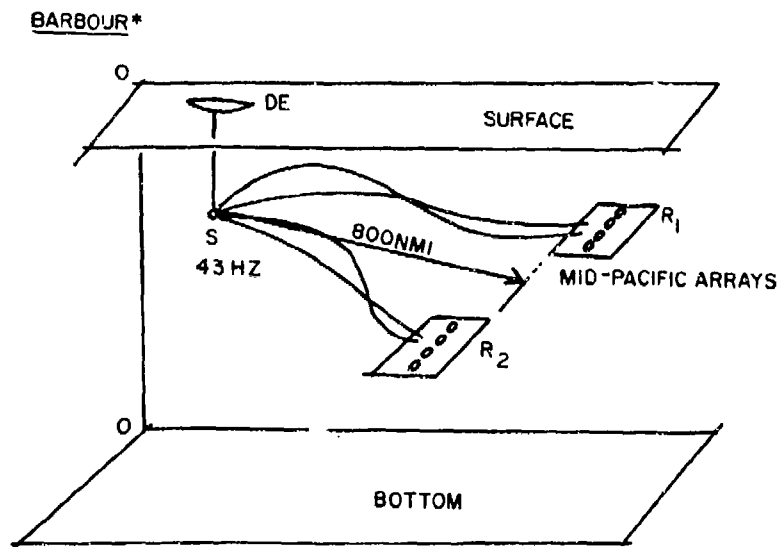
(C) Calculate coherence between transmitted PRN carrier (312.5 Hz) and received PRN as a function of integration time and processing bandwidth. Calculate power spectrum of signal phase modulation.



(C) Calculate "coherence surface" ($\Delta\tau, \Delta\Phi$) for processing band 1/4 Hz and integration time 2,4,6,8,16,32 min., using a 12.5 Hz line from sub.

*This sketch is either (1) the editor's concept of the underlying experimental situation of the paper, presented for convenience of the reader or (2) an actual experiment conducted by others. In all cases the material boxed in heavy lines is the author's contribution as reported at the Workshop.

CONFIDENTIAL



(C) Calculate coherence surfaces ($\Delta\tau, \Delta\Phi$) for processing band 1/4 Hz and 2 min. integration time, using a 43 Hz signal. Compare actual surfaces with ray trace model and source-receiver geometry. Calculate statistics of fluctuations in peak coordinates of the coherence surfaces as function of time.

Grace: Use Barbour data to distinguish between coherence peaks caused by platform motion and those caused by multipath.

*This sketch is either (1) the editor's concept of the underlying experimental situation of the paper, presented for convenience of the reader or (2) an actual experiment conducted by others. In all cases the material boxed in heavy lines is the author's contribution as reported at the Workshop.

CONFIDENTIAL

CONFIDENTIAL

Workshop Paper: "Effects of Fluctuating Signals and Noise on Detection Performance" (U)

Authors: J. Heine and J. R. Nitsche

Objective: (U) Analyze effect of fluctuations in noise caused by shipping, and fluctuations in the signal caused by multipath, upon systems ROC curves.

Research Approach: (U) Mathematical analysis, assuming ocean noise is not white Gaussian.

Chief Parameters: (U) Random SNR, Random P_D .

Principal Task: (U) Determine probability distribution of SNR.

Temporal Scales: (U) Slow fluctuations of characteristic time 2X to 3X receiver integration time.

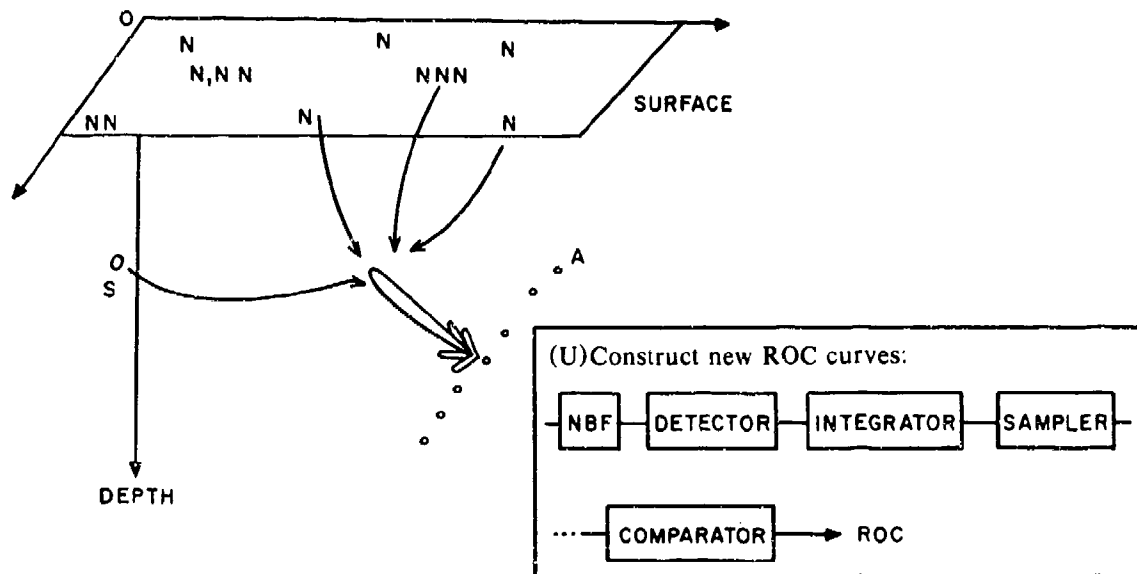
Principal Result: (U) Presentation of a set of ROC curves modified by fluctuations.

Principal Conclusions: (U) Predicted performance improvements based on non-fluctuating SNR can lead to gross overestimates.

A pictorial representation of this paper is shown next.

CONFIDENTIAL

Heine and Nitsche*



*This sketch is either (1) the editor's concept of the underlying experimental situation of the paper, presented for convenience of the reader or (2) an actual experiment conducted by others. In all cases the material boxed in heavy lines is the author's contribution as reported at the Workshop.

CONFIDENTIAL

CONFIDENTIAL

Workshop Paper: "A Working Fluctuation Model with Application to Performance Prediction" (U)

Author: R. Urick

Objective: (U) Review a signal intensity fluctuation model based on Rician statistics. Review the fluctuation time scale parameter. Review noise fluctuations. Discuss effects of fluctuations on detection.

Research Approach: (U) Compare models with data from numerous experiments.

Chief Conclusions: (U)

- (1) (U) Many experiments prove that the cumulative probability distribution of intensity of CW signals in a randomizing ocean Rician statistics. It is easier to predict fluctuations of signal level than to predict the mean level itself.
- (2) (U) The sea surface is responsible for fast fluctuations in the range 2-20 seconds. Slower fluctuations longer than 10 seconds, and up to 10 minutes appear to be caused by multipath reception.
- (3) (U) Fluctuations in ambient noise obey Gaussian statistics (but not always). Samples of noise power are random variables whose statistics depend on the time bandwidth product of the processor. A conventional processor yields chi-square statistics for these samples of noise power, with degrees of freedom equal to twice time-bandwidth product.
- (4) (U) Curves of P_D vs. SE have been plotted for Rayleigh, amplitude normal log, and normal signal fluctuations. Comparison with experiment shows that the log normal distribution with standard deviation between 6 and 8 dB best applies to real detection data. (Applies to short range, mobile sonar). This may be a consequence of the Central Limit theorem.

CONFIDENTIAL

Workshop Paper: Signal Fluctuations (U)

Author: K. Flowers

Objective: (U) To present characteristics of signals propagated over long range deep water paths, for which the data is currently insufficient to permit modeling. In particular, to determine probability density of received levels, and space/time statistics.

Research Approach: (U) Perform the experiments pictured below. From the data gathered remove the average signal level, then determine distribution of fluctuations about the mean. This is a function of frequency and range, but not of receiver position or direction.

(U) Use ray-tracing models to find average signal levels.

Chief Parameters: (U) Received signal level, its probability density and space/time statistics.

Chief Conclusions: (C) RMS fluctuation is directly proportional to average signal level.

(C) Radial (meaning along transmission path) correlation length for a 10 Hz acoustic field is about 1 km near the source, 4 to 5 km at a range from 10 km to 2000 km, and falling off above 2000 km to about 2 km at a range of 3000 km. Depth correlation only a few wavelengths. Transverse correlation quite large (many wavelengths).

(C) Bearing errors range between 1° and 2° over a period of hours. It is possible by removing a nearly linear trend in the data that a reasonably high bearing accuracy is obtained by observing wavefronts with short arrays.

(C) Variations of amplitude and bearing error are very sharp in going through convergence zones. No models are known to predict this effect.

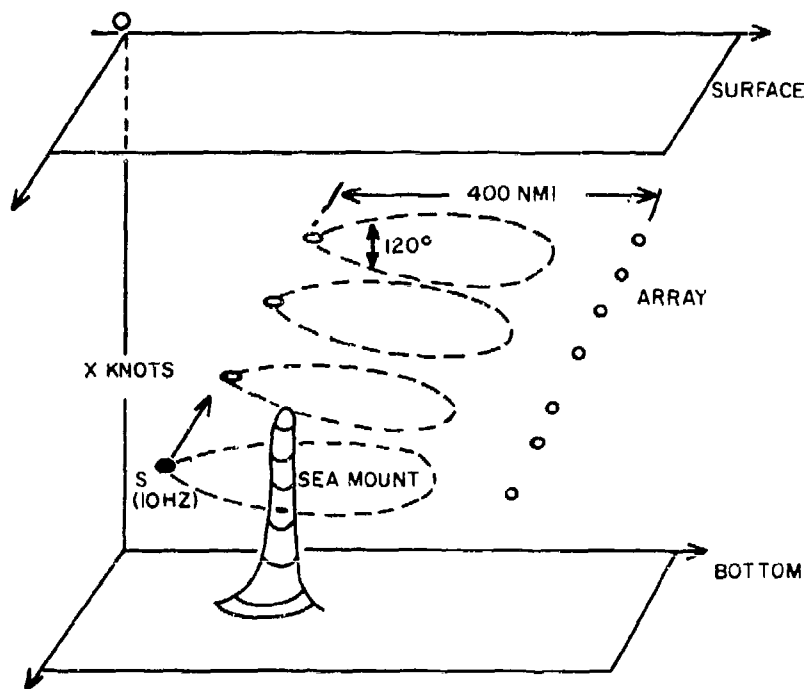
(C) Existing propagation models are capable of providing signal fluctuation statistics in long range, deep water experiments.

(C) For low frequencies bottom mounted arrays see nearly perfect plane waves. However their orientation is not understood.

Pictorial representations of this paper are shown next.

CONFIDENTIAL

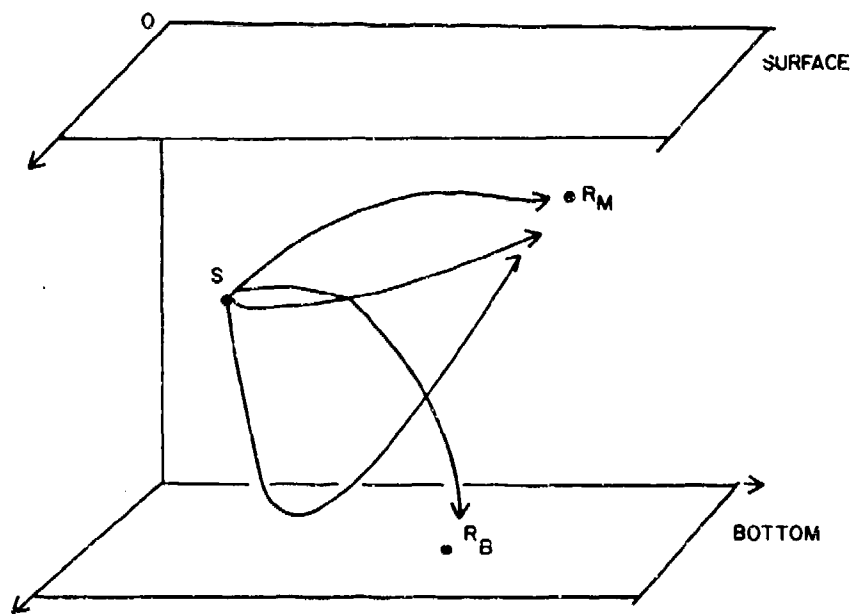
Flowers*



*This sketch is either (1) the editor's concept of the underlying experimental situation of the paper, presented for convenience of the reader or (2) an actual experiment conducted by others. In all cases the material boxed in heavy lines is the author's contribution as reported at the Workshop.

CONFIDENTIAL

Flowers*



(C) Experiment is designed to determine probability distribution of signal at receivers R_M , R_B , and correlation distance in depth, along transmission path and transverse to this path.

*This sketch is either (1) the editor's concept of the underlying experimental situation of the paper, presented for convenience of the reader or (2) an actual experiment conducted by others. In all cases the material boxed in heavy lines is the author's contribution as reported at the Workshop.

CONFIDENTIAL

CONFIDENTIAL

Workshop Paper: "A Model of Acoustic Propagation Through Internal Waves" (U)

Author: H. De Ferrari

Objective: (U) Develop numerical methods for computation of long range ocean propagation using the theory of Flatte, Dashen, Munk and Zachariasen, and the Garrett-Munk internal wave model.

Research Approach: (U) Use ray-tracing to get ray paths, then introduce fluctuation.

Chief Parameters: (U) Fluctuation strength Φ , diffraction parameter Λ .

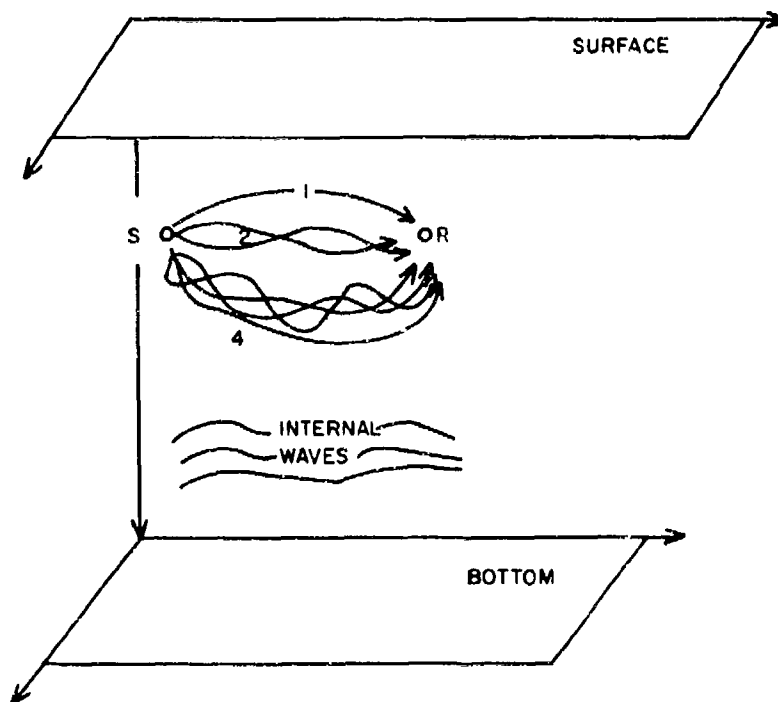
Number of Ray Paths: (U) The numerical study of single ray path completed. Next effort is to numerically calculate theoretical propagation with fluctuation for two channels, then four channels.

Chief Conclusions: (U) Λ parameter is very sensitive to ray geometry. Rays having turning points near the surface show less Φ variation than predicted.

A pictorial representation of this paper is shown next.

CONFIDENTIAL

De Ferrari*



(U) Calculate the quantities,

$$\Phi^2 = q_0^2 \int \int dx \, dx' \, \rho \left(z(x), z(x') \right)$$

$$\Lambda = \Phi^{-2} q_0^2 \int \int dx \, dx' \, \rho \left(z(x), Z(x') \right) (g_0 A L_y^2)^{-1}$$

*This sketch is either (1) the editor's concept of the underlying experimental situation of the paper, presented for convenience of the reader or (2) an actual experiment conducted by others. In all cases the material boxed in heavy lines is the author's contribution as reported at the Workshop.

CONFIDENTIAL

CONFIDENTIAL

Workshop Paper: "Prediction of Performance Behavior" (U)

Author: M. Moll

Objective: (U) Predict performance of a passive sonar receiver which has fluctuating acoustic inputs.

Research Approach: (U) Construct an analytical model of a multi-beam receiver with random input. For detection purposes choose a threshold for each beam which is a linear combination of the outputs on all other beams.

Chief Parameters: (U) Fluctuation is represented as ambient noise of form $N(t) = \sqrt{P(t)} G(t)$. Signal is sinusoid.

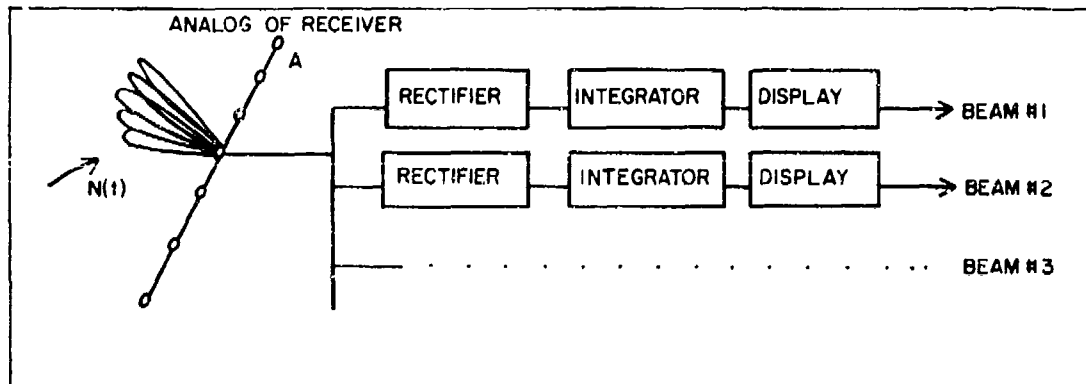
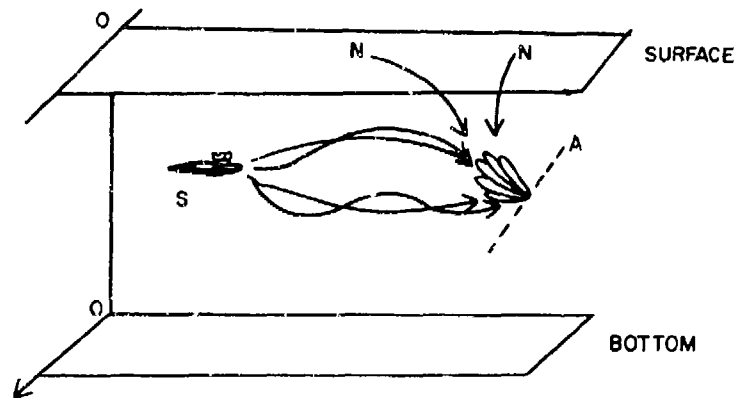
Chief Results: (U) Kurtosis of $N(t)$. Test statistic for detection, Z_D . Probability density of Z_D , its mean, variance, third moment.

(U) ROC plot of SNR vs. P_D with D/T as parameter (D is relaxation time of the envelope of the random process representing the output of a beam, T is the post rectification averaging time).

A pictorial representation of this paper is shown next.

CONFIDENTIAL

Moll*



(U) Choose THRESHOLD FOR BEAM #X = Linear combination of outputs of integrators on all other channels.

FLUCTUATION MODEL,

$$N(t) = \sqrt{P(t)} G(t)$$

$P(t)$ is a non-negative random process

$G(t)$ is a zero mean unit-variance stationary Gaussian process

*This sketch is either (1) the editor's concept of the underlying experimental situation of the paper, presented for convenience of the reader or (2) an actual experiment conducted by others. In all cases the material boxed in heavy lines is the author's contribution as reported at the Workshop.

CONFIDENTIAL

CONFIDENTIAL

Workshop Paper: "Acoustic Fluctuation Modeling for System Performance Estimation" (U)

Author: R. Cavanagh

Objective: (U) Evaluate the simulation random-process approach for modeling signal excess in system performance prediction.

Research Approach: (U) Construct signal and noise time series of received signal using available acoustic models of transmission loss and ambient noise. Simulate these series by random process models taking needed data from acoustic models. Compare acoustic models with random-process simulation, both as to statistics and as to detection history.

To evaluate, random process simulation model, choose data, one ocean environment (N. Pacific), single 25 Hz source, towed array receiver.

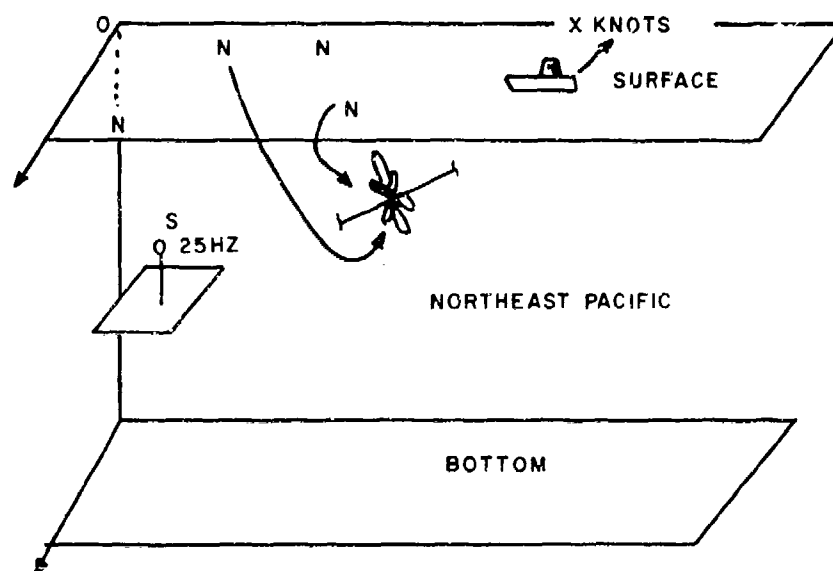
Chief Parameters: (U) Transmission loss, ambient noise, array gain, signal excess, detection threshold.

Chief Conclusions: (U) Given accurate inputs, random process simulation models give adequate simulation. Acoustic input data (statistics of signal excess, etc.) is biggest problem. Method is poor if data is poor.

A pictorial representation of this paper is shown next.

CONFIDENTIAL

Cavanagh*



(U) Acoustic Models of Above Test Case

To be compared with

Random-Process Simulation using

- a. Gauss-Markov
- b. Gauss Jump
- c. Ehrenfest

*This sketch is either (1) the editor's concept of the underlying experimental situation of the paper, presented for convenience of the reader or (2) an actual experiment conducted by others. In all cases the material boxed in heavy lines is the author's contribution as reported at the Workshop.

CONFIDENTIAL

CONFIDENTIAL

Workshop Paper: "Beam Output Fluctuations" (U)

Author: A. Fabuia

Objective: (C) Investigate the effectiveness of coherent multi-array processing (CMAP) for two towed arrays in a bottom-limited environment. Study the fluctuation characteristics of beam output signals from these arrays.

Research Approach: (U) Conduct an experiment featuring a moving source and two array receivers. Process data using the CMAP algorithms.

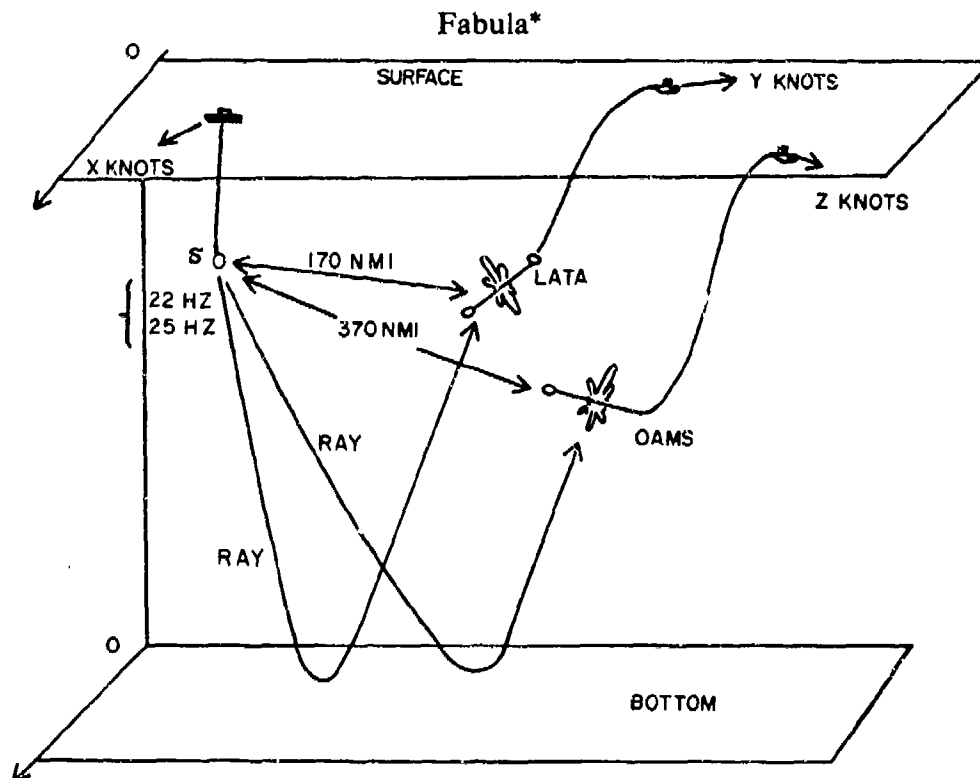
Chief Parameters: (U) Interarray signal coherence as a function of time difference of arrival. Beam Survey. Amplitude and phase fluctuations in beams. Doppler difference in beams.

Chief Conclusions: (C)

- (1) Maximum coherence between received signals at the two arrays range from 0.62 to 0.93.
- (2) Maximum signals "jump" from one beam to a neighbor beam due to multipath interference. A jump of 7° in 4 seconds has been recorded.
- (3) Null, or sharp amplitude fades, also occur, and are attributed to multipath interference. These fades are easily smoothed by making a 1° change in look angle.
- (4) Meander in phase is uncorrelated between the arrays. This meander is thought to be due to propagation effects, not platform motion.

A pictorial representation of this paper is shown next.

CONFIDENTIAL



(C) For digital signal processing of each beam data of LATA use 128 samples/sec, and obtain amplitude spectrum level in 1/4 Hz bins by use of FFT. On OAMS data use 125 samples/sec, and obtain spectrum level by use of DFT.

Plot coherence surface $E(\Delta\tau, \Delta\Phi)$ using CMAP algorithm (Coherent Multi Array Processor).

Make a "beam survey" by finding the loudest bin-beam pair (of beams) and record the relative levels of the signal s in the beam. To obtain alignment between arrays the projector signal is switched between two distinct frequencies (22 or 25 Hz).

Calculate fluctuations in relative amplitude and phase of the received signals as a function of beam number.

*This sketch is either (1) the editor's concept of the underlying experimental situation of the paper, presented for convenience of the reader or (2) an actual experiment conducted by others. In all cases the material boxed in heavy lines is the author's contribution as reported at the Workshop.

CONFIDENTIAL

CONFIDENTIAL

Workshop Paper: "Fluctuations Due to Range Rate" (U)

Author: I. Dyer

Objective: (U) By analysis construct a model of the power spectrum of fluctuations in a sinusoidal signal caused by platform motion. Compare this model with the power spectrum of fluctuations due to internal waves.

Research Approach: (U) Take a length of a single ray path and give it a velocity at each end. The frequency shift at each point in the path can be determined as a function of ray angle with the horizontal. Assuming fluctuation saturation, choose a sound speed profile, determine the energy of the ray in it, from it calculate its temporal correlation, and finally, by Fourier transformation determine the power spectrum of fluctuations.

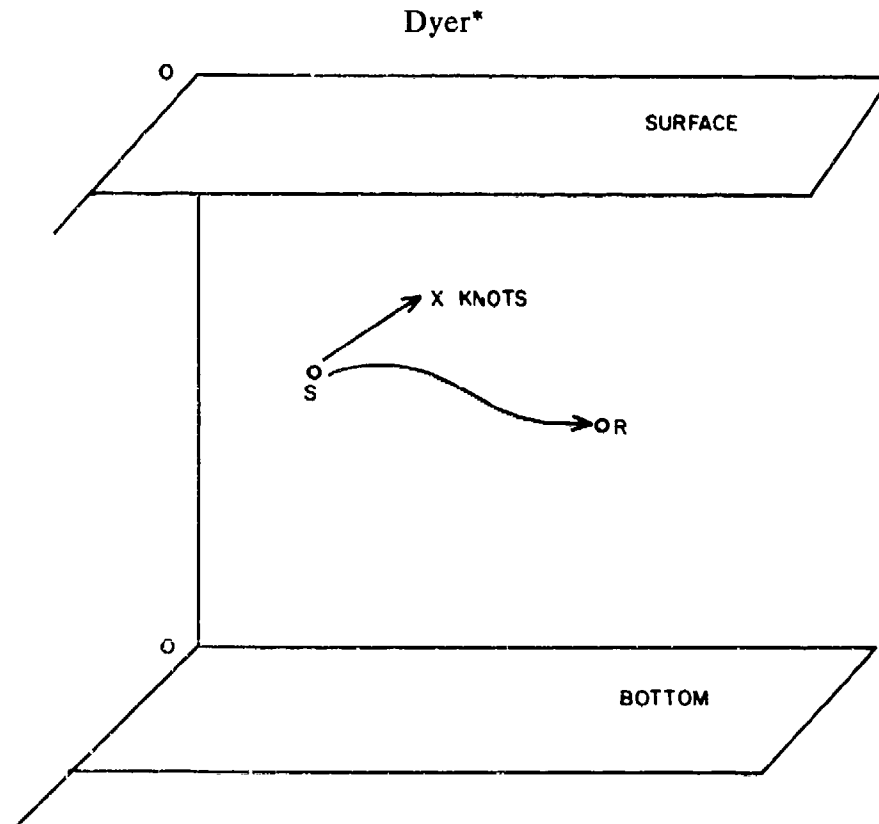
Chief Parameters: (U) Power spectra for range rate with the following choices of sound speed profiles (a) isospeed channel (b) bilinear channel, (c) Munk channel.

Chief Results: (U) Three power spectra are derived for the saturation fluctuation of sinusoids caused by platform motion, conforming to the three choices of sound speed profile.

Upon comparing fluctuations caused by phase rate with fluctuations caused by internal waves one can construct a *critical range rate* at which the frequency shift due to internal waves and that due to platform motion in a frozen ocean are equal.

A pictorial representation of this paper is shown next.

CONFIDENTIAL



(U) Analytic modeling of range rate statistics, particularly the power spectrum of fluctuations of frequency of a sinusoidal signal in the saturation regime.

*This sketch is either (1) the editor's concept of the underlying experimental situation of the paper, presented for convenience of the reader or (2) an actual experiment conducted by others. In all cases the material boxed in heavy lines is the author's contribution as reported at the Workshop.

CONFIDENTIAL

CONFIDENTIAL

Workshop Paper: "Impact of Source Motional Fluctuations on IAP" (U)

Author: A. Gerlach

Objective: (U) Determine correlation degradation between signals at two widely separated arrays caused by the motion of a transiting submarine and provide an estimate of the optimum integration time for use in passive correlation detection.

Research Approach: (U) From test data determine phase-difference fluctuations between the signals received at two remote sensors. Calculate from this the degradation of correlation coefficient between the two received signals.

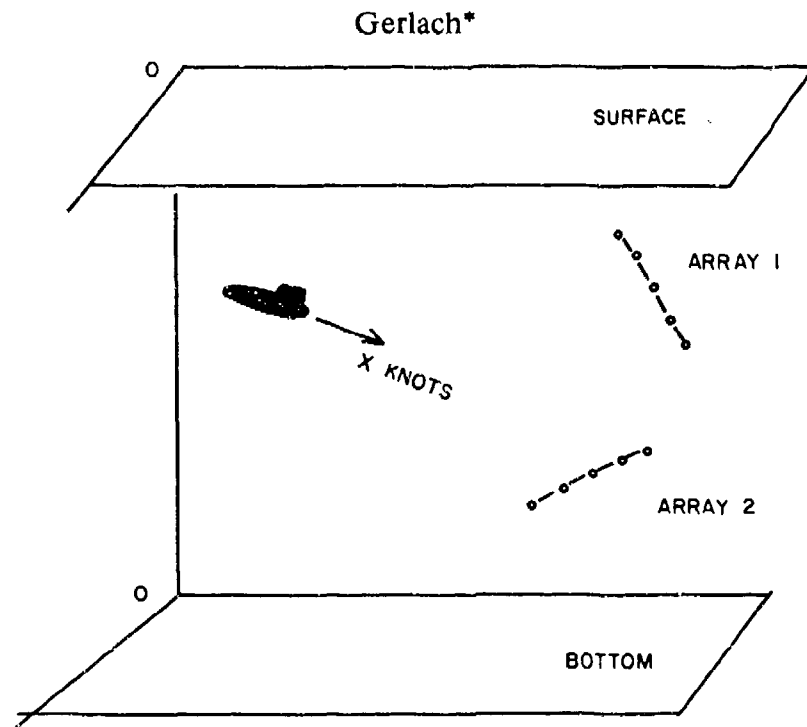
Chief Parameters: (U) Variance and Power Spectra of Target Speed and Course. Standard deviation of phase-difference fluctuations. Analysis time T . Cross correlation of signals at the two arrays.

Chief Conclusions: (1) (C) Temporal cross-correlation between signals at two arrays undergoes degradation as signal frequency, aperture angle between the sensors (taken at target location) target speed and integration time (T) increase. Standard deviation of phase-difference fluctuations increases *linearly* with T . Detailed data are available which give optimum integration time when signal frequency, target speed and course, and source-sensor angle are specified.

(2) (C) For received signals of time duration less than 30 minutes the dominant cause of fluctuations is platform motion (alternatively, multi-path interference).

A pictorial representation of this paper is shown next.

CONFIDENTIAL



(C) Calculate standard deviation of phase-difference fluctuations as a function of integration time. Calculate temporal cross-correlation of signals at arrays 1,2 and determine correlation degradation with course, speed, source-sensor angle and integration time.

*This sketch is either (1) the editor's concept of the underlying experimental situation of the paper, presented for convenience of the reader or (2) an actual experiment conducted by others. In all cases the material boxed in heavy lines is the author's contribution as reported at the Workshop.

CONFIDENTIAL

CONFIDENTIAL

Workshop Paper: "Acoustic Fluctuations" (U)

Author: R. Spindel

Objective: (U) The WHOI (Woods Hole) program is designed to study effects of oceanic variations on acoustic propagation, and determine limits on signal coherence in space and time, with concentration on narrowband (nominally 10 Hz) low frequency (100-400 Hz), long range (10-1500 km). The IGPP (Scripps) program is designed to study mesoscale processes in the ocean by acoustic means, concentrating on high frequency (2250 Hz), wideband, short range (25 km).

Research Approach: (U) Conduct experiments at sea. Show by calculation that study of mesoscales by acoustic signals is feasible.

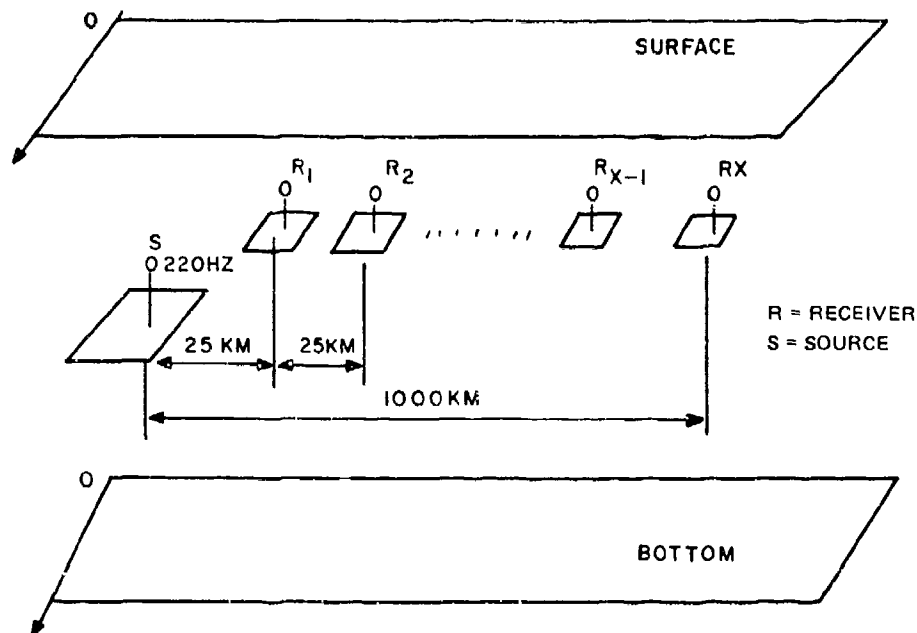
Chief Results: (U) (1) Study of mesoscales by acoustic means is feasible.

(2) Experiment still is to be conducted, or if conducted, to be reported.

A pictc representation of this paper is shown next.

CONFIDENTIAL

Spindel*



(U) WHOI-IGPP Proposed Experiments. (See paper.)

*This sketch is either (1) the editor's concept of the underlying experimental situation of the paper, presented for convenience of the reader or (2) an actual experiment conducted by others. In all cases the material boxed in heavy lines is the author's contribution as reported at the Workshop.

CONFIDENTIAL

CONFIDENTIAL

Workshop Paper: "Omni Noise Field Statistics Depth and Clutter" (U)

Author: J. Shooter

Objective: (U) Identify and understand the dominating source and environmental mechanisms that govern the ambient noise field as a function of depth, frequency and bandwidth. In particular, identify ambient noise caused by ships, and noise caused by wind.

Research Approach: (C) Use data of the vertical ACODAC sensor in the Church Opal experiment. Process the data into narrow band spectra, and obtain statistics of noise level spectra and false alarm rate.

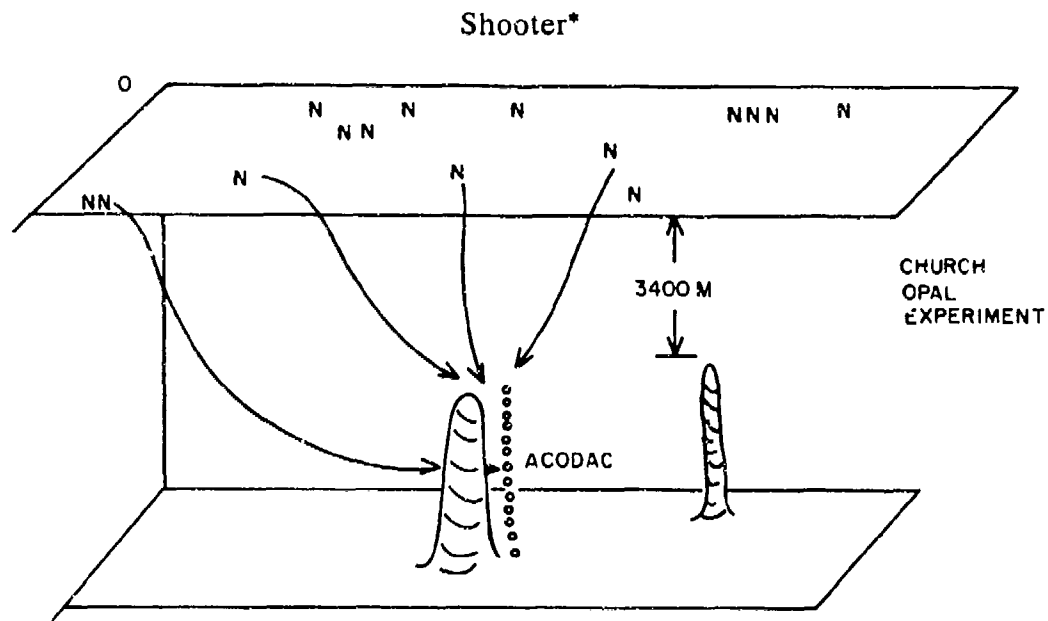
Chief Parameters: (U) Ambient noise spectrum SPL db re $\mu\text{Pa}/\text{Hz}^{1/2}$. Dynamic range of noise level. Covariance of broadband and narrowband spectral components of noise. "False alarm lines" in the noise field. Cell groups or "clutter."

Chief Conclusions: (C)

- (1) (C) If environment is stationary and homogeneous (limited to 3 to 6 HR) the noise obeys chi-square statistics.
- (2) (C) Noise levels varied from 65 dB to 105 dB re $\mu\text{Pa}/\text{Hz}^{1/2}$.
- (3) (C) Spectral components of broadband noise are uncorrelated in time or frequency for homogeneous conditions (3 to 6 HR); spectral components of narrowband (ship) noise are highly correlated across frequency band, High correlation between adjacent frequency bins also observed for wind generated noise.
- (4) (C) The number of single frequency bin false alarms during a "quiet period" is about 50 in 5 to 55 Hz range with 0.018 Hz resolution. Threshold at 10^{-3} probability of false alarms. When a ship passes number of false alarms rises to 200 over same period.
- (5) (C) Number of single bin false alarms is greatest for near-critical depth receiver.

A pictorial representation of this paper is shown next.

CONFIDENTIAL



(C) 13 hydrophones provided 13 data records in the form of time series. System dynamic range 80 dB. Process bandwidth was 0.147 Hz for frequencies 10 to 500 Hz and 0.018 Hz in band 5 to 75 Hz. Averaging time was one minute. Calculate ambient noise spectrum, covariance between spectral lines, false alarm statistics in single and multiple frequency bins, statistics of noise field "clutter."

*This sketch is either (1) the editor's concept of the underlying experimental situation of the paper, presented for convenience of the reader or (2) an actual experiment conducted by others. In all cases the material boxed in heavy lines is the author's contribution as reported at the Workshop.

CONFIDENTIAL

CONFIDENTIAL

Workshop Paper: "Characterization of Acoustic Propagation" (U)

Author: H. DeFerrari

Objective: (U) Characterize the transfer characteristics of a propagation channel rapidly in real time using a small computer and FFT.

Research Approach: (U) Using examples I,II,III pictured below, divide the spectrum of the received signal by the spectrum of the transmitted signal to find channel transfer function. From this by integration obtain the impulse response.

Chief Parameters: (U) Channel transfer function, channel impulse function.

Special Feature: (U) Source transmits pseudo random sequences to permit separation of multipaths, and to overcome noise at low end of spectrum.

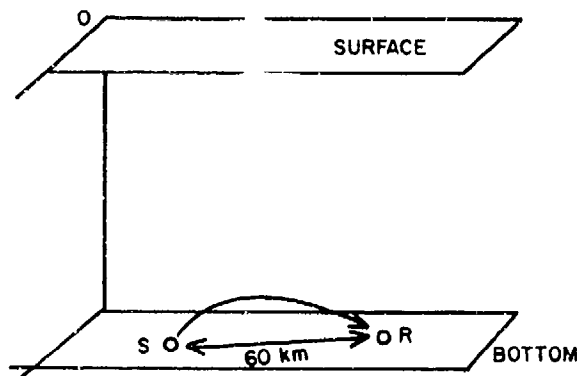
Principal Result of Research: (U) Inverse filtering on received pseudo-random sequences (examples I,II,III) has been used with success.

A pictorial representation of this paper is shown next.

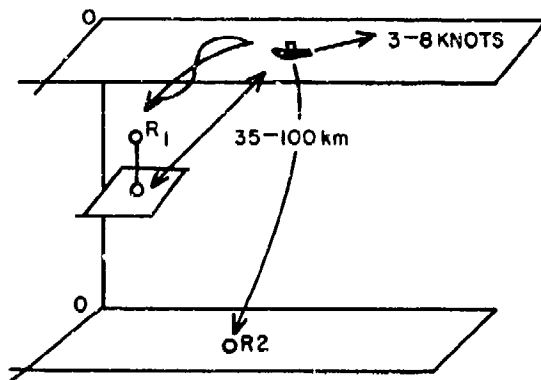
CONFIDENTIAL

De Ferrari*

EXAMPLE I



EXAMPLE II

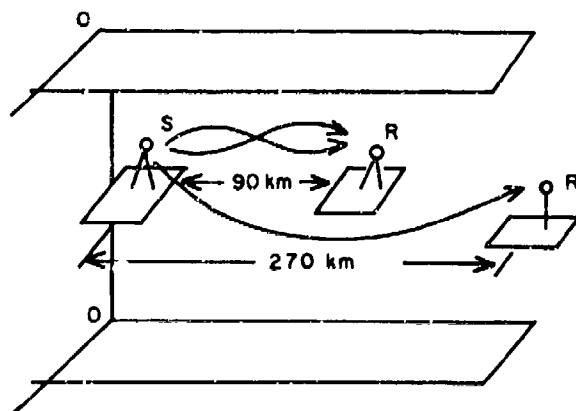


(U) Evaluate

$$\frac{R(W)}{S(W)} = H(W)$$

$$p(t) = \int_{-\Delta W}^{\Delta W} H(W) dW$$

EXAMPLE III



*This sketch is either (1) the editor's concept of the underlying experimental situation of the paper, presented for convenience of the reader or (2) an actual experiment conducted by others. In all cases the material boxed in heavy lines is the author's contribution as reported at the Workshop.

CONFIDENTIAL

CONFIDENTIAL

V. SUMMARY OF RESEARCH RESULTS (C)

(C) As a result of research effort completed thus far, answers to some of the original questions have been obtained. For example, based only upon the small sampling of research presented at the Fluctuations Workshop, we can say that the statistics associated with single point amplitude fluctuations over long paths at low frequencies are reasonably well known as a result of the experimental work of Flowers, Ramsdale and others, and Dyers' analytical work. Noise statistics have also been determined for omnidirectional sensors by Shooter and Flowers. Shooter has also investigated the covariance between noise in adjacent bins and found spectral levels uncorrelated. A number of beam noise models are now available as listed in Cavanagh's paper. Cavanagh has also compared the results of detailed acoustic fluctuation models with the results of mathematical random process simulations and has shown the utility of the latter when good input data are available. Gerlach has been able to recommend optimum integration times for multi-array processing based on his work with fluctuating signals at widely separated arrays. Urlick has shown that, for mobile sonar frequencies and ranges, a log normal model of signal-to-noise fluctuations is adequate. Similarly, work at lower frequencies by Flowers and Frish has shown that intensity fluctuations in transmission can also be represented by a log normal distribution. Thus, even this small sample of fluctuations research indicates that much useful information has been developed. However, the fluctuation effort does not appear to have been evenly distributed over the various applications areas.

(C) The matrix shown in Fig. 1 indicates that the experimental fluctuations work has been concentrated in the transmission loss and noise areas. The signal excess or signal-to-noise results have been almost exclusively model efforts. The signal gain, noise gain and array signal-to-noise performance areas have been neglected. To effectively enhance Navy capabilities, more effort should be devoted to experimental verification of signal-to-noise and signal excess results. In addition, more effort should be directed toward the utilization of fluctuation results for performance enhancement, as well as for descriptive and model applications.

CONFIDENTIAL

Applications Category	Fluctuation Category	Research Effort	■ Model & Expt ● Expt.	▲ Model • Related Info
TRANSMISSION LOSS				
mean				•
temporal amplitude statist		•	▲	•
temporal phase statist.			▲	•
spatial amplitude statist		•	▲	•
spatial phase statist			•	•
temporal ampl. autocorrel.		•	•	•
temporal coherence			•	•
spatial ampl. crosscorrel.		▲	•	•
spatial coherence				•
AMBIENT NOISE				
mean				•
temporal amplit. statistics		■		•
temporal autocorrelation				•
spatial coherence				•
SIGNAL GAIN				
NOISE GAIN				
ARRAY GAIN				
BEAM NOISE				
mean			▲	
temporal statistics			▲	•
spatial statistics				•
SIGNAL EXCESS				
mean			▲	▲
statistics		▲	▲	•
LOCALIZATION				
heavy accuracy-1 array		•		•
heavy accuracy multiarray			▲	•
holding statistics			▲	•

Figure 1

CONFIDENTIAL

CONFIDENTIAL

Additional Aid for Reader Orientation (C)

(C) To assist the reader of these proceedings in understanding the scope of each Workshop paper the sponsors requested each author to check out a "Player Card". On it were appropriate check boxes in columns and rows which indicated the Range, Geometry, Frequency Regime and Time Scales considered by the author in the preparation of his paper. The completed Player Card is reproduced here.

PLAYER CARD																				
SPEAKER	Pos ⁽¹⁾	RANGE ARENA				GEOMETRY ⁽¹⁾			FREQUENCY REGIME (Hz)				TIME SCALES							COMMENTS ⁽³⁾
		<CZ	CZ-3CZ	100-1000nm	>1000nm	Source	Rec.	Water	<1	1-50	50-2500	>2500	Sec	K'n	Hour	Day/Week	3M	Year		
Hanish																				
Larsen	0		✓	✓		D	D	DE-BL		10	< 30	to 200	< 300		15	4				
Fretwell																				
Plum																				
Cavanagh																				
Grace				✓		S	D	?	✓		✓			✓	✓					
Heine																				
Ulrich	E	✓	✓			D/S	D/S	D			✓		✓	✓	✓					
Flowers	D/E		✓	✓	✓	D/S	D	DE		✓	< 250			✓			depending on conditions		digital & analog	
DeFarrari																				
Ewert		✓																	weak scattering freq.	
Dlinthorpe																				
Moll	O/O	✓	✓	✓	✓	SD	SD	BL/DE		✓		✓	✓	✓	✓	✓	✓	✓	(4)	
Cavanagh	0		✓	✓		S	S	DE		✓				✓	✓	✓	✓	✓	(5)	
Tabula	E			✓		80nm	800nm	BL		✓									digital	
Dyer																				
Jobet																				
Gerlach	P			all	✓	all	all	all	✓	✓			✓		30 to 60					
Spindel	E		✓			DJ	DJ	BL/DE			✓	✓	✓	✓	✓	✓	✓	✓		
Fisher	E	✓	✓	✓		S	D	DE		✓		✓		✓	✓	✓	✓	✓		
Shooter	P/E	✓	✓	✓		S	D	DE		✓									analog & digital	
DeFarrari																				
Kerr																				

(1) POSITION

Sponsor (S)
Manager (M)
Modeler (O)
Signal Proc. (P)
Measurer (E)
System Des. (D)

(2) GEOMETRY:

Deep - D
Shallow - S
Bottom Limited - BL
Depth Excess - DE

(3) i.e.:

Saturated/non-saturated
Data - digital/analog

(4) This line is like a patent application. However, for prediction sonar performance, it is applicable to a broad range of acoustic environments.

(5) Model fluctuations in signal and noise are attributed to source/receiver motion in the multipath interference field.

CONFIDENTIAL

Conclusion (U)

(U) The Acoustic Fluctuation Workshop held Feb. 22-23, 1978 at the Naval Research Laboratory, Washington, D.C. is reported in this memorandum. A Technical Review, Editorial Summary and paper Synopsis have been provided to bring the great diversity of Workshop subject matter into perspective. Workshop papers which have reached completed form at the date of this publication are reproduced in Appendix A. Incomplete papers are summarized in Appendix B. An historical account of past achievements has also been briefly noted.

(U) All of the material in this memorandum has been used as a basis for structuring a future research program on the still unsolved aspects of the theory and application of acoustic fluctuations in the ocean. This proposed research is contained in NAVELEX Report dated November 28, 1978, Ref. 6. In itself it can be regarded as a set of Workshop conclusions from which recommendations for new work have been made.

CONFIDENTIAL

CONFIDENTIAL

REFERENCES

1. Encl (1) to AESD ltr to LRAPP mgr. AESD:PRT:ke Ser: S369 of 8 May 1974.
2. "International Workshop on Low Frequency Propagation on Noise, 14-19 Oct. 1974 (WHOI)," Vol. I and II, 1977. Coordinated at the Navy Center for Ocean Science.
3. Proceedings of the 1st Workshop on Operations Research Models of Fluctuations Affecting Passive Sensor Detection, Jan. 1976, (Vol. I (C), Vol II (S)).
4. Coherence Workshop, J.P. Beam, U.S. Navy Journal of Underwater Acoustics, Vol. 26, No. 3, July 1976.
5. Encl (1) "Planning Summary for Selected Navy Ocean Acoustic Program," to NORDA ltr 200:TM:sgt Serial S002-78 of 17 Jan. 1978 to OP-095.
6. "Acoustic Fluctuation: Guidelines for R&D Based on the Proceedings of the Fluctuation Workshop held at NRL, Feb. 22-23, 1978," NAVELEX Report dated November 28, 1978.

CONFIDENTIAL

APPENDIX A

**KEY ISSUES IN THE APPLICATION OF STATISTICS OF ACOUSTIC FLUCTUATION
TO SYSTEM PERFORMANCE MODELING**

S. Hanish

(See Volume 1 — Unclassified)

CONFIDENTIAL
(THIS PAGE IS UNCLASSIFIED)

CONFIDENTIAL

THE APSURV DETECTION MODEL (U)

R. W. Larsen
Naval Ocean Systems Center, San Diego, CA 92152

INTRODUCTION

(C) APSURV (ASW Programs Surveillance) is a computer model designed to analyze the performance of an Undersea Surveillance System. It includes a representation of dynamic acoustic targets, the acoustics of the ocean environment, the acoustic sensors, the signal processing capabilities and operational procedures involved in the detection, classification, localization and tracking of acoustic targets.

(U) To represent such a complex process, many simplifying assumptions and judicious compromises must be made in the model. The intended use of the model, as well as development and execution costs, are important considerations in the design of the model. The next sections review the historical background of the APSURV model, the overall model design and applications in order to provide a context in which to discuss the APSURV detection model and related development issues, such as the parametric representation of fluctuation processes.

HISTORICAL BACKGROUND

(U) The Manager, ASW Systems Project Office, System Analysis Office, was given the responsibility to develop Navy standard ASW performance models by the Chief of Naval Operations (OP-095) in 1967. As part of this effort, APSURV Mod 1 was completed in 1970. It was implemented on an IBM 7090 computer at the Naval Ordnance Laboratory (NOL). The primary application of this model was to support strategic force level studies conducted by OP-095.

(U) In 1974, the Performance Evaluation and Prediction (PEP) Program was established at the Naval Ocean Systems Center (NOSC) by the Undersea Surveillance Project Office, PME-124. After further development, APSURV Mod 2 became available on the UNIVAC 1108 computer at NOSC in early 1977. The primary application of APSURV Mod 2 is to support PME-124 in the development of the Undersea Surveillance System by relating test and evaluation results and operational data to system performance goals.

APSURV MOD 1 OVERVIEW

(C) APSURV Mod 1 is a single target, single frequency (50 Hz) model of the SOSUS system as it existed around 1970. Sonar equation information is derived by table look-up for an arbitrary target track in the Northern Hemisphere. Spherical geometry is employed. The major portion of the data base is a cellular grid of transmission loss for a single frequency (50 Hz), single target depth (300 ft) and a single season (unspecified). The

*APSURV MOD 1 -- ASW Program Surveillance Model Systems Analysis Office Report, Vol. I & II, Abstract/Analyst's Manual (S), (AD 513 177L).

CONFIDENTIAL

dependence of transmission loss on target depth is represented by correction factors called "coupling coefficients." This data base applied beyond a range of 300 n.mi. Within 300 n.mi., radial transmission loss curves are employed. General Oceanology, Inc. developed this data base by interpolation and extrapolation of Western Electric site survey data.

(U) Array processing is represented in APSURV Mod 1 by a single directivity index number per array.

(U) It turns out the detection model is one of the more sophisticated aspects of APSURV Mod 1. As it is the topic of interest, it is presented in detail in a subsequent section.

(U) Classification, localization and tracking are not modeled in APSURV Mod 1. However, it does produce a containment ellipse based on nominal bearing errors.

APSURV MOD 2 OVERVIEW

(C) APSURV Mod 2 is a multiple target, multiple frequency model of the current SOSUS system and SURTASS. Sonar equation data is derived from a data base computed by the Surveillance Analysis Model/Automated Signal Excess Prediction System (SAM/ASEPS). This data base contains "smoothed" boresight radial transmission loss for five frequencies (25 Hz, 50 Hz, 75 Hz, 150 Hz, 300 Hz), two source depths (60 ft, 300 ft) and two seasons (summer, winter). It also includes beam and frequency dependent array gains based on a directional noise model and array design parameters. It also contains frequency and seasonally dependent omnidirectional noise levels.

(U) In addition to modeling multiple frequency detection, APSURV Mod 2 also models classification, localization and tracking.

THE APSURV DETECTION MODEL

(U) Monte Carlo techniques are used in APSURV to develop detection statistics. At any prescribed time, an array, subsystem or system can be in only one of two detection states; either it is in contact with the target or it is not. The sonar equation forms the basis for this decision.

(U) The model is formulated to determine whether or not a target is detected for a specified value of the average signal excess at a specified time. A thresholding technique is employed for this purpose. Detection occurs when the instantaneous signal excess exceeds a threshold of zero; otherwise, detection does not occur. In mathematical notation,

$$D = \begin{cases} 1 & \text{when } SE(t) > 0 \\ 0 & \text{when } SE(t) \leq 0 \end{cases}$$

(U) The instantaneous signal excess, $SE(t)$, is related to the average signal excess, $\overline{SE}(t)$, by a random process, $X(t)$

CONFIDENTIAL

CONFIDENTIAL

$$SE(t) = \overline{SE}(t) + X(t) .$$

The average signal excess is computed in APSURV by extracting appropriate mean components of sonar equation terms from a data base and combining them appropriately; i.e.,

$$\overline{SE}(t) = \overline{SL}(t) - \overline{TL}(t) + \overline{AG}(t) - \overline{AN}(t) - \overline{RD}(t)$$

where

$\overline{SL}(t)$ = mean source level at time t

$\overline{TL}(t)$ = mean transmission loss at time t

$\overline{AG}(t)$ = mean array gain at time t

$\overline{AN}(t)$ = mean omninoise level at time t

$\overline{RD}(t)$ = mean recognition differential at time t.

(U) Of interest here is the representation of the random component $X(t)$ of signal excess. The process $X(t)$ represents random fluctuations associated with all component processes of the sonar equation. More precisely, $X(t)$ represents stochastic fluctuations as well as deterministic variations in signal excess which are not accounted for in the calculation of mean signal excess, $\overline{SE}(t)$.

(U) For convenience, the random variable $X(t)$ is selected as the deviation of the decibel value of the signal excess about the average of the decibel value. In APSURV, the random variable $X(t)$ is actually computed from a sum of random variables. Each component random variable is computed using a random walk called the Ehrenfest model.

THE EHRENFEST MODEL

(U) The Ehrenfest model provides the fundamental methodology for computing random fluctuations associated with the passive sonar detection process in APSURV Mod 1 and APSURV Mod 2. Mathematically, the Ehrenfest model is a random walk which represents diffusion in a central force field. Its mathematical properties which deem it useful to the sonar detection process are: (1) its distribution is approximately normal, (2) its autocorrelation function decays exponentially, and (3) transitions between states occur as relatively small steps. Thus, to the extent that a random process with normal distribution and an exponential autocorrelation function represents a component process of sonar detection, the process is simply described by its standard deviation and relaxation time (autocorrelation time-constant).

(U) The Ehrenfest random walk is a first-order Markov process in which the state space consists of integers with the property that, given the process is in state j , a single transition of the walk can only go to states $j - 1$ or $j + 1$.

CONFIDENTIAL

(U) For a state space $\{0, 1, \dots, n\}$, the transition probability matrix is of the form

$$P = \begin{bmatrix} 0 & 1 & 0 & 0 & \dots & 0 & 0 & 0 \\ q_1 & 0 & p_1 & 0 & \dots & 0 & 0 & 0 \\ 0 & q_2 & 0 & p_2 & \dots & 0 & 0 & 0 \\ \vdots & \vdots & \vdots & \vdots & & \vdots & \vdots & \vdots \\ 0 & 0 & 0 & 0 & \dots & q_{n-1} & 0 & p_{n-1} \\ 0 & 0 & 0 & 0 & \dots & 0 & 1 & 0 \end{bmatrix}$$

where $q_j = j/n$ and $p_j = 1 - j/n$.

(U) The steady state distribution of the Ehrenfest process is given by a binomial distribution of the form

$$p(k) = \binom{n}{k} \left(\frac{1}{2}\right)^n \quad \text{for } k = 1, \dots, n.$$

(U) The s -step autocorrelation function is given by

$$\rho(s) = \left[\frac{n-2}{n} \right]^s.$$

(U) To show how the Ehrenfest model may be used to represent the random deviations encountered in sonar applications, let $\{Y(t), t \in T\}$ be a stochastic process defined by the Ehrenfest model with state space $\{0, 1, \dots, n\}$. The index set T is taken to have the form $T = \{0, \tau, 2\tau, \dots\}$, where the stepping interval for the random walk is τ units of time. The process is extended to the continuum of time by letting $Y(t)$ remain constant between successive elements of T .

(U) A transform of the stochastic process $Y(t)$ may be used to determine deviations from average signal excess. Specifically, the random variable that represents deviations from the values of average signal excess is denoted as $X(t)$ and is defined in terms of $Y(t)$ as

$$X(t) = \sigma_{SE} \left(\frac{Y(t) - (n/2)}{\sqrt{(n/4)}} \right),$$

where

$X(t)$ = deviation from average signal excess,

$Y(t)$ = variate of the Ehrenfest model,

$n/2$ = mean of the Ehrenfest model,

$n/4$ = variance of the Ehrenfest model, and

σ_{SE} = standard deviation of the signal excess.

CONFIDENTIAL

CONFIDENTIAL

(U) Since $Y(t)$ possesses a binomial distribution, the distribution of $X(t)$ is asymptotically normal with a mean of zero and a variance equal to σ_{SE}^2 .

(U) Since $Y(t)$ has a finite state space, the induced distribution $X(t)$ also has a finite state space. Thus, the Gaussian distribution $X(t)$ is truncated at the \sqrt{n} sigma point. The model also contains an input truncation point for the combined random walk.

(U) In some applications, $X(t)$ may be partitioned into components. In APSURV Mod 1, this partitioning has been done on the basis of attributing fluctuations to the environment (X_E), to the target (X_T), and to individual sensors (X_S). The environmental component is the ocean condition that prevails and affects ambient noise and propagation loss. This fluctuation component is sampled independently for each sensor. The target component represents the fluctuations that occur about the mean source level. At any given time, this component is the same for all sensors regardless of type. For a particular sensor, the sensor component is independent of all other sensors.

(U) This partitioning is artificial in terms of the labels "environment," "target," and "sensors." The rules for combining the components are regarded as more important than any specific interpretation of the labels themselves. By studying the manner in which these components are combined, the user will be able to take full advantage of the flexibility afforded by this approach.

(U) An Ehrenfest random walk is used to represent each of these subprocesses. Different stepping intervals (τ) may be specified for the environment, the target, and the sensor; this feature provides a way of depicting both short- and long-term fluctuations. The stepping interval is related to the relaxation time for each of the fluctuations. Since all terms are obtained in the same manner, for convenience consider only the term $X_E(t)$. Let τ_E be the stepping interval associated with $X_E(t)$ and let the state space be the set $\{0, 1, \dots, n_E\}$. It is commonly assumed that the process being simulated is a Gaussian Markov process, in which the autocorrelation coefficient (ρ_G) between successive glimpses is given by an equation of the form

$$\rho_G(\Delta t) = \frac{-\Delta t}{\tau},$$

where

Δt = time interval between glimpses, and

τ = the relaxation time.

(U) The problem is to find τ_E given τ . From equations given previously, it can be shown that

$$\tau_E = \tau \ln \left(1 - \frac{2}{n_E} \right).$$

(U) Separate standard deviations are associated with each of the terms X_E , X_T , and X_S . This association relates to the standard deviation in signal excess (σ_{SE}) as follows:

CONFIDENTIAL

$$\sigma_{SE}^2 = \sigma_E^2 + \sigma_T^2 + \sigma_S^2,$$

where

σ_E = standard deviation associated with environment,

σ_T = standard deviation associated with target, and

σ_S = standard deviation associated with sensor.

Note that σ_E is condition-dependent in the same sense that the value may vary with the target range from the sensor (near or far) and the target depth (shallow or deep).

(U) For example, suppose Y_E , Y_T , and Y_S denote the Ehrenfest random walks that represent fluctuations for the environment, the target, and the sensor. Assume that the state spaces for these walks are defined over integers from zero through n_E , n_T , and n_S , respectively. Then, at any prescribed epoch,

$$X_i(t) = \frac{Y_i(t) - (n_i/2)}{\sqrt{n_i/4}} \quad \text{for } i \in \{E, T, S\}$$

$$X(t) = \sigma_E[X_E(t)] + \sigma_T[X_T(t)] + \sigma_S[X_S(t)]$$

$$X(t) = SE(t) - \bar{SE}(t).$$

(U) The distribution of $X(t)$ may be symmetrically truncated by input. The quantity that is input is the maximum absolute deviation from zero that $X(t)$ can assume and is given in units of σ_{SE} . Therefore, if the distribution is to be truncated at the $3.5 \sigma_{SE}$ point, the truncation input would be 3.5, thereby limiting the range of $X(t)$ to $-3.5 \sigma_{SE} \leq X(t) \leq 3.5 \sigma_{SE}$.

(U) For any two sensors of the same subsystem, the correlation coefficient (ρ) between their fluctuations at a given epoch is

$$\rho = \frac{\sigma_T^2}{\sigma_E^2 + \sigma_T^2 + \sigma_S^2} = \frac{\sigma_T^2}{\sigma_{SE}^2}$$

which is an immediate consequence of the assumption that $X_T(t)$ is presumed to be the same for all sensors of the same subsystem, that $X_S(t)$ and $X_E(t)$ are generated independently for each sensor, and that all crosscorrelations among $X_E(t)$, $X_T(t)$, and $X_S(t)$ are zero.

(U) As a matter of historical interest, the fluctuation parameters used in APSURV Mod 1 at the time of its delivery to NOSC in 1973 are listed below.

	Standard Deviation	Relaxation Time
Target	4 dB	4 hrs
Environment	6 dB	4 hrs
Sensor	4 dB	4 hrs

CONFIDENTIAL

FLUCTUATION SURVEY

(C) As part of the development of APSURV Mod 2, a brief review was conducted to determine the applicability of the fluctuation model and its parameters as specified in APSURV Mod 1. The primary differences between APSURV Mod 2 and APSURV Mod 1 which motivated this review are: (1) APSURV Mod 2 is a multifrequency, multi-target model, whereas APSURV Mod 1 is a single frequency, single target model; (2) APSURV Mod 2 accounts for more deterministic variations in sonar equation parameters than APSURV Mod 1; and (3) APSURV Mod 2 attempts to model coherent interarray processing, whereas APSURV Mod 1 does not.

(U) So far, the review process has raised more questions than answers and it is by no means complete. This paper only summarizes the current status of this effort. The variability of each term in the sonar equation will be discussed briefly. For this purpose, it is convenient to write the sonar equation in the following form,

$$SE = SL - TL + SG - BN - RD$$

where

SL = source level

TL = transmission loss

SG = beamformer signal gain

BN = beam output noise level (omninoise level plus the beamformer noise gain)

RD = recognition differential.

Source Level Variations

(C) APSURV Mod 2 deterministically computes the aspect, speed and operating mode dependence of source level and frequency for the five dominant signature components for each class of target.¹ Thus, only the measurement uncertainty and/or random variation in source level of a specific submarine need be considered in the fluctuation model. For primary targets of interest, the reported standard deviation of measurement error is 2 dB. For lack of a better information, a standard deviation of 3 dB and a four-hour relaxation time is associated with random source level variations in the model.

Transmission Loss Fluctuations

(U) Transmission loss fluctuations account for about one-half of the total random fluctuations in the model and transmission loss is presumed to be the dominant source of fluctuations which impact the detection process. No list of references on this subject would be complete. Suffice to say, this is a current and relevant topic of discussion.

(U) Generally speaking, stochastic transmission loss fluctuations can be categorized as temporal fluctuations and spatial fluctuations. Temporal fluctuations are attributed to

¹Radiated Noise Levels from Foreign Ships, Defense Intelligence Agency.

CONFIDENTIAL

scattering from time-dependent inhomogeneities in the ocean and its surface (internal and surface waves). The internal wave theory² characterizes fluctuations of refracted-only propagation (RR paths) in terms of saturated and unsaturated regions. As the saturated region generally applies to long-range detection, its properties have been chosen to characterize temporal fluctuations in APSURV Mod 2. In particular, transmission loss fluctuations due to internal waves in the saturated region are described by a Rayleigh distribution (with a standard deviation of 5.6 dB independent of frequency) and a nominal relaxation time of 1.5 hrs at 50 Hz and 500 n.mi. The relaxation time is inversely proportional to frequency and weakly dependent on range.

(U) In order to apply the temporal fluctuation theory further, a global description of environmental conditions yielding saturated and unsaturated regions is required. In addition, regions of bottom bounce (BB), RSR (refracted, surface reflected), and RR propagation must be defined. The internal wave theory must also be extended to include BB and RSR paths.³

(U) Spatial fluctuations can be attributed primarily to the rangewise correlation interval associated with the transmission loss multi-path structure.⁴ Characterization of these fluctuations is complicated. However, for targets with range rates in excess of one knot, which is generally the case of interest, the relaxation time of this process is on the order of minutes for frequencies of primary interest. This time is less than the integration time for passive incoherent processing and post-processing operator integration which is usually on the order of 10 min. to 30 min. In such cases, the spatial transmission loss fluctuations due to source motion are termed fast-fading and have no effect on the performance of the incoherent detection process.⁵

(U) A particular exception to the above is the case of coherent interarray processing. In this case, spatial decorrelation effects directly impact the time over which coherent integration can be performed when moving targets are considered. This topic is beyond the scope of this paper.

(U) Besides stochastic transmission loss fluctuations, considerations must also be given to deterministic or predictable transmission loss variations. Such is the case with convergence zones. Except for half-channel and bottom-bounce conditions, convergence zone structure is important in predicting the detection performance of shallow receivers out to ranges on the order of 150 n.mi. Beyond a range of 150 n.mi., convergence zone structure is usually weak. For bottom-mounted sensors, convergence zone structure usually exists but it is not a dominant effect like it is for shallow receivers.

(C) APSURV Mod 2 does not currently account for deterministic convergence zone structure for SOSUS arrays. Presumably it is compensated for in a nondeterministic sense by using at short ranges (less than 150 n.mi.) the intensity variation associated with internal waves at long ranges (the saturated region); the claim being that the loss in intensity variation due to internal waves at short ranges (the unsaturated region) is roughly compensated for by the increased predominance of convergence zone structure at short ranges.

²Sound Transmission Through a Fluctuating Ocean, Platte, S.M., Dasher, R., Monk, W.H. and Zachariasen, F., Stanford Research Institute Technical Report JSR-76-39, May 1977.

³Fluctuations Caused by Internal Waves in Ocean Sound Transmission Via RSR Paths, Bolt, Beranek and Newman, Report No. 3668, by Preston Smith.

⁴Spatial Coherence in Multipath or Multimodal Channels, P.W. Smith, Jr., JASA 60, 306-310 (1976).

⁵Detection Performance for Fading Signals, A. D. Whalen, 1967.

CONFIDENTIAL

(U) The transmission loss fluctuation parameters currently used in APSURV Mod 2 are summarized below. It is assumed that there is no inter-frequency nor inter-sensor correlation of transmission loss fluctuations.

Frequency	Standard Deviation	Relaxation Time
25 Hz	5.6 dB	3.0 hrs
50 Hz	5.6 dB	1.5 hrs
75 Hz	5.6 dB	1.0 hrs
150 Hz	5.6 dB	30 min
300 Hz	5.6 dB	15 min

Signal Gain Fluctuations

(C) The variation in signal gain due to target motion through the beam pattern structure of an array is computed deterministically in APSURV Mod 2. For SURTASS arrays, additional signal gain variations due to array motion are expected but have not as yet been modeled. Effects such as signal gain variation due to changes in wavefront coherence is not considered, although the mean loss in signal gain due to loss in wavefront coherence is included for selected SOSUS arrays where this phenomena has been observed.

Beam Noise Fluctuations

(U) Beam noise fluctuations are attributed primarily to shipping below 150 Hz and to wind noise above 300 Hz with the intermediate frequency range being a nominal transition region. Both analytic models and Monte Carlo models of beam noise have been developed. In addition, measured beam noise statistics have been collected for selected sites. It is expected that generalized descriptions of the characteristics of beam noise fluctuations as a function of frequency, site, season, and/or array design will be forthcoming.

(C) The current assumptions in APSURV Mod 2 concerning the parameters describing beam noise are shown below. These numbers are based on average measured values for a particular SOSUS array. APSURV Mod 2 has provision for site-dependent beam noise fluctuation parameters, but the numbers have not been provided. No frequency or array interdependence of beam noise fluctuations is currently assumed. Although there is provision in the model for correlated beam noise effects, quantitative descriptions are not available.

Frequency	Standard Deviation	Relaxation Time
25 Hz	3.0 dB	4 hrs
50 Hz	3.5 dB	4 hrs
75 Hz	3.5 dB	4 hrs
150 Hz	3.5 dB	4 hrs
300 Hz	3.0 dB	4 hrs

CONFIDENTIAL

Recognition Differential Variations

(C) The concept of recognition differential is modeled in APSURV Mod 2 by line detection thresholds and decision rules which represent the classification process. The line detection thresholds are based primarily on test and evaluation results. These tests involve the injection of threat signatures into beam noise in a manner which attempts to maintain constant signal-to-noise ratio during the test. Thus, the standard deviation of a particular detection threshold measurement can be attributed principally to operator differences. Usually this amounts to about 2 dB.

(U) Other variations in detection thresholds are modeled explicitly in APSURV Mod 2. This includes the variation in detection threshold associated with the assignment of allocatable signal processing equipment to specific beam bands.

SUMMARY

(U) The following table is a summary of the parameters currently used in APSURV Mod 2 to represent random acoustic fluctuations:

	Standard Deviation	Relaxation Time	Inter-Sensor Correlation	Inter-Frequency Correlation
SL	3.0 dB	4 hrs	100%	0%
TL	5.6 dB	(75/f) hrs	0%	0%
BN	~3.5 dB	4 hrs	0%	0%
RD	2.0 dB	4 hrs	0%	0%

CONFIDENTIAL

PSEUDO—SURVEILLANCE SYSTEM PERFORMANCE SIMULATOR (U)

Lyman Fretwell
Bell Telephone Laboratories
Whippany, New Jersey

ABSTRACT

(U) System Performance model evolution is guided by the user's needs, subject to computer resource constraints. Models are used to gain insight not obtainable in other ways, and their limitations require that care be exercised in interpreting their results.

(U) PSEUDO is a Monte Carlo code simulating ocean acoustics and the system processes of detection, resource allocation and localization and tracking. It is a large scale simulation that simulates the system-related results of the component processes rather than duplicating their functioning in detail. In general, the system wet end is characterized by data input to the model whereas the shore processing is represented by software. It is most often used to compare system alternatives.

(U) Fluctuations are modeled in PSEUDO according to the components of the Sonar equation with individual components represented by Gauss-Markov processes. Temporal correlation is modeled explicitly, and frequency and spatial correlation are implicit in the way random numbers are shared among the sonar equation computations of signal-to-noise. Recommendations are made from PSEUDO's viewpoint of those fluctuations areas most in need of further research.

(U) Recent work at Bell Laboratories inspired by PSEUDO's needs is presented on beam dependence of beam noise standard deviation and on the temporal character of the total signal-to-noise process.

**PSEUDO (PROGRAMMED SIMULATIONS TO EVALUATE
UNDERWATER SURVEILLANCE SYSTEMS DYNAMIC OPERATIONS)**

(U) Systems application of performance modeling needs a tradeoffs guide model evolution for current needs encompassing total system design. PSEUDO has become a complex, large scale simulation. The goal is to simulate system performance potential by using simplified representation and not duplicating the physics. A history of simulation at Bell Laboratories is shown in Table I. We must model system function capabilities and not expect to reproduce field data anomalies. Computer resource limitation are a trade-off against model complexity and uniformity of simplification is important. Aspects needed for user application should be emphasized.

CONFIDENTIAL

Table I — History of simulation at Bell Laboratories (U)

<u>DATE</u>	<u>REFERENCE</u>	<u>MODEL</u>	<u>REMARKS</u>
1967	23rd INTERIM RPT	DSS	FIRST KNOWN ACOUSTIC SIMULATION
1968	24th INTERIM RPT	OSS	FIRST SYSTEM SIMULATION; USED OFF-LINE LOCALIZATION AND TRACKING
1969-72		OSS	SIMULATED DATA FOR ALGORITHM EVALUATION
1973		PSEUDO	STUDY OF SEARCHLIGHT CONCEPT
1974	OSTP-43	SPAN	SIMULATED HYDROPHONE AND DIRECTIONAL AMBIENT NOISE
1974-75		PSEUDO, BMT, SSM	ASSORTED SYSTEM SIMULATIONS
1976	IUSS RPT	PSEUDO	EVALUATION OF SHORE PROCESSING CONCEPTS
1977	WL BROCHURE	PSEUDO	COMPARISON OF UNDERWATER DEPLOYMENT OPTIONS

(U) Modeling system performance leads to insight not obtainable in other ways. Estimation of future as well as present system performance will be done. Deployment planning requires a wide spectrum of model application e.g. wet end system design and dry end system design. The role of models in deployment planning is illustrated in Fig. 1. Adaptability is important. Models can also provide operational performance assessment and aid in functional development (resource allocation). It also identifies anomalous performance and provides guidance.

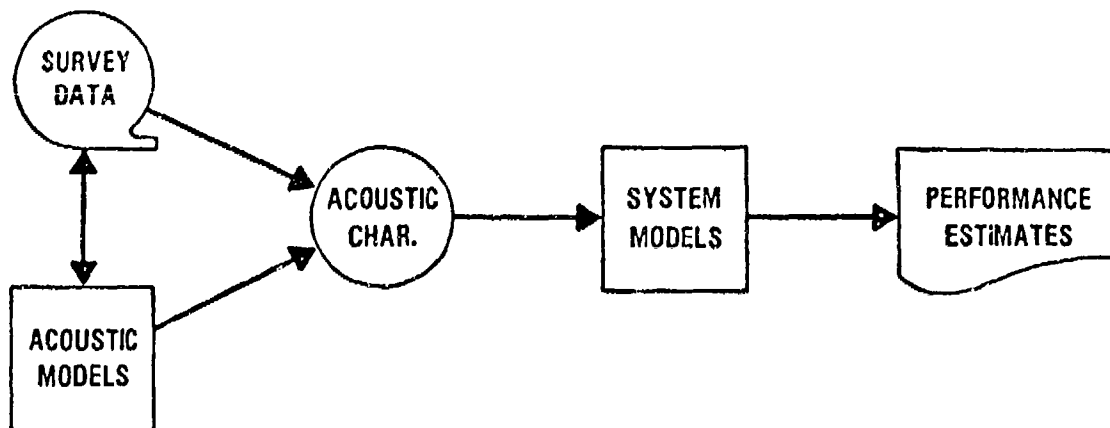


Fig. 1 (U) — The role of models in deployment planning (U)

CONFIDENTIAL

(U) Care is needed in interpreting model results. Simplification without oversimplifying, total system performance (detection, localization and tracking), and components of answer should make sense in the presentation of results. Uncertainties should be taken into account in how results are used. Complexity means potential for uncertainty in absolute estimates. The objective is usually robustness of a system-related decision. Relative measures are better than absolute. Multiple realizations may indicate sensitivity. The user's reaction to uncertainties motivates further modeling and research. There is no single answer as it depends on the user and is especially true of fluctuations.

(U) Acoustic models provide data where no survey data exists. They guide survey planning and extrapolate survey data to other areas and seasons. System models provide comparative data for evaluating alternatives and in evaluating new deployments in total surveillance contexts.

(C) Programmed simulations to evaluate underwater surveillance systems dynamic operations. (PSEUDO) is a Monte Carlo multi-target, multi-line, multi-sensor simulator. It is the most advanced simulator available to address detection, localization and tracking, and has a potential for intercept/handover. The large scale simulation has: 44 sensors, 35 targets, and 8 lines per target. The multiple modes of target prosecution are for general surveillance (detection) (1) Unalerted acquisition (2) Alerted reacquisition and for searchlight surveillance; (with tracking) (1) Interstitial beams (2) IAC, Spear processing allocations.

SYSTEMS APPLICATION OF PERFORMANCE MODELING

NEEDS, TRADEOFFS GUIDE MODEL EVOLUTION

- Current needs encompass total system design
 - PSEUDO has become complex, large scale simulation
- Goal is to *simulate system performance potential*
 - Use simplified representations — don't duplicate the physics
 - Must model system functional capabilities
 - Don't expect to reproduce field data anomalies
- Computer resource limitations trade off against model complexity
 - Uniformity of simplification is important
 - Emphasize aspects needed for user application

MODELING SYSTEM PERFORMANCE LEADS TO INSIGHT NOT OBTAINABLE IN OTHER WAYS

- Estimate future as well as present system performance
- Deployment planning requires wide spectrum of model application
 - Wet end system design
 - Dry end system design
 - Adaptability is important

CONFIDENTIAL

- Models can also provide operational performance assessment
 - Aid in functional development (resource allocation)
 - Identify anomalous performance, provide guidance

CARE IS NEEDED IN INTERPRETING MODEL RESULTS

- Presentation of results: simplification without oversimplification
 - Total system performance (detection, localization and tracking)
 - Components of answer should make sense too
- Take uncertainties into account in how we use results
 - Complexity means potential for uncertainty in absolute estimates
 - Objective is usually robustness of system-related decision
 - Relative measures are better than absolute
 - Multiple realizations may indicate sensitivity
- User's reaction to uncertainties motivates further modeling, research
 - There's no single answer — depends on user
 - Especially true of fluctuations

(C) PSEUDO SIMULATES RATHER THAN DUPLICATES (U)

(U) The acoustics formulation is done as follows. The Sonar equation relating significant parameters is: $S/N = SL - TL - N + SG - NG$. Average values are supplied for these parameters from a preprogrammed table lookup, interpolation. For fluctuating components we employ a lognormal distribution with correlation (Gauss-Markov model).

(C) The detection/classification function is carried out next. A line is detected if $S/N >$ some threshold selected. Then a target is detected when specific classification criterion is met. These classification algorithms depend upon:

- 1) Target state (alerting)
- 2) Target line signatures
- 3) Length of time held
- 4) Signal excess

While the threshold varies, depending upon:

- 1) Target state (alerting provided)
- 2) Special resources, correctly allocated
- 3) Processing bandwidth, line stability considerations

An example of how long a target is held depending upon number of resources allocated is given by Fig. 2.

CONFIDENTIAL

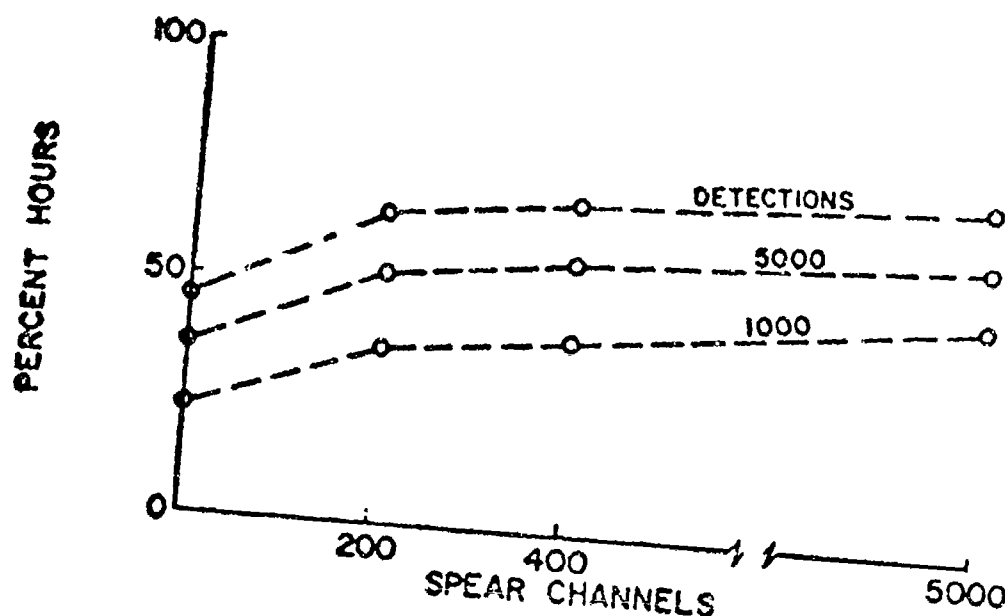


Fig. 2 (C) — Sensitivity to resources (U)

PSEUDO IS A MONTE CARLO MULTI-TARGET, MULTI-LINE
MULTI-SENSOR SIMULATOR

- The most advanced simulator available to address
 - Detection
 - Localization and tracking
 - Potential for intercept/handover
- Large scale simulation
 - 44 sensors
 - 35 targets
 - 8 lines per target
- Multiple modes of target prosecution
 - General surveillance (detection)
 - Unalerted acquisition
 - Alerted reacquisition
 - Searchlight surveillance (tracking)
 - Interstitial beams
 - IAC, Spear processing allocated

(C) Localization and tracking functions are included. PSEUDO models NESB procedures on fixed beams. It contains versions of MST, MSL/D, SBL and simulates results of station operations.

CONFIDENTIAL

(C) Resource allocation is also provided whereby an allocation is based on estimated position and uncertainty ellipse. For example, IAC Spear for searchlight surveillance is modeled with improved thresholds and localization capability. A dynamic algorithm sets a priority based on the number of beams required to cover uncertainty ellipse for a given probability of detection. The size these uncertainty ellipses are strongly depends upon a system continuity of operation. System outages cause large exponential increased in these areas as shown by Fig. 3.

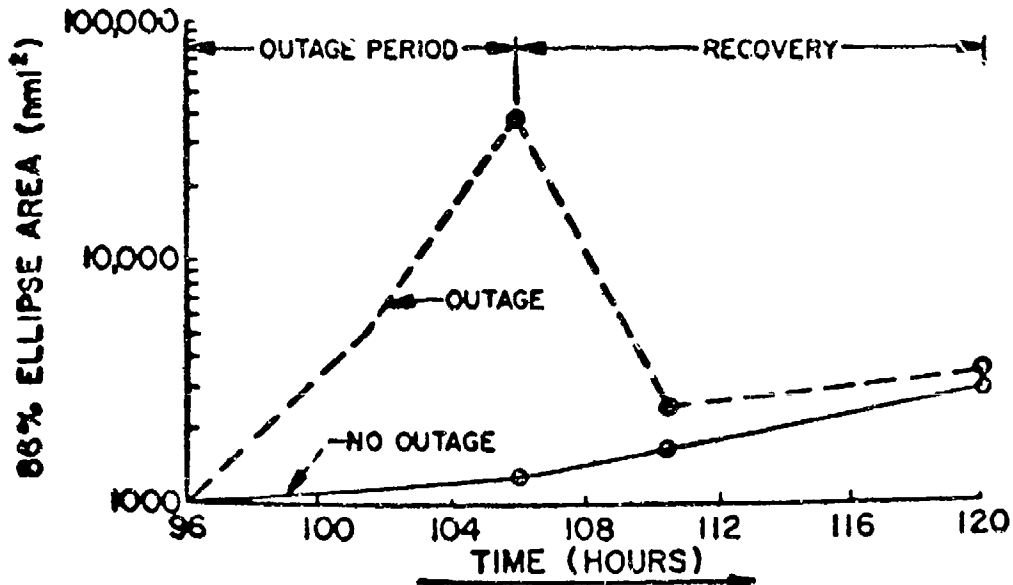


Fig. 3 (C) — Sensitivity to system outage (U)

(C) Beam signal and noise component fluctuations are included where each component modeled as Gauss-Markov process. The noise standard deviation, correlation coefficient can vary from beam to beam. The following commonality of random components is used to effect space, frequency correlation structure:

— Target	— Each source	dB
— TL	— Each array-target	(2.0)
— N (Ambient)	{ Each beam	(3.3)
— SG	{ Each array	(2.0)
— Detection	— Each octave	(2.9)
	— Each array-line	(2.5)
		(1.5)
	TOTAL	(6.0)

Typical correlation used — 0.7 one hour

NOTE: If time correlations differ, total process is not Gauss-Markov

CONFIDENTIAL

(U) Fluctuations understanding is needed for performance modeling. The correlation structure needs most work now; as those involving time, frequency and space. Appropriate correlation between data gathering, modeling is needed. Data is to be taken at prime sites to develop and check models; also review available data. Need models to run a multitude of cases to obtain statistics. There is a need to develop fluctuations understanding for those new system components 1) shore processing improvements (IRP, ABF) and 2) sensor alternatives (SURTASS, RDSS, distributed sensors, large aperture arrays).

CONFIDENTIAL

FLUCTUATIONS FOR THE APAIR, APSURF, APSUB MODELS (U)

R. S. Flum, Sr. (ASW-115)
ASW Systems Project Office (PM-4)
Washington, D.C. 20360

(U) We present a brief description of all the Anti-Submarine Warfare Program (AP) models—lumped together—with application to ASW and engagement. These models are computer written, user oriented Monte Carlo types. They are documented and validated math models.

When using them the word Monte Carlo means the model is replicated a number of times for a "run"—to get the statistical distribution of the output.

The models are:

APAIR — AP for Air deployments (1, 2)

APSURF — AP for Surface deployments (3)

APSUB — AP for Submarine deployments (4)

In applying these models we need a correlation of fluctuations between terms in Signal Excess (SE) equation, defined in the conventional manner by the equations:

Active applications: $S.E. = S_L - (N_L - R_{DA}) + T_S - 2T_L \pm \sigma_A$

Passive applications: $S.E. = T_S - (N_L - R_{DP}) - T_L \pm \sigma_P$

in which σ represents a correction for fluctuations of component terms.

RANDOM FLUCTUATION

(C) In APAIR there are four input fluctuations provided; when put to use these models require the following fluctuation inputs:

V_1 = operator degradation factor — drawn once each replication for each operator
0 mean, normal* with $\sigma = 0 \pm 6$ dB.

V_2 = long term fluctuation — open field environment — for each frequency — drawn once each replication
0 mean, normal with $\sigma = 3$ dB

V_3 = short term fluctuation — for each frequency — drawn at 30 min. intervals within each replication
0 mean, normal with $\sigma = 5$ dB

V_4 = buoy to buoy variation — for each buoy drawn when dropped — for each replication
0 mean, normal $\sigma = 3$ dB

*Statistics are Gaussian with standard deviation σ .

CONFIDENTIAL

CONFIDENTIAL

(C) APAIR random variations are given by

$$VR = -V_1 + V_2(J) + V_3(J) + V_4$$

where

- V_1 - Represents an operator degradation factor which is selected for each individual iteration from a user specified distribution (0 + 6 dB).
- V_2 - Represents a frequency dependent combination of threat radiated noise variation and ambient noise variation from iteration to iteration. These are drawn from zero mean, normal distributions with user specified standard deviations (~3 dB).
- V_3 - Represents frequency dependent short term ambient noise variations within each iteration. Drawn from zero mean, normal distributions with user specified standard deviations (~5 dB).
- V_4 - Represents a buoy-to-buoy variation within each iteration. Drawn from a zero mean, normal distribution with user specified standard deviations (~3 dB).

(C) In APSURF for active performance

There are three input fluctuations -

1. ping to ping - drawn each ping for signal excess calculations
0 mean, normal $\sigma = 6$ dB
2. sonar to sonar - drawn once each replication for each sonar
0 mean, normal $\sigma = 6$ dB - 5 dB
3. day to day - drawn once each replication to represent the long term fluctuations
0 mean, normal $\sigma = 5$ dB

For the submarine target - *active* - there is a variation on the modified cookie cutter representation of a ping-to-ping difference in range amounting to

0 mean;

(C) In APSURF for passive performance

There are three input fluctuation values -

1. σ_{LT} long term, environment, frequency, drawn once per replication
0 mean, normal $\sigma = 5$ dB
2. σ_{ST} short term, drawn once each integration interval of environment, frequency $\sigma = 2$ dB
3. σ_{ST} buoys-short term, drawn once each integration interval, environment, frequency $\sigma = 2$ dB

CONFIDENTIAL

- (C) In a APSUB and active performance there are three input fluctuations —
ping to ping. These are drawn for each ping, function of prop. mode., B_B , E_Z , etc.
- (C) In APSUB and passive performance there are two models:

PFLUCT1

Near surface and convergence zone. This model assumes fluct. are exponentially correlated in time or serial correlated or MARKOV process. These are functions of in, across, or below layer — drawn each sample time.

For bottom bounce—

Has two components of fluctuation — the above kind of MARKOV component and a jump component. These are functions of bottom area, each area has a new jump fluct. component. Assumes no correlation.

PFLUCT2

Fluctuations represents sig to noise. They are drawn from normal dist. and uncorrelated — mean 0 and $\sigma = 1$. This number is then multiplied by a constant which is a function of propagation model added to S.E. code.

A. SUBROUTINE AFLUCT - Several Fluctuation Models

(U) Introduction

Since the ocean is not a static medium, the acoustics of underwater sound is not a static process. Many parameters of the active sonar equation vary with time. Both short term and long term fluctuations tend to exist; however the nature and distribution of these fluctuations are yet unknown and require further study, especially for active sonar considerations.

(U) Description

The fluctuation model described herein assumes signal fluctuations to be uncorrelated from ping to ping. A normal distribution is assumed with a standard deviation set by input. Each parameter in the active sonar equation is assumed to be a mean value, making the signal excess a mean value. Then signal fluctuations are considered, and an instantaneous signal excess is determined.

This subroutine is called from the active sonar model (ASONAR). It is entered with the mean signal excess and the standard deviation or sigma value. An instantaneous signal excess is drawn from a normal distribution having the mean signal excess as its mean and a sigma by input. This process may be referred to as a Monte Carlo experiment.

(U) Limitations

This subroutine is for use with active sonar only.

CONFIDENTIAL

CONFIDENTIAL

B. SUBROUTINE PFLUCT1

(U) Introduction

Fluctuations in signal strength are poorly understood but must be considered when solving the sonar equation. Fluctuations may be due to transients such as noise spikes in the target radiated noise patterns, self noise variations, and changes in propagation loss. This model simulates signal fluctuations by adding a random, time correlated component to the computed mean signal to noise ratio. Since the signal fluctuation process is poorly understood at present, this model can be assumed to be only a reasonable approach to the problem.

(U) Description

Two different algorithms are used to compute signal fluctuations in this model, one for near-surface and convergence-zone and another for bottom-bounce transmissions. The first of these assumes that successive fluctuation components are exponentially correlated in time. Thus, samples which are widely separated in time will be uncorrelated, while those which are closely spaced will be strongly correlated. This technique is very similar to the statistical process called serial correlation and is sometimes called a MARKOV process. The magnitude of this fluctuation component also varies depending on whether the transmission is in, below, or across the layer. A random component is drawn at every sample time in the time.

In the bottom reflected mode the fluctuation is assumed to be composed of two parts, a MARKOV component as described above and a jump component. The jump component is assumed to be associated with a particular area of ocean bottom. The size of the area and the jump fluctuation are chosen randomly. After relative motion considerations show that the game participants have left the area, another area is randomly chosen together with another jump fluctuation component. Successive jump fluctuations are assumed to be uncorrelated.

(U) Limitations

The output of this model should be considered representative of deep water transmissions. Shallow water environments may require a fluctuation model different from the present one.

C. SUBROUTINE PFLUCT2

(U) Introduction

Fluctuations in signal strength are poorly understood at present but must be considered when solving the sonar equation. Fluctuations may be due to transients such as noise spikes in the target radiated noise patterns, self noise variations, and changes in propagation loss.

(U) Description

PFLUCT2 is a routine to simulate fluctuations in the signal-to-noise ratio. Fluctuations are drawn from a Gaussian distribution and are uncorrelated.

CONFIDENTIAL

On each call to PFLUCT2 the subroutine draws a number from a Gaussian distribution with standard deviation equal to one. The random number is then multiplied by a constant which depends on the propagation mode.

The same fluctuation model is used regardless of propagation mode. Only a constant is changed when the mode changes. There is no jump fluctuation in bottom bounce.

It should be realized that this formulation is only a rough approximation of observed fluctuations.

(U) Limitations

The logic of this routine assumes that signal fluctuations are uncorrelated in time. This approximation may not be adequate if the sonar is sampled frequently.

Details on Choices and Algorithms

<u>APSURF</u>	<u>PASSIVE (σ)</u>	<u>ACTIVE (σ)</u>
$\sigma_{LT} = 5$ dB	per replication	ping to ping = 6.0 dB
$\sigma_{ST} = 2$ dB	per replication	sonar to sonar = 5.0 dB
$\sigma_{ST_{buoys}} = 2$ dB	per replication	iteration to iteration = 5.0 dB
		target strength = aspect
		submarine sonar = 10% true range

D. ASUB FLUCTUATION (Passive)

Passive signal fluctuation is simulated by creating a random time correlated component which is added to the signal to noise ratio.

Three separate computations are made depending on the propagation mode.

There are two separate passive fluctuation routines PFLUCT1 (random time correlated components) and PFLUCT2 (components from a Gaussian distribution).

1. SUBROUTINE PFLUCT1 Details

$$DELTAT = TSA - FLTIME$$

where

TSA = sonar sample time

FLTIME = last fluctuation sample time

NSPROP (Near Surface Propagation)

$$FLUC = AKE(69)[YNS]$$

$$YNS = CRN \sqrt{1 - e^{-2 \cdot DELTAT \cdot AKE(67)}} + e^{-DELTAT \cdot AKE(67)}(YNS)$$

YNS = near surface correlation coefficient

CONFIDENTIAL

AKE(67) = coef for correlating NS fluctuations in time (NWL value 60/hrs)

AKE(69) = standard deviation for NS fluctuations (NWL value 5 dB)

GRN = Gaussian random number with mean = 0 and $\sigma = 1$.

CZPROP

FLUC = AKE(70)[YCS]

YCS = $\text{GRN} \sqrt{1 - e^{-2 \cdot \text{Deltat} \cdot \text{AKE} 68}} + e^{-\text{Deltat} \cdot \text{AKE} 68}(\text{YNS})$

YCS = convergent zone correlation coef.

AKE(68) = coef. for correlation CZ fluctuations in time (NWL value 60/hrs)

AKE(70) = standard deviation for CZ fluctuation (NWL value 5 dB)

GRN = same as NS.

BBPROP

FLUC = AKE(73) FJUMP + AKE(74)[YBB]

YBB = $\text{GRN} \sqrt{1 - e^{-2 \cdot \text{Deltat} \cdot \text{AKE} 71}} + e^{-\text{Deltat} \cdot \text{AKE} 71}(\text{YBB})$

YBB = bottom bounce mode correlation coef.

AKE(73) = σ of the jump component of bottom bounce mode (NWL value 3 dB)

AKE(74) = σ of the MARKOV component of bottom bounce mode (NWL value 3 dB)

AKE(71) = coef. for correlation BB mode fluctuation in time (NWL value 60/hrs)

FJUMP = jump component of fluctuation in BB mode

FJUMP = Gaussian random number from a normal distribution with 0 mean and $\sigma = 1$.

New FJUMP values are drawn when BB area moves a distance RADBB.

RADBB = $-\text{AKE}(72) \log(\text{RMRG})$

AKE(72) = average ocean floor radius where jump component stays constant (NWL value 3 NM)

RMRG = uniform random number between 0 and 1.

YNS, YCZ and YBB are the random time correlated (MARKOV) components.

2. SUBROUTINE PFLUCT2 Details

Random numbers from a Gaussian distribution with a $\sigma = 1$ are multiplied by a different constant for each prop. mode.

NS mode FLUC = GRN · AKE(69)

CZ mode FLUC = GRN · AKE(70)

BB mode FLUC = GRN · AKE(74)

CONFIDENTIAL

REVIEW OF BEAM-NOISE FLUCTUATION MODELS

R. C. Cavanagh

(See Volume 1 — Unclassified)

CONFIDENTIAL
(THIS PAGE IS UNCLASSIFIED)

CONFIDENTIAL

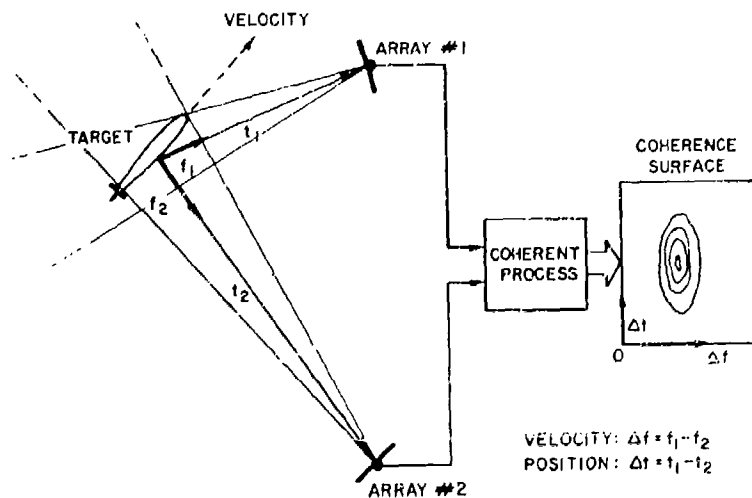
THE EFFECT OF ACOUSTIC FLUCTUATIONS IN THE OCEAN UPON COHERENCE (U)

O. D. Grace
NOSC, San Diego, California

ABSTRACT

(U) The effects of acoustic fluctuations on the coherence function peak value and peak location are discussed. These discussions are elaborated by the results from four sea born experiments in which the effect of acoustic fluctuations upon the coherence function are measured. Possible causes are presented some cases.

(C) Signals that have been received at different SOSUS arrays from a common target have been observed to be correlated. This shows that the ocean does not completely decorrelate the signal over long propagation paths. It also suggests that this property can be exploited to detect, locate and track distant targets at sea. Under the Coherent Multi-Array Processing (CMAP) program at NOSC this concept has been transformed into a working technology. As indicated in Fig. 1 it has been shown that distant targets can be detected using the signals received at two arrays and that these targets can be located and tracked using the differential time delay and Doppler shift of the signals. It has also been found that the performance of this technique has limitations due to acoustic fluctuations in the ocean and it is these limitations that are of interest here.



(C) Figure 1 -- Coherent multiarray processing (CMAP) (U)

CONFIDENTIAL

(C) The algorithms currently under test at NOSC are variants of the coherence function, as opposed to the correlation function, i.e., for the broadband surveillance problem it is more convenient to search for targets in the frequency domain. The algorithms, as shown in Fig. 2, are formulated in terms of an integration of Fourier components over time and an integration of Fourier components over frequency. In both cases a search over time difference and Doppler difference is performed until the coherence peak exceeds a detection threshold. Having detected the target the location of the peak gives the coordinates that are used to locate and track the target.

(C) For the case of coherent signals in stationary Gaussian noise the noise threshold of the coherence function approaches zero as the processing time-bandwidth, TW, product is increased while the signal coherence remains unchanged. This implies that all targets can be detected by increasing TW. Also, for coherent signals in stationary noise the shape of the peak is controlled by the integration time and processing bandwidth. The width of the peak along the Doppler difference axis decreases with increasing integration time while the width of the peak along the time difference axis decreases with increasing processing bandwidth. This implies that all targets can be located and tracked with unbounded precision by increasing TW. In practice, neither effect is observed which implies unsurprisingly,

Coherence Equation

$$\gamma^2(n, \theta) = \frac{\left| \sum_{k=1}^K F_T^*(n, k) F_R(n, k) e^{jk\theta} \right|^2}{\sum_{k=1}^K F_T^*(n, k) F_T(n, k) \sum_{k=1}^K F_R^*(n, k) F_R(n, k)} \quad \begin{array}{l} \text{Integration} \\ \text{over time} \end{array} \quad (1)$$

$$\rho^2(n_d, \tau) = \frac{\left| \sum_{n=1}^{N_s} F_T^*(n) F_R(n + n_d) e^{j2\pi n\tau/N} \right|^2}{\left[\sum_{n=1}^{N_s} F_T(n) F_T^*(n) \right] \left[\sum_{n=1}^{N_s} F_R(n + n_d) F_R^*(n + n_d) \right]} \quad \begin{array}{l} \text{Integration} \\ \text{over frequency} \end{array} \quad (2)$$

where

- N_s = the number of bins in the signal band
- $F_T(n)$ = DFT coefficient for bin n of the transmitted signal
- $F_R(n)$ = DFT coefficient for bin n of the received signal
- N = DFT length in samples
- τ = time delay in samples
- n_d = Doppler shift in bins.

(U) Figure 2 — Coherence equation (U)

CONFIDENTIAL

that the signal radiated by a moving target and received at a distant array is not completely coherent and that the noise is not stationary and Gaussian. We note though, in addition, that if multipath components are present or if the target or medium changes state during the integration time, then multiple peaks may be resolved as the TW product is increased. This may reduce coherence through energy spreading or may produce false peaks or displaced peaks. Since this problem is not directly relevant to the fluctuations problem, we ignore it till later. In the following, as indicated in Fig. 3, we give examples of coherence degradation and random perturbations of the coherence peak location due to medium effects and platform motion. We also discuss the problem of distinguishing between coherence peaks due to fluctuations and those due to multipath.

(U) Mohnkern [1] has examined the problem of degradation of coherence value with increasing integration time and processing bandwidth. His results are summarized in Fig. 4. His data was obtained from an experiment performed by the University of Miami and Woods Hole Oceanographic Institute near Bermuda. A PRN sequence modulated a carrier tone at 312.5 Hz. The clock period was 0.0256 sec, giving the signal a 40 Hz bandwidth, and the sequence length was 3.2768 sec, giving a line separation of 0.3 Hz. Only the side band lines were processed. The signal was transmitted by a source suspended 1100 feet from a moored ship and was received by the TRIDENT array 145 n.mi. away at a depth of 13,700 feet.

(U) The received and transmitted signals were partitioned in time and two sets of Fourier coefficient sequences were generated for each signal having the resolutions 0.019 Hz and 0.076 Hz. The replica coherences between the transmitted and received signals were calculated using both the time integration and frequency integration algorithms. The 0.076 Hz resolution data was integrated over a sequence of time windows in the range of 0.5 min to 128 min. The 0.019 Hz resolution data was integrated over the frequency bands of 5, 10, 20, and 40 Hz.

(U) The results of these calculations are summarized in Fig. 4 as coherence vs TW product. From an examination of these curves, we infer:

1. Increasing the TW product decreases coherence.
2. The rate of decrease of coherence is less than the rate of decrease of the detection threshold.
3. Increasing the integration time decreases the coherence more than increasing the bandwidths.

The latter result implies that the movement of the medium and platform more strongly degrades coherence than multipath energy splitting.

(U) Mohnkern examined the spectrum of the signal phase modulation, which is presented in Fig. 5. This graph shows a -30 dB per octave decay as would be expected for internal waves 2, 3. The effect of small random platform motions is believed to be small as shown in the following experiments.

(C) The degradation of the coherence value due to platform movement has been examined by Sloat [4]. He considered the case of random perturbations about a constant motion and obtained curves for coherence degradation due to the target constant course and speed and also due to the random course and speed fluctuations. He has compared these curves to data and a representative case as shown in Fig. 6.

CONFIDENTIAL

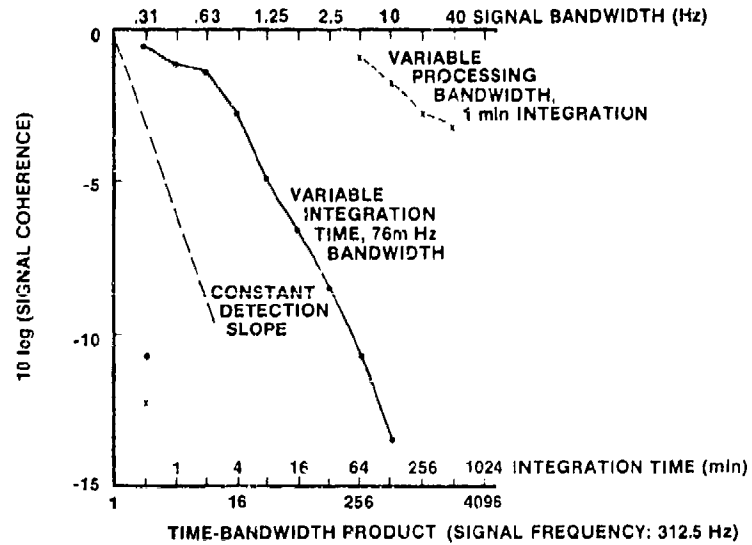
A. Degradation of coherence value

1. Internal waves
2. Platform motion

B. Variation in peak location

C. Separation of fluctuation effect from multiple effects

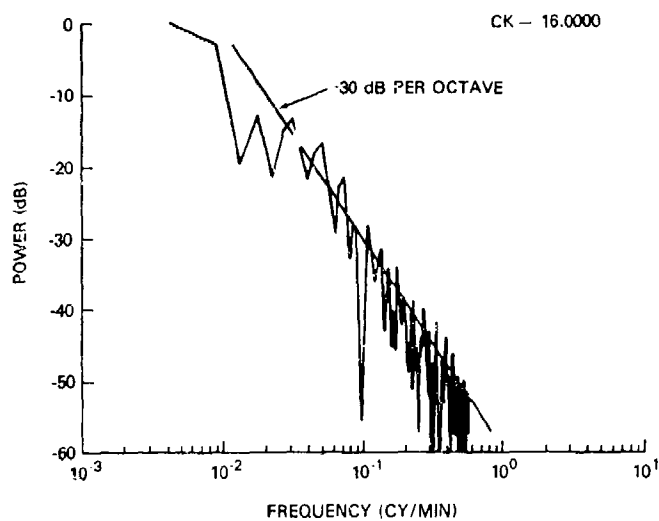
(U) Figure 3 -- Coherence surface fluctuations (U)



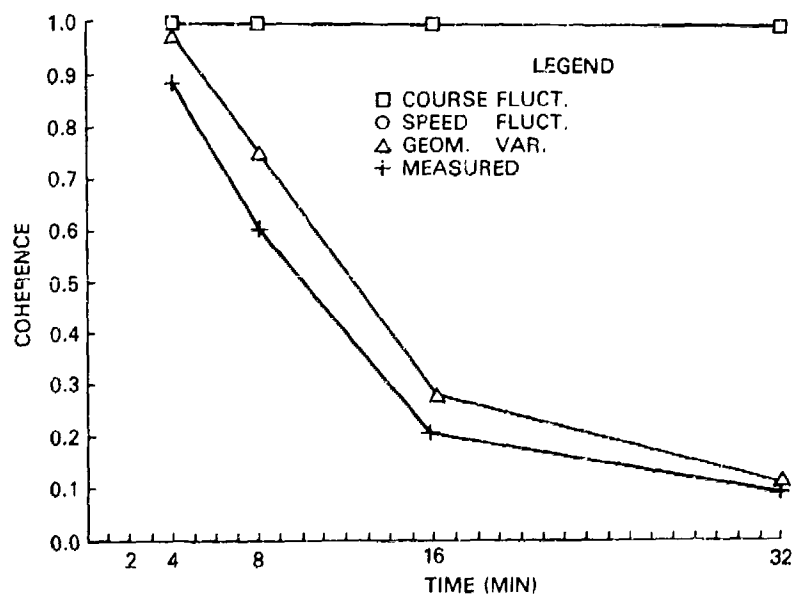
(U) Figure 4 -- Signal coherence vs time-bandwidth product (U)

CONFIDENTIAL

CONFIDENTIAL



(U) Figure 5 — Spectrum of phase fluctuations (U)



(U) Figure 6 — Degradation of coherence (U)

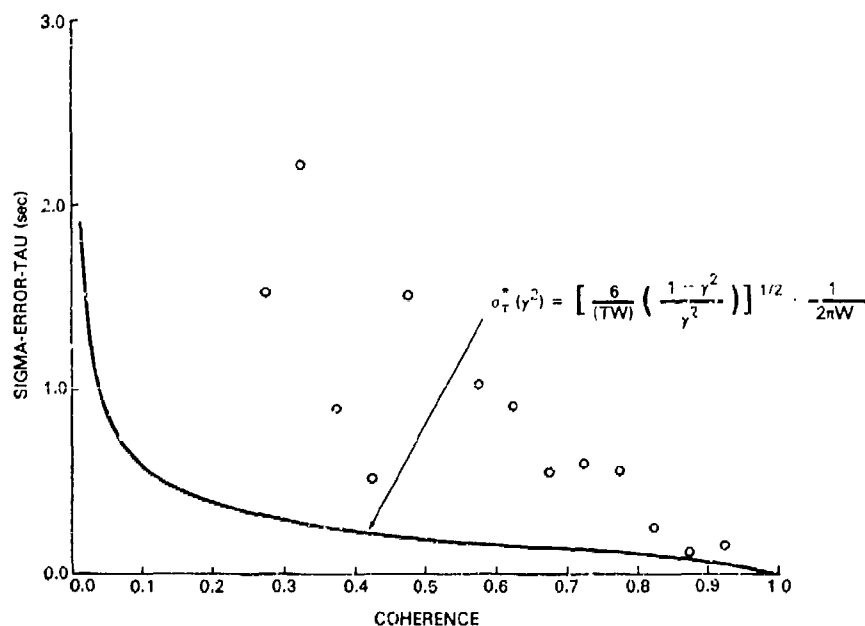
CONFIDENTIAL

CONFIDENTIAL

(C) The data was obtained at the mid-Pacific arrays 1321 and 1322 during SUBICEX 1-75 from the USSN BLUEFISH. The target speed was 15 knts and was closing upon the arrays at the ranges of 40 n.mi. and 100 n.mi. The frequency of interest was the blade line at 12.5 Hz. Sequence of cross coherence surfaces were generated having a processing band of 1/4 Hz and integration times of 2, 4, 8, 16, 32 min. Averages of the coherence values at each integration were obtained and are presented on Fig. 7, along with the theoretical curves. From an examination of these curves, we infer that:

- Random course and speed fluctuations produced a small effect on the coherence values.
- The constant course and speed produced a pronounced effect on the coherence value.
- The consistently lower than predicted measured coherence value implies that medium effects are also contributing to the coherence degradation.

We note also that the first result supports Mohnkern's conclusion that the small random velocity fluctuations of the source contributed a minimal effect on the coherence.



(C) Fig. 7— $\sigma(\hat{\tau} - \tau)$ vs coherence (measured and theoretical lower bound); coherence cells -0.05 for measured data (U)

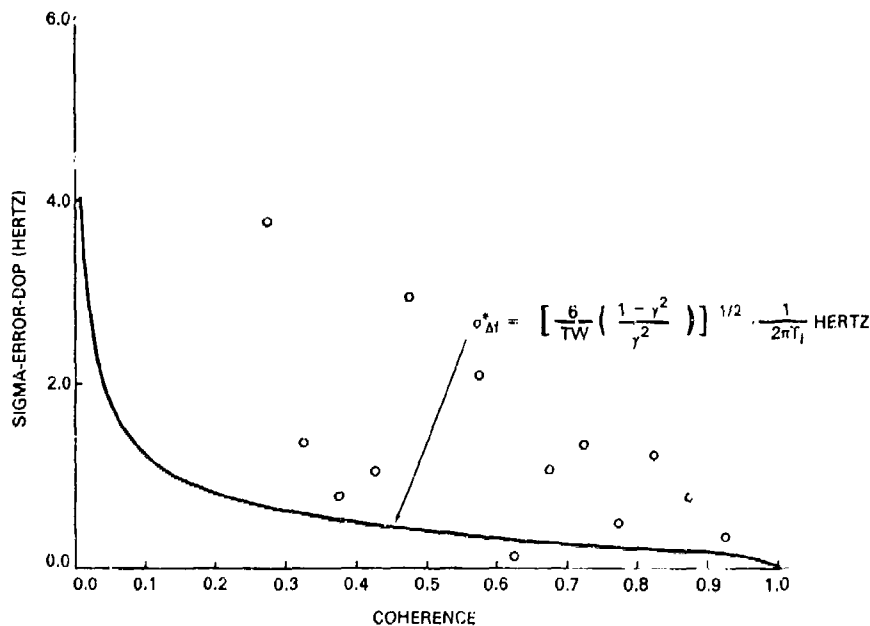
CONFIDENTIAL

(C) In the above, we have seen that both platform motion and the medium can cause coherence degradation. It has also been observed that the coherence peak location is effected by platform motion and the medium.

(C) Barbour [5] has examined the variance of the coherence peak coordinates. He obtained his data from the FME experiment. The source was an HX231F DE Steiguer at depths of 400 feet to 500 feet. The receivers were the mid-Pacific arrays 1322 and 1323. The target to receiver ranges were approximately 800 n.mi., and were opening. The signals were 1/4 Hz bandwidth tones at 44.125 Hz and 43.125 Hz.

(C) A sequence of approximately 60 coherence surfaces were generated having 1/4 Hz processing bandwidth and 2 min integration times. The coherence peak coordinates were measured and corresponding errors were computed from predicted values based upon NAVSAT position fixes, the ship log and the FACT ray trace model. Histograms of the errors vs coherence were generated and the graphs of the error standard deviation vs coherence are shown in Figs. 8 and 9. Also shown on these figures are theoretical curves of the error standard deviation vs coherence. These calculations assume coherent signals in additive stationary Gaussian noise. A comparison of the data to the theory indicates that the standard deviation of the estimate is substantially greater than expected. The exact source of these discrepancies are unknown but they are presumably due to fluctuations in the target speed and course as well as to medium fluctuations.

(C) In the preceding discussions we have ignored the multipath problem. In each case we assumed that a single peak was obtained that was degraded or displaced due to platform motions or to medium fluctuations. In fact multiple peaks are frequently found. These multiple peaks may be due to changes in the motion of the target or medium or may be due to multipath; i.e., increasing the integration time may resolve multipath components in differential Doppler while increasing processing bandwidth may resolve multipath components in differential time delay.



(C) Fig. 8— $\sigma(\hat{\theta} - \theta_{LLS})$ vs coherence (measured and theoretical lower bound); coherence cells—0.05 for measured data (U)

CONFIDENTIAL

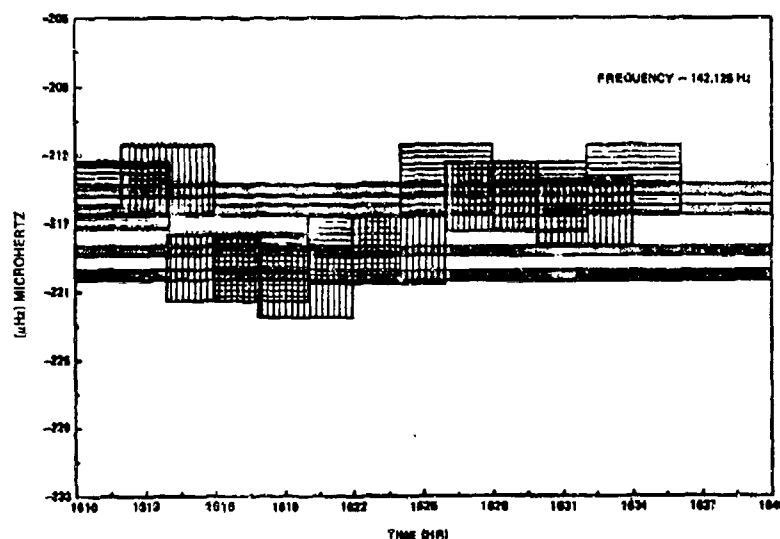


Fig. 9—Time-frequency history of the coherence peaks (Day -252) (U)

(C) Grace [6] has examined the problem of distinguishing between coherence peaks caused by platform motion and those caused by multipath. Using the above mentioned data set [5] he has found that if the platform medium fluctuations are sufficiently slow and if the differential Doppler between multipath components is sufficiently great, these phenomena can be separated. One such case was obtained using a 142.125 Hz line and is shown in Fig. 9. Each rectangle represents an integration time—differential Doppler window. In the absence of target and medium variability, the sequence of short time integration surfaces would have a constant frequency displacement and the long time integration surface would resolve the multipath components. In the presence of target and medium dynamics the short time integration surfaces would have a variable frequency displacement and the interpretation of the long time integration surfaces would be obscured. We conjecture that the data in Fig. 9 represents two multipath components separated by approximately 2 mHz and are radiated by a target having speed variations of approximately 0.1 knt.

(U) In summary, we have seen that the coherence peak value and peak location can be adversely effected by target motion and medium variations. To understand their effects on the CMAP algorithms the standard second order statistics must be known, especially the power and cross power spectrum of the amplitudes and phase modulation induced in the signal by the medium and platform fluctuations.

CONFIDENTIAL

CONFIDENTIAL

REFERENCES

1. Mohnkern, G.L., Measurements of Signal Coherence Near Bermuda, NOSC, San Diego, CA, CMAP Progress Report No. 77-005, Sept. 1977.
2. Jobst, W. and Clark, J., Modulation of Acoustic Phase by Internal-Wave Vertical Velocity, *J. Acoust. Soc. Am.*, 61, 688-93, March 1977.
3. Dyson, F., Munk, W. and Zetler, B., Interpretation of Multipath Scintillations Eleuthera to Bermuda in terms of internal waves and tides, *J. Acoust. Soc. Am.*, 59, 1121-33, May 1976.
4. Sloat, S., Target Motion Effects on Signal Coherence(C), NOSC, San Diego, CA., CMAP Progress Report No. 77-011, Sept. 1977.
5. Barbour, D., Time-Difference and Doppler Difference Errors (C), NOSC San Diego, CA, CMAP Progress Report No. 77-010, Sept. 1977.
6. Grace, O.D., Multipath Recombination (S), NOSC, San Diego, CA, CMAP Progress Report No. 77-001, Sept. 1977.

CONFIDENTIAL

**THE EFFECTS OF FLUCTUATING SIGNALS AND
NOISE ON DETECTION PERFORMANCE**

J. C. Heine and J. R. Nitsche

(See Volume 1 — Unclassified)

CONFIDENTIAL

WORKING FLUCTUATION MODELS WITH APPLICATION TO DETECTION PREDICTION (U)

R. J. Urick
Rockville, Maryland 20850

SIGNAL FLUCTUATION MODEL (U)

(C) Assume that the signal from a distant steady single frequency source consists of two components: a constant, nonfluctuating component plus a random component. Near the source, the former is greater than the latter; at long ranges from the source, the reverse is the case and the signal is completely random. This physical model results in the so-called "Rician" distribution of the received signal amplitude, having as its single parameter, the randomness—defined as the ratio of random to the total power—in the received signal (Ref. 1). Field data observed for a wide variety of conditions (propagation paths, range, frequency and integration time) have been found to obey this distribution. Even the narrow-band noise of a submarine recorded in the Mediterranean with the TASS towed-line array was found to follow the Rician distribution (Ref. 2). Evidently we can predict the fluctuation of signal level—once the randomness is crudely estimated from the propagation conditions—better than we can predict the mean level itself. Cumulative Rician distribution curves are shown in Fig. 1.

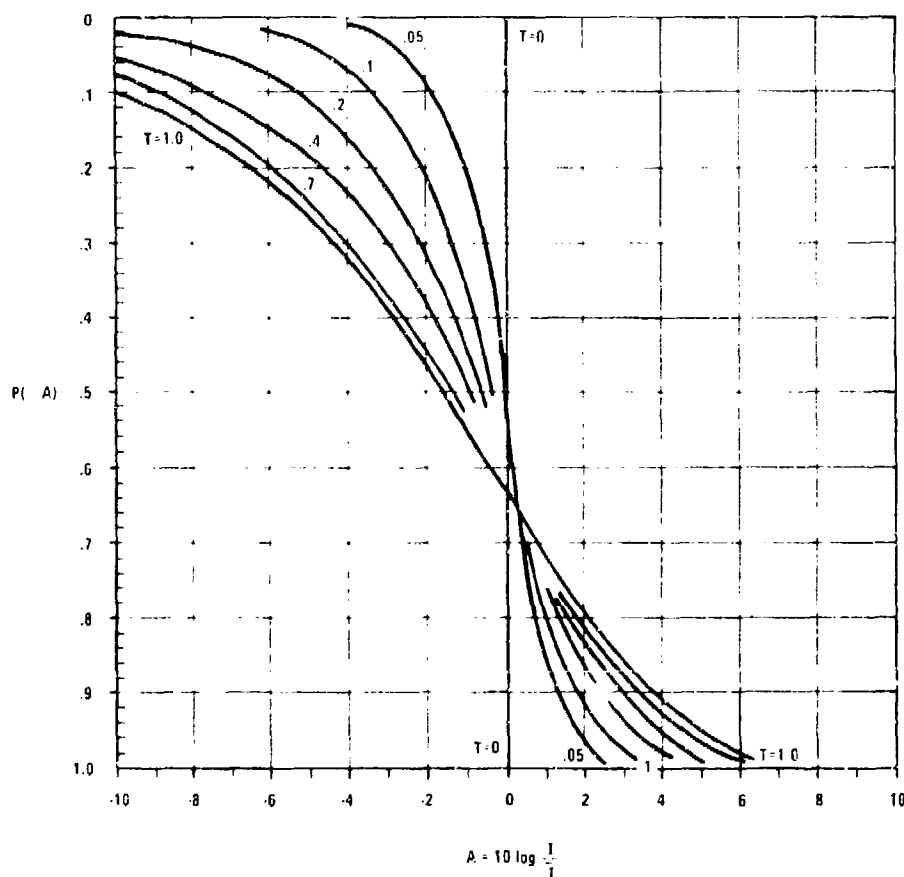
FLUCTUATION TIME SCALE (U)

(U) The other fluctuation parameter—its time scale—has been investigated by an intensive analysis of a two-frequency CW bottom-bounce transmission run (142 and 275 Hz) out to the first CZ recorded on hydrophones at 90 and 300 ft. Fluctuation spectra were found to be similar to those of ocean waves, indicating that the sea surface is responsible for fast fluctuations with periods in the range 2 - 20 seconds (Ref. 3). Slower fluctuations of periods longer than 10 seconds had correlation times tending to increase with range out to the CZ from a fraction of a minute to several minutes—doubtless the rate at which the bottom-bounce multipaths were caused to interfere by the motion of the source (Ref. 4).

NOISE FLUCTUATIONS (U)

(U) On the other hand, while the fluctuations of a sinusoidal signal depend primarily on the ocean medium, the fluctuations of the ambient background depend primarily on the processor employed. Ambient sea noise is known to be often (but not always) Gaussian, and is stationary over periods shorter than those of any significant changes in shipping density and local sea state. For stationary Gaussian noise simple considerations show that samples of the noise power at the output of a conventional processor are chi-square distributed with degrees of freedom equal to twice the bandwidth-time product. Verification of this prediction for integration times from 4 to 64 seconds has been obtained for the

CONFIDENTIAL



(U) Fig. 1—Cumulative distribution curves of the level of a received sinusoidal signal. Vertical scale is the fraction of signal samples equal to or less than the number of decibels relative to the mean, as abscissa. T is the randomness, or fraction of random power in the received signal (Ref. 5). (U)

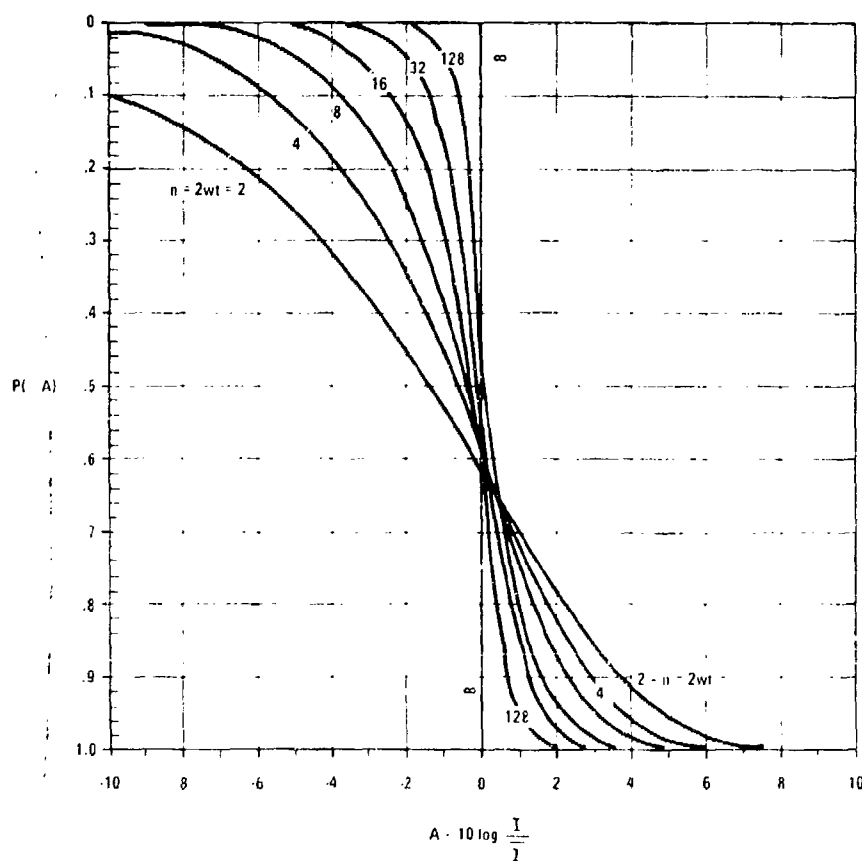
beam noise of a towed array at a frequency of 300 Hz (Ref. 5). Cumulative chi-square distribution curves are shown in Fig. 2.

EFFECT OF FLUCTUATIONS ON DETECTION (U)

(U) A curve of probability of detection against signal excess is known in audition as a transition curve. Transition curves have been obtained theoretically for Rayleigh, amplitude normal signal fluctuations (Ref. 6, Part I). Such curves make possible the ready solution of the sonar equations when predicting detection probability in a fluctuating environment (Ref. 7).

CONFIDENTIAL

CONFIDENTIAL



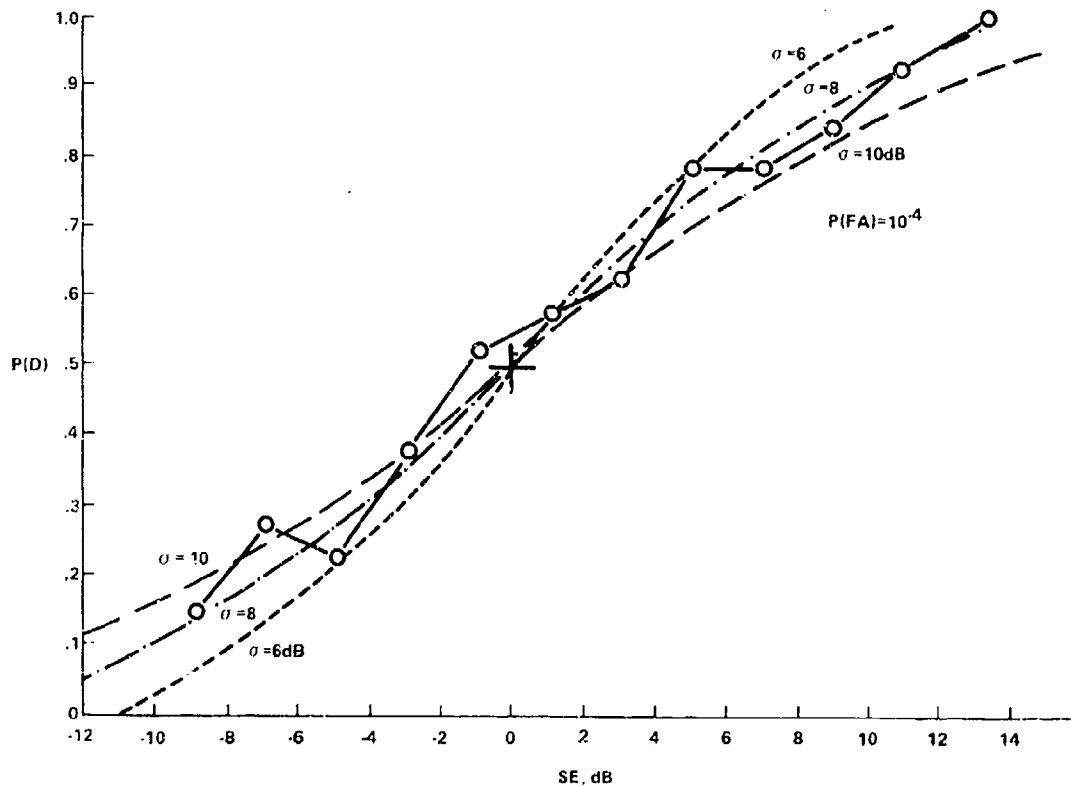
(U) Fig. 2—Cumulative distribution curve of the level of Gaussian noise at the output of a processor of bandwidth w and integration time t (Ref. 5) (U)

THE REAL WORLD (U)

(C) The 64-dollar question now is what fluctuation model best represents the real world. To answer this question, the results of seven different field exercises were examined (Ref. 6, Part II). Included in the survey was a SHAREM exercise involving AN/SQS-23 echo-ranging, a Fixwex exercise involving 142 and 152 Hz one-way transmission out to the first CZ, and AN/SQS-26 echo ranging data. The resulting transition curves, when averaged together, show that the log-normal distribution, with a σ between 6 and 8 db, applies to this sampling of real detection data (Fig. 3).

(C) The physically unreasonable log-normal distribution is doubtless the result of the Central Limit Theorem applied to the product of the (more-or-less) independently quantities occurring in the sonar equations.

CONFIDENTIAL



(C) Fig. 3—Composite plot of detection probability $p(D)$ signal excess $S(E)$ from the examples. The plotted points are averages in 2-dB intervals (Ref. 6). (C)

SUMMARY (U)

(C) Field-data-verified models have been obtained for the amplitude fluctuations of CW signals and ambient noise. Similar models appear not to exist as yet for the other quantities in the sonar equation. However, when everything is put together in terms of detection results, the fluctuation of the signal-to-noise ratio (or signal excess) appears to be log-normal in consequence of the Central Limit Theorem.

(C) This result—the normality of db's—is a convenient one for performance modelling, and has been widely used for many years (Ref. 8) to explain the results of sonar fleet exercises.

REFERENCES (U)

1. R.J. Urick, A Statistical Model for the Fluctuation of Sound Transmission in the Sea, Naval Surface Weapons Center Report TR 75-18, 1975.
2. R.J. Urick and R.H. Kirklin, Fluctuations of Submarine Signals and Narrow-Band Noise in a Towed Line Array, Tracor Contract N00019-76-C-0508, March 1977 (Confidential).

CONFIDENTIAL

CONFIDENTIAL

3. R.J. Urick, Fluctuation Spectra of Signals Transmitted in the Sea and Their Meaning for Signal Detectability, Naval Ordnance Laboratory Report NOLTR 74-156, 1974.
4. R.J. Urick, Time-Scale of the Fluctuation of a Bottom Bounce Narrow-Band Signal from a Moving Source in the Sea, NSWC TR 75-83, 1975.
5. R.J. Urick, Models for the Amplitude Fluctuations of Narrow-Band Signals and Noise in the Sea, Journal Acoustical Society of America 62, 878, 1977.
6. R.J. Urick, Signal Excess and Detection Probability of Fluctuating Sonar Signals in Noise, Part I: Theoretical Models (Unclass), Part II: Field Data (Confidential), *USN/JUA* 27, 569, July 1977.
7. R.J. Urick, Solving the Sonar Equations with Fluctuating Signals in Noise, Proceedings 1977 IEEE Conference on Acoustics, Speech and Signal Processing, May 1977.
8. T.G. Bell, Comparisons of Target Detection Results with Expectations Based on USL Range Prediction Methods, Underwater Sound Lab, Report 576, 1963.

CONFIDENTIAL

SIGNAL FLUCTUATIONS (U)

K. D. Flowers

Naval Research Laboratory, Washington, D.C. 20375

(U) We have previously presented fluctuation models for signals and noise applicable to long range, deep water, passive surveillance systems. These models are to be published in the July issue of the Journal of Underwater Acoustics, and a user manual will be published shortly as an NRL report.

(U) What I would like to discuss today in addition to these models are some of the characteristics of signals that we have measured but have insufficient data to model.

(U) For long range passive surveillance we adopt the point of view that only the gross features of the environment are known and the location of the target is only approximate. Thus we consider the problem as a statistical one.

(U) From Fig. 1 what we would like to know is the probability distribution of the acoustic signal at a receiver R due to a source S at range r and frequency F . We also require the nature of the field in three orthogonal directions at the receiver which we characterize with the correlation distances in depth, along the transmission direction, and transverse to the transmission direction.

(U) Knowledge of these quantities aids in the determination as to what type of system should be deployed and how well it will operate at a given location. Unfortunately, this information is not readily obtained because the medium in which we operate is inhomogeneous and anisotropic. I don't refer here only to the inhomogeneity or anisotropy in the water column itself but also that due to the presence of boundaries and in particular the ocean bottom.

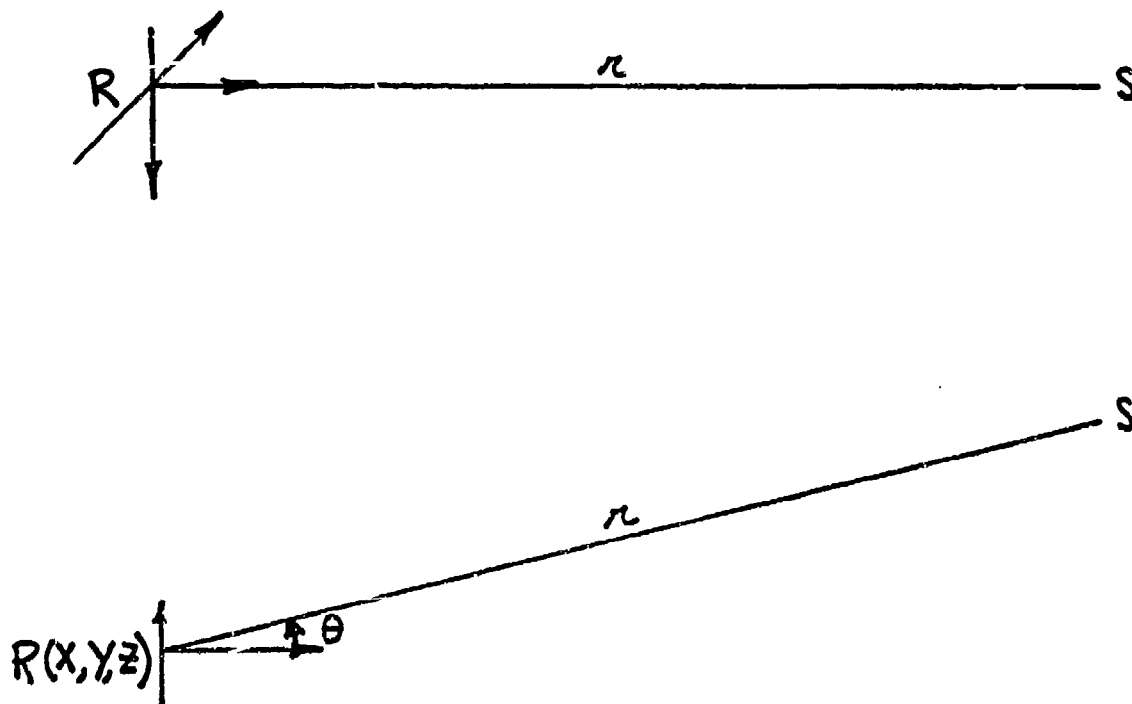
(U) Therefore, in general, the distribution of signal level is a function of direction and absolute position as well as range and frequency. The correlation distances are similarly affected.

(U) However there appears to be a way around this problem. In Fig. 2 we found that by removing the average signal level from our data we could determine the probability distribution of the fluctuation about the mean. This distribution was independent of receiver position and direction. It remained a function of frequency and an easily modeled function of range.

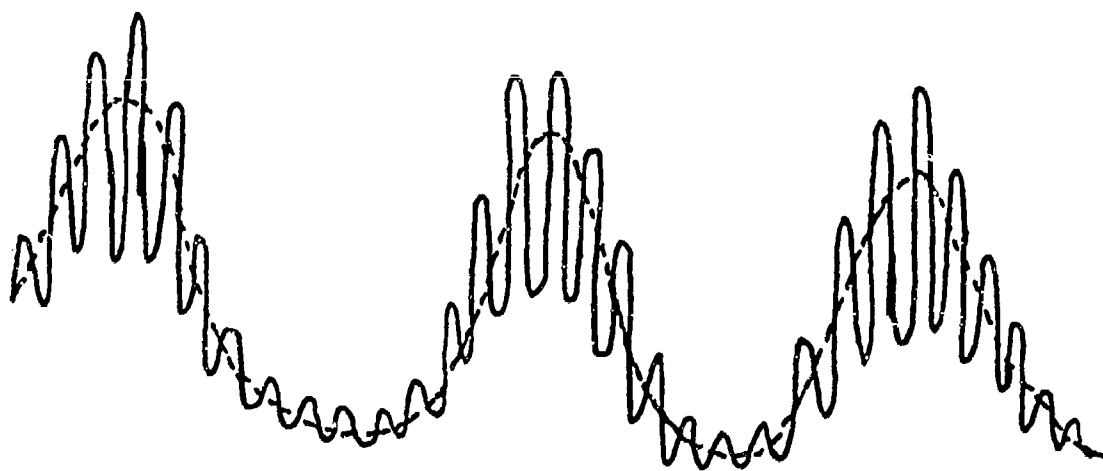
(U) So the problem reduces to the determination of the average signal level for each possible source-receiver geometry. Fortunately with only a few environmental inputs the average can be computed using ray tracing, normal mode models, or by using the parabolic equation method. That is, we need only the average sound speed profile and major variations to it, such as the existence of a front along the propagation path, and the existence of topographic blockage such as a seamount.

CONFIDENTIAL

CONFIDENTIAL



(U) Figure 1 - Geometry (U)



(U) Figure 2 - Typical signal fluctuation and average representation (U)

CONFIDENTIAL

(U) The range dependence of the fluctuation models is small and linear. Models for only two frequency regions have been determined ~ 10 Hz and frequencies greater than 100 Hz. The single model for frequencies greater than 100 Hz arises from the fact that the field is well represented at these frequencies by ray tracing.

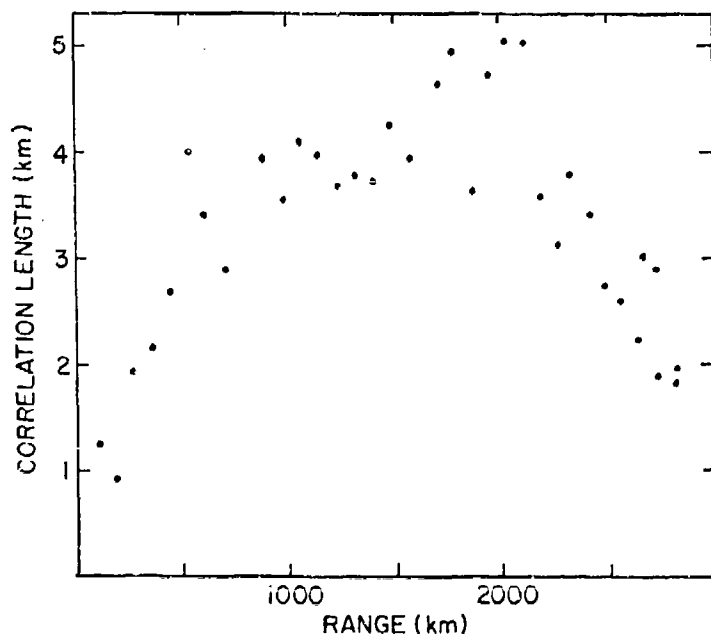
(U) It has been shown that these fluctuation models can be determined from the same propagation models that we used to determine the average signal level. Thus models should be available for any range and frequency.

(U) The models generally give the not unexpected result that the rms fluctuation is directly proportional to the average signal level, although the shape of the distribution is determined by a higher order moment.

(U) Although these models were developed for signals propagated to long ranges in the deep ocean, we feel they may be more generally applicable. At least it is hoped that the method is generally applicable and that models could be constructed for shorter ranges and shallow water.

(U) The radial correlation of the acoustic field, i.e., the correlation length of the field along the line connecting source and receiver turns out to be a little more complicated but easily understood.

(C) Figure 3 shows the measured correlation length of a 10 Hz acoustic field as a function of range for a specific bottom mounted receiver. The increasing correlation length with range is attributed to the decreasing influence of bottom interacting modes and the leveling off due to the stabilization of the number of modes. The decrease at long ranges is due to these modes losing their ordered phase.



(C) Figure 3 -- Measured correlation lengths for long ranges at 10 Hz (U)

CONFIDENTIAL

(U) For high frequencies (greater than 100 Hz) bottom interacting modes are rapidly attenuated and for these ranges we only see a slowly decreasing radial correlation length with range.

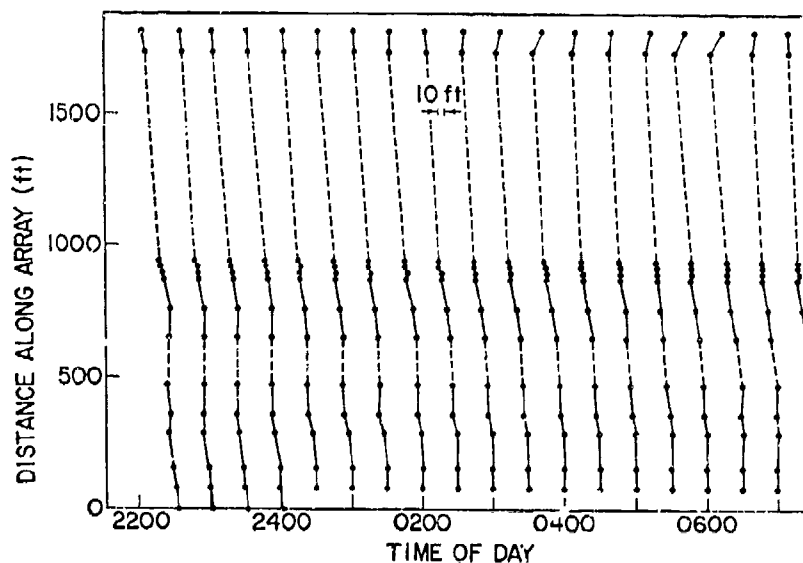
(U) As expected, the field correlation in the radial direction is controlled by the modes present and their phase relationship. One should be able to model this quantity for any given situation.

(U) NOTE TWO THINGS: (1) This is a radial correlation length of the fluctuation and not of the total acoustic field, and (2) receiver depth is not important in these models, only the water depth along the propagation path

(U) Acoustic field correlations in directions orthogonal to the propagation paths are more difficult to obtain. It is felt that correlation in the depth direction is relatively short (a couple of wavelengths) and the horizontal transverse correlation distance is quite large (many wavelengths). We have no information on correlation in depth and only a small amount on the transverse correlation.

(C) We have measured signal phase differences across existing bottom mounted arrays for low frequencies. The possible correlation lengths measurable are short, ranging from 3 to 7 wavelengths. Since we are observing such a small increment of the acoustic field we construct the constant phase wave fronts of the field, test them for linearity, and construct normals to them. For example in Fig. 4 there are measured wavefronts at an array where the source was fixed approximately 200 nm away.

(U) If the wavefronts are highly linear we consider the field perfectly correlated over the observed aperture. The normals to these wavefronts are the bearings to the target as observed by the array. By knowing the exact bearing to the target, target bearing errors can be constructed.



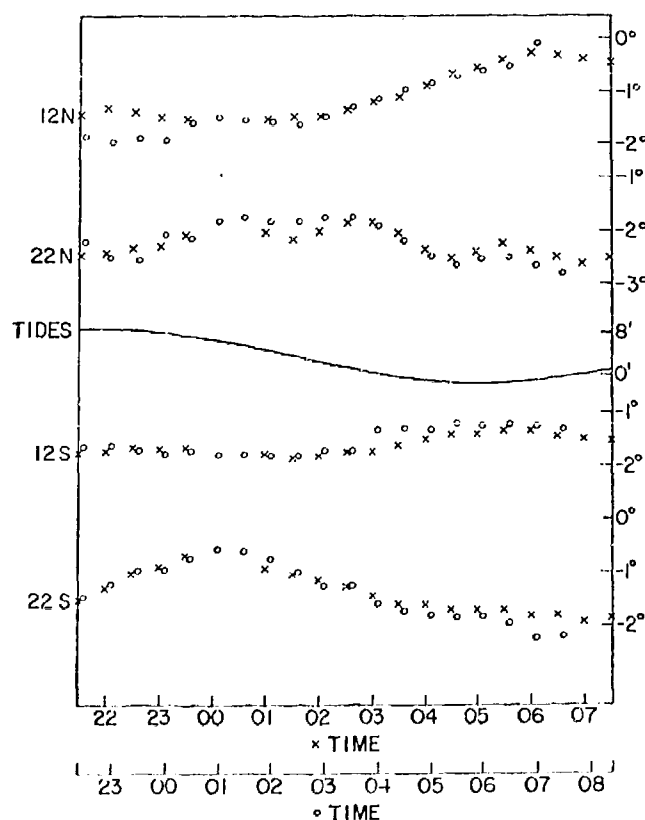
(C) Figure 4 -- Measured wavefronts at a bottom array for a 22 Hz source at 200 nm (U)

CONFIDENTIAL

(U) In Fig. 5 is an example of how the bearing error can change with time. Both source and receiver are fixed. Shown are simultaneous results at two arrays (N and S) for two frequencies. Thus even for a "good" case target bearings fluctuate. Here it is felt that the effect of medium variations are enhanced by bottom interactions to produce these variations.

(U) We see in Fig. 6 that a low frequency source was towed along a track crossing in front of an array (B) at about 400 nm. The bearing ϕ of the source varied over a range of 120° . Note the existence of a seamount at point A. The measured bearing using the above technique deviated from the actual bearing by the amount shown in Fig. 7. Here Ω is the relative amplitude of the received signal, θ is the bearing error, σ_θ is the slope error in fitting a straight line to the wavefronts, and σ_y is the rms deviation of the measured phase from the straight line fit.

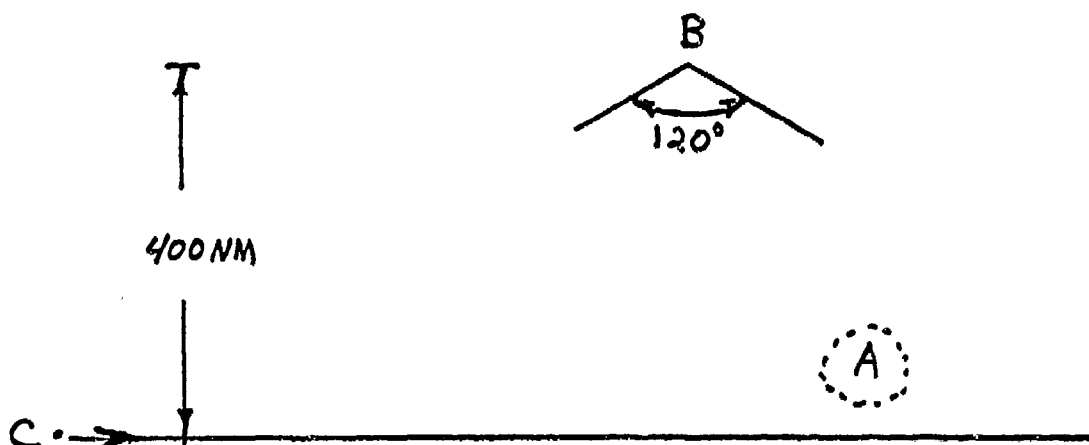
(C) As expected, when the signal is low the wavefront becomes rougher but signal level alone is not the only factor. At point A is where the source went behind the seamount noted in the last figure. The *signal-to-noise ratio* is still good but the loss of the unobstructed RSR propagation results in poor transverse spatial coherence. Note that this effect applies equally to receivers fixed on the bottom, suspended, or towed.



(C) Figure 5 - Deviation in apparent direction of sources for two consecutive days (o and x). The time scales for the data have been shifted (50 min.) with respect to each other in order to align the shift in tidal cycle for the 2 days. The tidal prediction for Graylands Washington is shown as a solid line in the center of the figure (U).

(C) Figure 5

CONFIDENTIAL



(U) Figure 6 — Tow track geometry (U)

(U) We note that with the possibility of removing this nearly linear trend from the data that a reasonably high bearing accuracy is obtainable by observing wavefronts with short arrays.

(U) On the other hand, when the source is observed by an array at a location as in Fig. 8, the wavefronts are not as consistent as in the previous case. A particularly interesting effect is observed when the source is in this region where convergence zone structure may be seen in the received signal. Figure 9 shows the received amplitude as the source is towed through a convergence zone. The first part of the zone is attributed to deep cycling RR and the second part corresponds to RSR propagation paths. Note the behavior of the bearing error for these different propagation conditions. I am not aware of any model which predicts any such wavefront behavior.

(U) Note however, that the bearing error remains relatively constant for the majority of the time.

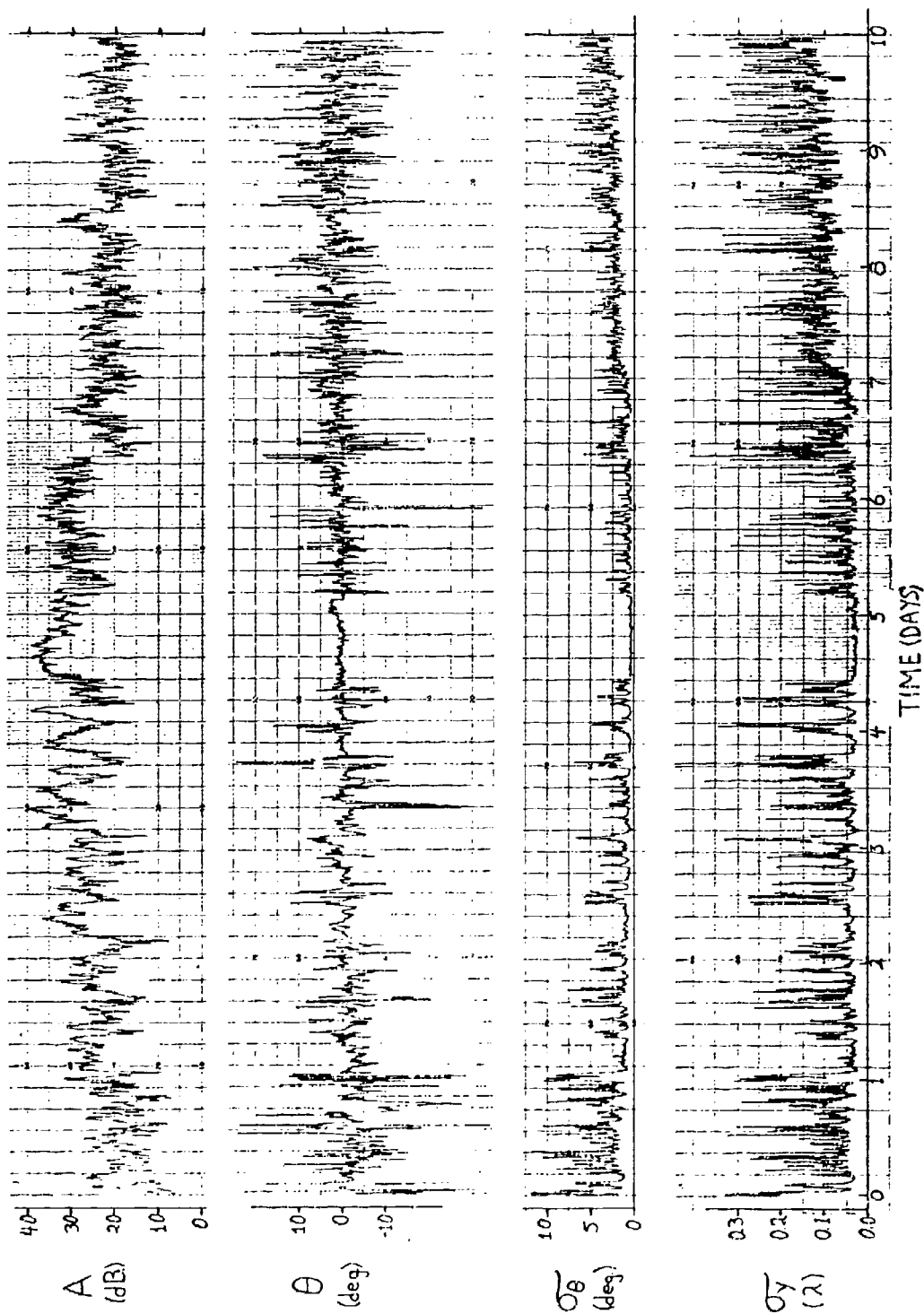
(U) On one array no observable wavefronts were present.

(C) The deep sound speed profiles associated with these measurements and approximate depth and local sea floor slopes at the arrays are illustrated in Fig. 10. At points A, B, E, and for the most part C, near perfect correlation was observed over the length of the arrays. At point D however, despite good signal to noise no coherent wavefronts were observed. For one experiment the propagation path was in shallow water for a considerable distance which we feel would produce the observed results. For the other experiment the slope dropped rapidly, but this was a stationary source experiment so the RSR path may not have directly connected the source and receiver for this case.

(U) Restricting ourselves to long range, deep water, passive surveillance requirements, we have presented data in support of the following:

- (1) Existing propagation models are capable of providing the required signal fluctuation statistics.

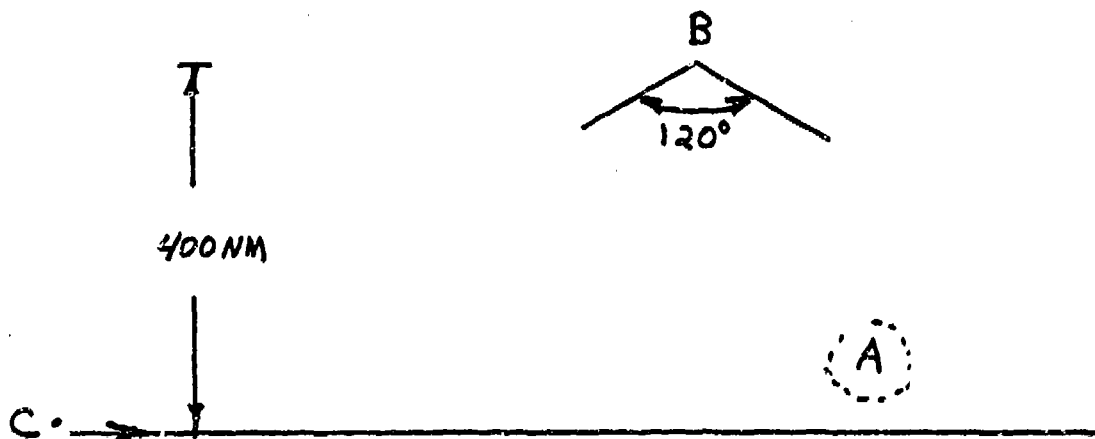
CONFIDENTIAL



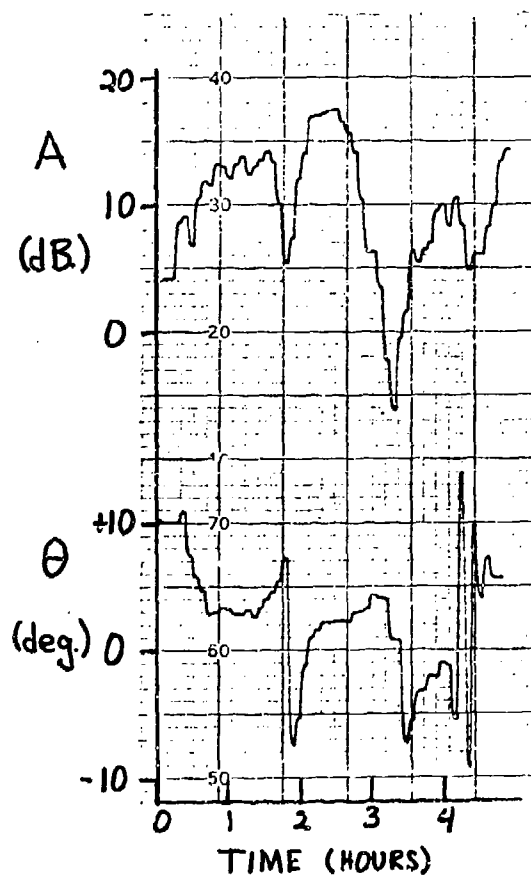
(C) Figure 7 — Bearing error related to array received signal levels waveform slope (data sampled once every 8 min.) (U)

CONFIDENTIAL

CONFIDENTIAL

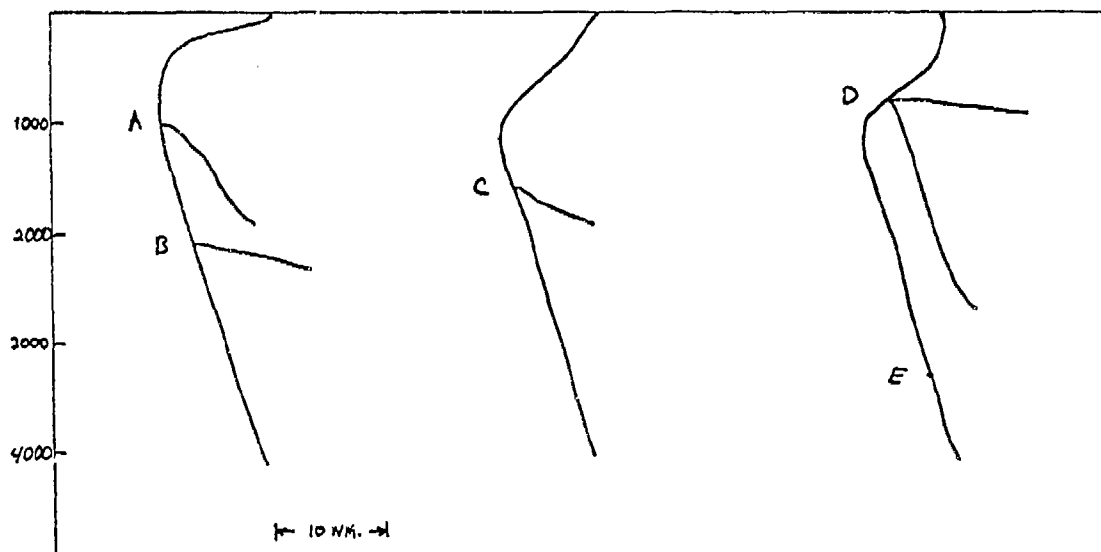


(U) Figure 8 — Tow track geometry (U)



(U) Figure 9 — Bearing error within a convergence zone (U)

CONFIDENTIAL



(C) Figure 10 — Sound speed and bathymetry at selected sites (U)

- (2) That topographic interference anywhere along the propagation path will affect equally receivers that are bottom mounted, suspended, or towed.

and finally,

- (3) That for low frequencies, properly positioned bottom mounted arrays are operating in nearly perfect plane wave fields. However, the orientation of these fields vary and these variations are not completely understood.

CONFIDENTIAL

CONFIDENTIAL

**NUMERICAL MODELS OF ACOUSTIC PROPAGATION
THROUGH INTERNAL WAVES**

H. A. DeFerrari and R. Leung

(See Volume 1 — Unclassified)

CONFIDENTIAL

SINGLE PATH-PHASE AND AMPLITUDE FLUCTUATIONS

T. E. Ewart

(See Volume 1 -- Unclassified)

CONFIDENTIAL
(THIS PAGE IS UNCLASSIFIED)

CONFIDENTIAL

PREDICTION OF DETECTION PERFORMANCE

M. Moll

(See Volume 1 — Unclassified)

CONFIDENTIAL

ACOUSTIC FLUCTUATION MODELING FOR SYSTEM PERFORMANCE ESTIMATES

R. C. Cavanagh

(See Volume 1 — Unclassified)

CONFIDENTIAL
(THIS PAGE IS UNCLASSIFIED)

CONFIDENTIAL

BEAM OUTPUT FLUCTUATIONS ON TWO TOWED ARRAYS* (U)

Andrew G. Fabula
NOSC Code 5311

INTRODUCTION

(C) During the recent Bearing Stake exercise (Ref. 1), two towed arrays, called OAMS and LATA, simultaneously received CW signals from a towed source. The characteristics of the two arrays are described in Ref. 1. An hour of beam output recordings on both arrays was obtained incidentally to propagation loss and intra-array coherence measurements (Ref. 2). The recorded data are being used to investigate the effectiveness of coherent multi-array processing for two towed arrays (Mobile/Mobile CMAP). As an important part of that work, the characteristics of the beam output signal at each array have been investigated.

(C) Figure 1 shows the area and geometry of the experiment. The Mk 6 source was towed by the USNS KINGSPORT. Approximate parameters for 1700Z, 13 Apr 1977 were as follows:

	Mk 6	OAMS	LATA
Depth (m)	80	200	300
Speed (knots)	9.9	2.8	2.3
Track heading ($^{\circ}$ T)	211	133	239
Source range (naut. miles)	--	170	370
Source bearing ($^{\circ}$ T)	--	221	313
Source aspect ($^{\circ}$)	--	170	78
Source relative bearing ($^{\circ}$)†	--	76	74

The inter-array aperture angle is 92° , and the source track heading is at 124° to the bisector of that angle. Because of the aspect angles, the doppler shift at LATA is more sensitive to source heading perturbations, while the doppler shift at OAMS is more sensitive to source speed changes. For both arrays, the source is about 15° forward of broadside.

*See also NOSC TR294 "A Mobile-Mobile CMAP Experiment," A.G. Fabula, Aug. 78 (Confidential)
† 0° = front endfire.

CONFIDENTIAL

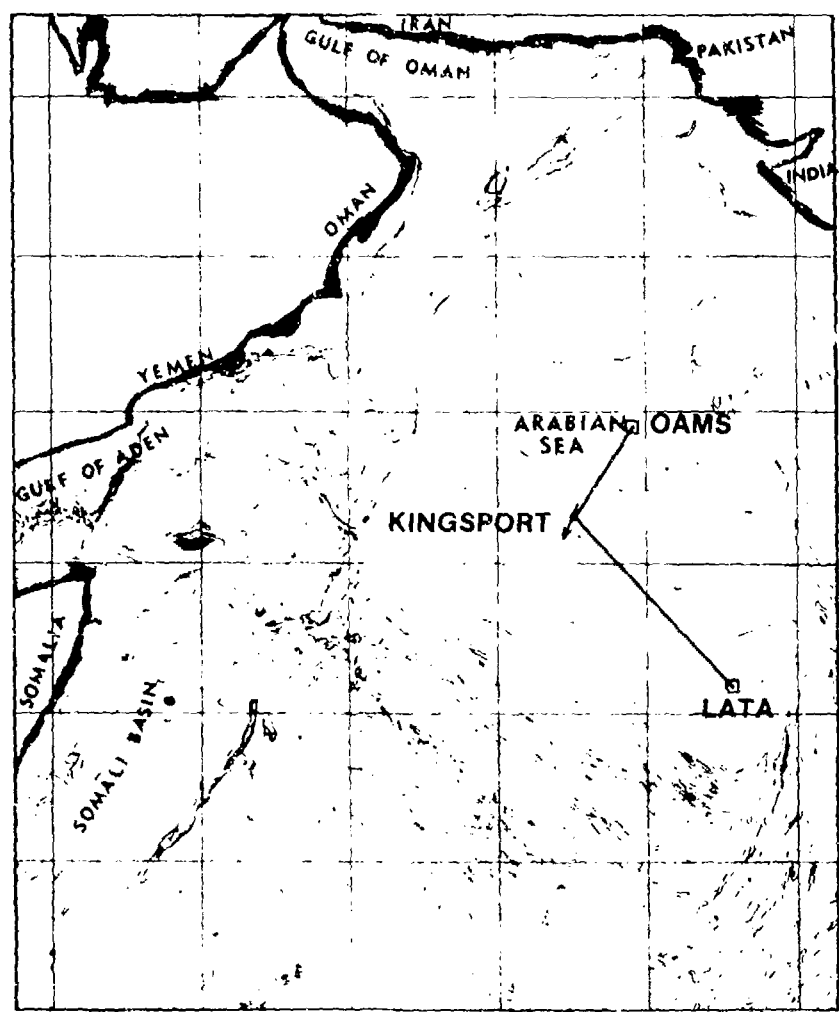


Figure 1. (C) Mobile/Mobile CMAP Experiment Geometry. (U)

(C) According to the pre-exercise ray trace predictions (Ref. 3), the important propagation paths interact with the bottom at low grazing angles (the source is above the bottom conjugate depth; the receivers are below). Due to thick bottom sediment of the Indus Fan, the low frequency bottom reflection loss at low angles is very low, and the source was received at both arrays at high signal-to-noise ratio.

CONFIDENTIAL

CONFIDENTIAL

(C) The LATA hydrophone outputs were digitized at 512 Hz and recorded at sea and later beamformed digitally. Digital anti-alias filtering was done before sub-sampling to produce the LATA beam data sampled at 128 Hz for this work. The OAMS beamforming and analogue recording was done at sea. The simultaneously recorded time code 1 kHz carrier was used to command the analogue-to-digital conversion at 125 Hz. In this way the effects of tape speed fluctuations were eliminated. Figure 2 summarizes the FFT and DFT processing for CMAP analysis for 1/4 Hz bin width.

LATA:

- 128 Hz sampling available
- 512 point FFT s, $\frac{1}{4}$ Hz bin width
- For 75% overlap, shift 128 points

OAMS:

- 125 Hz sampling to be synchronized by time code carrier divided by 8
- 500 point DFT s, $\frac{1}{4}$ Hz bin width
- For 75% overlap, shift 125 points

Figure 2. (C) Mobile/Mobile CMAP inputs. (U)

CMAP RESULTS

(C) Only preliminary CMAP results are available so far. Due to the narrow bandwidth of the Mk 6 signal and its frequency switching, a mixture of narrowband and wideband analysis has been used, as in Figure 3. The narrowband results showed coherence ridges with peaks as high as 0.9. The wideband results for OAMS Beam 7 and LATA Beam 8 and four successive frequency switch events were as follows:

Event	Max. Coherence	Tau(s)
1	.76	290.0
2	.69	296.1
3	.93	295.9
4	.62	287.6

The scatter in tau is not consistent with the known track geometry which implies a monotonic decrease of tau. In order to study the cause of such scatter in CMAP results, the fluctuations of the signals received at each array have been studied in detail.

CONFIDENTIAL

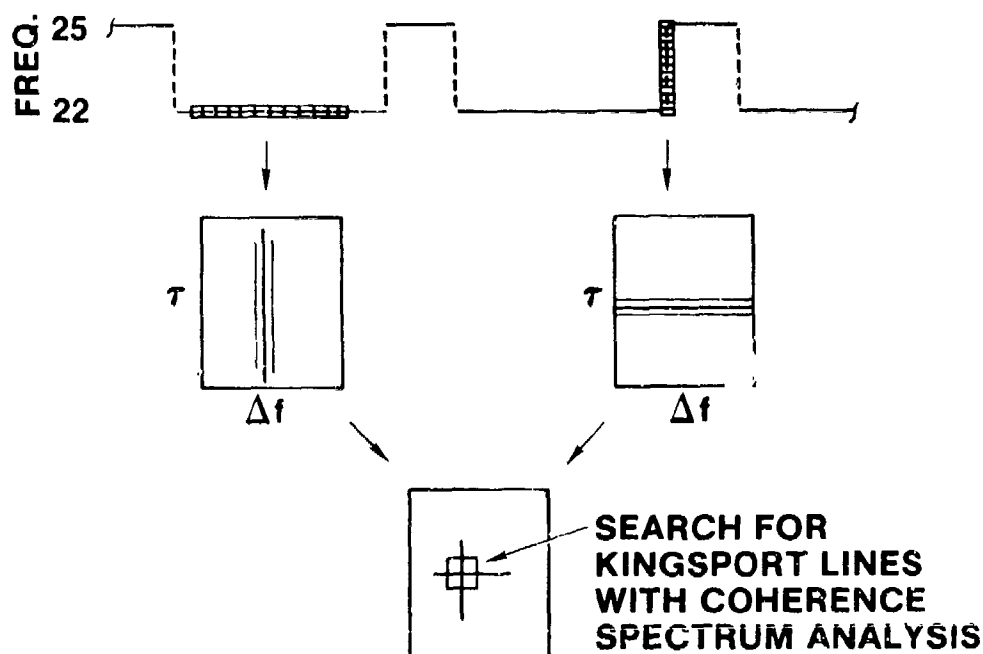


Figure 3. (C) Plan for Mobile/Mobile CMAP analysis. (U)

BEAM SURVEY

(C) Figure 4 is a 20-minute survey of sixteen LATA beams 1° apart in look angle. For two sets of FFT bins each containing one of the projector frequencies (22 or 25 Hz), the loudest bin-beam pair has been found for each independent FFT (4 seconds block length and separation). For each FFT, the three plots of Figure 4 give the following:

- | | | |
|-------------|---|--|
| top plot | — | bin numbers for the two loudest bin-beam pairs |
| middle plot | — | beam numbers for those same pairs, with the loudest beam for the signal emphasized |
| bottom plot | — | relative levels for those same pairs |

The projector switching action is seen in the top plot. Although the projector switches frequency abruptly, there is considerable overlap in the top plot, apparently due to the spread of multipath travel times. The middle plot shows loudest beam drift and "jumping" due to

CONFIDENTIAL

CONFIDENTIAL

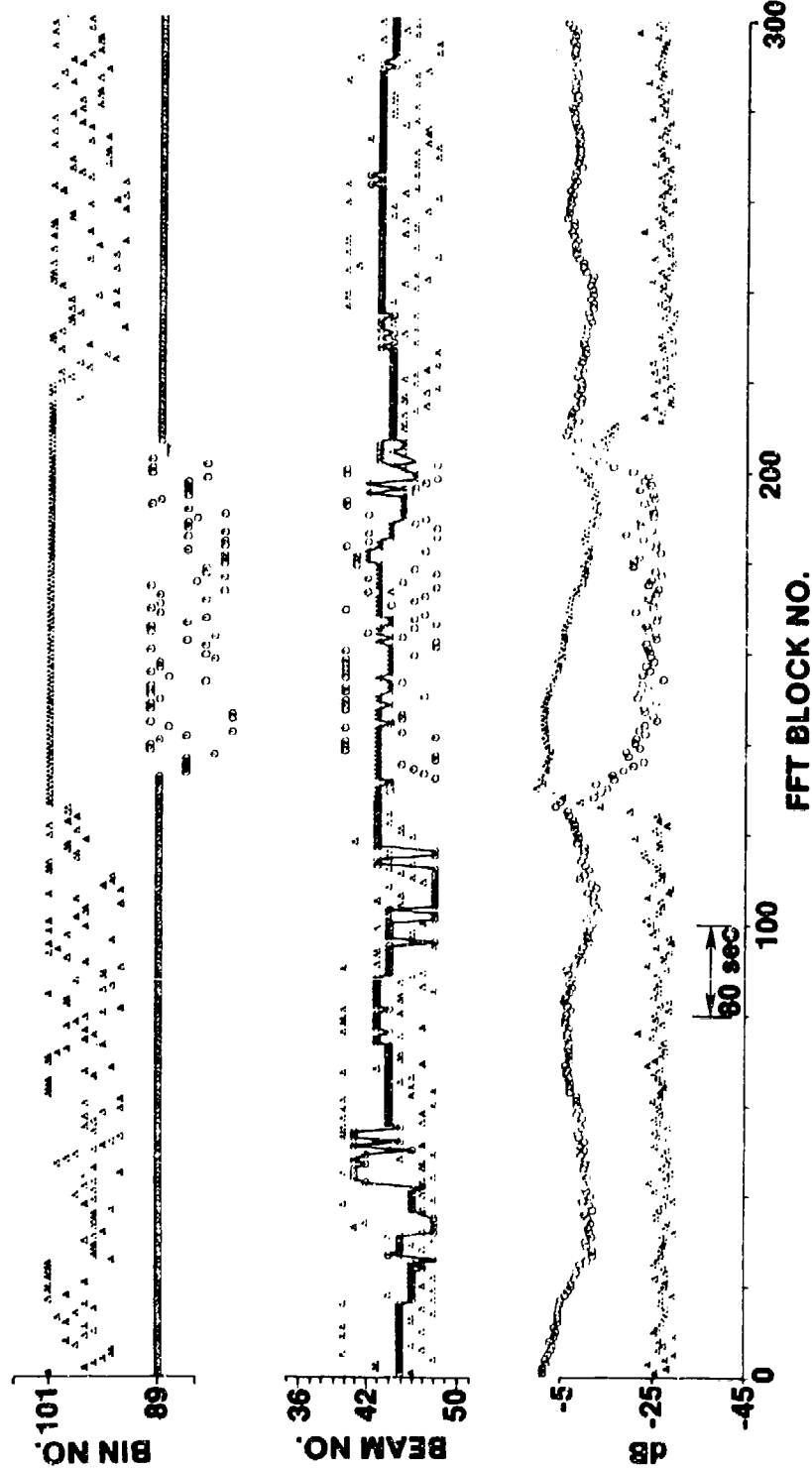


Figure 4. (U) Survey of LATA Beams for 1710 - 1730Z, 13 April 77. (U)

CONFIDENTIAL

(C) multipath interference and (possibly) array meander. The jumping is as much as 7° in 4 seconds. Whenever beam jumping is intense, the bottom plot shows slow fading of the loudest beam with 5-10 dB level reduction and time scale of about 100 seconds. Because the towing conditions were very good for the experiment, it seems likely that such rapid beam jumping is not due to array meander but is due to changing multipath interference. The observed time scale of about 100 seconds for the major amplitude fluctuations is of the same order as the aperture length divided by a predicted trace speed of sound field structure as discussed later.

(C) Beam jumping is presumably mainly due to multipath interference between paths with different vertical arrival angles. While one might think that the amount of jumping is limited by the spread in vertical arrival angles, these data clearly show otherwise. For example in the present case, with a horizontal array with a horizontal arrival at 74° from end-fire, a shift to a vertical arrival angle to $\pm 20^\circ$ would move the loudest beam from 74° to 75° ; a shift of vertical arrival to $\pm 40^\circ$ would give only 74° to 78° . Arrival angles of $\pm 40^\circ$ are unreasonable at the range involved in this case, so that the beam jumping seen in Figure 4 cannot be explained by vertical arrival angle only. Instead one must consider how the interference pattern across the array can cause the loudest beam to not match any of the actual arrivals (Ref. 4, 5). The case of beam "nulls" discussed later is an example of related behavior.

AMPLITUDE AND PHASE FLUCTUATIONS

(U) The high SNR of the loudest beam outputs (typically over 20 dB in the source bin) allows direct examination of the phase stability of the received signal on each array. Doppler shift of both signals can be measured and continuous doppler difference can be measured.

(U) Figure 5 is an example of such data for LATA Beam 44 giving the FFT relative amplitude in decibels and $\Delta\theta$, the increment of FFT argument from block to block, i.e., in one second. At the start of the figure, the projector is on 22 Hz and later it switches to 25 Hz so that temporal characteristics of both signal-plus-noise and noise are seen. (Note that a steady $\Delta\theta$ of $+8^\circ$ corresponds to a doppler shift of $8/360 = +.022$ Hz.)

(C) The "null" or sharp amplitude fade on Beam 44 seen in Figure 5 is clearly due to a multipath interference pattern, with a phase jump, which moved across the array. Such patterns were frequently seen on the hydrophone signals in the at-sea coherence analysis. The beam phase jump corresponding to the beam null is seen more clearly in Figure 6, where $\Sigma\Delta\theta$ is the accumulation of the $\Delta\theta$ values, thereby giving the residual total phase of the received signal. In Figure 6, $\Sigma\Delta\theta$ is given also for Beam 43. (The two sets of $\Sigma\Delta\theta$ values were arbitrarily aligned at the start of the time period for the plot.) Thus a 1° change in beam look angle eliminates the phase jump. (The accompanying amplitude null is also smoothed over.)

CONFIDENTIAL

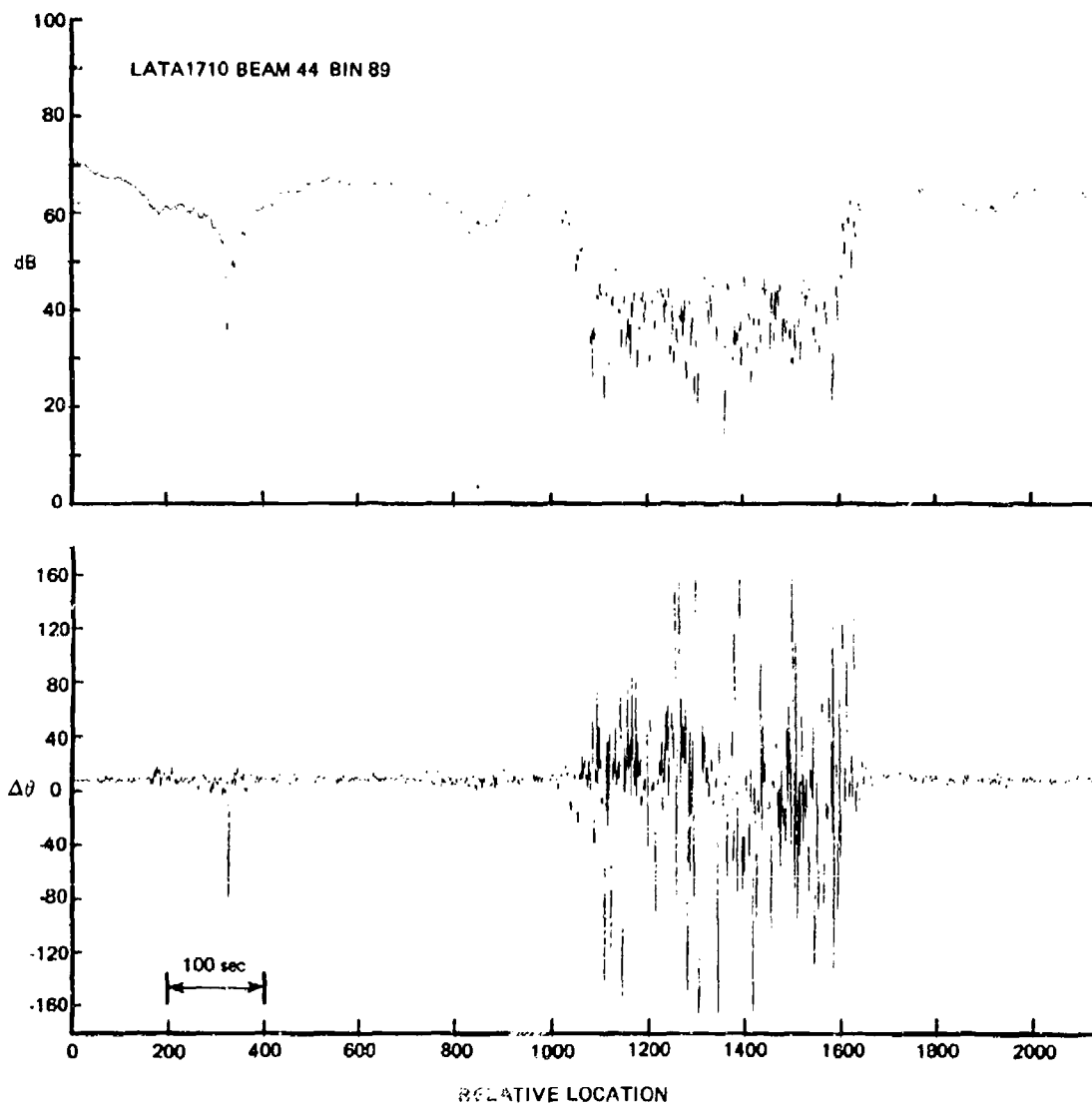


Figure 5. (U) Sample of LATA Beam Data. (U)

CONFIDENTIAL

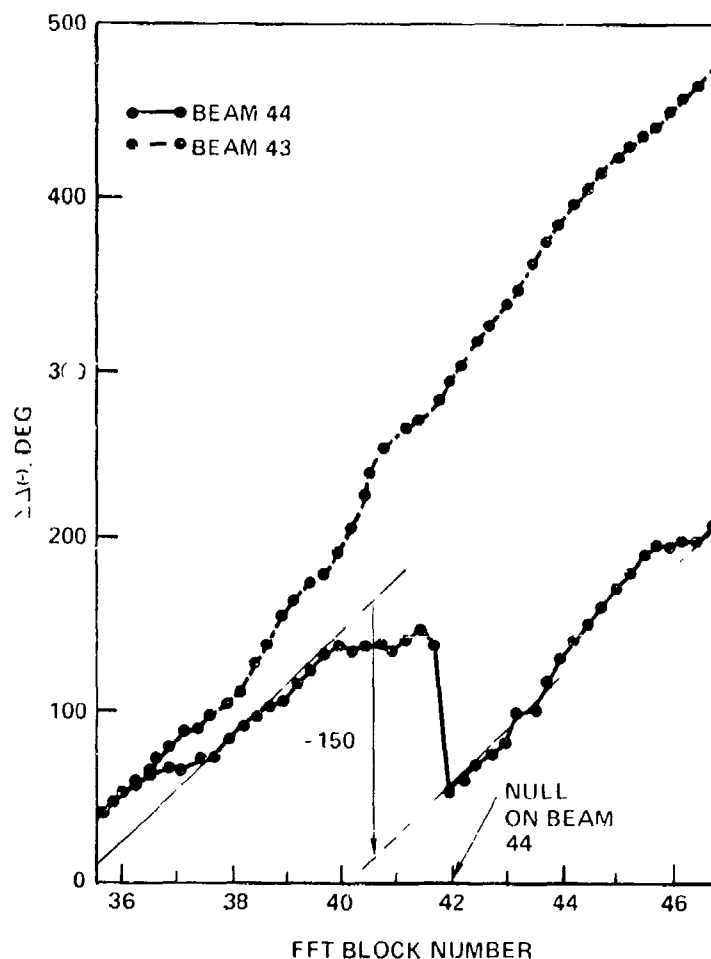


Figure 6. (U) Beam Phase Behavior around the Null in Figure 5. (U)

(C) It is not surprising that 1° change of look angle makes such a difference in signal behavior. For example, if the signal field has a 180° phase jump at the aperture midpoint, so that the beam steered directly at the source is nulled, then that change in look angle which corresponds to $\frac{1}{2}$ period change in time delay across the full aperture will largely smooth out the null. (At 22 Hz, a 180° phase jump corresponds to .023 s, while the change from LATA Beam 44 to Beam 43 in maximum beamforming time delay is .013 s.)

(C) Since the estimated trace speed of sound field structure across LATA, as discussed below, is about 5 m/s, it would take about 240 s for a given feature of the sound field to pass over the array. Presumably this is so much longer than the duration of very depressed signal level in Figure 5 because that deep depression only occurs while the phase sharp jump is nearly centered on the array.

CONFIDENTIAL

CONFIDENTIAL

(C) The type of phase behavior seen in Figure 6 occurred systematically. The approximate frequency of such sharp nulls was about 1 per array beam hour (from 3 nulls on two loudest or near loudest beams for each of two arrays in 37 minutes). It is unexpected that the greater number of nulls (two out of three) should occur on LATA with its much slower range rate. This may have been due to severe OAMS hydrophone gain perturbations (due to damage) which raised relative side lobe levels and presumably also made the beam outputs less sensitive to multipath interference.

DOPPLER DIFFERENCE

(U) Figure 7 is an example of how the $\Delta\theta$ data has been smoothed in order to leave only the major features of the doppler variations. $\tilde{\Delta\theta}$ is a running average of 11 $\Delta\theta$ samples. $\Delta\theta$ is obtained by further band smoothing.

(C) Figure 8 is a summary of 1600 seconds of $\tilde{\Delta\theta}$ data and the corresponding values of β , the normalized doppler difference, with

$$\beta = (\Delta f_{\text{LATA}} - \Delta f_{\text{OAMS}}) / f_{\text{source}}$$

for

$$\Delta f = \tilde{\Delta\theta} / 360$$

In order to align the LATA data with the OAMS time scale, two notably sharp switch events were aligned by inspection. The time alignment shift decreased 6 seconds in 15 minutes compared with an expected decrease of about 4 seconds based on track reconstruction.

(C) The plots in Figure 8 show no evidence of correlated frequency meander at both arrays. This is consistent with the estimated source frequency steadiness to .01%, which corresponds to $\Delta\theta$ constancy to about 0.8° at 22 Hz. Thus, the uncorrelated meanders of the $\tilde{\Delta\theta}$ data are presumably due to propagation effects or to receiver or source motions.

(C) Lateral meander of the track of the source would mainly affect the doppler received at LATA. A $\pm 1^\circ$ variation in the heading of the source two ship would produce a $\Delta\theta$ variation at LATA of only about $\pm 1^\circ$. In view of the calm seas at the time, it seems unlikely that the source tow ship would have had heading variations large enough to explain the major meanders in $\tilde{\Delta\theta}$ for LATA.

(C) Similar reasoning eliminates other source or receiver motion perturbations as likely causes of the larger $\tilde{\Delta\theta}$ meanders seen in Figure 8, leaving propagation effects as the tentative explanation. Propagation effects can arise due to range-only-dependent structure of the signal sound field moving across the array. From the track reconstruction data, the corresponding trace speeds should be around 20 m/s for OAMS and 5 m/s for LATA. Thus,

CONFIDENTIAL

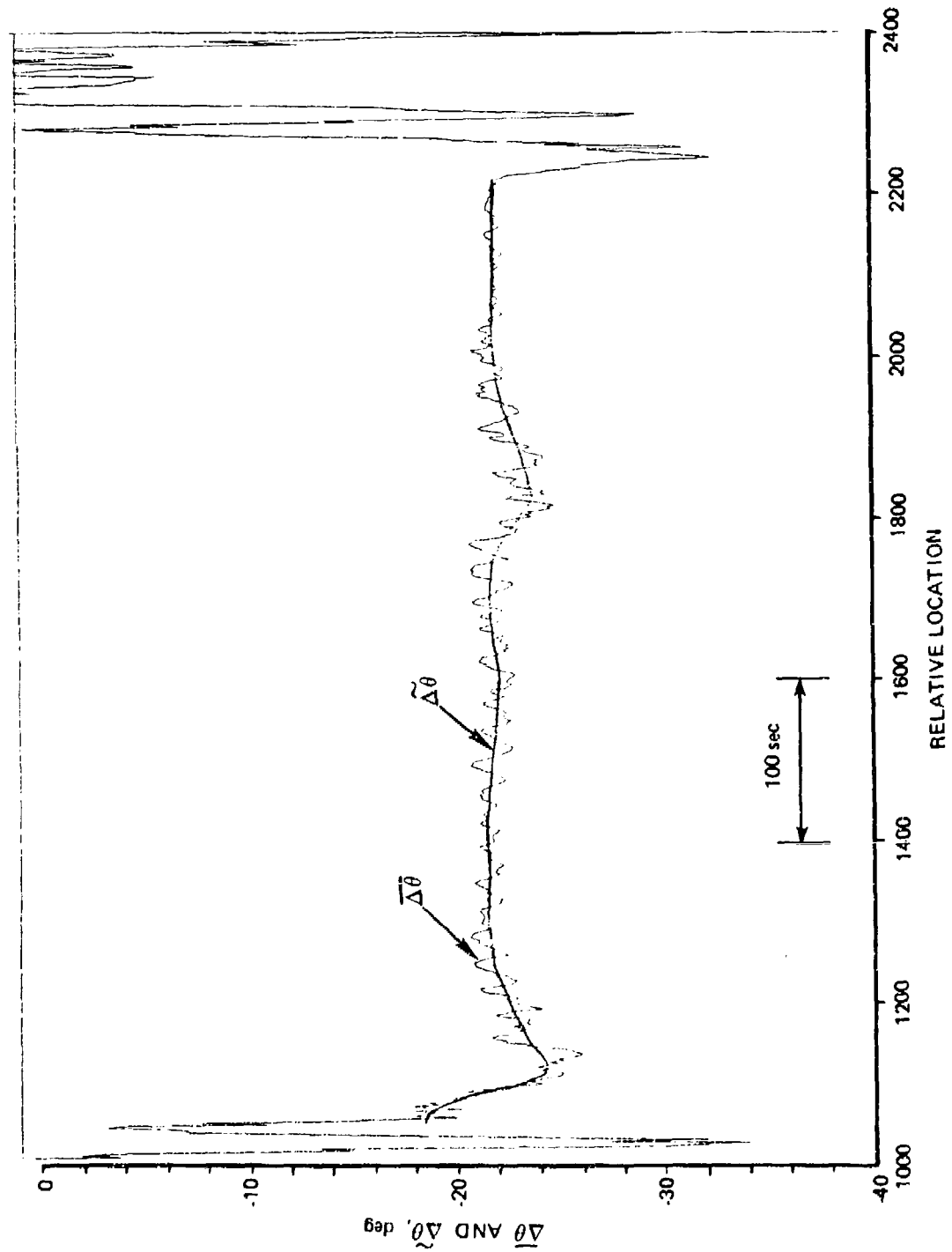


Figure 7. (U) Example of $\Delta\theta$ and $\Delta\tilde{\theta}$ Data (OAMS Beam 7, 22 Hz). (U)

CONFIDENTIAL

CONFIDENTIAL

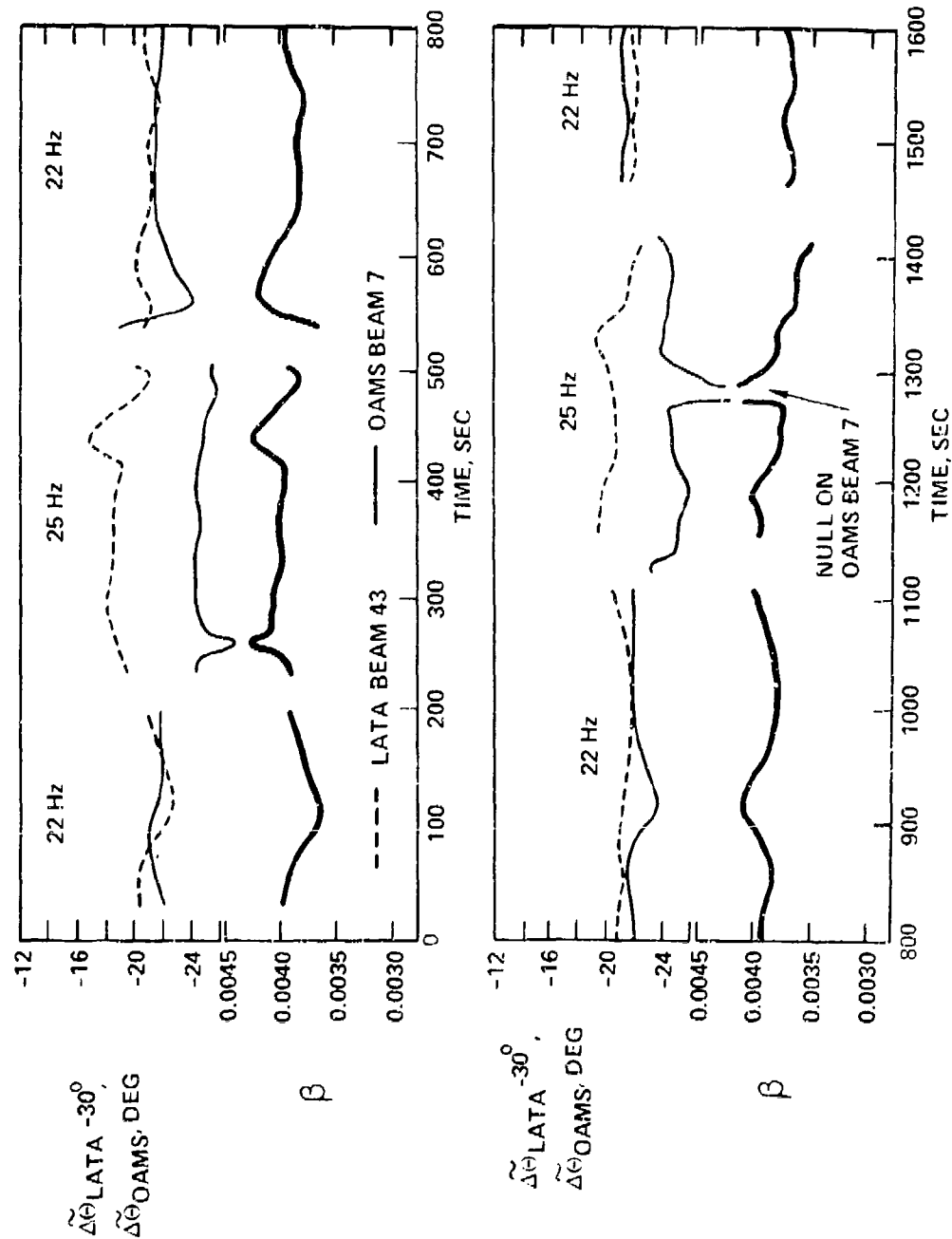


Figure 8. (U) Summary of Smoothed Residual Phase Increments and Resultant Normalized Doppler Difference. (U)

CONFIDENTIAL

CONFIDENTIAL

(C) the slow meanders of $\Delta\theta$ in Figure 8 could be caused by changing range. More definitive conclusions will be sought via a propagation modeling investigation which may also consider possible bottom waviness.

SUMMARY

(C) Towed array beam output fluctuations of signals from a moving CW source received at high signal-to-noise ratio for long range, bottom-limited propagation, display significant and correlated amplitude and phase fluctuation behavior. Occasional sharp amplitude "nulls" and associated phase jumps are seen which are remarkably smoothed over for a 1° change in beam look angle. Most of the characteristics of the received signals for this experiment can be understood in terms of multipath interference patterns moving across the arrays.

REFERENCES

1. Western Electric Company - Government Systems Division, "Technical Specification for Project Bearing Stake (U)", WECO TS No. 296-76. Naval Electronics Systems Command, 18 Nov 1976, SECRET.
2. NOSC, "Bearing Stake Exercise: Preliminary Results (U)", NOSC TR 169, 31 Oct 1977, CONFIDENTIAL.
3. Northrop, J. et al., "Environmental Acoustic Predictions for the Northwestern Indian Ocean (U)", NOSC TN 104, May 1977, CONFIDENTIAL.
4. Gordon, D. F. and E. R. Floyd, "Acoustic Propagation Effects in Beamforming of Long Arrays (U)", presented at the 30th Navy Symposium on Underwater Acoustics, San Diego, Oct. 1976; submitted to U.S. Navy Journal of Underwater Acoustics, CONFIDENTIAL.
5. Floyd, E. R. and D. F. Gordon, "Effects of Propagation on Linear Array Performance", NUC TN 1774, Sept 1976, UNCLASSIFIED.

CONFIDENTIAL

FLUCTUATIONS DUE TO RANGE RATE

I. Dyer

(See Volume 1 — Unclassified)

CONFIDENTIAL

THE IMPORTANCE OF SOURCE MOTION RECEIVER ORIENTATION,
AND THE OCEAN ENVIRONMENT

W. Jobst

(See Volume 1 — Unclassified)

CONFIDENTIAL
(THIS PAGE IS UNCLASSIFIED)

CONFIDENTIAL

IMPACT OF SOURCE MOTIONAL FLUCTUATIONS ON INTERARRAY SIGNAL COHERENCE (U)

Albert A. Gerlach
Naval Research Laboratory
Washington, D.C. 20375

ABSTRACT

(U) A dominant cause of phase fluctuations in signals propagating the ocean is due to the motional fluctuations inherent in a moving source. When the source signal is received at two widely separated receiving arrays, the impact of the phase fluctuations is to degrade the signal coherence between the two array signals. The extent of the coherence degradation has been determined to be a complex function of the correlation analysis time and parameters associated with the signal, the source motion, and the system geometry. The interrelationship between the coherence degradation, the correlation time, and the relevant system parameters has been derived and verified experimentally. The results of this study are presented in graphical form for ease of data assimilation. A most useful result is the estimation of an optimum correlation integration time as a function of the relevant system parameters. It is concluded that the motional fluctuations inherent in a moving source limit the correlation integration time which is optimum in passive sonar applications.

TECHNICAL SUMMARY

INTRODUCTION

(U) Acoustic signal transmission over long ranges in the deep ocean is subject to fluctuations in the propagation delay resulting from both temporal and spatial medium variability, and from fluctuations in the source and/or receiving sensor motion. Except for unusual conditions it can be expected that, over analysis intervals of less than about 30 minutes, the propagation delay fluctuations will be dominated by the relative speed and course fluctuations between the source and the receiving sensor. This was demonstrated in the CASE sea tests conducted in 1973.

(C) The impact of the propagation-delay fluctuations is to produce phase-difference fluctuations between the target-emitted signal received at two remote receiving sensors (after correcting for both time difference in arrival and mean doppler difference). In turn, the motion-induced phase-difference fluctuations will degrade the correlation-coefficient between the two received signals. A recent study shows that the amount of coherence degradation due to this cause can be expected to increase with the temporal length of the analysis interval (correlation integration time) [1,2]. The objectives of this paper will be to quantify the amount of correlation degradation which can be expected from a transiting submarine target, and to provide a suitable estimate of the optimum integration time to use in passive correlation detection. In the results to be presented the target was assumed to emit a narrowband acoustic signal while conducting a routine underwater transit along a base course at an assigned speed of advance between 5 and 30 kts.

CONFIDENTIAL

EXPERIMENTAL TEST DATA

(C) To obtain data on the motional fluctuations of a transiting submarine, ship speed and course were measured aboard a nuclear submarine during a normal underwater transit. The data were measured at one minute intervals (from the ship's inertial navigation system) over eight test runs of one-half hour duration each. The test runs encompassed several ship headings while the submarine proceeded at a speed of approximately 10 knots.

(U) In computing the correlation degradation for a given analysis interval T , only the motional fluctuation data within the given time interval are relevant. Consequently, the data from the 8 test runs afforded an opportunity to accumulate a significant sample size for statistical analysis (when T is less than 30 minutes). In the data computations the analysis window T was varied from about 6 minutes to 30 minutes in 10 discrete steps.

VARIANCE AND POWER SPECTRA OF TARGET SPEED AND COURSE

(C) The variance of both the submarine speed and course was computed and found to increase monotonically with the length of the analysis interval T . For T between 5 minutes to 30 minutes, the mean standard deviation of the speed and course ranged from 0.05 to 0.10 kt and from 0.35 to 0.62 degrees, respectively. The variance about the mean measures was quite high.

(U) The average power spectral density of both the speed and course fluctuations was found to be a generally decreasing function of frequency. However for a limited sequence of observations, the power spectral density did peak at a frequency large with respect to $1/T$ Hz. This implies that the correlation degradation for a given analysis (integration) time can be expected to vary rather significantly over extended periods of observation.

PHASE-DIFFERENCE FLUCTUATIONS

(U) The phase-difference fluctuations between two remote receiving sensors are a function of: the analysis time T , the frequency of the signal source, the motional parameters of the source, and the source-sensor geometry. All other factors being equal, the expected standard deviation of the phase-difference fluctuations was found to increase monotonically with the analysis time T (over the range of 5 to 30 minutes). Knowledge of the standard deviation of the phase-difference fluctuations was used to compute the correlation degradation as a function of all of the relevant parameters. It was determined that the expected correlation degradation increases monotonically with; the signal frequency, the aperture angle of the two receiving sensors (taken at the target location), the target speed, and the correlation integration time.

OPTIMUM INTEGRATION TIME

(C) Of primary utility in undersea surveillance applications is the selection of the optimum integration time for an interarray correlation detector. Assuming that the motional fluctuation data acquired on the test submarine are representative of all nuclear submarines, the optimum integration time was derived as a function of; the source signal

CONFIDENTIAL

frequency, the target mean speed and course, and the aperture angle of the receiving sensors (relative to the source). It was determined that for signal frequencies less than about 50 Hz, optimum integration times in excess of 8 to 10 minutes are realizable over a wide range of both target speed and sensor-pair aperture angle. On the other hand, for signal frequencies greater than 100 Hz, long integration times (10 minutes or more) will be sub-optimal except for small aperture angles and low target speeds or a highly favorable base course. Detailed data are available which give the optimum integration time when the signal frequency, the target speed and course, and the source-sensor aperture angle are specified [3,4].

CONCLUSIONS

(U) It can be concluded that the impact of source motional fluctuations on interarray signal coherence is to limit or bound the maximum correlation integration time which can be usefully employed in passive sonar applications. The limitation is well-defined in the sense that knowledge of the relevant signal, motional, and geometry parameters is sufficient to specify an optimum integration time for a given application.

REFERENCES

1. A.A. Gerlach, "Correlation Degradation Resulting from Target Motion," *NRL Report 7894*, July 1975.
2. A.A. Gerlach, "Motion Induced Coherence Degradation in Passive Systems," *IEEE Trans. ASSP* 26, February 1978.
3. A.A. Gerlach and W.L. Anderson, "Limitations on the Coherence of an Acoustic Signal Emanating from a Transiting Submarine," *NRL Report 8079*, January 1977.
4. A.A. Gerlach and W.L. Anderson, "Optimum Coherence Time for the Detection of a Transiting Submarine in Passive Sonar," *JUA(USN)* 27, No. 4, October 1977.

CONFIDENTIAL

ACOUSTIC FLUCTUATIONS

R. C. Spindel

(See Volume 1 — Unclassified)

CONFIDENTIAL

RANGE INDEPENDENT FLUCTUATIONS AND
PATTERN RECOGNITION OF VERTICAL ANGLE OF ARRIVAL STRUCTURE (U)

F. H. Fisher
University of California, San Diego
Marine Physical Laboratory
Scripps Institution of Oceanography
San Diego, California 92152

(C) The results to be presented here are from the CONTRACK IV cruise of May 1977. The origin of this work stemmed from a talk that VADM Waller gave at a meeting of the Under Sea Warfare Research and Development Council (USWR & DC) in which he discussed problems in holding contact with and tracking submarines. In connection with solving these problems, I felt it might be advantageous to use a vertical array to eliminate or reduce interference effects by separating the various multipaths by their vertical angles of arrival. The idea was to make multipaths work for us and to see how far we could push towards a goal of continuous tracking of third generation sources. Hence, the name of our cruises, CONTRACK for continuous tracking.

(U) The results I am going to present will indicate what sort of limits the medium places on long range sound propagation. The results are encouraging with respect to goals cited above.

(U) In CONTRACK IV, we measured the vertical arrival angles of signals at 195 Hz and 400 Hz transmitted from a source towed at about 4 kts at a depth of 100 m to simulate a submarine on a radial run away from FLIP.

(U) The experiment was done in the convergence zone region nearest to San Diego as shown in Figure 1. FLIP was deployed in a 3 point moor with the 532 meter, 20 element array centered at the sound channel axis as shown in Figure 2. We used a pseudorandom spacing of the elements as shown in Table A1 and the beam pattern response at 400 Hz is shown in Figure 3.

(U) In Figure 4 we see the kind of data we took at sea. In order to have an on-line display at-sea, the analog hydrophone signals were bandpassed and sampled at a 2.5 kHz rate for two seconds at three minute intervals. Using the complex amplitude at the signal frequencies we normalize, beamform and display the vertical arrival angle structure between $\pm 20^\circ$ as shown. A positive angle of arrival corresponds to energy that is arriving from above the horizontal at the array. Thus, as the source range increases we see energy coming from below (the near side of the zone) and then after the energy has vertexed above the array, we see the onset of energy coming from above. As range increases and ray paths spread out, we see that we begin to receive signals over most of a convergence zone.

(U) In order to obtain the pattern of vertical arrival angles at 195 Hz and 400 Hz the data are displayed on a linear scale in power that has been normalized. The normalization for each two second sample consist of dividing the signal level at each hydrophone by the average of the signal levels for all hydrophones. The reason for the normalized display was to improve the continuity of the vertical arrival angle pattern. That is, given the large variations that are

CONFIDENTIAL

observed in amplitude, we minimize these effects by the normalized display. The average signal level across the array is also displayed in Fig. 4. In addition, the standard deviation (σ) across the array at 400 Hz is also displayed; the σ appears to be range independent at 195 Hz and 400 Hz as shown with a value of about ± 3 db.

(U) The pattern of vertical arrival angle structure seen in Fig. 4 is virtually identical to that obtained in CONTRACK III in June 1976 during which we were processing only 0.2 second data samples at 400 Hz. The weather conditions during CONTRACK III were much more favorable. It should be noted that we were in a sea state 5 to 6 for nearly the whole CONTRACK IV run.

(C) The limited results from CONTRACK IV suggest that the vertical arrival pattern is rather simple with two dominant arrivals. It is robust and reproducible without requiring array motion compensation. Each zone has a characteristic pattern which may be useful in identifying a range for a source. The progression of the angle of arrival with range is easily understood on the basis of ray tracing.

(U) In Fig. 5 we display, on a linear scale, the power as a function of the vertical arrival angle in a three dimensional display beginning at the seventh zone. Here we see the caustic region at the beginning of the seventh zone and the large variations in absolute power as a function of range. Note the course change in Figs. 4 and 5 just before we approach the eighth zone. This represents a course change from 315° to 090° .

(U) A very important feature in Fig. 5 occurs when the 400 Hz source is turned off at the end of the record (see also Fig. 4), where no energy at any angle between ± 20 is seen; that is, we see no effects of ambient noise in Fig. 5. However, because of the normalization process, the record in Fig. 4 appears noisy even when the source is turned off. As yet we cannot answer the question, do we have just two dominant arrivals or are there other weaker ones present in Figs. 4 and 5.

(C) Another aspect of the pattern recognition potential of displaying the data as seen in Fig. 4 or 5 is that it may be possible to distinguish between a submerged and a surface source. Also, it is seen that since the 195 Hz and 400 Hz patterns are virtually identical, the potential exists for relating frequencies to a source on the basis of pattern recognition, and subsequently combining identical patterns at various frequencies from a common source to enhance tracking.

(C) For a source on a constant course and at constant speed it is possible to recognize CPA and zone intercept times and therefore deduce range and speed using a single vertical array. This is shown in the Appendix.

(U) In the high energy caustic region at the beginning of the seventh zone, the square of the coherence at 400 Hz is typically greater than 0.7 across the array, using a center hydrophone as a reference. The coherence was calculated from 32 samples (20 Hz bandwidth) within each two second data sample. The variations in power seen in Fig. 5 do not significantly degrade the ability to resolve the vertical arrival structure (in Fig. 4) at 400 Hz. Even though the source level at 195 Hz is 16 db lower than the 400 Hz level, the patterns in Fig. 4 are still very prominent and virtually identical to the 400 Hz patterns.

CONFIDENTIAL

(U) At 400 Hz, and a range of ~200 miles, the S/N ratio for a single hydrophone is about 20 db. In the 0.6 Hz bandwidth corresponding to the ~2 second sample we find the ambient noise to be 68 db/1 μ Pa, which corresponds to a spectrum level of ~71 db/1 μ Pa, about that to be expected for sea state 5 to 6. The propagation loss averaged over the array in the region of 200 miles is 100 db.

(C) Our preliminary results for array gain at both frequencies average about 8 db for the seventh zone; it is as high as 11 db in the caustic region. This says that by going to a 200 element array of the same aperture we should achieve an 19 db array gain. Our data suggests that integration times of 10³ seconds or greater are reasonable to consider. If a 50 mHz bandwidth is used to improve signal to noise, we gain 10.8 db; allowing 5 log T for going from 20 seconds to 1000 seconds, we gain 8.5 db; allowing 13 db for recognition differential, we conclude that with a 200 element 532 meter array, we can obtain a signal excess of 45.3 db at a range of 200 miles; the results are summarized in Table 1.

(C) If we take advantage of the oceanographic environment by looking at sources in northerly directions, most of the propagation loss occurs within the first two hundred miles. Therefore, it appears that our results indicate a substantial probability of detecting and holding (targets) out to long range in northerly directions, in the northern hemisphere.

(C) Our preliminary analysis of the on-line data taken at-sea therefore appears to be very encouraging as to what might ultimately be achieved using a vertical array. We expect to learn more from the CW data, which was taken on two ten channel analog recorders in conjunction with inter-array correlation work with NOSC.

(C) The principal questions to be addressed are the ultimate capabilities of vertical arrays for detection and tracking, the utility of pattern recognition as a means of discriminating between submerged and surface sources, and the fact that amplitude fluctuations over the array appear to be independent of range. The fluctuation aspect bears on the ideas of the Jason group (1) regarding saturation and coherence in an individual multipath.

Table I — (C) Projection of preliminary 400 Hz results to a 200 element array (U)

Experimental S/N	20 db	Average for single element 0.6 Hz bandwidth, 200 mile range
Array Gain*	19 db	For 200 element array based on measured array gain for 20 element array average gain
Bandwidth Gain	10.8 db	600 mHz to 50 mHz
Post Detection Gain	<u>8.5 db</u>	20 seconds to 1000 second sample
Output S/N	58.3 db	
Recognition Differential	<u>13 db</u>	
Signal Excess	45.3 db	

*Peak values of array gain are ~2 db higher

CONFIDENTIAL

(C) The work of Ross Williams (2) at 400 Hz at ranges of 700 nm encourages us to be optimistic in that he found little wavefront distortion over an aperture similar to ours. This leads us to believe that coherence for a single arrival over the array does not degrade significantly with range and that we might expect to be able to detect and hold low level targets at ranges of 1000 miles or more.

(U) Analysis of the CW data will give us added insight in how to plan a critical test of the ideas advanced in this presentation.

ACKNOWLEDGMENTS

The results reported in this talk represents research supported by the Office of Naval Research Code 222 and Naval Ocean Research and Development Activity Code 500.

REFERENCES

1. Munk, W. H., and F. Zachariassen "Sound Propagation Through a Fluctuating Stratified Ocean: Theory and Observation" JASA 59.818 - 838, 1976.
2. Williams, R. E. and C. H. Wei "Spatial and Temporal Fluctuations of Acoustic Signal Propagated Over Long Ocean Paths" JASA 59 1299 - 1309, 1976.

CONFIDENTIAL

CONFIDENTIAL

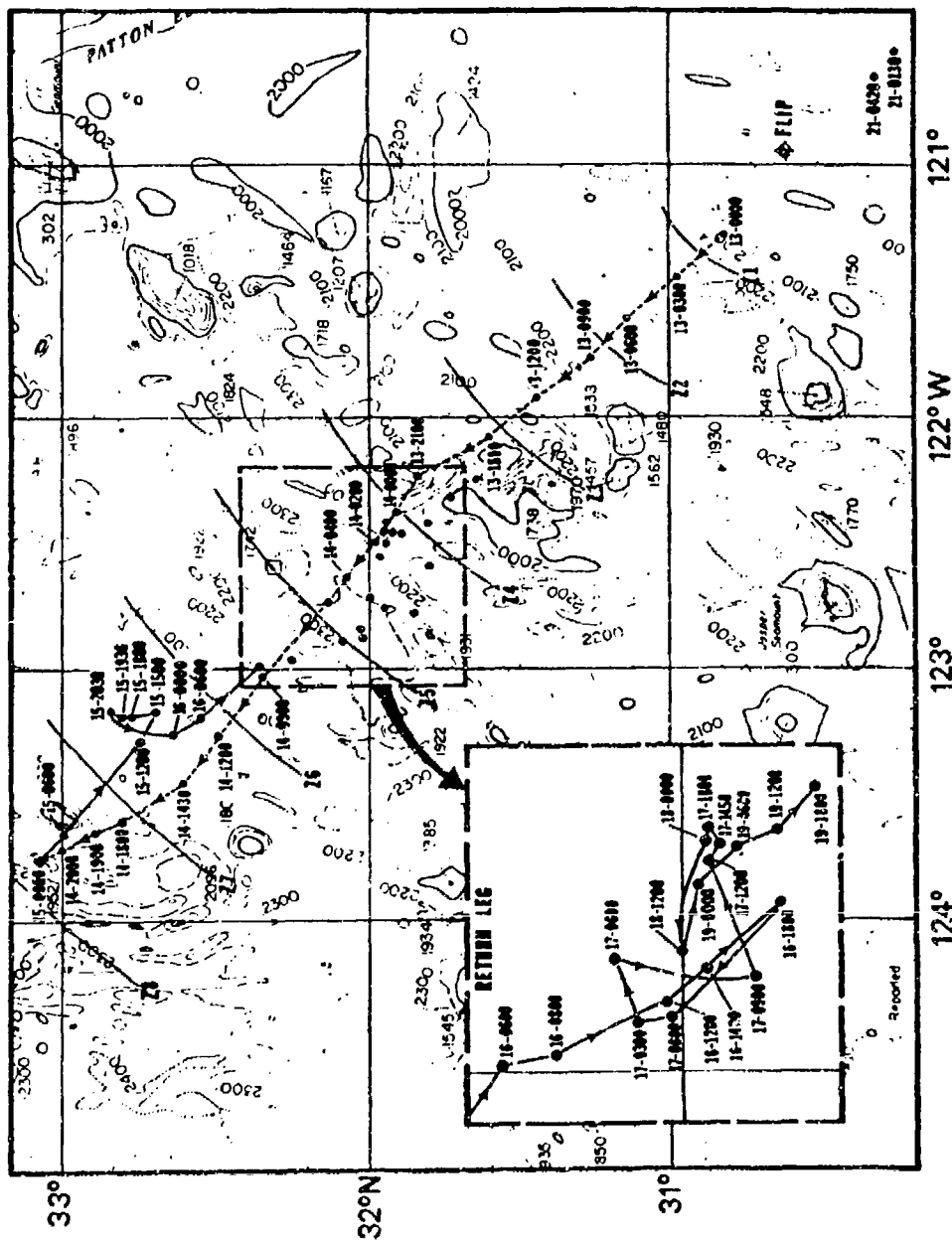


Figure 1 (U) — Map of operating area for CONTRACK IV showing FLIP location and course of USNS UTE. Convergence zone ranges to FLIP are shown. (U)

CONFIDENTIAL

CONFIDENTIAL

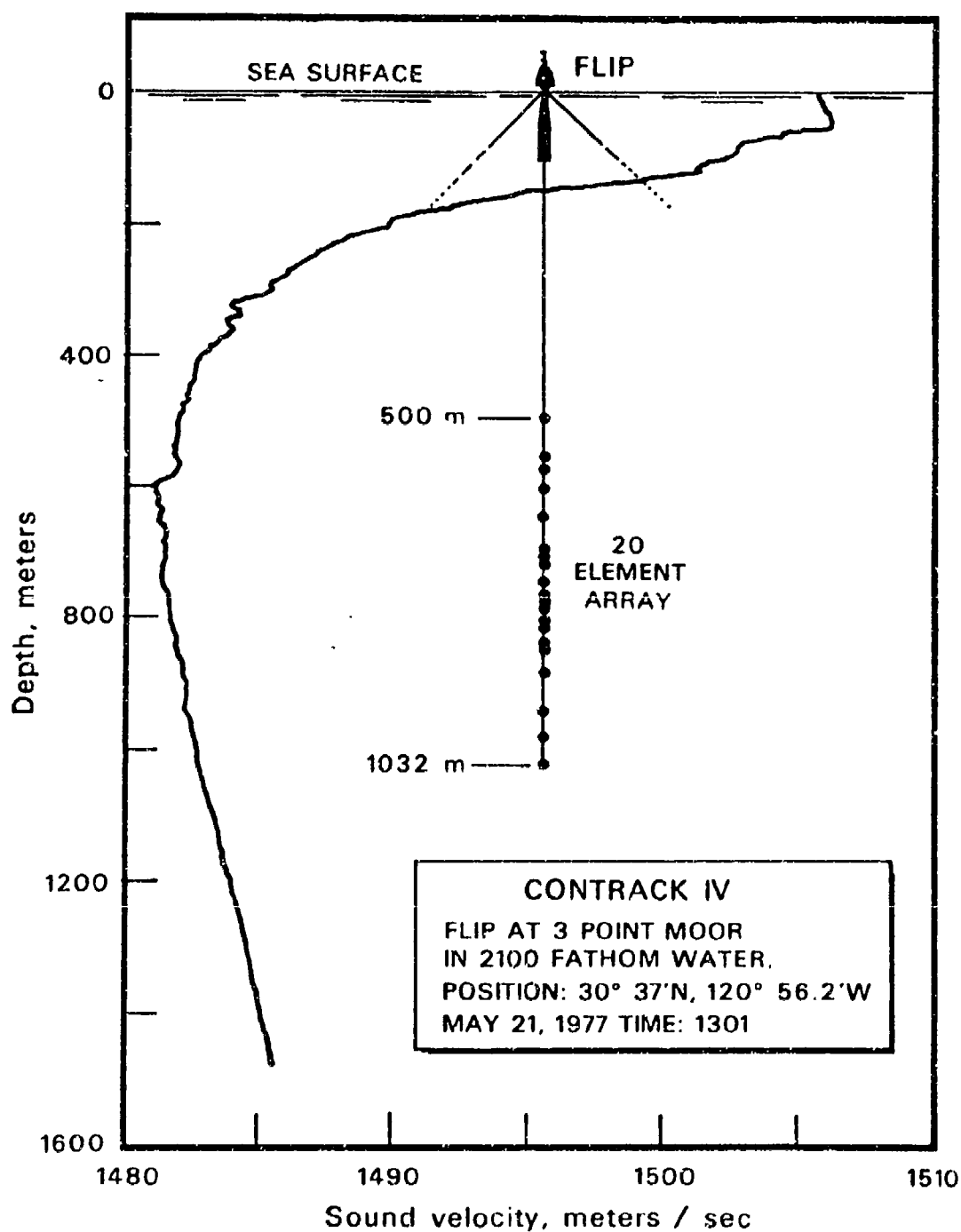


Figure 2 (U) — Schematic diagram of FLIP in a 3 point moor with 20 element 532 meter hydrophone array deployed. Center of array is at axis of deep sound channel as determined from sound velocity profile. (U)

CONFIDENTIAL

CONFIDENTIAL

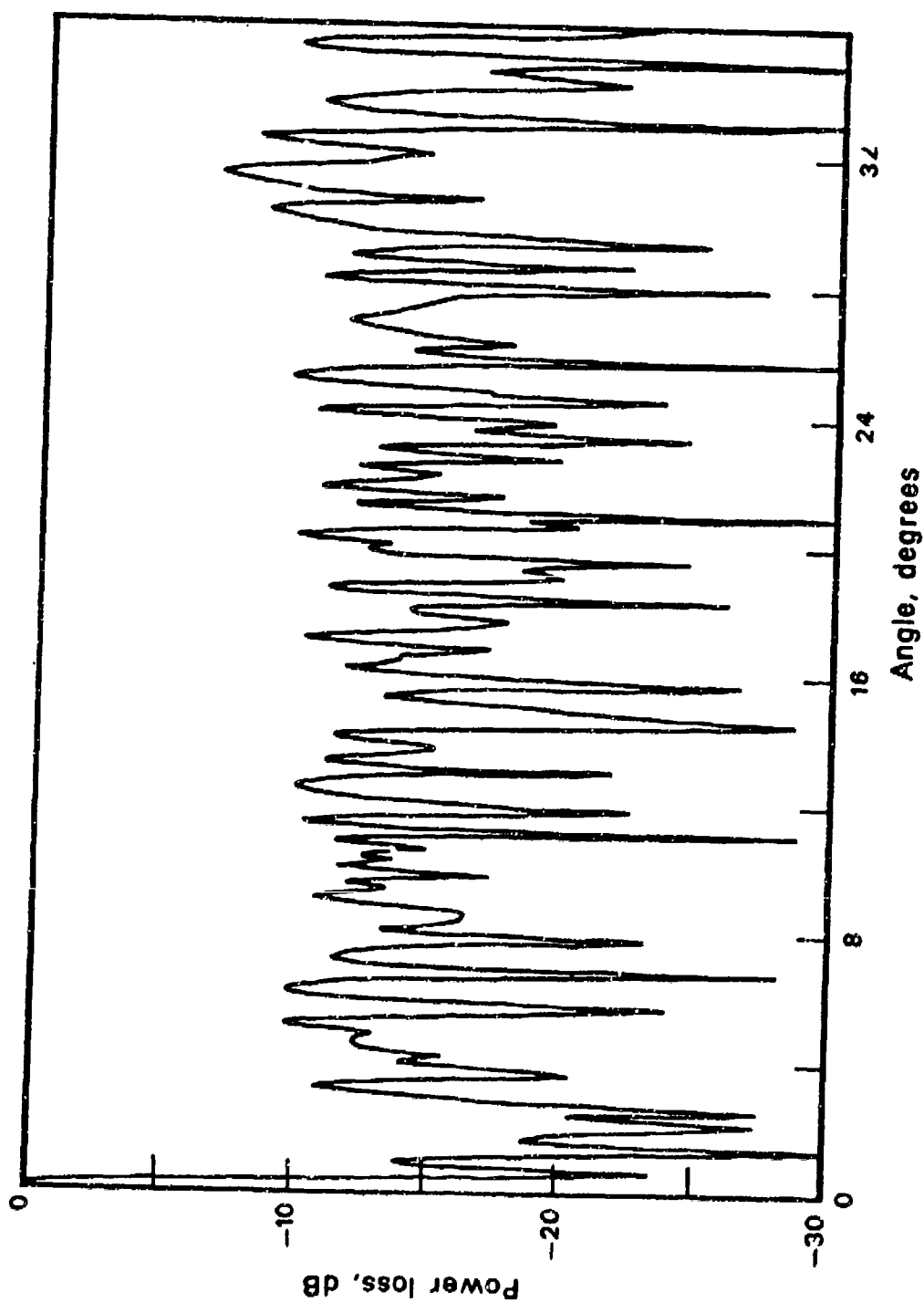


Figure 3 (U) -- Array response as a function of angle at 400 Hz. (U)

CONFIDENTIAL

CONFIDENTIAL

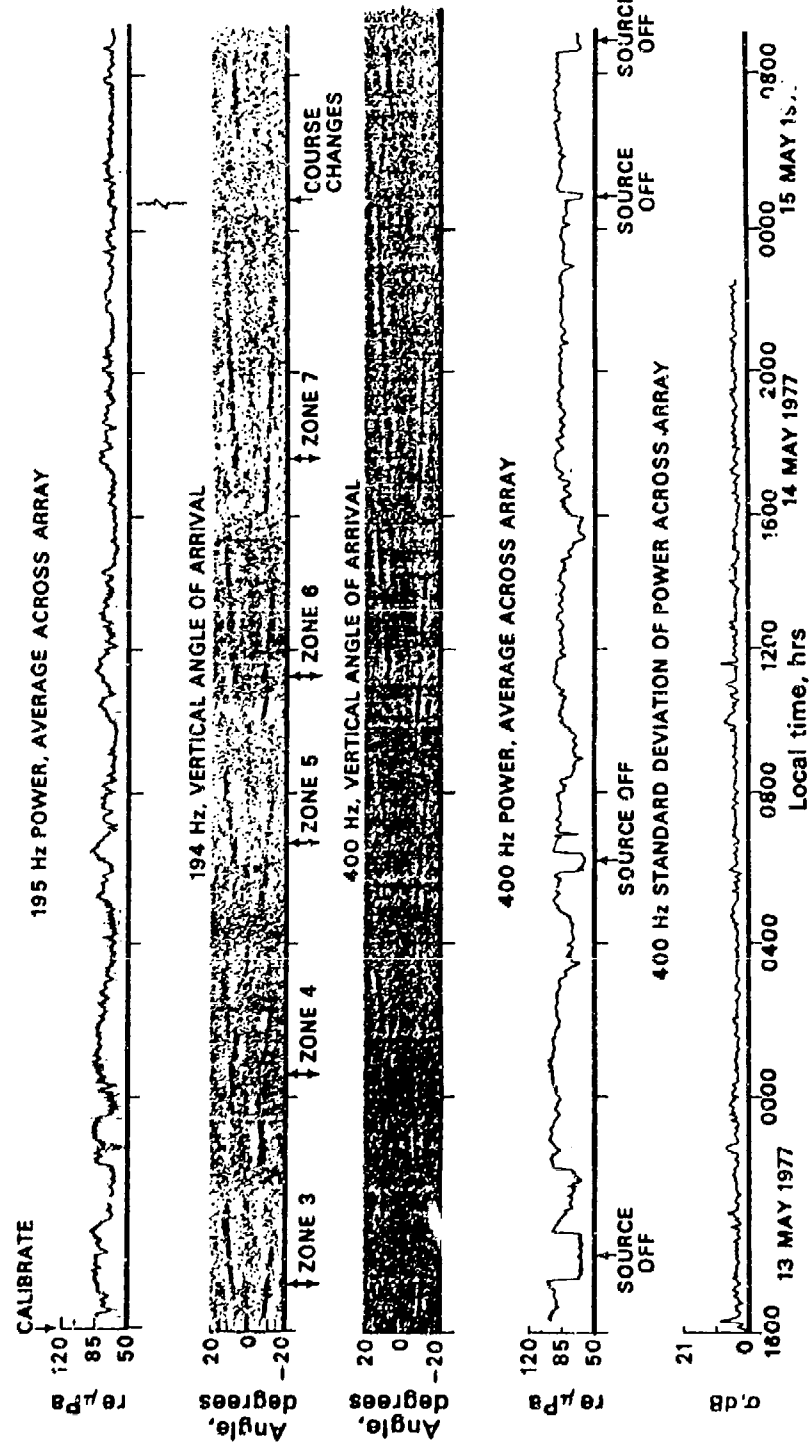


Figure 4 (U) — Normalized display on a linear scale of vertical arrival angle structure of acoustic energy at 195 and 400 Hz as a function of range, along with average power across array at 195 Hz and 400 Hz, and standard deviation of energy across array at 400 Hz. Source depth was 100 meters and source speed on radial run was about 4 kts. (U)

CONFIDENTIAL

CONFIDENTIAL

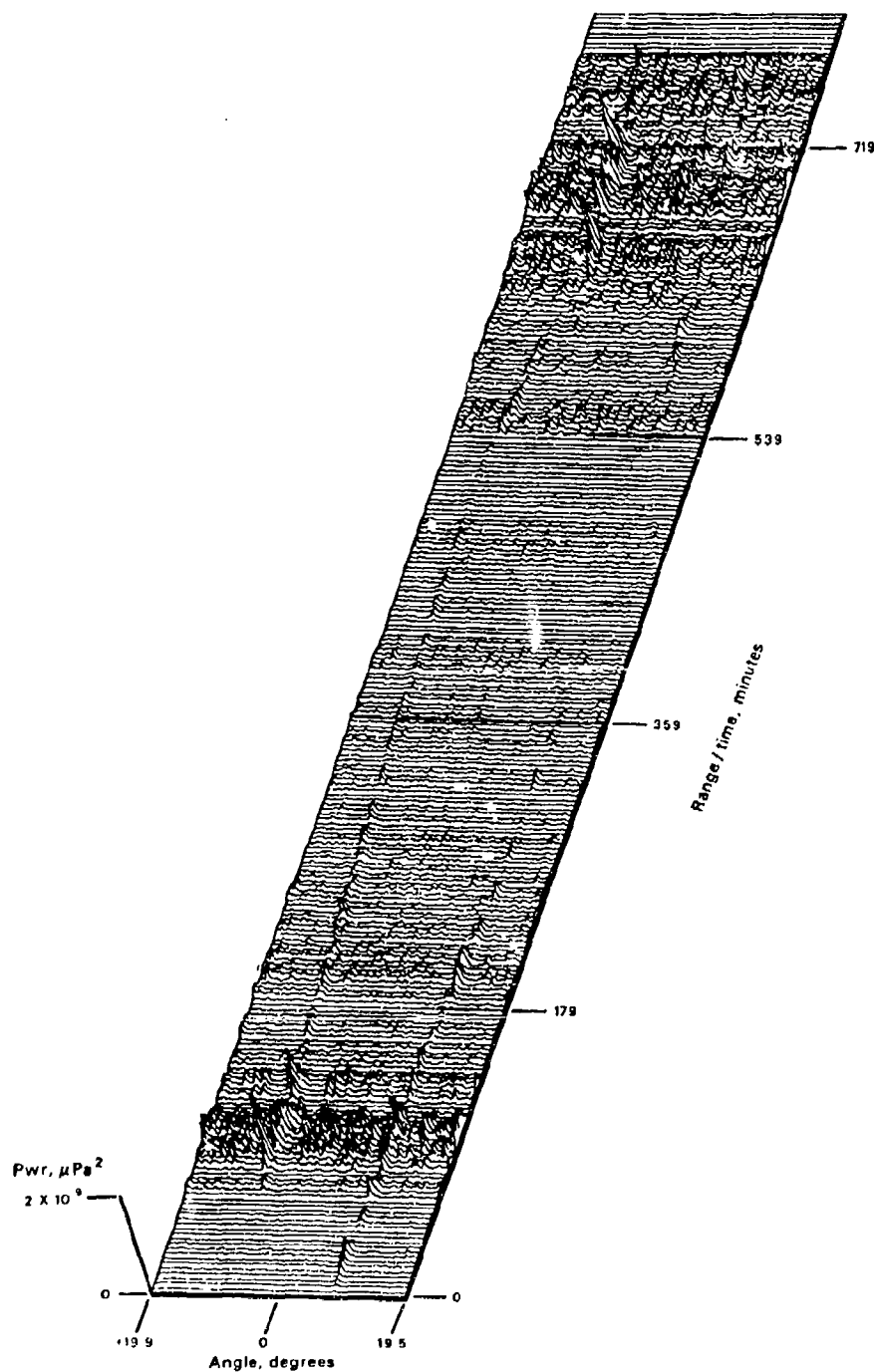


Figure 5 (U) — Three dimensional unnormalized power display on a linear scale of vertical angle arrival structure as a function of range commencing near the beginning of the seventh convergence zone, about 1700 on 14 May 1977. Compare with Fig. 4 to see how normalized display improves pattern continuity. Note last few sweeps when sound source is turned off; in the normalized display it is difficult to tell when the source is off. (U)

CONFIDENTIAL

APPENDIX A

EXPERIMENTAL DETAILS (U)

(U) The vertical array was deployed from FLIP which was in a tight 3 point moor in 2100 fm water as shown in Fig. 2. The center of the array was located at the sound velocity minimum. The sound velocity profile shown in Fig. 2 was obtained just before the array was deployed. The top hydrophone of the 532 m array was at a depth of 500 m. The hydrophone outputs are amplified and coupled through an FM telemetry link over a single coaxial cable to FLIP where a set of 20 receivers demultiplex and demodulate the signals. The signals are band-pass filtered from 100 Hz to 1 kHz and digitized at 2.5 kHz for 2 second intervals. An integer FFT processing system is used to obtain the complex phase and amplitude of desired signal frequencies. At 3 minute intervals an on-line display of the vertical arrival angle structure is plotted for the two signal frequencies at 195 Hz and 400 Hz. The vertical beam patterns of noise and of signals at other frequencies from 100 Hz up to 1 kHz can be displayed by reprocessing the digitized data.

(U) In Table AI the hydrophone spacings are listed; hydrophone 1 is at the bottom of the array. The spacings are pseudorandom and represent an unfilled array with a 1.75 m unit interval.

Table AI — (U) Element spacings of the LRAPP array (U)

Hydrophone Number	Spacing, Meters
20	63
19	21
18	31.5
17	36.75
16	50.75
15	8.75
14	14.0
13	28.0
12	15.75
11	5.25
10	15.75
9	28.0
8	5.25
7	28.0
6	7.0
5	38.5
4	56.0
3	36.75
2	42.0
1	

CONFIDENTIAL

(U) The source was towed between 3 and 4 knots by the USNS UTE with the source depth at 100 m. Source levels were checked at a range of 1000 yards and were 188 db/ μ P at 400 Hz and 172 db/ μ P at 195 Hz with both signals being transmitted simultaneously. The source frequencies were generated either by frequency synthesizers or by a crystal-controlled oscillator. The source was a single HX-90 unit driven by a 5 Kw CML power amplifier. XBT drops were made every 6 hours on both FLIP and UTE.

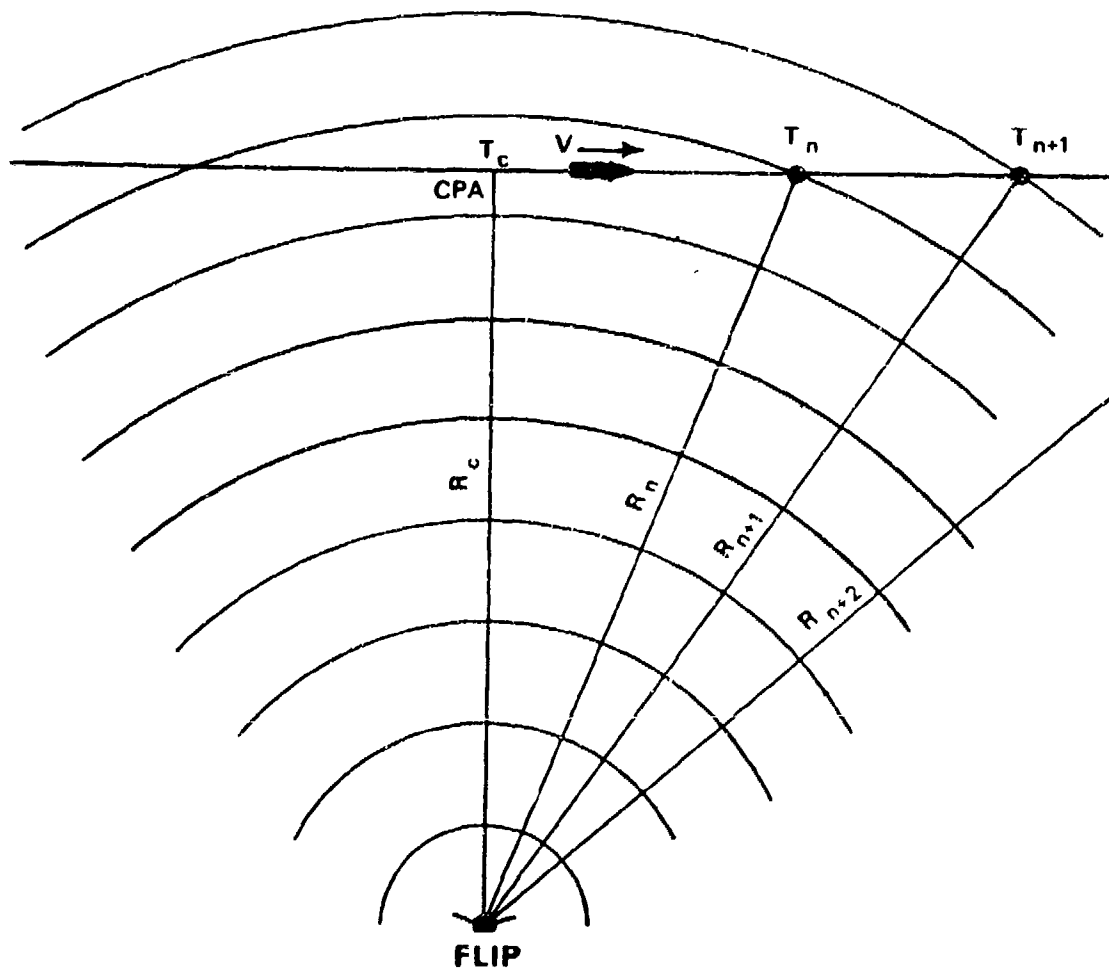


Figure A1 (U) — Schematic of geometry for recognition of CPA and zone intercepts from behavior of vertical arrival angle as a function of time. (U)

CONFIDENTIAL

APPENDIX B

(U) PATTERN RECOGNITION FOR CPA AND ZONE INTERCEPTS (U)

(U) In Fig. 4 we see that the arrival angle pattern changes in a uniform way as range increases. Suppose the source were moving at a constant speed on a tangential run as shown in Fig. 6 instead of a radial one. From the pattern of vertical angles of arrival we can identify a time T_n when it intercepts the n th zone (n unknown) from FLIP at a range R_n where $R_n = nR_z$, R_z being the zone range for the region of interest. For a source moving at constant speed, course and depth the time T_c at which the closest point of approach (CPA) occurs, corresponding to a range R_c , can be identified by a reversal in the progression of the pattern of vertical angles of arrival as a function of time. The range to the zone n is therefore

$$R_n^2 = R_c^2 + V^2 (T_n - T_c)^2 \quad (1)$$

Similarly for the range to zone $(n + 1)$

$$(R_n + 1)^2 = R_c^2 + V^2 (T_n + 1 - T_c)^2 \quad (2)$$

From these two equations we obtain

$$(R_n + 1)^2 - R_n^2 = V^2 [(\Delta T_n + 1)^2 - \Delta T_n^2] \quad (3)$$

where $\Delta T_n = T_n - T_c$, etc.

(U) The zone range R_z is known from the oceanography and location. Noting that $R_n + 1 = R_n + R_z$ we obtain

$$(2R_n + R_z)(R_z) = V^2 [(\Delta T_n + 1)^2 - \Delta T_n^2] \quad (4)$$

Similarly we obtain

$$(2R_n + 2R_z) 2R_z = V^2 [(\Delta T_n + 2)^2 - \Delta T_n^2] \quad (5)$$

Knowing R_z we can solve these two equations for the two unknowns R_n and V . Further zone-crossing times would increase the accuracy of the result.

(C) This exercise demonstrates in principle how the pattern of vertical arrival angles can be used to track and range on a moving source; for a reasonable speed and range we can calculate the times involved for a typical zone range. At $R_c = 195$ nm, $V = 10$ kts, $T_n - T_c = 7.8$ hours and $(T_n + 1) - T_n = 6.2$ hours with $R_z = 30$ nm.

(U) Doppler analysis of course could also be used to recognize CPA and obtain T_c .

CONFIDENTIAL

CONFIDENTIAL

**OMNIDIRECTIONAL AMBIENT NOISE AS A FUNCTION OF DEPTH AND
FREQUENCY IN THE DEEP NORTHEAST PACIFIC (U)**

Jack A. Shooter
*Applied Research Laboratories
The University of Texas at Austin
Austin, Texas 78712*

ABSTRACT

(U) A recent acoustic exercise was held in the mid northeast Pacific in 500 m of water. A vertical ACODAC with sensors distributed between 3400 m and the bottom was deployed to record the depth dependence of the omnidirectional ambient noise field. Data were recorded for a duration of 10 days and selected portions of data have been analyzed representative of periods of time when the acoustic field was dominated by single merchant ships and selected wind speed periods when no single merchant ships dominated the field. The data were processed into one minute spectra with frequency resolutions of 0.147 Hz over the range of 10 to 600 Hz and 0.018 Hz over the range 5 to 75 Hz which has allowed a detailed study of the spectral characteristics of the noise field and a clear separation of the noise field into its dominating source mechanisms. The emphasis of this work has been on the identification and understanding of the dominating source and environmental mechanisms that govern the ambient acoustic field.

TECHNICAL SUMMARY

Introduction

(U) The goal of the ARL:UT Ambient Noise Program is to characterize the physical and statistical nature of the ambient noise field as a function of depth, frequency and bandwidth with emphasis on narrowband data. The primary purpose is to provide support for ambient noise modeling and system evaluation.

(C) This program started in FY 77 under NAVELEX-320 sponsorship and this first year was devoted to the development of "tools" with which to measure and analyze the noise field and to the study of noise field physical and statistical parameters. The initial data base chosen for this study was the vertical ACODAC data from the NORDA/LRAPP exercise CHURCH OPAL. These data, because of the vertical noise field gradient or "depth quieting" presented an almost unique opportunity for the study of the physical mechanisms that made up the total field. As will be discussed, it is quite easy to identify the spectral components of nearby merchant ships in this data base.

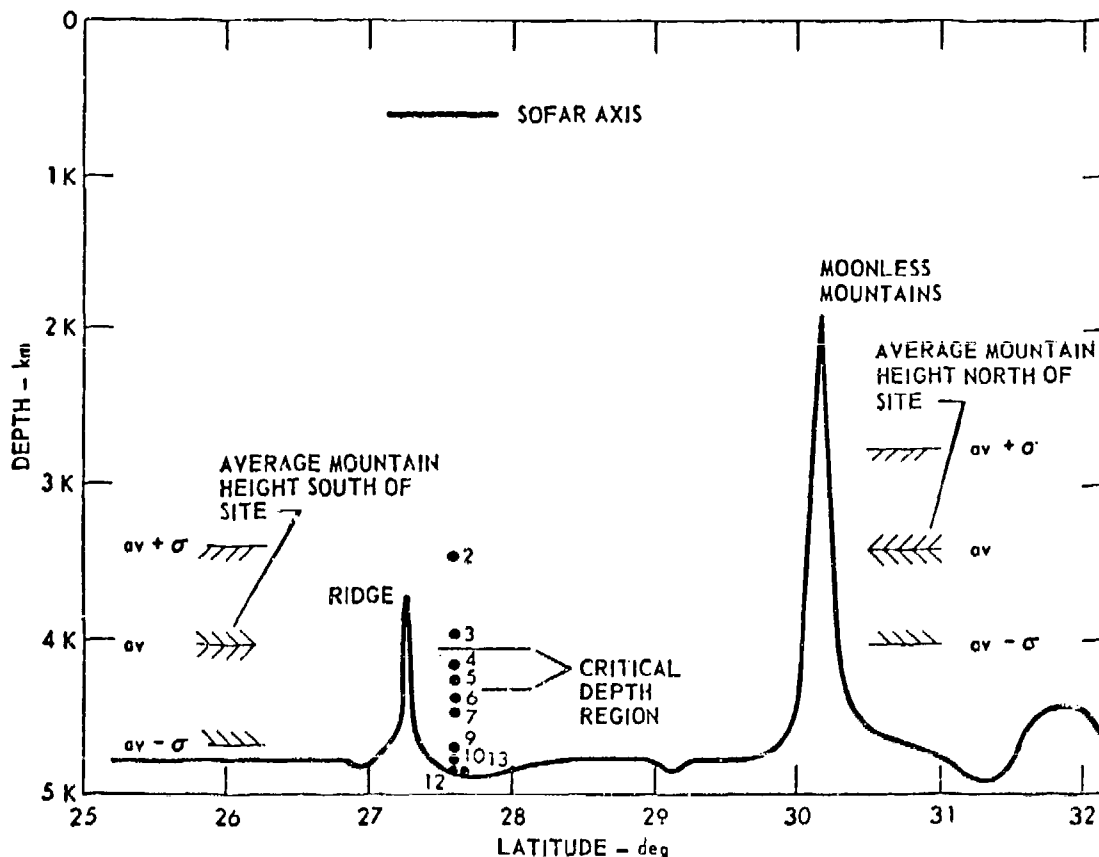
(U) The fundamental approach to this problem has been to process the data into narrowband spectra and to use that, plus ancillary information such as ship positions and wind speed, to identify the dominant acoustic sources. The physical properties of the source and environmental parameters are then determined and the statistical properties of the data are measured.

CONFIDENTIAL

Data Base

(C) The vertical ACODAC in the CHURCH OPAL exercise was deployed in 5000 m of water in the mid northeast Pacific. The hydrophones as seen in Fig. 1 were distributed from 3460 m depth to within 30 m of the ocean bottom. The ACODAC recorded 13 data channels onto analog tape for a duration of 10 days with a usable bandwidth of 500 Hz per channel. A 14th channel was used for recording time of day plus encoding of data channel gain states. The data channel gain ranging is independent for each channel and allows a system dynamic range of more than 80 dB. As will be shown, this dynamic range allowed the recording of nearby ship signatures as well as some of the lowest noise levels ever recorded by LRAPP.

(U) For analysis purposes these data were processed into narrowband calibrated spectra for selected time periods. These time periods were those times when the dominating acoustic sources could be identified. Several merchant ship signatures were selected as well as periods of time when there were no known nearby sources and the wind generated noise was the dominating source mechanism. The primary analysis bandwidth was 0.147 Hz over the frequency range 10 to 500 Hz. Because of an interest in very low



(U) Fig. 1—CHURCH OPAL ACODAC site showing bathymetry along the Meridian 137° 55' W

CONFIDENTIAL

frequency, some data were also processed with a 0.018 Hz bandwidth over the range 5 to 75 Hz and it is these higher resolution data that have served as the primary data base for the study of false detections in the spectra or "clutter" measurements. The spectra are stored on digital tape in the form of one minute averages. The noise level fluctuations of the low frequency data are shown in Figs. 2 and 3 for a 10 day period. The large (10 to 40 dB) excursions mark the passage of merchant ships.

Physical Environment

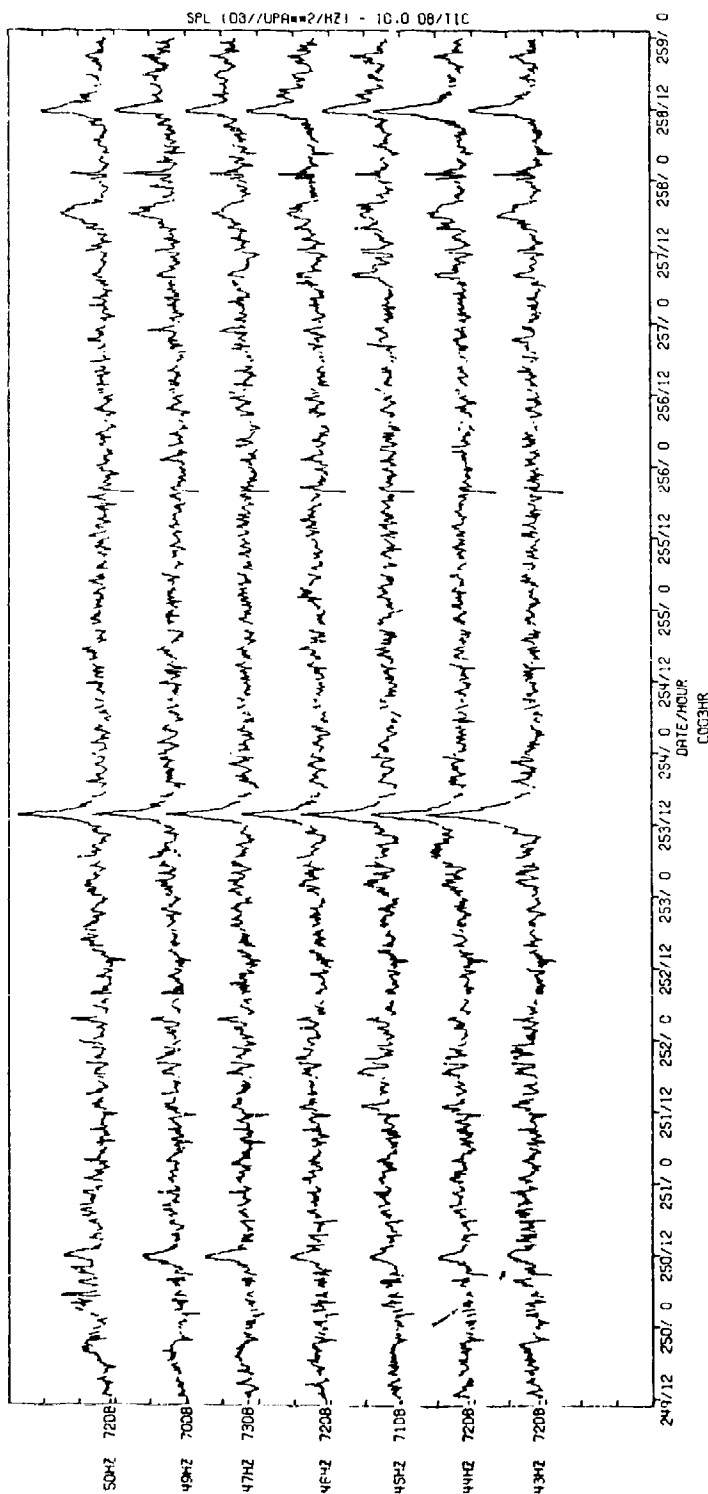
(C) In order to properly understand the impact and significance of the CHURCH OPAL data base, some discussion of the physical environment will be given. The CHURCH OPAL area was located in the deep water of the mid northeast Pacific and the ACODAC site was 180 km south of the Moonless Mountains which act as a bathymetric shield to the north and northeast. The ocean bottom in this area is characterized as a high loss area and at the ACODAC site there was more than 800 m depth excess with the nominal critical depth at 4000 m and the actual ocean bottom at 4883 m. The sound axis was near 600 m depth and in general the sound axis and critical depths decrease at the more northerly latitudes. The shipping density in the area is low compared to the high density shipping to the north at 50° latitude (Yokomoma-San Francisco). In fact, there are periods of 18 to 24 hours when no ship came within 300 km of the site. Most of the identified ships transiting the area were on the Hawaii to San Francisco route and were traveling at nominal speeds of 15 kt. At least four ships approached the site to within 18 km and completely dominated the acoustic field observed by the near bottom hydrophone over the frequency range 5 to 500 Hz.

Noise Depth Dependence

(C) All of the physical parameters including the shipping density just mentioned in the physical environment are critical to contributing to the observed depth quieting at the ACODAC site. An additional contributing mechanism to depth quieting may be the down slope conversions of the merchant ship noise as they pass over the continental shelves and near sea mounts. At least one significant example of a fluctuation in the ambient noise field due to slope conversion is seen in the CHURCH OPAL data at time 251 1500-252 0000 when a merchant ship passes near a sea mount. Several propagation loss model computations have indicated that sources on the continental slopes are either not observed or are greatly attenuated relative to deep receivers in deep water where there is significant depth excess. An example ray trace model is shown in Fig. 4.

The observed depth quieting in these data shows a 20 to 25 dB decrease in level from 3460 m (540 m above critical) to 4853 m (30 m above bottom). Most of the attenuation of level with depth happens below critical depth. A summary of the difference in noise level between critical depth and near bottom depth is shown in Fig. 5 for four nominal wind speeds. It is emphasized that this decrease in level with depth is observed only under distant source conditions when there are no dominating source mechanisms within 300 km. In the case of a dominant nearby (less than 18 km) source such as a transiting merchant ship or a strong local wind the noise field is essentially independent of depth.

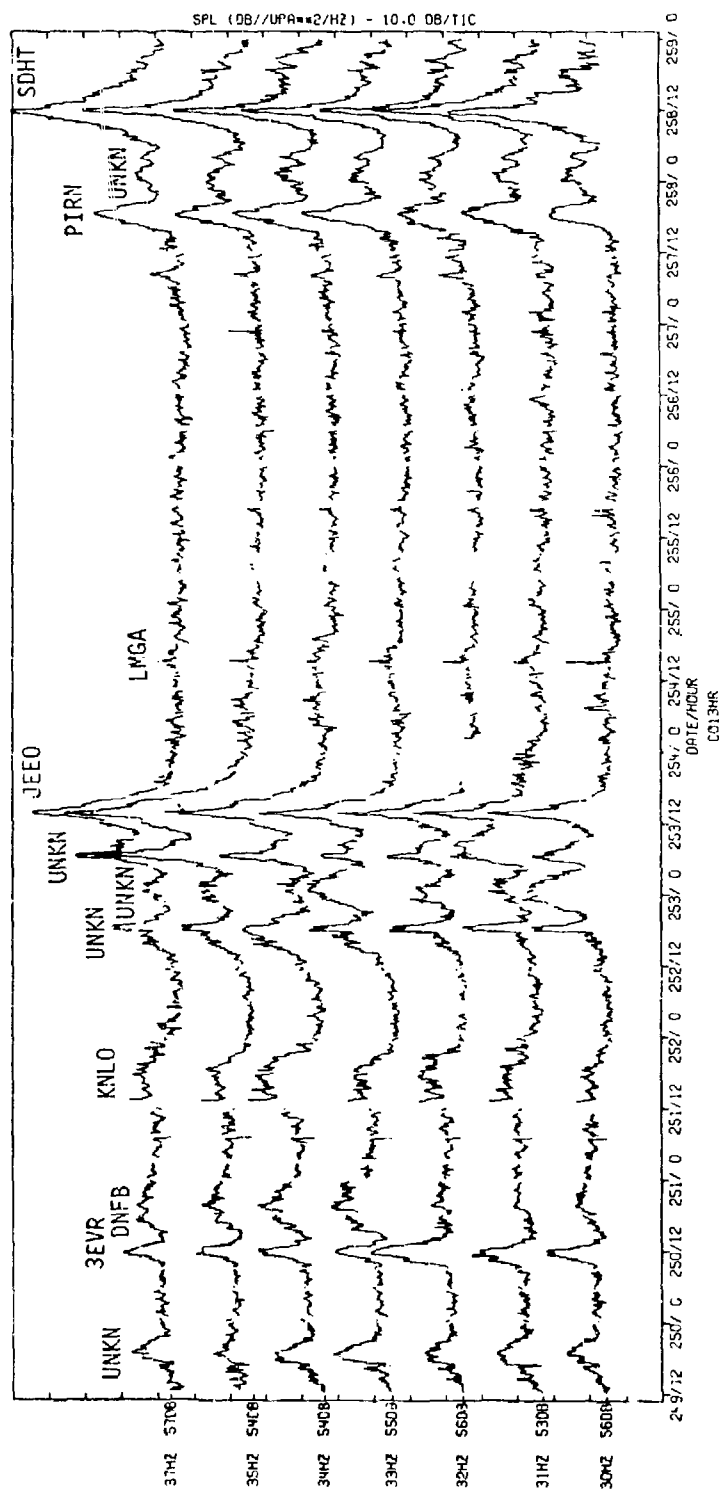
CONFIDENTIAL



(U) Fig. 2—Noise levels for the critical depth receiver 0.147 bandwidth, 10 minute averages (levels in dB// $\mu\text{Pa}/\text{Hz}^{1/2}$)

CONFIDENTIAL

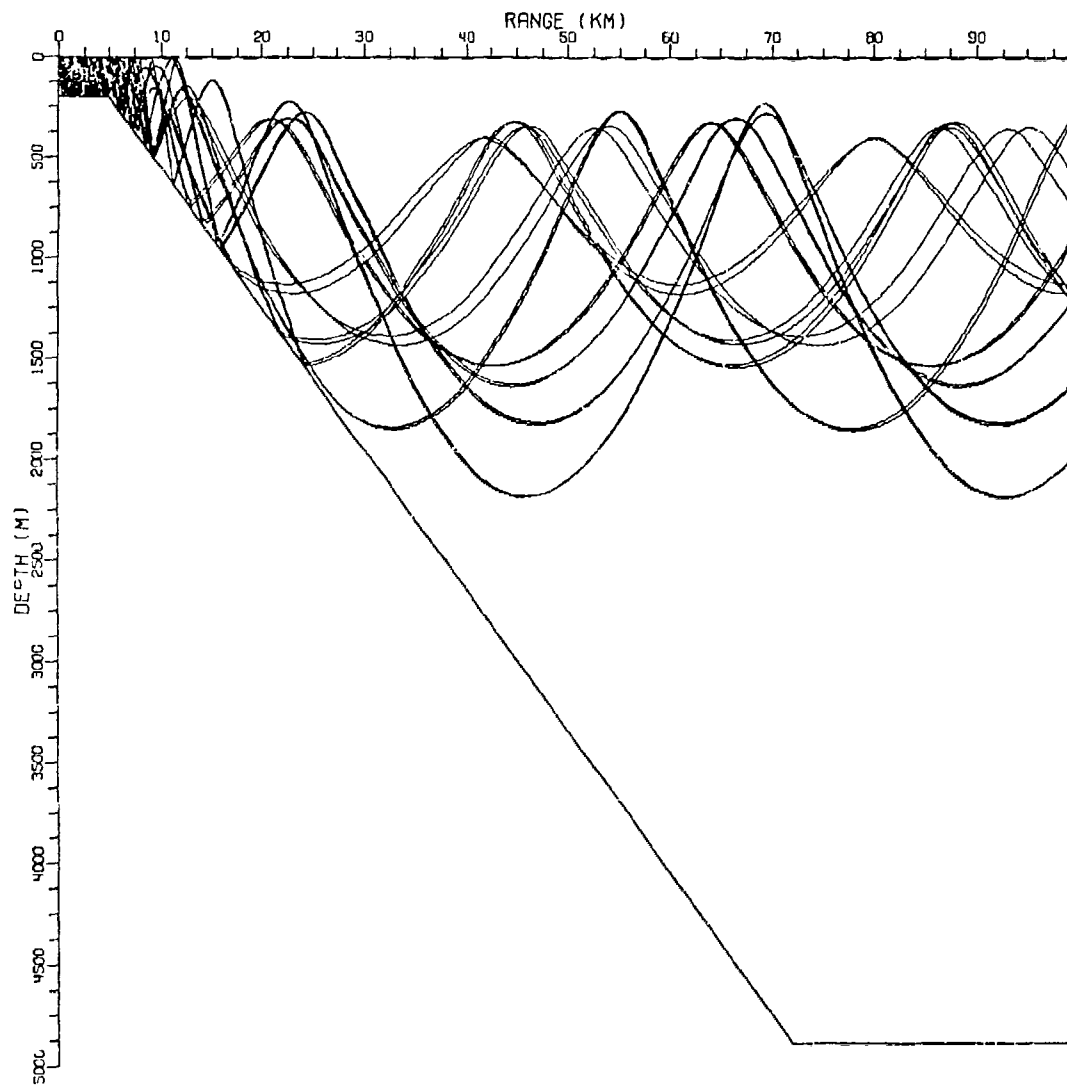
CONFIDENTIAL



(U) Fig. 3—Noise levels for the near bottom receiver 0.147 bandwidth, 10 minute averages (levels in dB/ μ Pa/Hz^{1/2}.)

CONFIDENTIAL

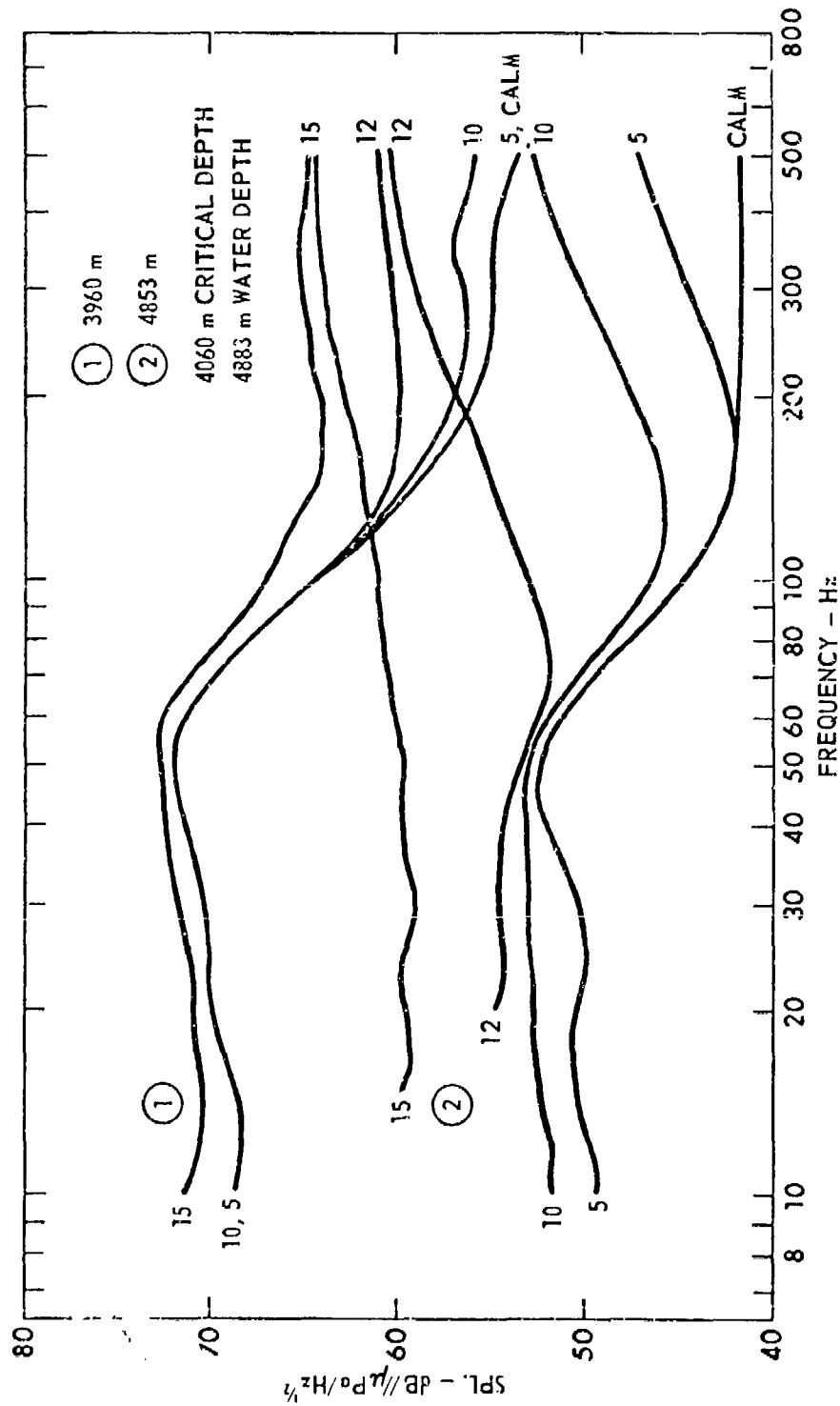
CONFIDENTIAL



(U) Fig. 4—Ray trace model showing the sound field due to a source on the continental shelf

CONFIDENTIAL

CONFIDENTIAL



(U) Fig. 5—Representative ambient noise spectra as measured on the 3960 m and the 4853 m hydrophones for indicated wind speeds (0.2 Hz frequency resolution, 10 min. integration time)

CONFIDENTIAL

CONFIDENTIAL

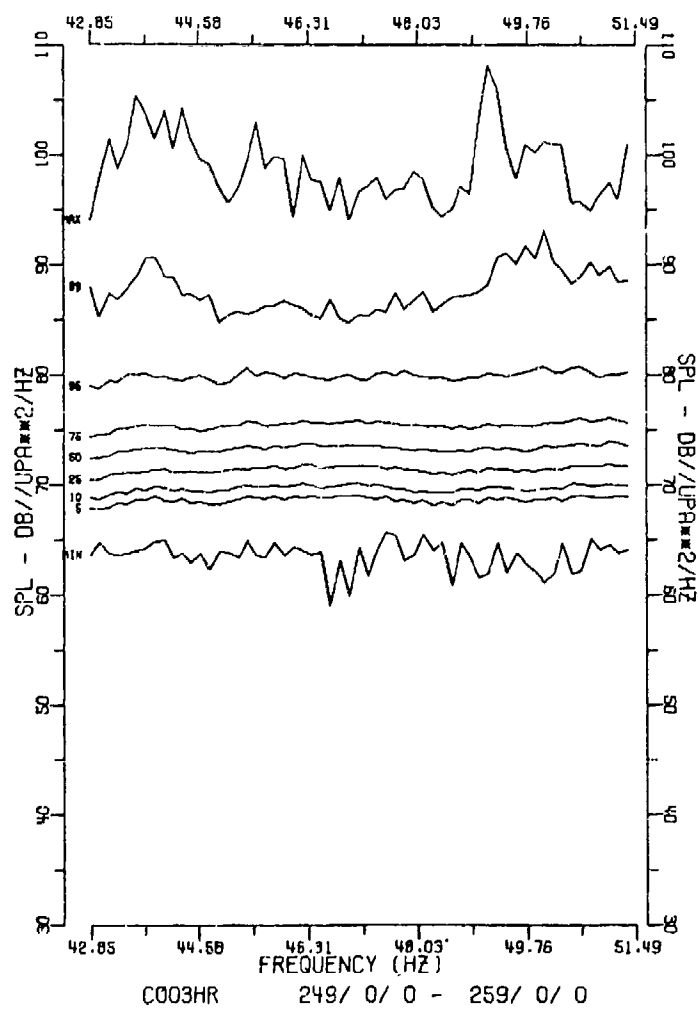
Noise Field Statistics

(U) In the case of the narrowband spectra the data have been shown to obey chi-square statistics where the conditions are stationary and homogeneous. Of course, this almost never happens and it was nearly impossible to find short (3 to 6 hour) segments of data that could be statistically tested for stationary and homogeneous conditions. However, when these conditions are met for independent data it appears that the data behave in a chi-square predictable way independent of depth, frequency, or bandwidth.

(C) Because of the almost unique conditions at the CHURCH OPAL site the dynamic range of the noise levels are enormous. The levels of noise observed at the near critical depth receiver range from a minimum of near 65 dB re $\mu\text{Pa}/\text{Hz}^{1/2}$. These levels, seen in the percentile levels of Fig. 6, represent the extreme variations in level over a 10 day period. The minimum level represents distant source conditions and the maximum level represents the passage of a merchant ship to within 18 km. In this case the frequency range was 40 to 50 Hz. In the same frequency range for the near bottom receiver the corresponding levels seen in Fig. 7 range from 45 to 105 dB in level. This even greater difference of 60 dB is, of course, due to the much lower levels detected by the near bottom receiver. The median levels for these two receivers was 58 dB and 73 dB for the near bottom and critical depth receivers, respectively.

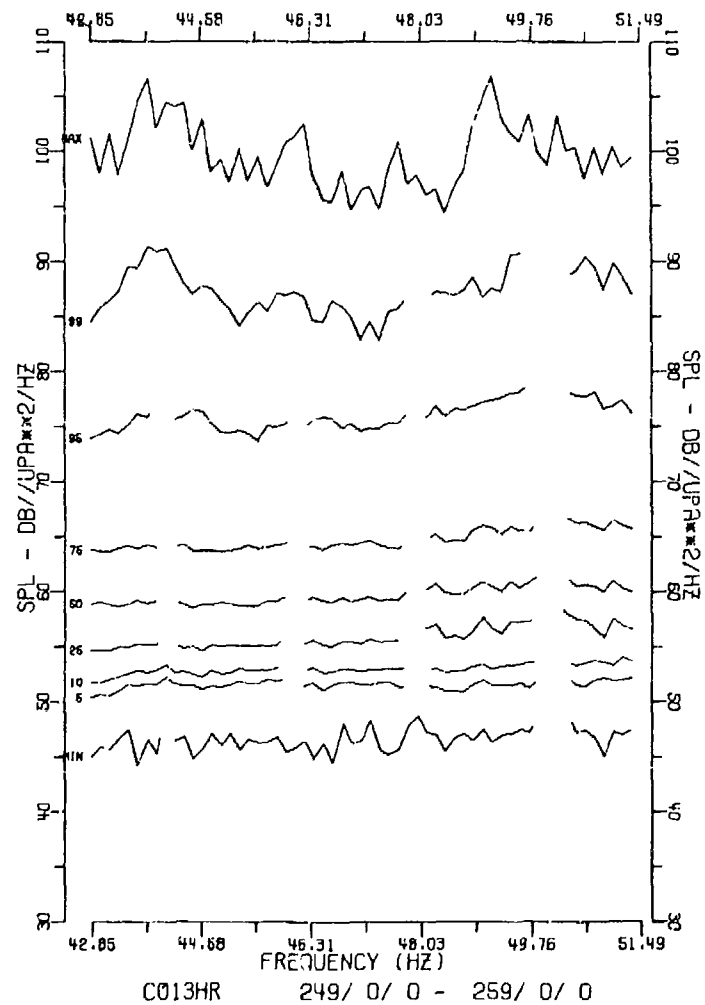
(C) The spectral components for broadband portions of the noise field again for homogeneous conditions which happens for only very short time periods (3 to 6 hours) are essentially uncorrelated in time or frequency. An example of the independence of the spectral components is shown in Fig. 8 which is a normalized spectral covariance matrix for the critical depth receiver during a quiet time of random homogeneous data. A more detailed view of these data is seen in Fig. 9, which represents cross sections of the same matrix for three arbitrary frequencies. The frequency spacing of these data was 0.147 Hz. A contrasting piece of data can be seen in Fig. 10 which is the normalized spectral covariance matrix observed during the close passage (less than 18 km) of a Swedish merchant ship. In this case the spectral components are highly correlated all across the frequency band and a more detailed view can be seen in Fig. 11 which are cross sections for three frequencies. The physical interpretation here is that although the spectrum may have peaks due to blade rate and shaft harmonics as seen in Fig. 12, the entire spectrum rises and falls together as the ship makes its transit. This same degree of high correlation can be observed in the portion of the spectrum dominated by wind generated noise.

CONFIDENTIAL



(U) Fig. 6—Percentile noise levels for the critical depth receiver
(0.147 Hz bandwidth, one minute sample every 10th minute)

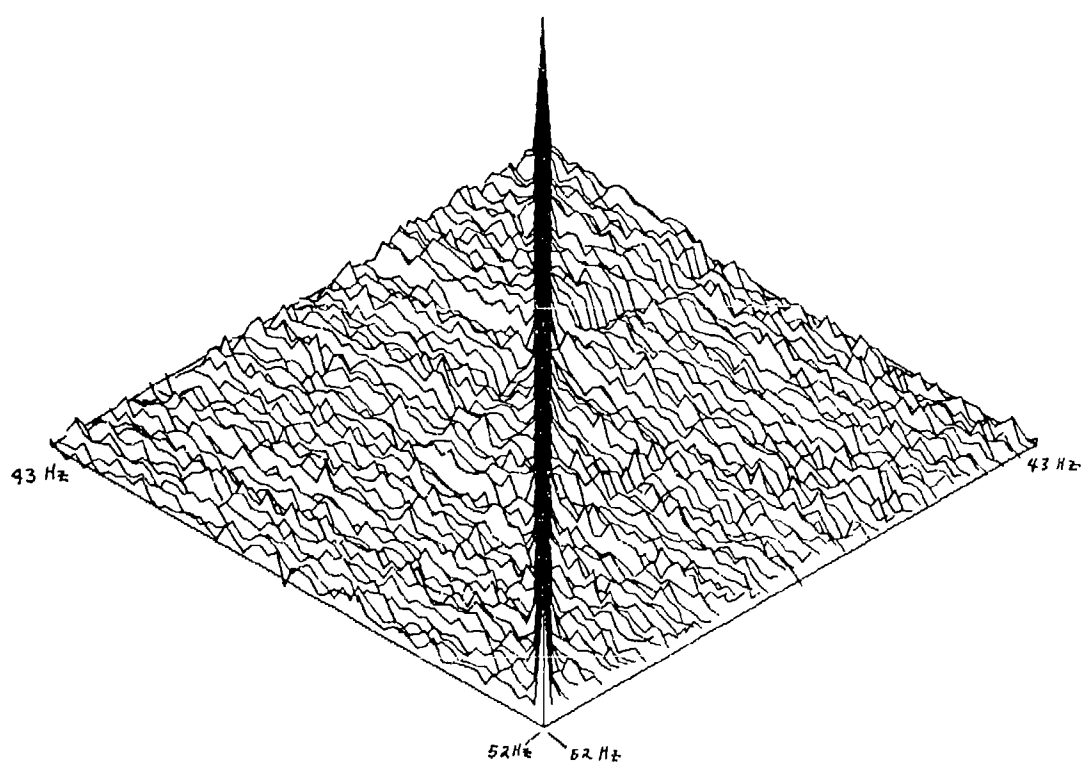
CONFIDENTIAL



(U) Fig. 7—Percentile noise levels for the near bottom receiver
(0.147 Hz bandwidth, one minute sample every 10th minute)

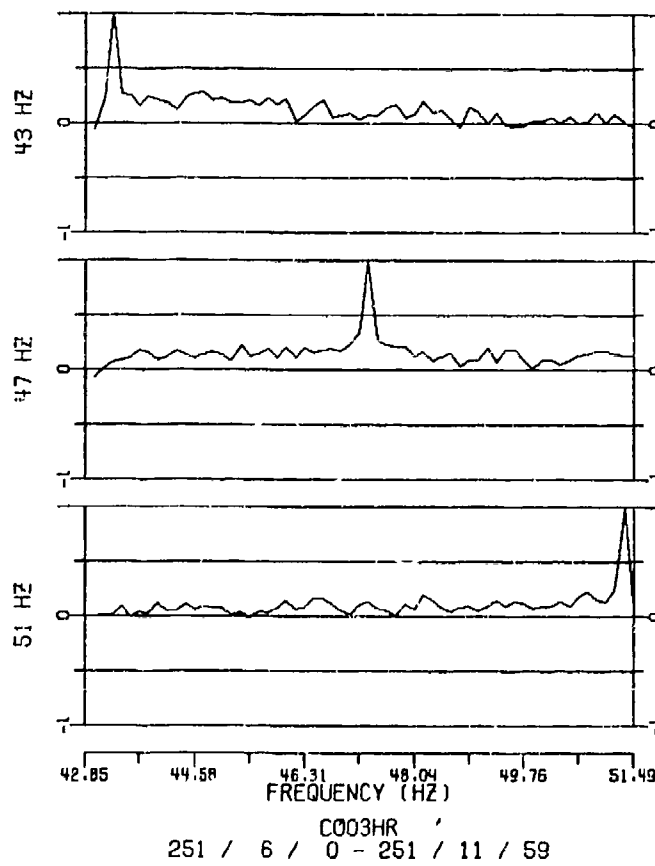
CONFIDENTIAL

CONFIDENTIAL



{U} Fig. 8--Normalized frequency covariance matrix of spectral levels
C003HR
251/6/0-251/11/59
(0.147 Hz bandwidth)

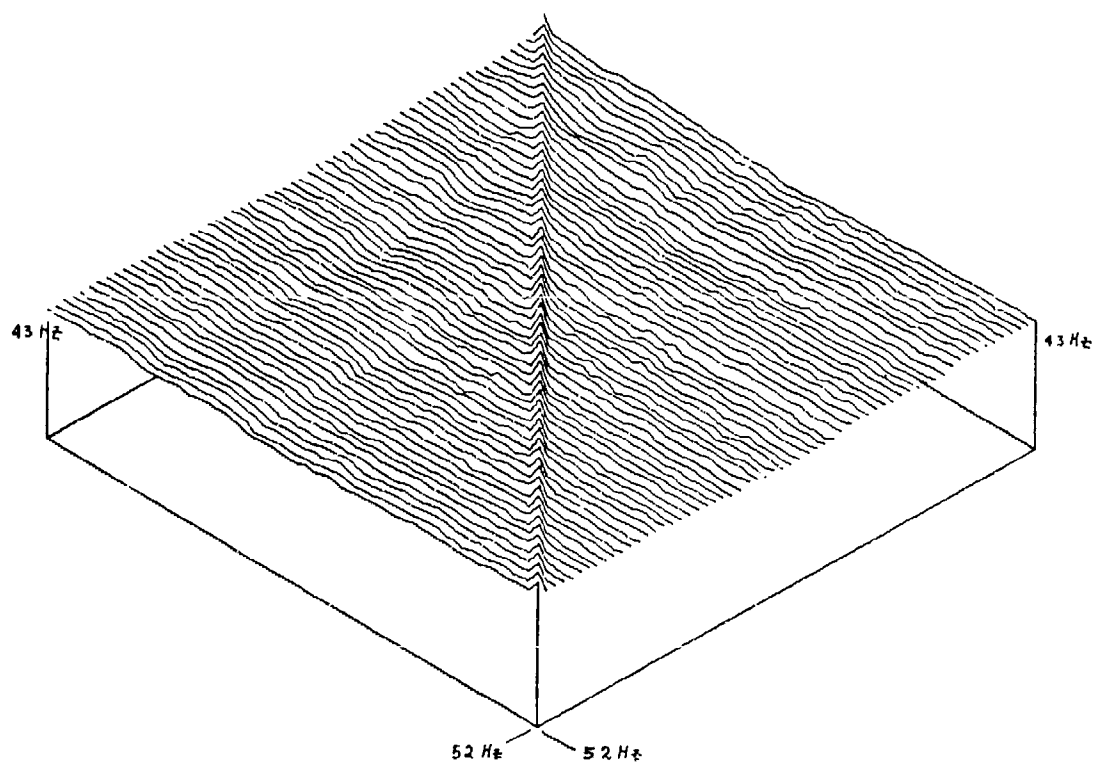
CONFIDENTIAL



(U) Fig. 9—Normalized frequency covariance matrix of spectral levels

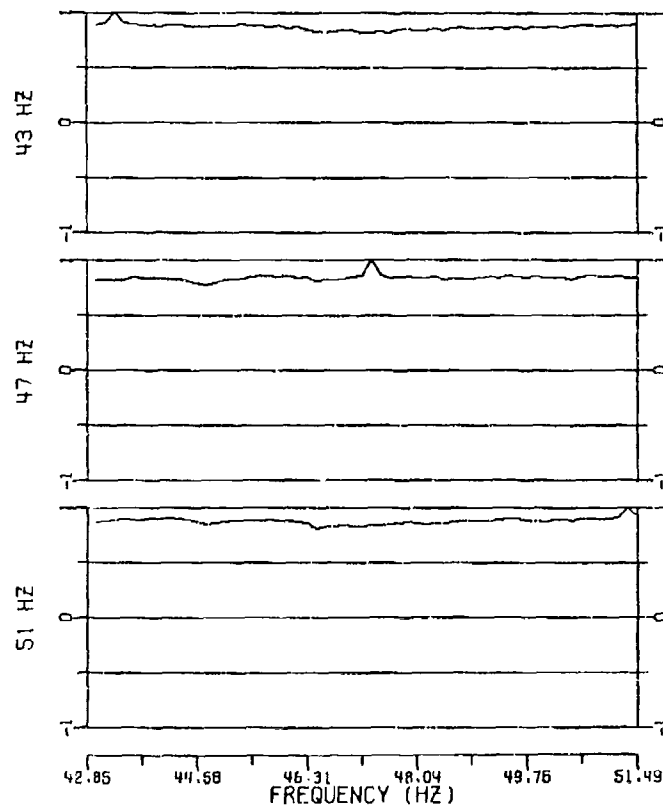
CONFIDENTIAL

CONFIDENTIAL



(U) Fig. 10—Normalized frequency covariance matrix of spectral levels
C003HR
258/9/0-258/14/59
(0.147 Hz ban dwidth)

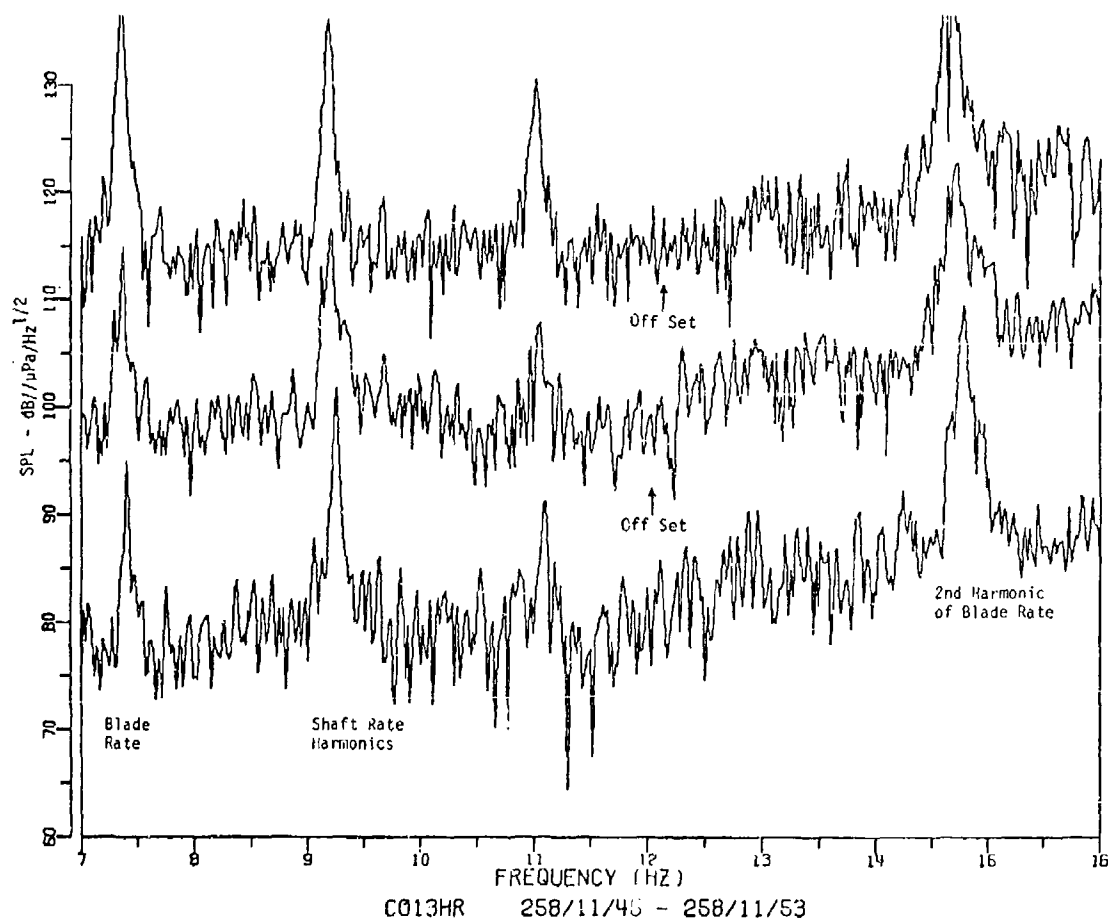
CONFIDENTIAL



C003HR
258 / 9 / 0 - 258 / 14 / 59
(U) Fig. 11—Normalized frequency covariance
matrix of spectral levels

CONFIDENTIAL

CONFIDENTIAL



(U) Fig. 12--Spectrum levels of a nearby ship (0.018 Hz resolution)

CONFIDENTIAL

Noise Field Clutter

(C) One of the important noise field characteristics are the number and characteristics of lines that appear in the noise field. At this writing the false alarm statistics (i.e., detection of "peaks" in the spectra) are just becoming available for these data and only a few preliminary results can be given. One preliminary result is that during periods of "quiet" times the number of single frequency bin false alarms across frequency is typically 50 over the frequency range 5 to 55 Hz with 0.018 Hz resolution. This number was measured at a 0.1% probability of false alarm rate based on chi-square statistics. The expected number of false alarms would have been three for the conditions of true chi-square data. For the case of a ship passage the number of single frequency bin false alarms at the same threshold appears to typically increase from 50 to 200. The number of false alarms is summarized in Fig. 13 for the critical depth receiver and in Fig. 14 for the near bottom receiver. The number of single bin false alarms are typically greater for the near critical depth receiver. It is also obvious that most of the merchant ship lines are broad and most false alarms can be described as multiple bin false alarms. For the purpose of data analysis the multiple bin false alarms have been collapsed into cell groups of contiguous bin false alarms to allow estimates of line frequency and line widths. For the 0.018 Hz data it was observed that ship lines were frequently over resolved and the number of cell groups could be further reduced by allowing skips in between single bin false alarms and still count the noncontiguous single bin false alarms as a part of a single cell group. A parameter study has been carried out for these data which indicate that it is reasonable to allow 3 to 10 skips between single bin false alarms within a single cell group.

(C) Some examples are shown in the following figures for a quiet time. Figure 15 shows the noise levels for the 6-hour period 256 1800-257 0000 using bands of 0.147 Hz for the critical depth receiver. The number of single bin false alarms for these data is shown in Fig. 16 along with the number of cell groups detected for 0, 3, 5, 10 and 15 bin skips. The same kind of data are shown in Figs. 17 and 18 for the near bottom receiver. A display of cell groups on a frequency-time plot is shown in Fig. 19 for the critical depth receiver and in Fig. 20 for the near bottom receiver, and it is clear that there are several persistent lines in these data. Also, it can be seen upon close examination that the frequency estimates of these lines are slightly variable. The frequency of a cell group is defined to be the weighted frequency

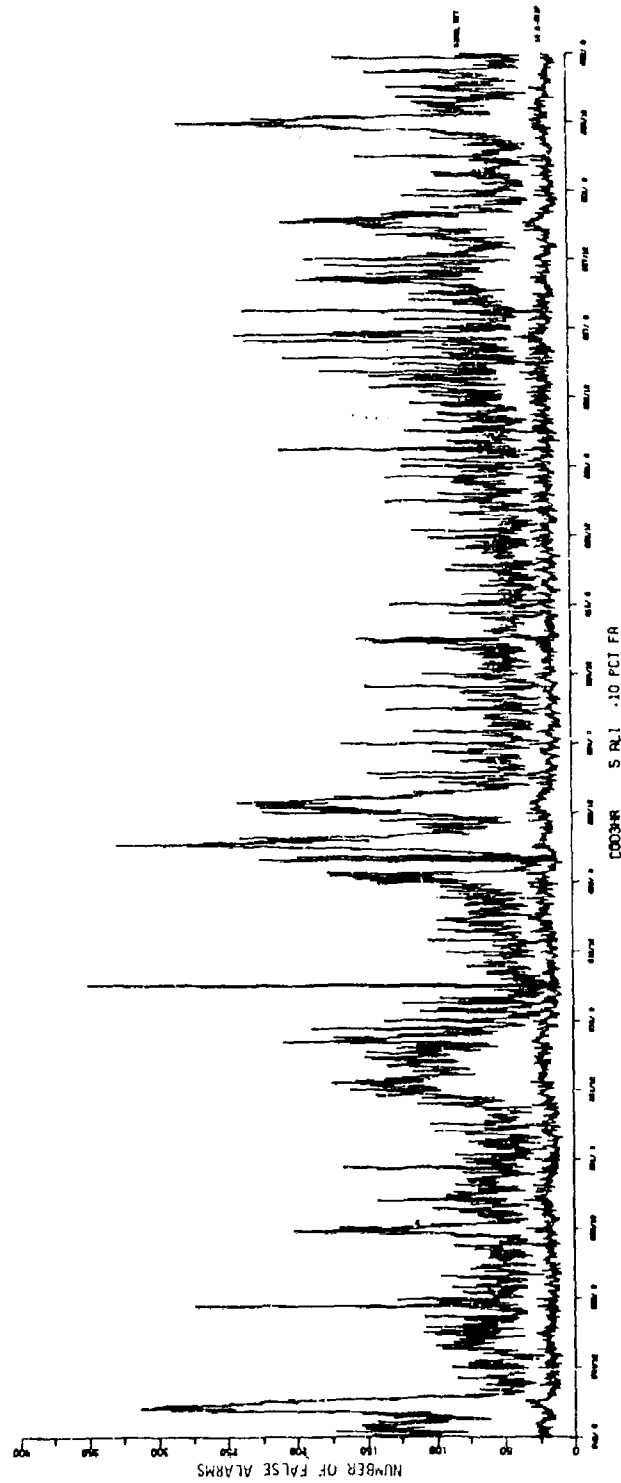
$$f_0 = \sum_i f_i P_i / \sum_i P_i,$$

where P_i is the mean square pressure at frequency f_i and the index, i , is summed over the cell group. The bandwidth of a cell group is defined to be

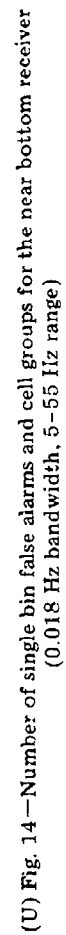
$$W_0 = \left[\sum_i (f_i - f_0)^2 P_i / \sum_i P_i \right]^{1/2},$$

which is twice the weighted RMS value.

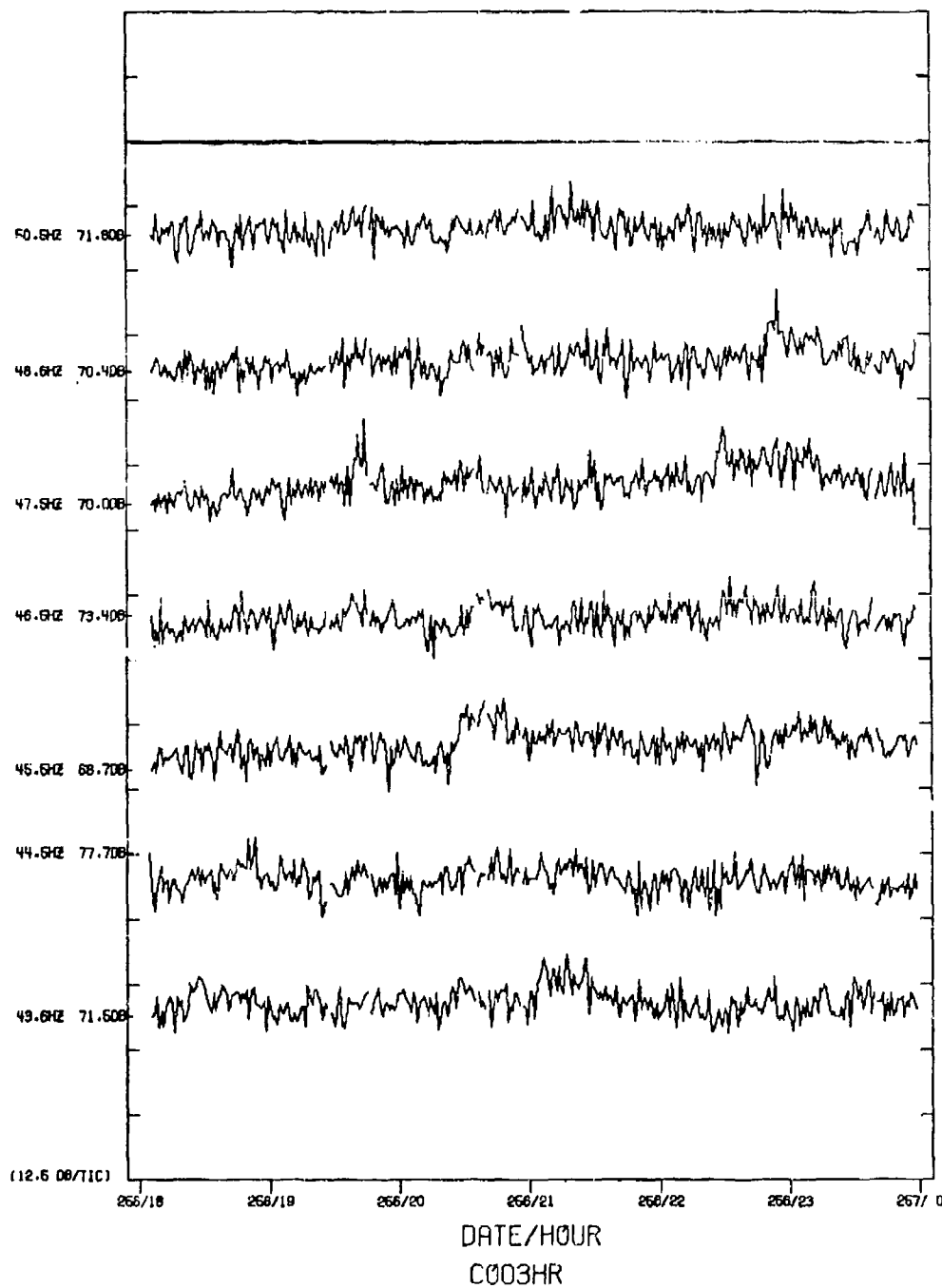
CONFIDENTIAL



(U) Fig. 13—Number of single bin false alarms and cell groups for critical depth receiver
(0.018 Hz bandwidth, 5-55 Hz range)

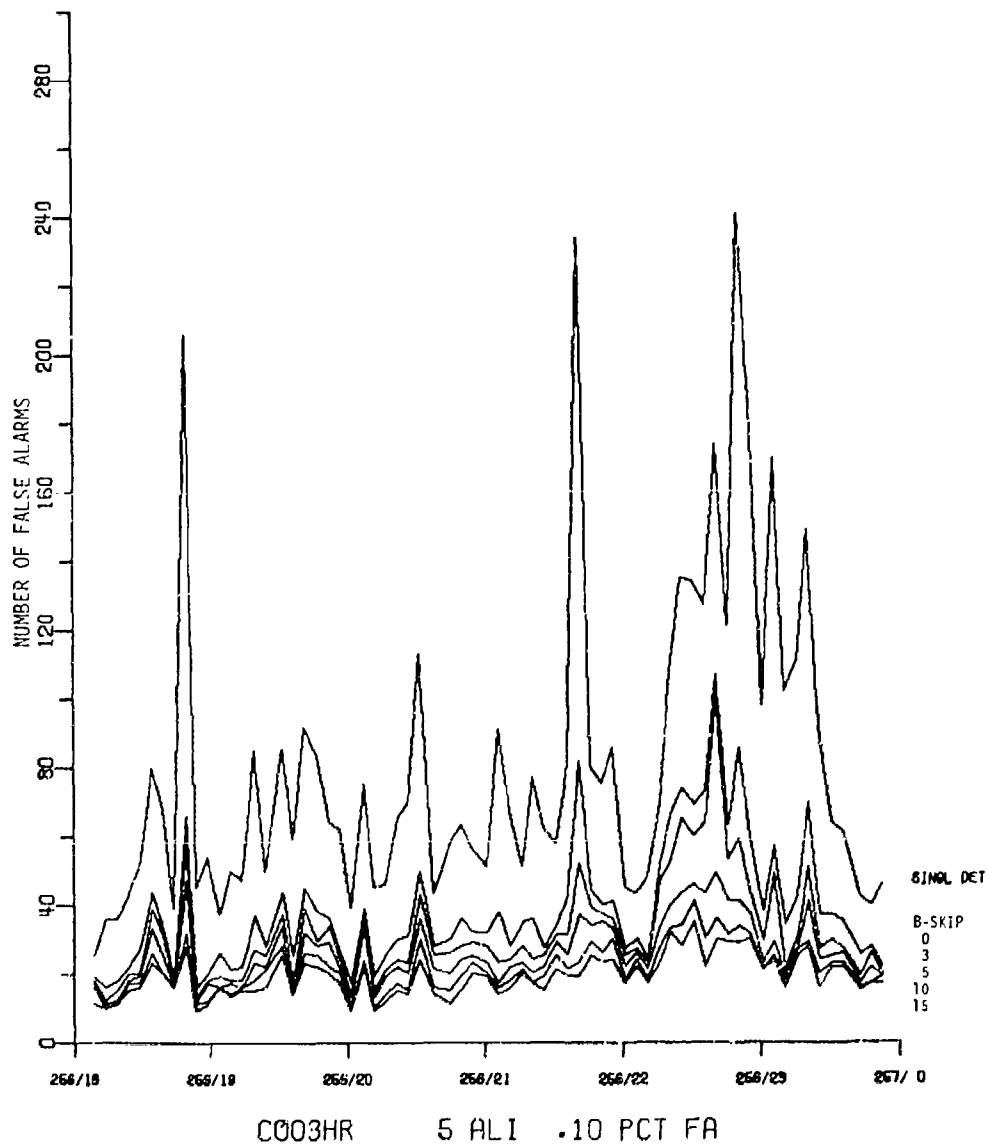


CONFIDENTIAL



(U) Fig. 15—Noise levels for critical depth receiver (0.147 Hz bandwidth, one minute samples)

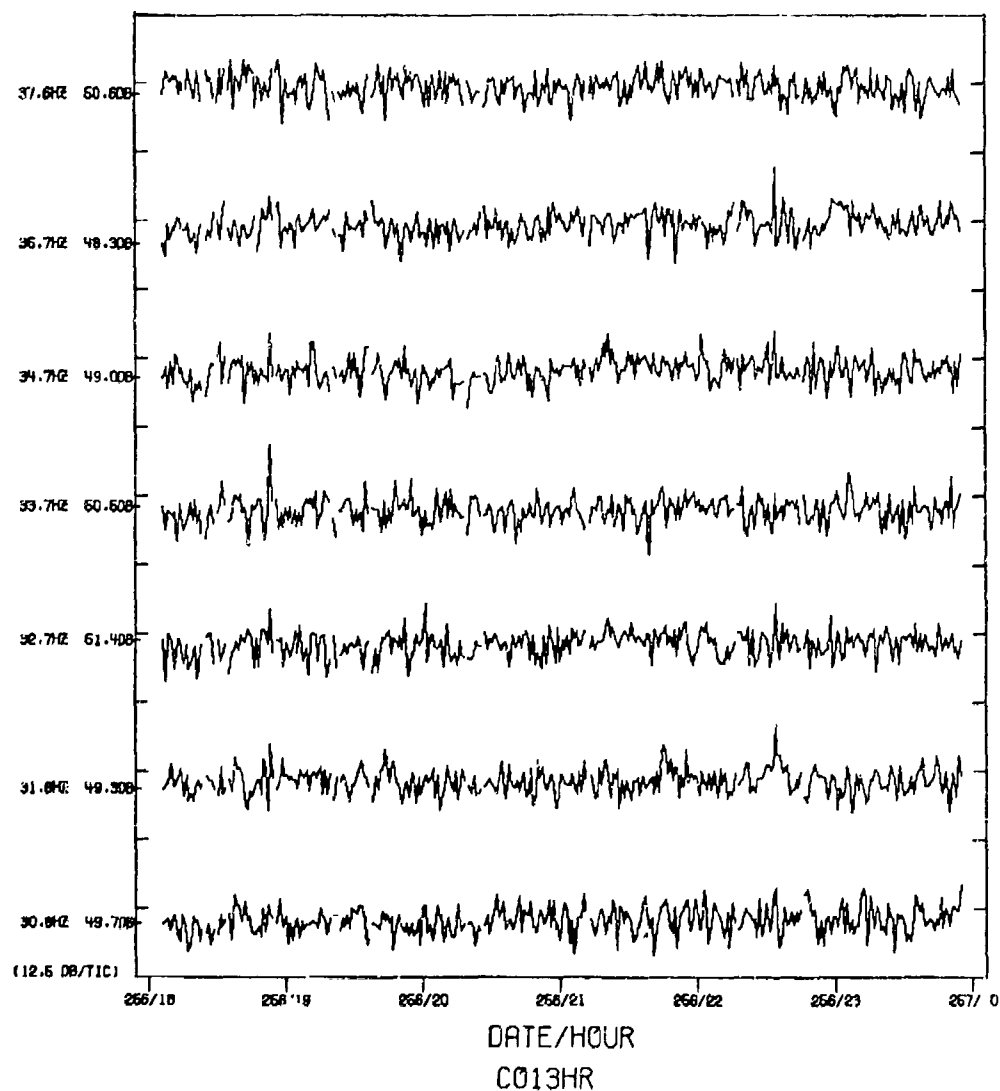
CONFIDENTIAL



(U) Fig. 16--Number of single bin false alarms and cell groups for critical depth receiver, allowing skips between detected bins (0.018 Hz bandwidth, 5-55 Hz range)

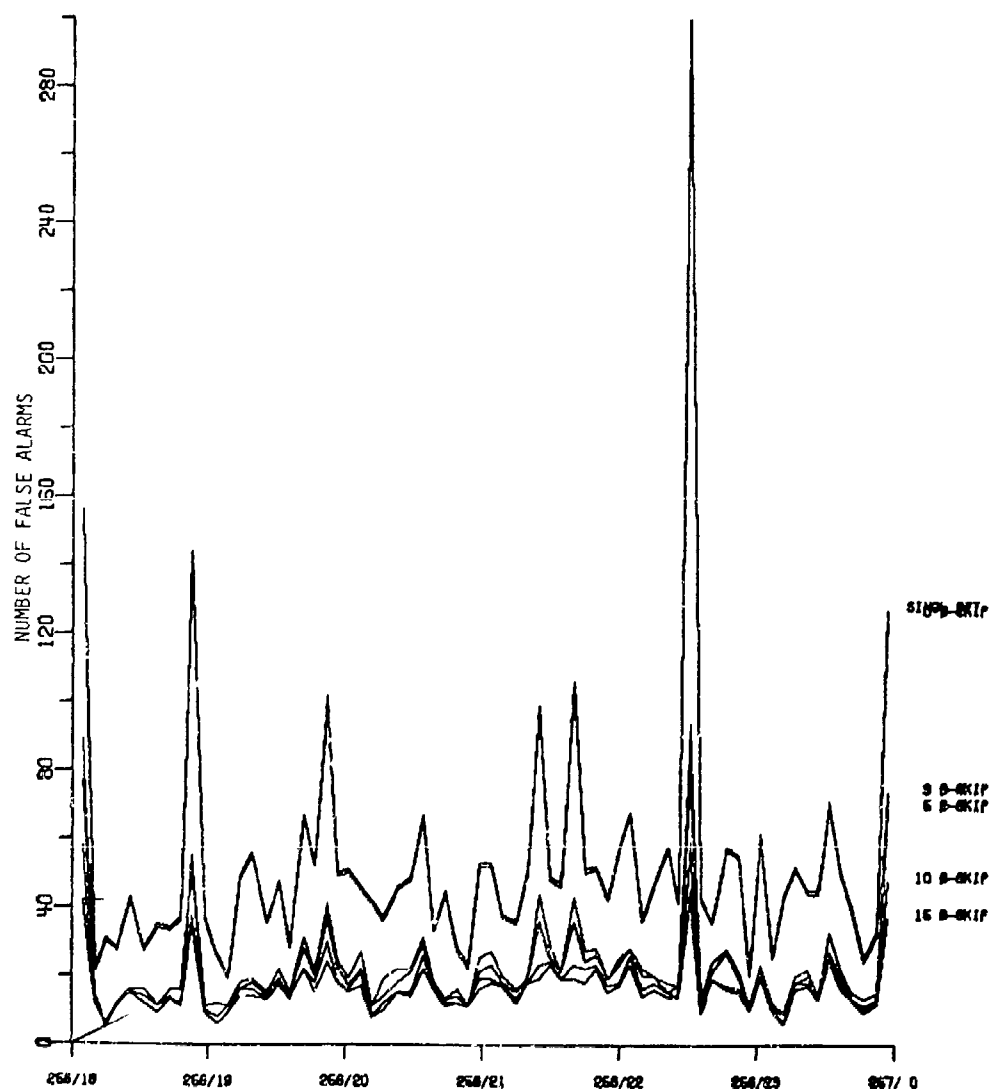
CONFIDENTIAL

CONFIDENTIAL



(U) Fig. 17—Noise levels for near bottom receiver (0.147 Hz bandwidth, one minute samples)

CONFIDENTIAL

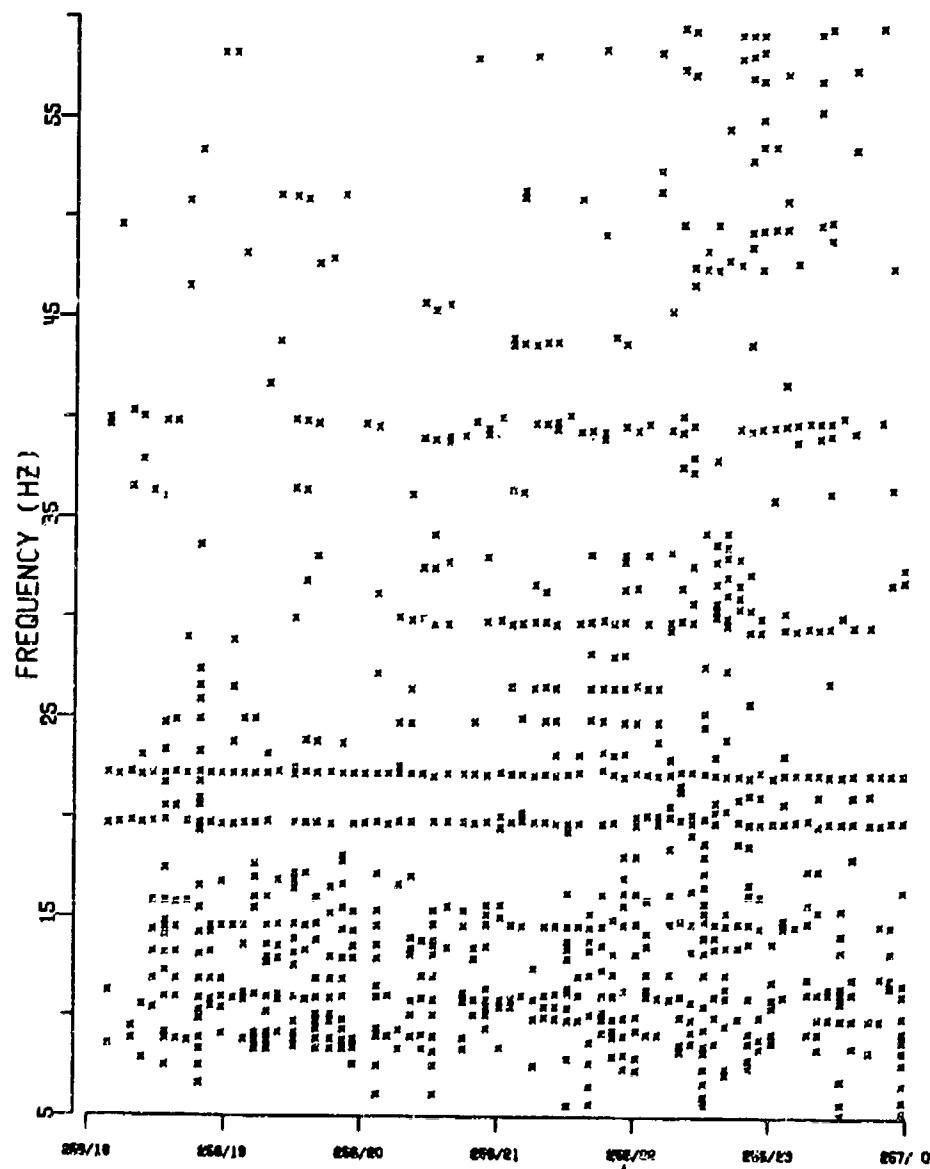


013HR 5 ALI .10 PCT FA

(U) Fig. 18--Number of single bin false alarms and cell groups for near bottom receiver allowing skips between detected bins (0.018 Hz bandwidth, 5--55 Hz range)

CONFIDENTIAL

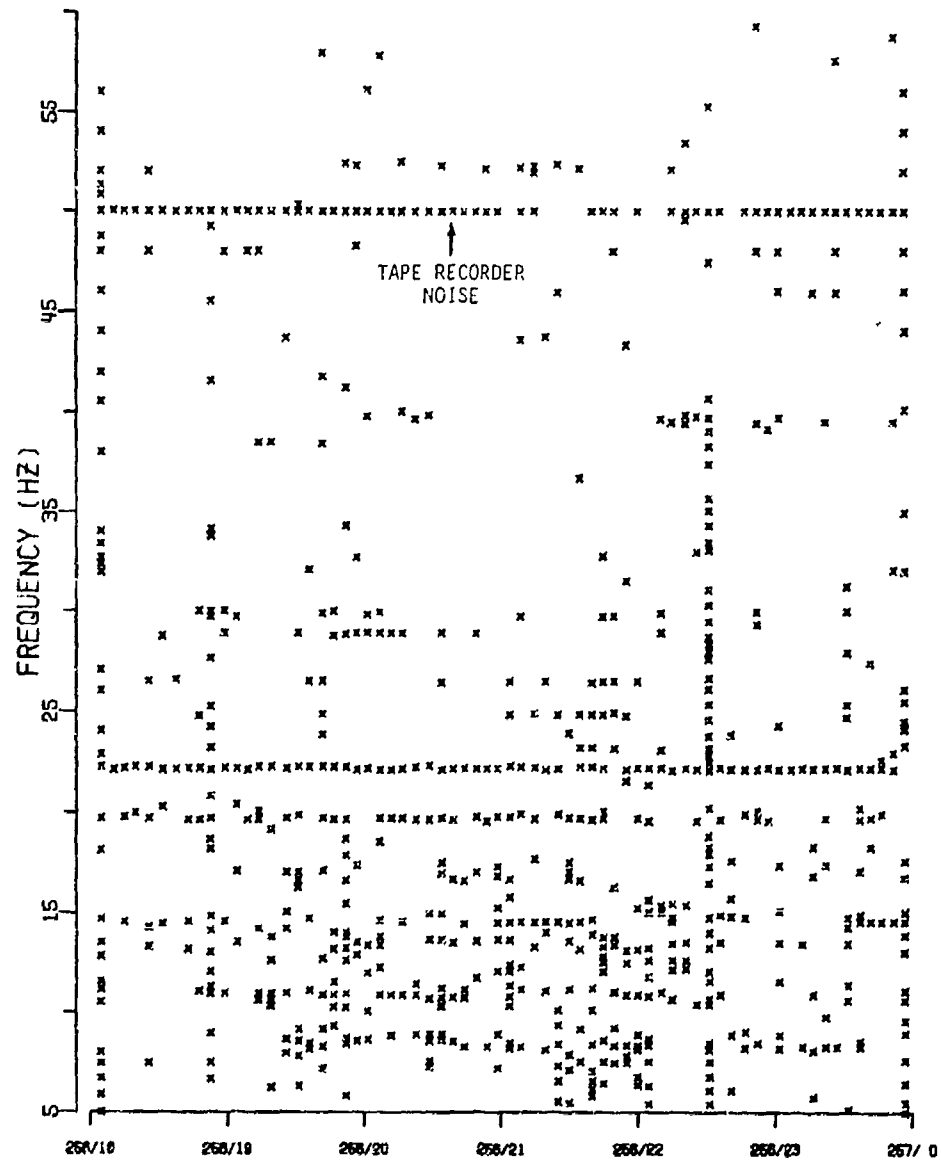
CONFIDENTIAL



0003HR .1 PCT FA
5 MIN AVG 10 FREQ BIN SKIPS

(U) Fig. 19—Cell groups or "clutter" detected by critical depth receiver

CONFIDENTIAL



C013HR .1 PCT FR
5 MIN AVG 10 FREQ BIN SKIPS

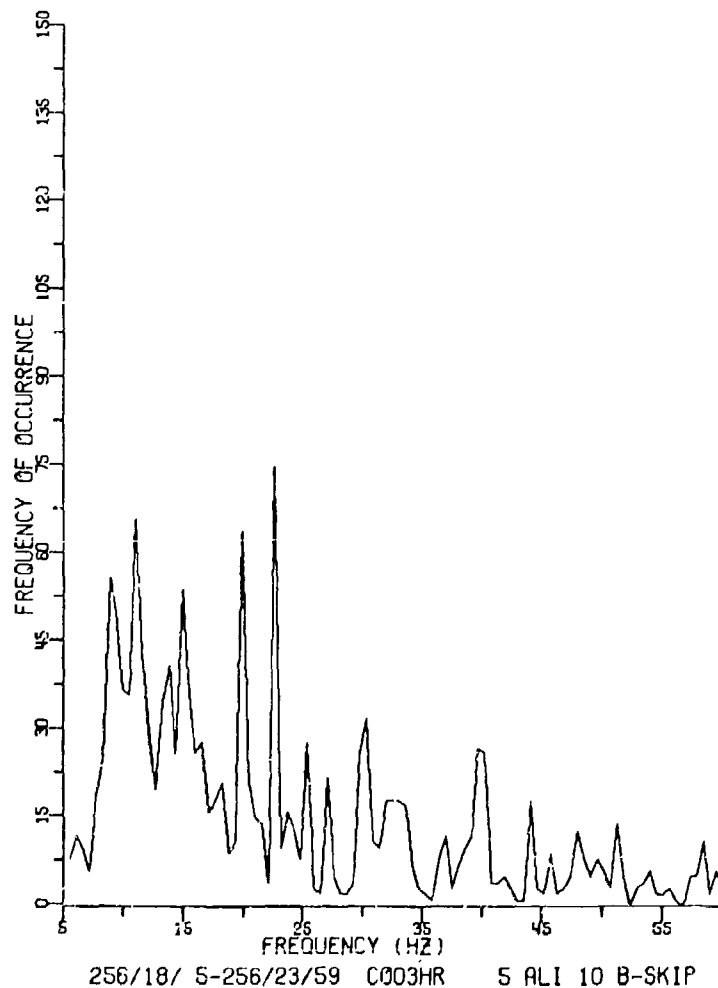
(U) Fig. 20—Cell groups or "clutter" detected by near bottom receiver

CONFIDENTIAL

CONFIDENTIAL

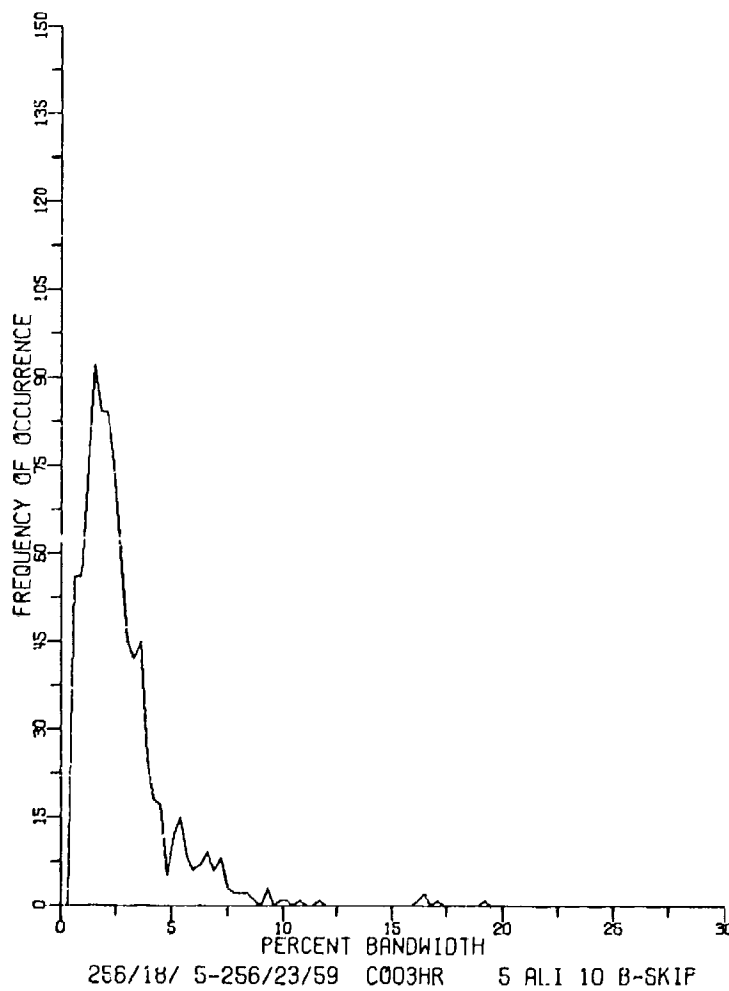
(C) A histogram of the cell group frequencies for the critical depth receiver is shown in Fig. 21 followed by Fig. 22, which is a histogram of percent bandwidths defined to be W_0/f_0 . In this case the most probable percent bandwidth was found to be 2.5%. A histogram of signal excess is shown in Fig. 23, which represents the average single bin power level of a cell relative to the average background power level. In this case all of the cell groups were lumped together and the low cutoff is determined by the 0.1% detection threshold near 5 dB, which was used for this example. The same statistical measures are shown for the near bottom receiver in Figs. 24 through 26. The peaks in the distribution of frequencies are essentially the same for both receivers. The percent bandwidth probability for the near bottom receiver peaks at a smaller value than for the near critical depth receiver and no reason is offered here as to why. The signal excess for the two receivers was about the same.

(U) These data are preliminary and the next phase of this program will be to link cell groups in the time domain to form lines so that additional measures can be made on line frequency and amplitude stability in the background noise.



(U) Fig. 21—Distribution of cell group frequencies
critical depth receiver

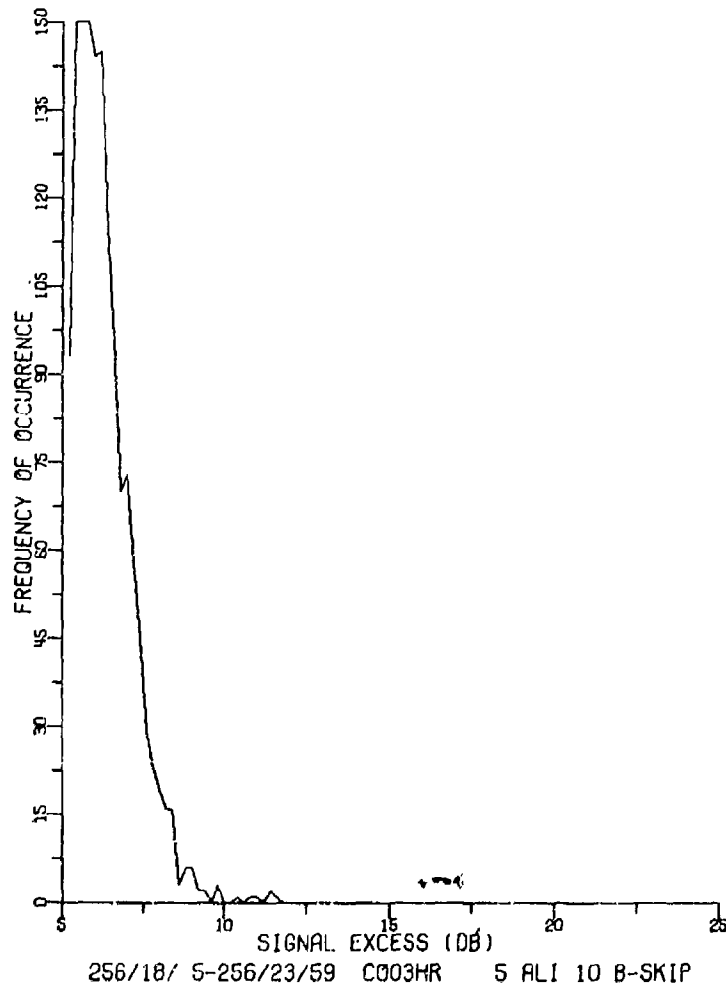
CONFIDENTIAL



(U) Fig. 22—Distribution of cell group percent bandwidths
critical depth receiver

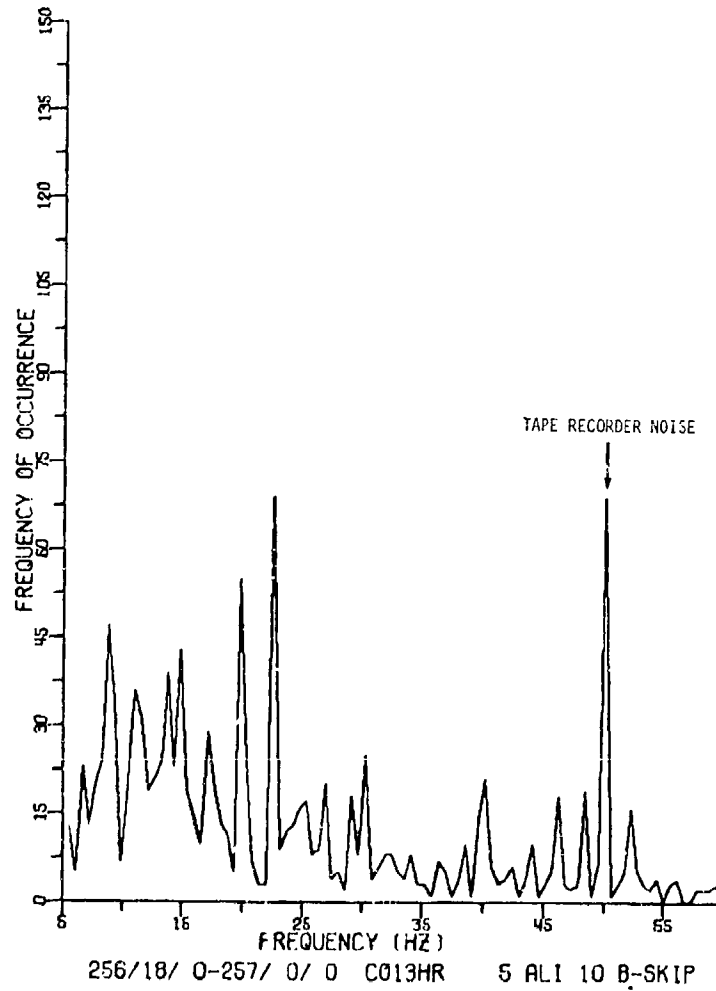
CONFIDENTIAL

CONFIDENTIAL



(U) Fig. 23—Distribution of cell group signal excess
critical depth receiver

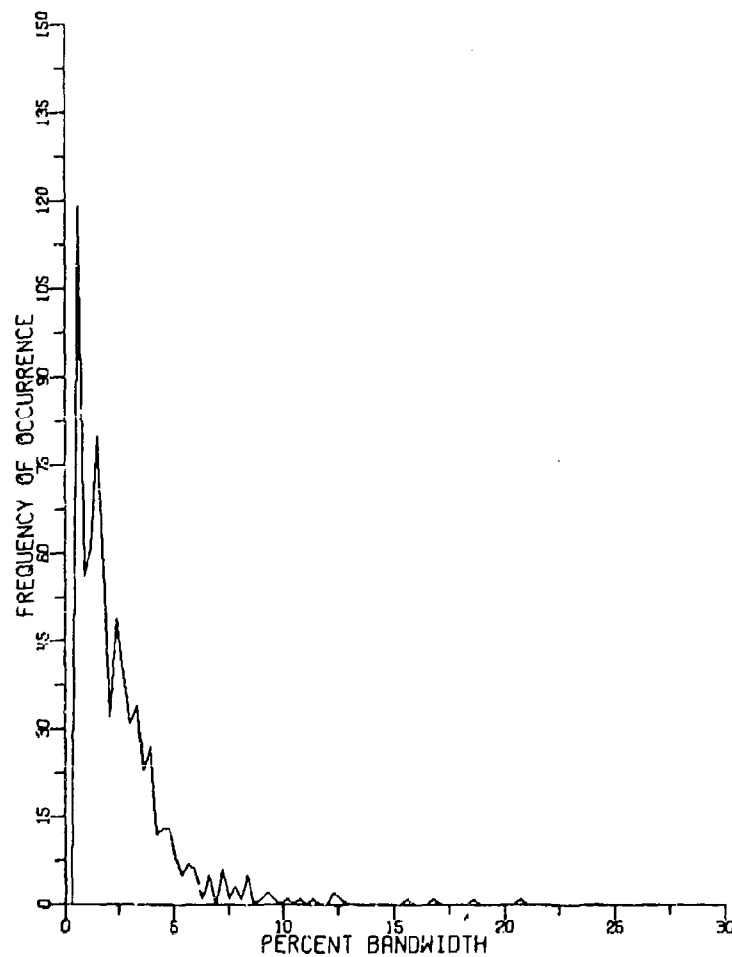
CONFIDENTIAL



(U) Fig. 24—Distribution of cell group frequencies
near bottom receiver

CONFIDENTIAL

CONFIDENTIAL

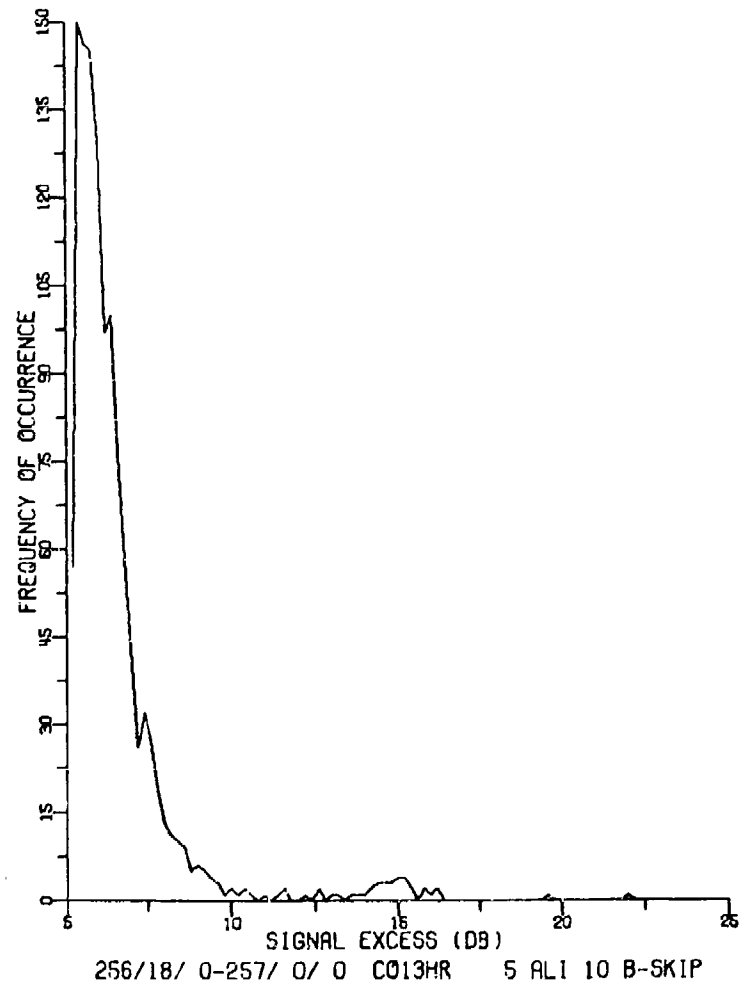


256/18/ 0-257/ 0/ 0 C013HP. 5 ALI 10 B-SKIP

(U) Fig. 25—Distribution of cell group percent bandwidths
near bottom receiver

CONFIDENTIAL

CONFIDENTIAL



(U) Fig. 26—Distribution of cell group signal excess
near bottom receiver

CONFIDENTIAL

CONFIDENTIAL

**MEASUREMENT OF CHARACTERISTICS OF AN
ACOUSTIC PROPAGATION CHANNEL BY INVERSE FILTER**

H. A. DeFerrari and R. F. Tusting

(See Volume 1 — Unclassified)

CONFIDENTIAL

MEASUREMENT TOOLS (U)

Dave Keir
Naval Electronics Systems Command
PME 124-6124
Washington, D.C. 20360

ABSTRACT

(U) Four acoustic sensor systems which can be applied to the measurement of acoustic fluctuations are discussed. These systems are the Long Bottomed Array (LBA), Mid-Frequency Array (MFA), Ocean Measurement and Acoustic Technology (OMAT) System and Versatile Experimental Kevlar Array (VEKA). These systems have been built under the auspices of various naval and defense organizations and span a variety of frequency and deployment regimes. Although most of these systems were not built for the purpose of investigating acoustic fluctuations per se each one is capable of looking into new areas of fluctuations not previously investigated.

LONG BOTTOMED ARRAY (LBA)

(C) The LBA project is sponsored by PME-124-6C. Figure 1 shows a view of the LBA which was implanted off Bermuda in November of 1977. The LBA is 8206 m in length and its 21 quad signal cable terminates at Tudor Hill Laboratories, a NUSC facility. The 21 quad cable was chosen for use as it was already terminated at the Tudor Hill Laboratories. Standard SOSUS moving coil hydrophones were recovered from antiquated systems, recalibrated and reused in the LBA.

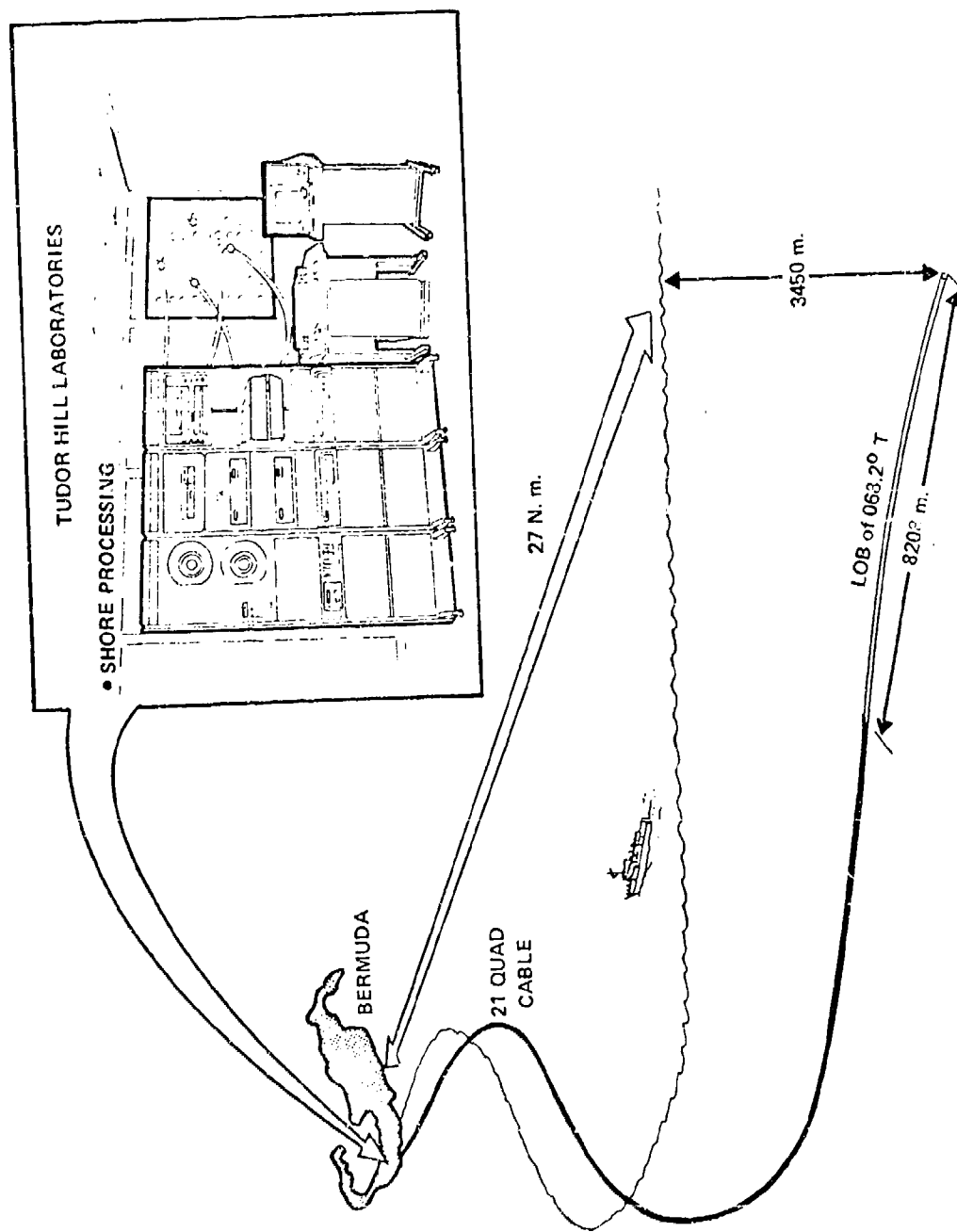
(U) The noise measurement analysis (NMA) system which can be seen in the upper right hand corner of Fig. 1 consists of: (1) an array processor for frequency analysis of up to 64 channels of data and (2) a controlling computer. A set of magnetic delay lines for beam forming and variable antialiasing filters precede the NMA system. The throughput data rate capability for the NMA is equivalent to a 40 kHz total input rate for a 50% overlap Hanning weighted FFT.

(C) Figure 2, which is to scale, shows the proposed LOB for the array at 68.2° . In laying the array, however, a 67° LOB was used. The array is in 3450 m of water and still lies well within its vertical and horizontal "lay box."

(C) Figure 3 shows an expanded view of the array which consists of 72 hydrophones. Sixty of these hydrophones have been hardwired together to form 30 hydrophone pairs. Twelve hydrophones have been left scattered throughout the array as singly wired elements. The combining of hydrophones in this way was done because of the limited number of conductor pairs. Forty-two pairs were available with the 21 quad cable. The hydrophones have a uniform spacing of 114 m with the exception of hydrophone No. 1 at the seaward end of the cable which is 228 m from its nearest neighbor. At 10 Hz the array can form 7 one degree wide beams to either side of broadside without aliasing. Additionally, 2 interstitial 1 degree beams are formed on either side of broadside and three 2 degree beams are formed utilizing one half the full aperture of the LBA.

CONFIDENTIAL

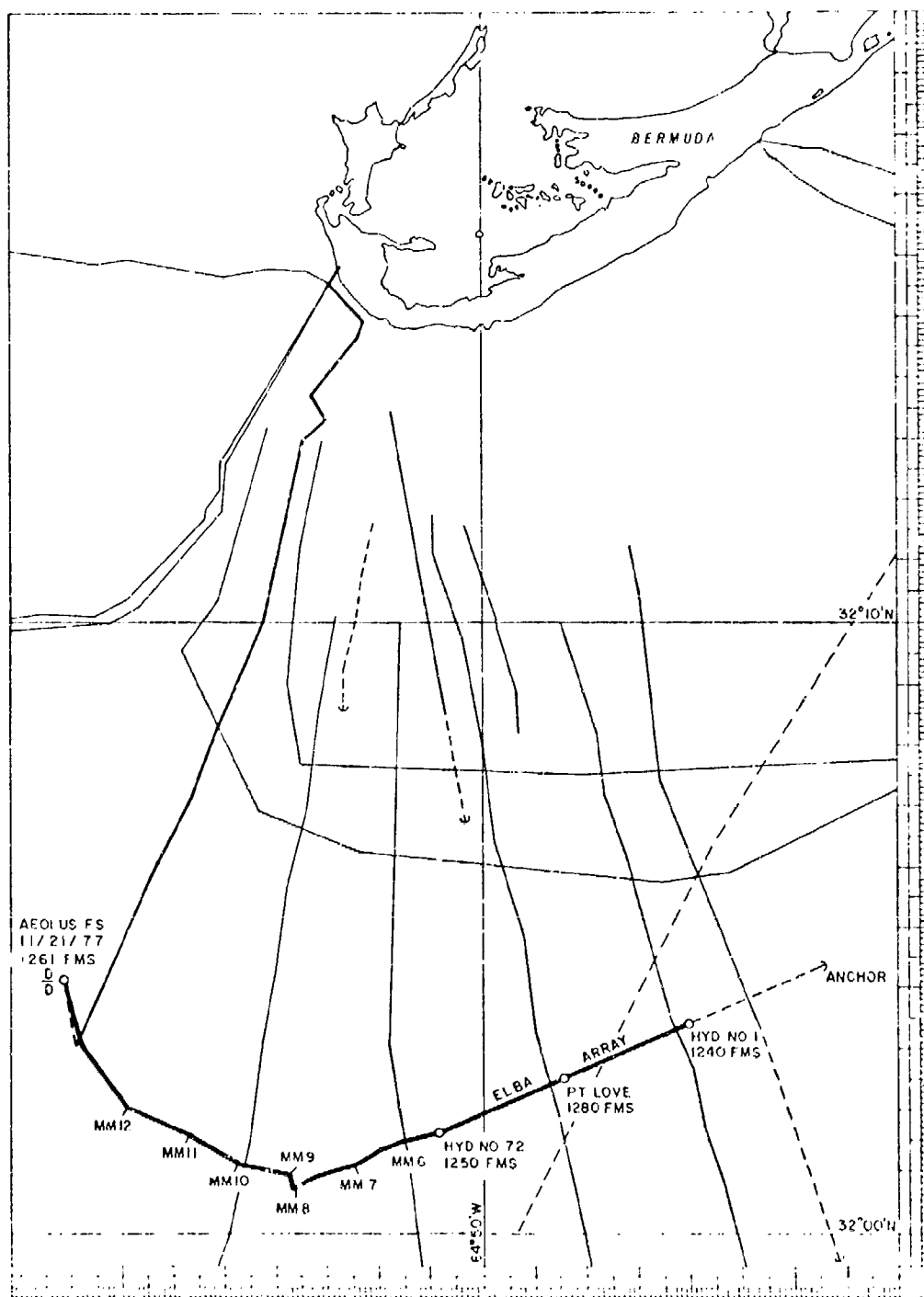
CONFIDENTIAL



(C) Fig. 1 — The long bottomed array system (U)

CONFIDENTIAL

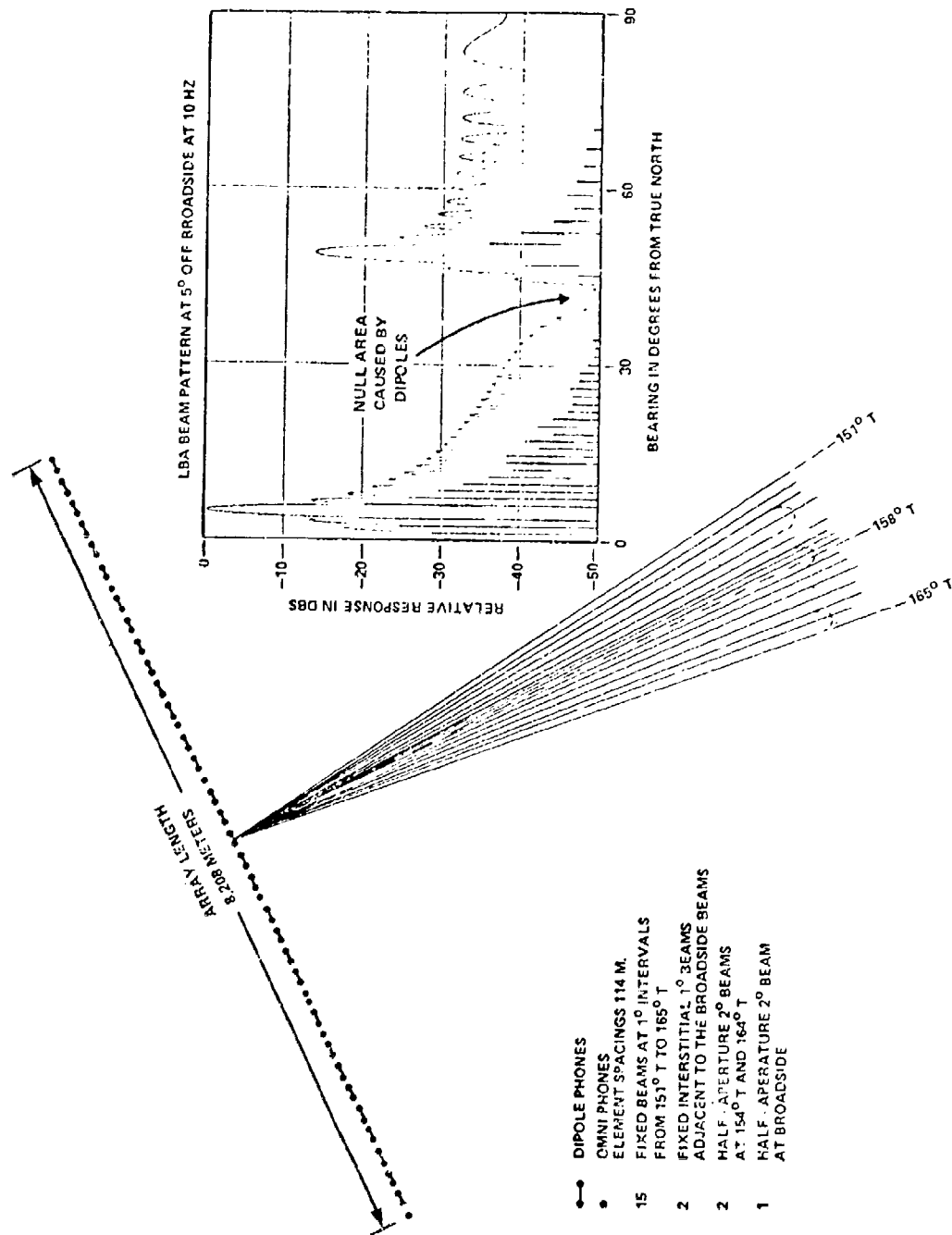
CONFIDENTIAL



(C) Fig. 2 — Proposed lab for LBA (U)

CONFIDENTIAL

CONFIDENTIAL



(C) Fig. 3 — Long bottomed array characteristics (U)

CONFIDENTIAL

(C) Figure 4 shows the geographical coverage of these beams. The new LOB points the array beams more seaward than originally planned. Because of the general orientation of the array, it is ideally situated to "look" between the ships in the shipping lanes to the south. These lanes are nearly perpendicular to the beam axis.

(U) Much of the information contained in this synopsis of LBA characteristics and capabilities was found in Ref. 1. Further inquiries regarding possible usage of the system should be directed to: Commander, Naval Electronic Systems Command, attention: Douglass W. Gaarde, PME-124-624, Washington, D.C. 20360.

OCEAN MEASUREMENTS AND ARRAY TECHNOLOGY (OMAT) SYSTEM

(C) The OMAT system is sponsored by Defense Advanced Research Projects Agency (DARPA). The OMAT system was conceived and built for the purpose of investigating the increases in array and array signal gain which might be obtained in the low frequency region from very long arrays.

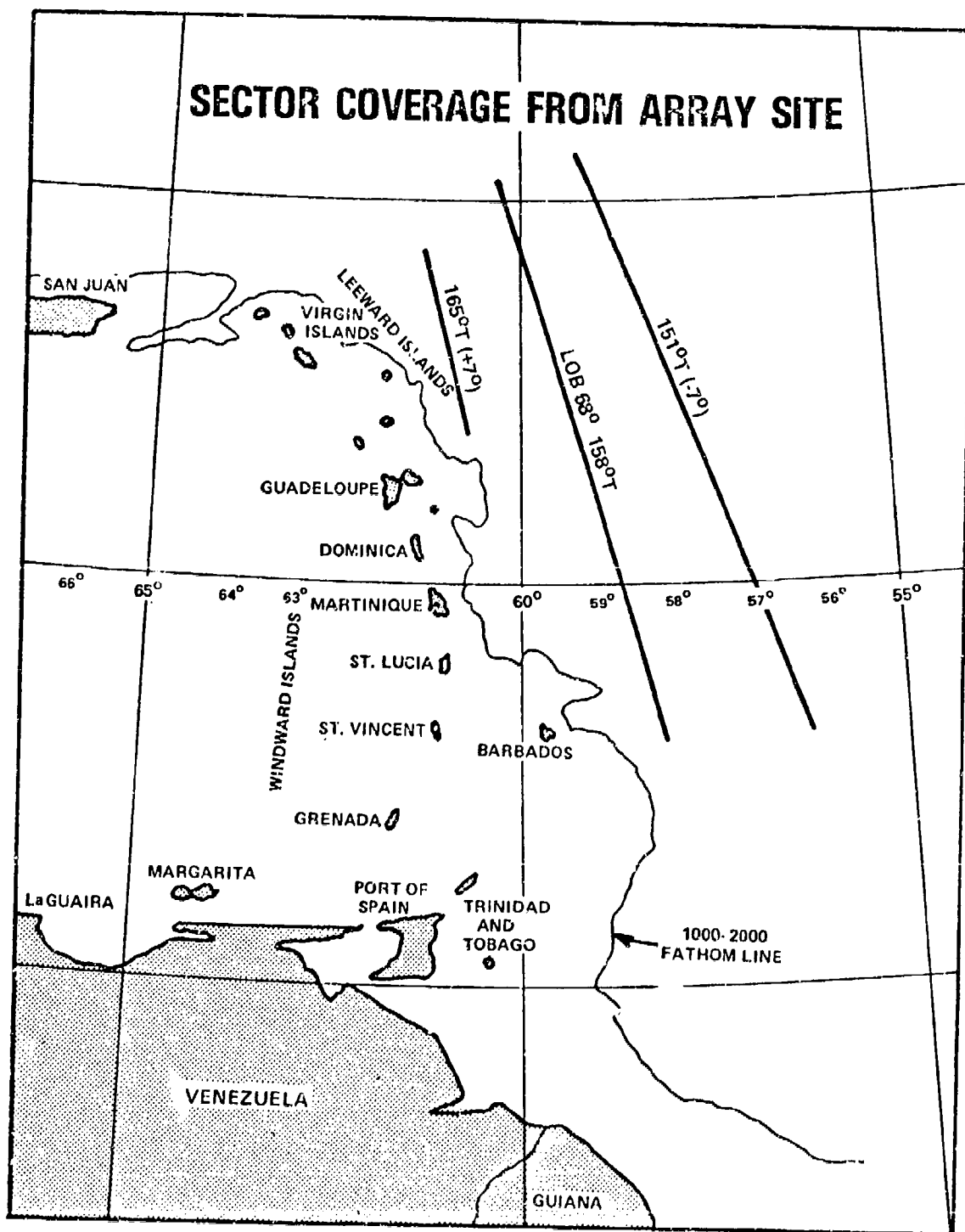
(C) Figure 5 shows a possible configuration for the OMAT system. Each of the A and B subarray modules (Fig. 6), has 60 and 55 acoustic hydrophone groups respectively and can be combined to form a symmetric geometrically tapered array of 230 hydrophone groups with 4 hydrophones per group. The individual hydrophones in each hydrophone group are 2.25 m apart. The taper ratio is 1.012 resulting in approximately a 4 to 1 ratio between the narrowest and broadest hydrophone group spacings. The OMAT system in its full configuration should be able to form beams 0.5 degree wide with adjacent clean sweep areas greater than 40 dB down and plateaus greater than 20 dB down.

(U) The necessity of calibration of the array electronics has been eliminated by utilizing a completely digital telemetry system for the acoustic and engineering data channels.

(C) Figure 6 shows possible launch configurations. The whole system can be 20 km or more in length from the end of the tag line to the array termination at the ship. In spite of its length a specially equipped LSD can launch the system in 6 hours and recover it in 12. The launch and recovery procedures have been tested for suspended operation with the system complete except for the acoustic modules of which only one small submodule was present. The submodule contained only a few acoustic channels. Several minor problems were uncovered but the test was considered to validate the basic system and the launch procedures. Other configurations have not been tested but are in practice less complex than the suspended mode of operation.

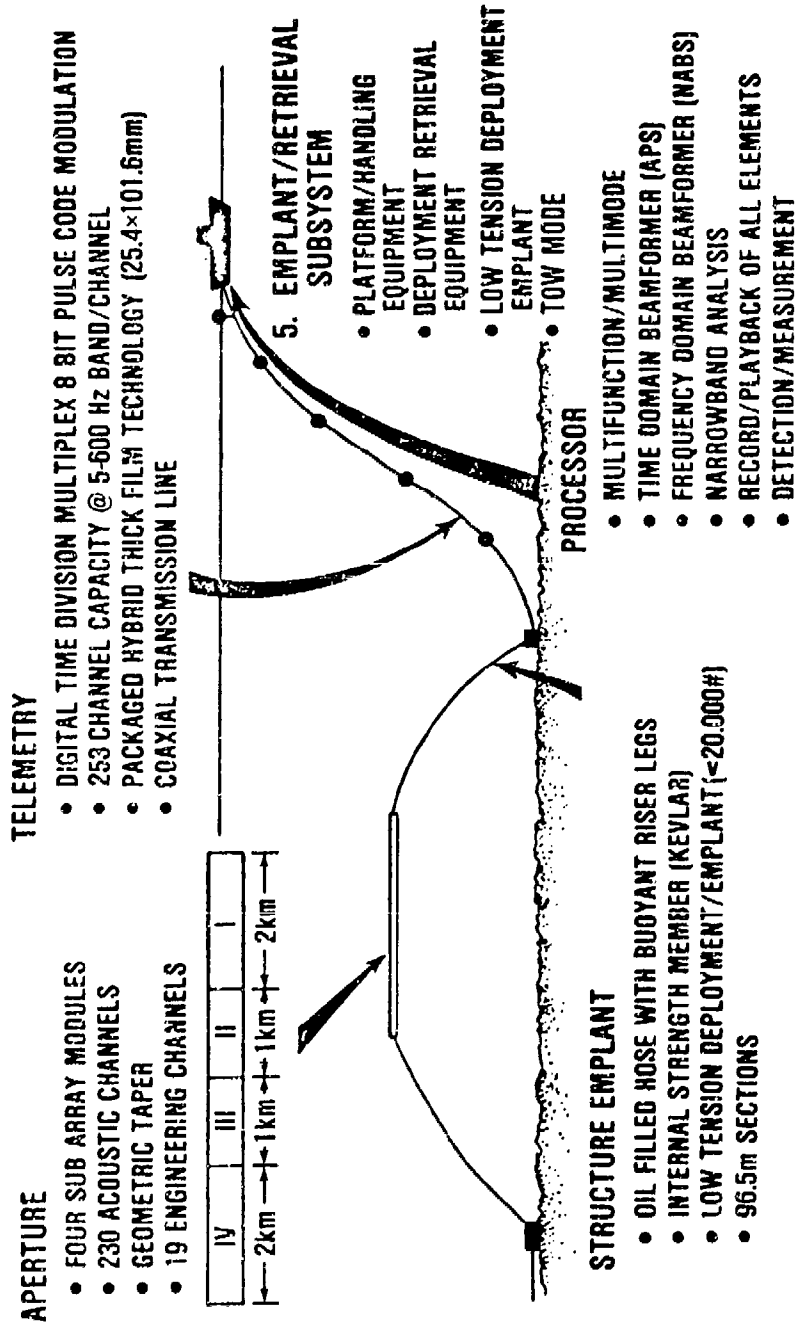
(U) In order to form optimal beams with a slowly oscillating suspended array, a high frequency projector at one end of the array will operate in conjunction with bottom mounted transponders to determine the array shape once every 15 minutes. A spare projector is mounted at the other end of the array (see Fig. 7). This transponder time delay information will be fed to a computer which will recalculate time delays to be used for each hydrophone in forming beams.

CONFIDENTIAL



(C) Fig. 4 — Geographical coverage of LBA (U)

OMAT OCEAN MEASUREMENTS AND ARRAY TECHNOLOGY

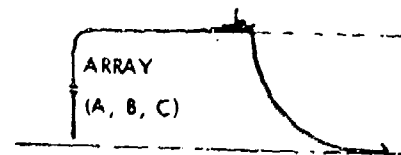
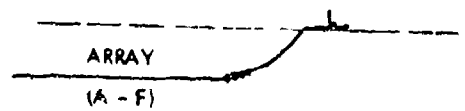
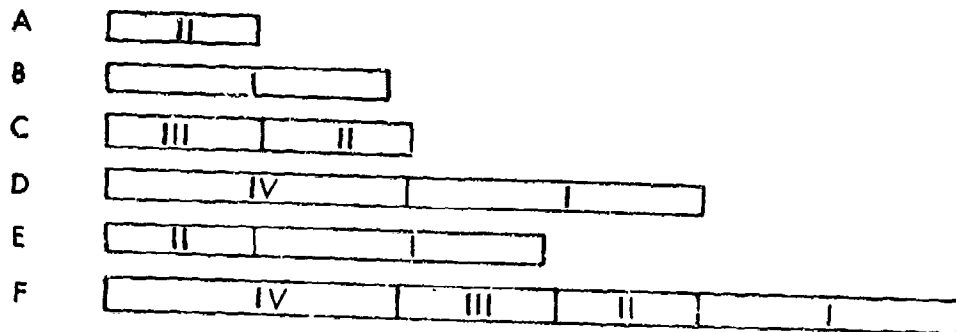


(C) Fig. 5—Ocean measurements and array technology system concept (U)

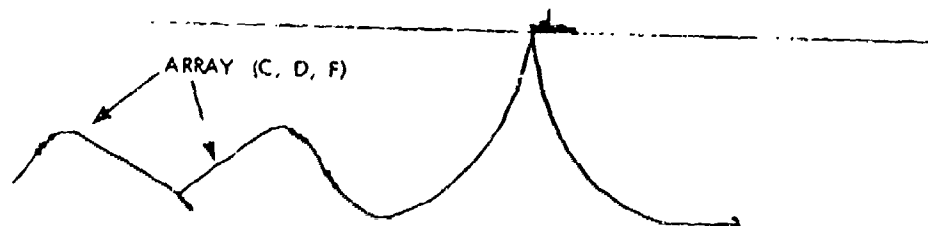
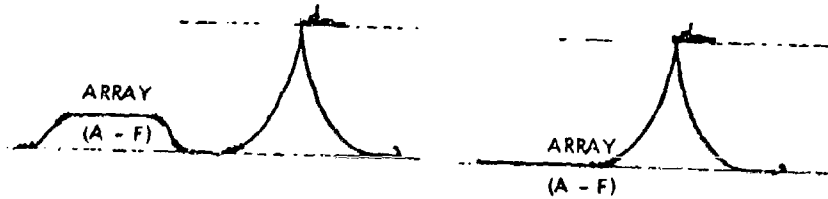
CONFIDENTIAL

CONFIGURATION

MODULES



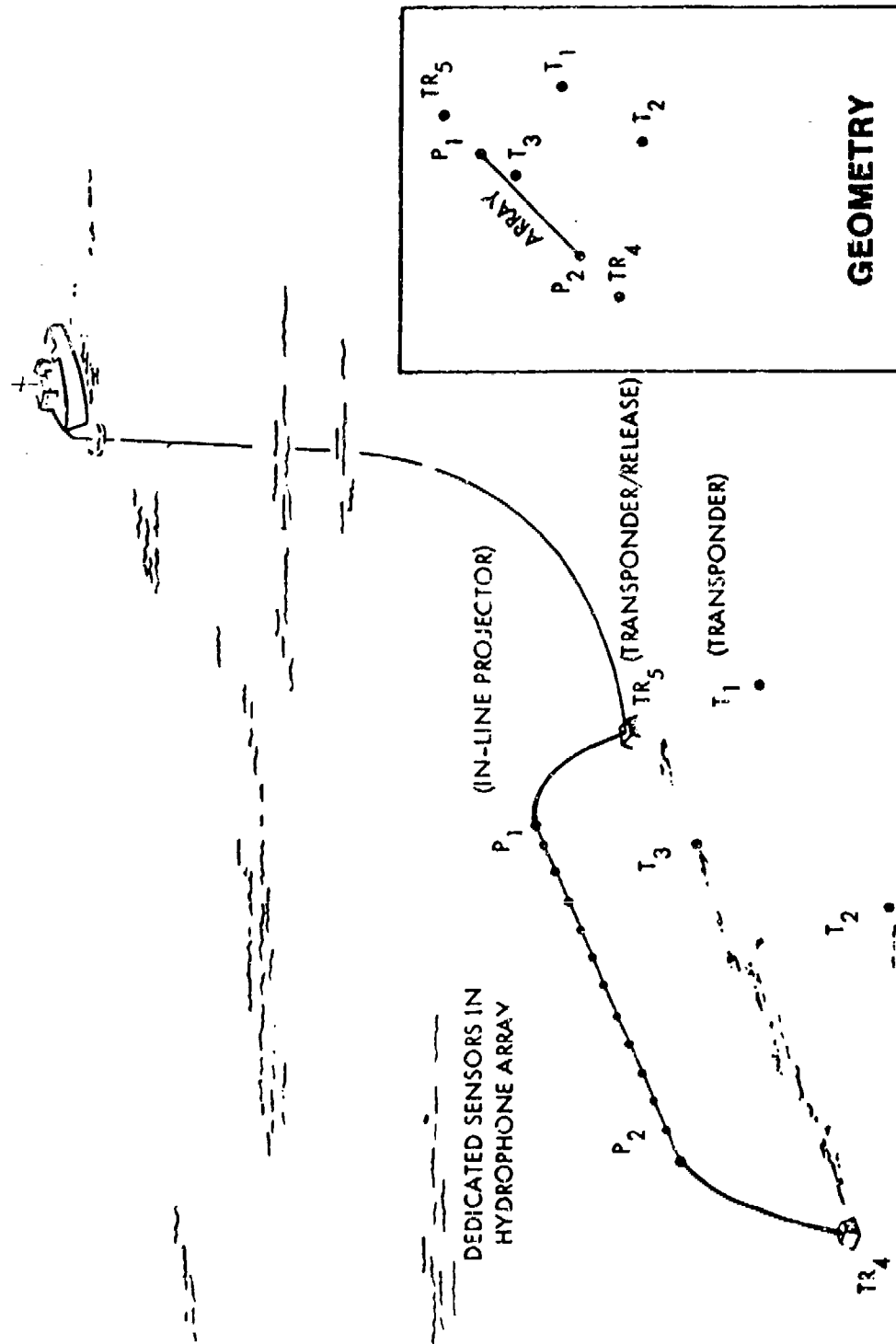
SURFACE SUPPORTED ARRAY CONFIGURATION



BOTTOM SUPPORTED ARRAY CONFIGURATIONS

(C) Fig. 6—Array configurations (U)

CONFIDENTIAL



(U) Fig. 7—Active array motion compensation system (U)

CONFIDENTIAL

CONFIDENTIAL

(C) The array has been designed for use in the very low frequency, 5 to 37.5 Hz, region. Because of the large number of hydrophone channels involved, beam forming is limited to 32 beams of 0.5° width with the beam sector centered at 30° from broadside. Frequency processing can be done with either course (1.0 Hz) or fine (0.1 Hz) resolution on any of 112 hydrophone or beam outputs. In addition 48 vernier processing channels are available with 10 and 1 mHz resolution. Sixteen lofargram channels are also present in the processing system. The computer has software for periodically calculating among other things, array shape, moments of the noise levels, histograms, spectrum level vs sensor position, and fluctuation statistics.

(U) Much of the information contained in this synopsis of the OMAT system capabilities was found in Ref. 2. Further inquiries regarding the possible use of this system for fluctuation studies should be made to: DARPA; Attn: Mr. Randy Cook; 1400 Wilson Blvd.; Arlington, VA 22209.

MID FREQUENCY ARRAY (MFA)

(C) The MFA is a system sponsored by DARPA. The MFA has been built for the purpose of investigating the limits of the increase in array and array signal gain obtainable in the mid-frequency region from very long towed arrays.

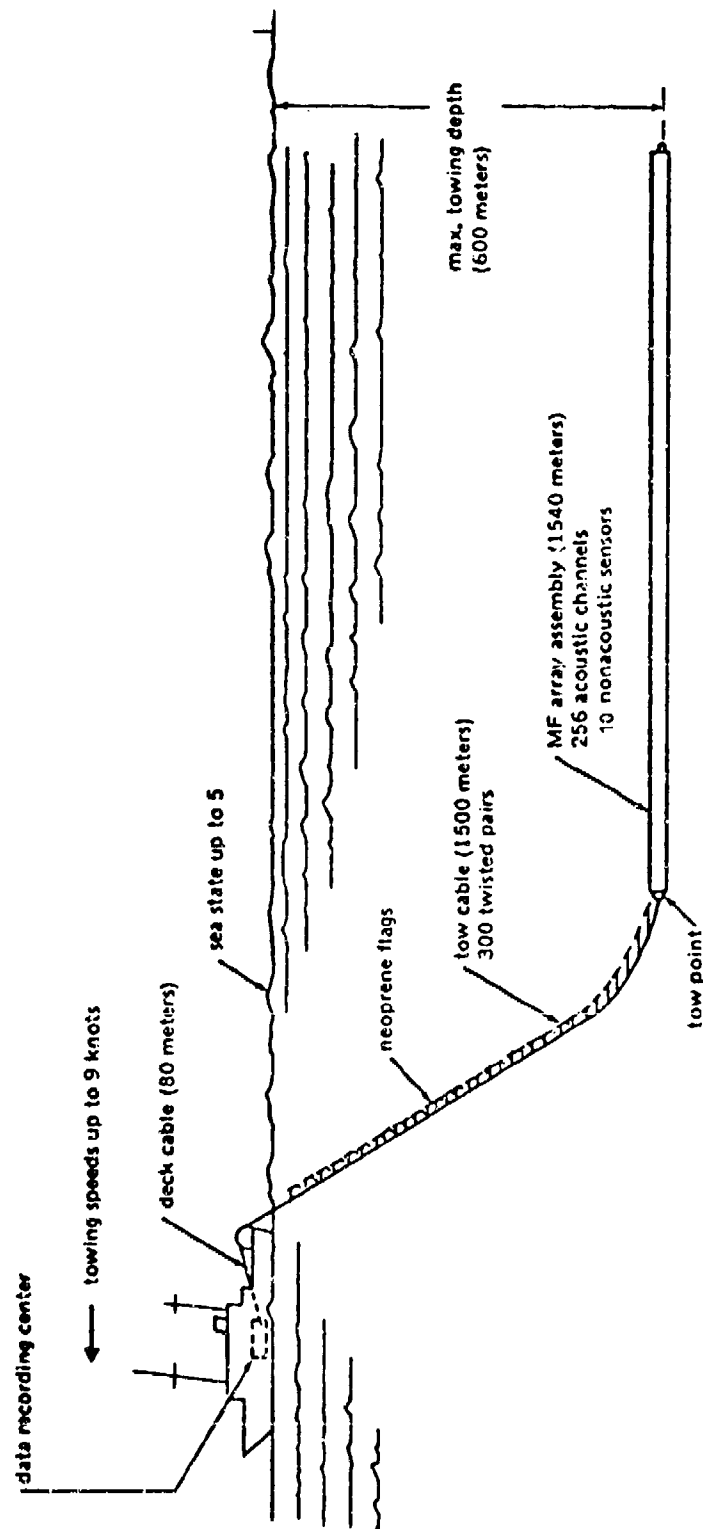
(C) Figure 8 shows a schematic of the MFA configuration. The MFA consists of 256 acoustic and 10 nonacoustic sensors. There are 4 depth and 4 heading sensors spaced evenly over the length of the active portion of the array with one heading and one depth sensor occupying a single module 7.5 m in length. The tension and temperature sensors are in a module just aft of the tow cable junction.

(C) The hydrophone groups are uniformly spaced with 2.5 m between group centers. There are four hydrophones per group to reduce flow noise and balance hydrophone acceleration. The array is designed to operate in the 25 to 300 Hz region. Three hundred twisted pairs bearing the acoustic and nonacoustic signals on board the tow ship through 1500 m of tow cable. High and low speed vibration isolation modules (VIMs) of 180 m each in length are mounted fore and a low speed VIM (180 m) only is mounted aft of the acoustic portion of the array.

(C) Before going into the beamformer the hydrophone signals are first 500 Hz low pass filtered and digitized. Because of the present limited memory capacity of the digital time delay beamformer only 32 full aperture beams or 64 half aperture or quarter aperture beams can be formed at any one time. However, different shadings and different apertures for the same steer angle may be examined simultaneously.

(U) Figure 9 shows a schematic of the data flow in the processing system. The HP 21MX-E can perform 48 1024 pt, 1/2 second FFTs every 20 seconds. Alternately, 48, channel chan, 4 freq bands/chan, 64 pt 16 sec FFTs can be performed every 15 seconds in a selected frequency band. These frequency data are stored on magnetic tape for later analysis by an HP 2100 computer and associated software. All 256 channels of time series hydrophone data are stored on HDDR tape for later playback. Real time spectrum analyzers (BQR-20, BQR-23's, HP 5420A) provide an additional frequency analysis capability.

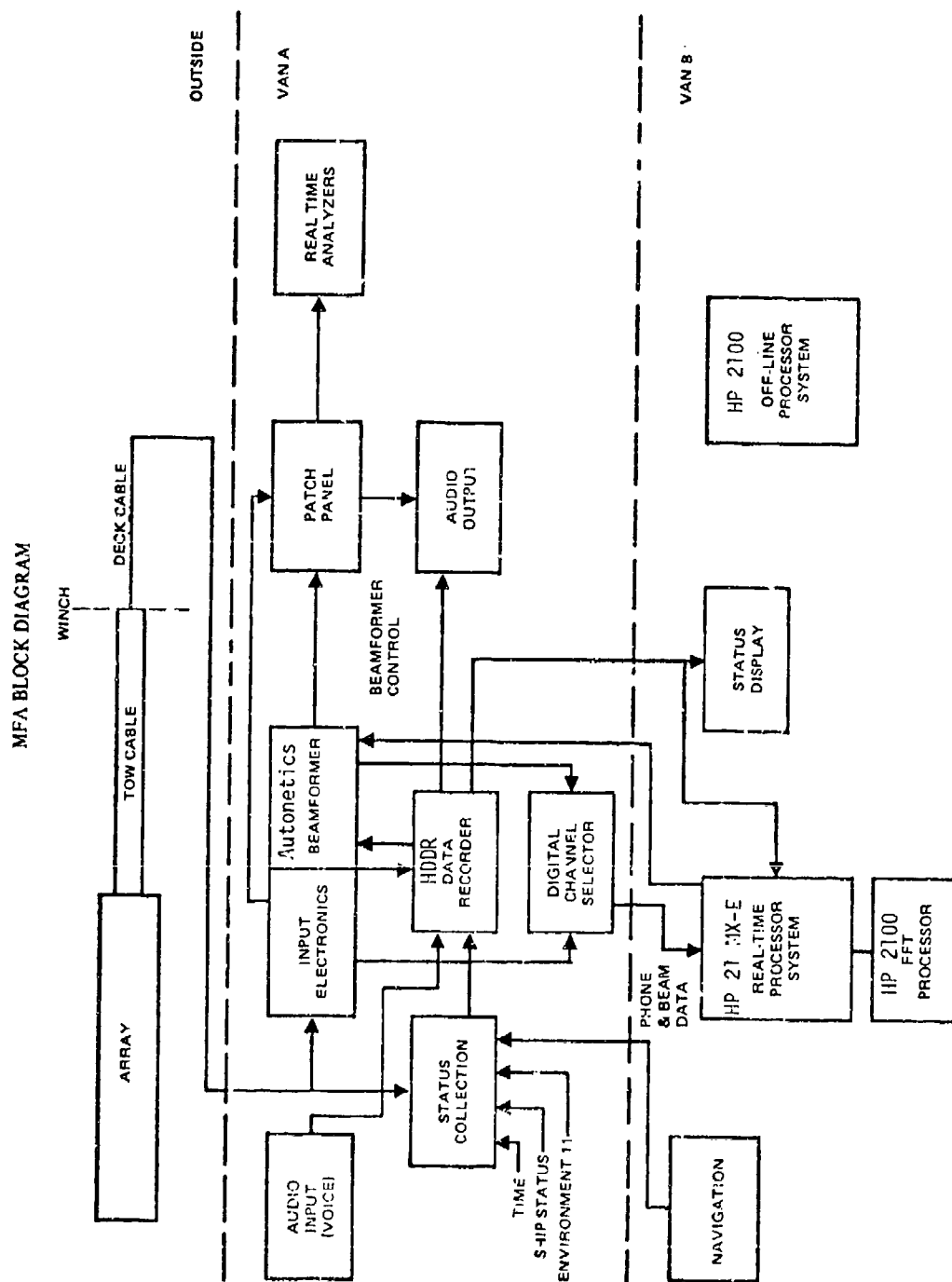
CONFIDENTIAL



(C) Fig. 8 — Mid-frequency towed array (U)

CONFIDENTIAL

CONFIDENTIAL



(C) Figure 9

CONFIDENTIAL

(C) Initial tests with this system are expected to commence this summer in the Atlantic south of Bermuda. Much of the information in this synopsis on the MFA was obtained from correspondence with Jim Reese, of Code 7111, NOSC San Diego. Further inquiries regarding the possible use of this system or its resultant data for fluctuation studies should be made to: DARPA; Attn: Mr. R. Cook; 1400 Wilson Blvd.; Arlington, VA 22209.

VERSATILE EXPERIMENTAL KEVLAR ARRAY (VEKA) SYSTEMS

(U) VEKA systems were developed by NORDA as a lightweight, shipboard configurable, acoustic measurement tool. Kevlar, a synthetic fiber, is utilized as the strength member for the array cable. As a result, hydrophones may be broken out at any point along the array and a minimal amount of flotation is needed to configure the system in any of several modes. The VEKA system can be configured as a bottomed, suspended, vertical, or towed array; the first three of which may exist in any combination.

(U) Tests off New Zealand (Ref. 3), demonstrated the easy deployability and reliability of a 6000 ft. Kevlar cabled suspended array in deep water. In December 1977 (Ref. 4), tests were conducted in the Gulf of Mexico by NORDA with a 40 acoustic and 4 nonacoustic channel VEKA. The array was 510 m and the tow cable was 1500 m in length. The array was proposed to be towed in both a horizontal and vertical configuration (see Figs. 10 and 11).

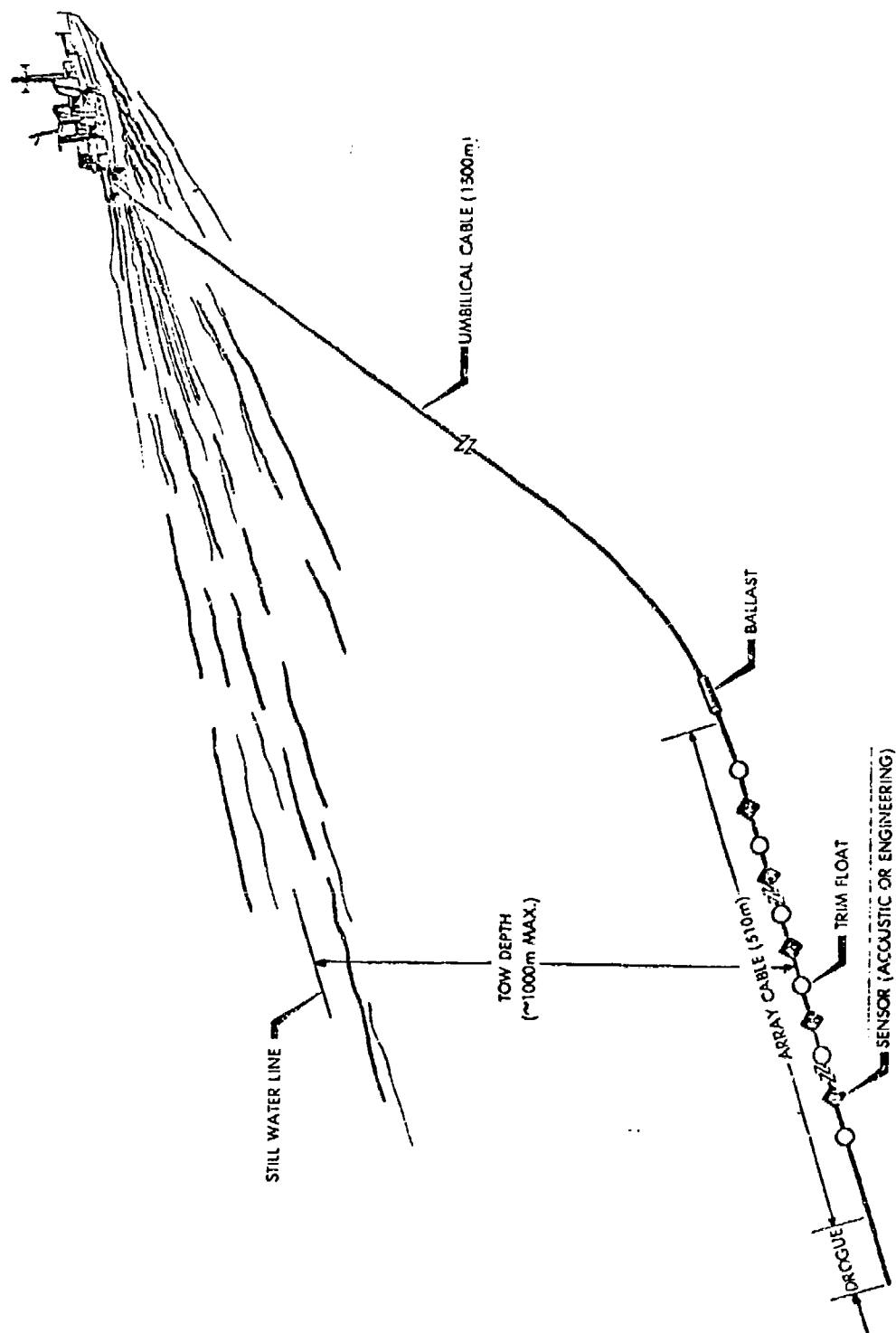
(U) Nonmultiplexed acoustic channel bandwidth of the various VEKAs is presently 5 to approximately 1000 Hz. If at some time in the future the proposed RF link from a surface buoy to the analysis ship with its concomitant multiplexing of the data channels is incorporated into the VEKA, the channel bandwidth could drop to 300 Hz depending on the number of channels incorporated into the array. A proposed VEKA system could accommodate array lengths up to 6000 m and transmission cables up to 9000 m with up to 500 hydrophones.

(U) Further information regarding present and future VEKA system capabilities and characteristics should be directed to Rick Swenson, Naval Ocean Research and Development Activity, Bay St. Louis, MS 39529.

REFERENCES

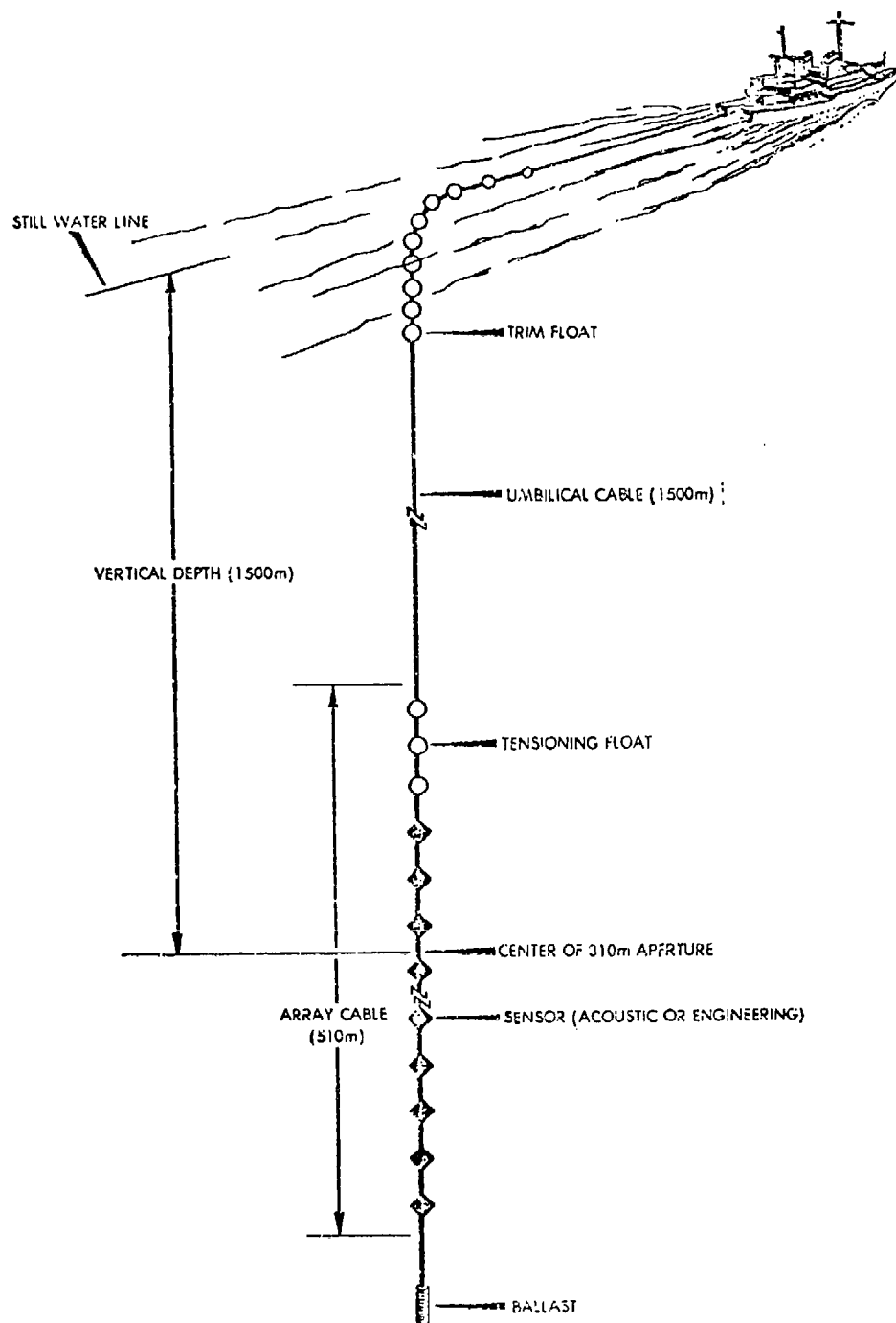
1. Confidential Report "The Long Bottomed Array (U)," by D. Gaarde, PME-124-60, dtd 4 November 1977.
2. Confidential Report "Project Seaguard (U)," by NUSC 5401-1A, dtd 19 September 1977.
3. Unclassified Report "Technical Specifications for Gulf of Mexico Array Tests Aboard USNS HAYES," by R.S. Anderson, Ocean Acoustics Division, Code 340 NORDA, dtd 3 November 1977.
4. Unclassified Report "Proposal for Lightweight Survey Array (LASA) (U)," by Ocean Technology Division, Code 350 NORDA, dtd 12 August 1977.

CONFIDENTIAL



(C) Fig. 10 — VEKA in horizontal configuration (U)

CONFIDENTIAL



(C) Fig. 11 — VEKA in vertical configuration (U)

CONFIDENTIAL

CONFIDENTIAL

APPENDIX B

SYNOPSIS OF THE FLUCTUATION WORKSHOP PAPERS NOT SUBMITTED FOR PUBLICATION (U)

(U) Of the 23 papers presented at the Workshop three were discussed in some detail in Section II of Ref. 6, while 14 have been editorially summarized in the preceding section and for five of these a synopsis was prepared because at the time no additional information was available. The one by Mr. Keir on latest arrays is included in its entirety together with all the other papers submitted for publication as Appendix A Ref. 6.

R. FLUM

(C) APETC consists of a group of engagement models devoted to detection of submarines by sonobuoys. The fluctuation aspects of the models are treated as random "draws" from a statistical population whose probability distribution *simulates* (but does not duplicate) the fluctuation of a sonar parameter. The first model, APAIR, is devoted to air launched sonobuoys. It has for each replication four Monte Carlo "draws": (1) an operator degradation factor which accounts for fluctuation in operator recognition differential (2) an environment draw, which accounts for long term fluctuation of acoustic signals, modeled as a zero mean normally distributed random variable (3) a second environment draw which accounts for the short term fluctuations in acoustic signals (4) a buoy variation draw which accounts for deployment fluctuations of buoy to buoy. The second model, APSURF, is devoted to surface launched sonobuoys. It has several Monte Carlo draws for each replication of both active and passive modes. In the active mode the draws are: (1) fluctuations in source level of a single buoy from ping to ping (2) fluctuation of sonar performance from sonar, say 3 sonars per convoy (3) fluctuation of acoustic signals with long term duration. In the passive mode the Monte Carlo draws for each replication provide estimate of standard deviation of target strength and relaxation time. The draws are: (1) an environment draw to account for long term fluctuations, (2) an environment draw to account for short term fluctuations within the duration of an integration time, (3) a similar short term environmental fluctuation associated with helicopter launched sonobuoys. The third model, APSUB, is devoted to submarine launched sonobuoys. It too has both active and passive modes. In the active mode a Monte Carlo draw provides an estimate of the standard deviation in source level from ping to ping based on transmission path. In the passive mode attention is given to fluctuations in signals propagating in paths near the surface out to convergence zones, for the geometry of one hostile submarine facing one friendly submarine. A Monte Carlo draw provides an estimate of standard deviation for this type fluctuation.

CONFIDENTIAL

(C) As an overall comment on APETC it is important to realize that there is little justification for the numbers used to correct for fluctuations. The basis of the Monte Carlo trial is the Markov chain which remains an arbitrary choice. More work is needed to help APETC. In particular, present models assume all components of the sonar equation are statistically independent. There is need to investigate the correlations between components.

(U) Concerning validation, all models have been tested. However, they have been found to be very sensitive to certain sonar parameters, particularly range of detection.

T. EWART

(U) An objective of project MATE is to study oceanographic phenomena by use of "high frequency" sound. In such studies it is important to work with a single refractive path. Hence there is a necessity to develop techniques for extracting one Fermat path from a group of multipaths. The limit on resolution of paths is the size of the Fresnel zone. To explore path isolation we have devised two experiments, both in the unsaturated regime, and have assumed that the perturbations in sound transmission are caused by internal waves. The first experiment is in a local fjord, source on one side, receiver on the other. The transmitted signal is a known waveform (narrow band, broad band, pulsed tone, etc.). The received signal is assumed to be a random time-delayed version of this waveform with random amplitude, to which ambient noise has been added during transmission. In the signal processing the techniques of inverse filtering, matched filtering and maximum likelihood have been used to obtain estimates of fluctuations in amplitude and time of arrival. It is found that maximum likelihood yields the best results. The resolution into multipaths is obtained by the technique of sequential pulsing. Data has been obtained for frequencies at 4, 8, and 13 Hz. A noticeable feature of the data is the dominating effect of tides which is clearly evident. Theoretical analysis compared with experiment showed that geometric optics gives best agreement with data on phase fluctuations, but fails to agree with data on amplitude fluctuation. The latter should be calculated from the JASON diffraction parameter.

(U) The second experiment is at the Cobb seamount, at a range of 18 km where the ocean at the depth of the experiment does fit the Garrett-Munk model of internal waves. A moored sensor was used in conjunction with a 12 Hz signal to obtain reasonable estimates of internal wave phenomena.

A. ELLINTHORPE

(C) The objective of our research is to develop an underwater communication system in which the sensors are to be mounted on the hull of warships. The intended range is 100 nmi. and the frequencies in question span 500 to 5000 Hz. Our present concern is the degrading effect on ocean-induced fluctuations. Since communication signaling is a sequence of pulses we must study the transmission of transients. A typical transient is a delta function. After transmission it is no longer a delta but appears spread out in amplitude. The amplitudes are randomly distributed. It is found that the probability is more like Rayleigh than log-normal; however, both are hypotheses.

CONFIDENTIAL

(C) Our approach is to do experiments at sea. Formerly we used the AFAR range, but we now use submarines for our communications experiments, particularly the Nautilus. When the path of the communication signal is near the surface of the sea we think we understand the propagation well enough. It is a random modulation process. Actually we use the Pierson-Moskowitz model of surface waves, and deal with a modulation of a carrier that results in two side bands. We experimented and signal processed the data to find an empirical probability distribution for amplitude of received signal. We compared this with the log normal and Rayleigh distributions, and found that the data for surface paths more nearly agrees with the Rayleigh distribution. We next undertook to study fluctuations due to internal waves. We isolated a single ray path and performed towed array experiments. In particular, we measured the variance of sound speed fluctuations with depth and found that portions of it roughly agree with the Garrett-Munk model. We then made plots of $[\mu^2(Z)]$ vs. depth, correlation time vs. frequency, and roughness scales of the bottom. Several conclusions were drawn from our work. (1) transmitted signals along direct paths which fall into the category of unsaturated statistics fits the log normal distribution, while saturated paths fit the Rayleigh distribution. (2) Bottom effects on fluctuation associated with ship motion are much stronger than volume effects. (3) Most of the experiments present evidence of good direct path propagation followed by strong randomization of received signal caused by bottom roughness. Understanding bottom effects remains to this day our chief problem.

W. JOBST

(U) When source-receiver pairs are in relative motion the acoustic field can be regarded as momentarily frozen, during which time the receiver moves through the field. The received pressure waveform is sampled by individual hydrophones of an array of hydrophones, and the spatial coherence between pairs of hydrophones can be calculated for the specific moment of freeze. In the following moment a new portion of the frozen field is sampled, and a different spatial coherence is measured. Thus the spatial coherence matrix which accounts for all pairs of hydrophones in the array becomes a function of time. A critical parameter in determining the statistics of this spatial coherence matrix is the time-bandwidth of the signal processor. Particularly, if the integration time is too long the statistics become nonstationary.

(U) It is the purpose of this study to use data from recent experiments in the Atlantic and Pacific to characterize the coherence of signals in the context of moving source/receiver.

(C) The experiment actually considered had a source centered at 88.8 Hz, and a moving receiver of conventional type. The range was 200 nmi. and reception was both on omni and on beamform. From the received data a plot of transmission loss vs. time was made, and its mean and variance calculated. Then the data was used to calculate coherence in space, time and frequency. To calculate spatial correlation coherence we took the averaging time to be 40 minutes. Although one expected (and found) quite a bit of change in ocean structure with range, the data showed that the spatial correlation index in deep ocean paths is near unity. The data was also calculated to produce plots of temporal coherence vs. time, and it was found that the decorrelation time was about 80 sec. A plot of correlation envelope vs. time was also made. The results pointed up the importance of projector motion, hence the importance of placing an accelerometer on the projector to monitor its motion.

CONFIDENTIAL

(U) As a result of the data reduction exercise reported here the *spatial coherence* of the received field was obtained as a function of array orientation, arrival angle of the multipath and spread in arrival angles over different multipaths; the temporal coherence was obtained as a function of the source ship speed; and the frequency coherence was obtained as a function of time.

CONFIDENTIAL

CONFIDENTIAL

APPENDIX C
A REVIEW OF SIGNIFICANT PAPERS ON
FLUCTUATIONS AT THE 94th ASA MEETING

S. Hanish

(See Volume 1 -- Unclassified)

CONFIDENTIAL

APPENDIX D

BIBLIOGRAPHY (U)

A

AESD Fluctuations Workshop, Encl (1) to AESD ltr to LRAPP mgr. AESD:PRT:ke
Ser: S269 of 8 May 1974.

APAIR MOD 2, ASW Programs Air Engagement Model (U), Vol. I, Part 1: Users Manual
(Uncl) (AD 860 261L), Systems Analysis Office Report (SAOR) 69-10 June, Prepared by
J.D. Kettelle Inc.

APAIR MOD 2.5, ASW Programs Air Engagement Model (U), Users Manual (Uncl)
(AD 872 929L), SAOR 70-3 Feb., Prepared by J.D. Kettelle, Inc.

APAIR MOD 2, ASW Programs Air Engagement Model (U), "Evaluation of APAIR Air
ASW Engagement Model Passive Acoustic Detection Phase (U)" (Conf) SAOR 70-6
(AD 513 215), Prepared by C.W. Kissinger.

APAIR MOD 2.6, ASW Programs Air Engagement Model (U), Vol. I: Users Manual (Uncl)
SAO Tech. Memo 71-12 July, (AD 890 139L), Prepared by J. McCain and J. Parkerson.

APAIR MOD 2.6, ASW Programs Air Engagement Model (U), Vol. II: Programmers Manual
(Uncl), ASW Document 75-102, Jan., (AD B00 G017L), Prepared by J. Parkerson.

APAIR MOD 2.6, ASW Programs Air Engagement Model (U), "Evaluation of APAIR Air
ASW Engagement Model Localization and Attack Phases (U)" (Conf), ASW Report 14-72-1
(AD 529 362L).

APSUB MOD 2, ASW Programs Submarine Engagement Model (U), Vol. I: Technical
Description (Conf), Naval Weapons Laboratory Technical Report 2858 (AD 525 118L).

APSURF MOD 1, ASW Programs Surface Ship Engagement Model (U), Vol. I, Part 1
(Sec. 1-5): Users Manual (Uncl), Prepared by J.D. Kettelle, Inc., Systems Analysis Office
Report 68-16 Jan. (AD 881 385L).

APSURF MOD 1, ASW Programs Surface Ship Engagement Model (U), "A Destroyer
Passive Sonar Simulation for the ASW Programs Surface Ship Engagement Model (APSURF)
(U)," ASW Document 74-002 (Uncl), (AD-B014259L), Prepared by J. Mandelbaum.

APSURV MOD 1, ASW Program Surveillance Model (U), Vol. I & II: Abstract/Analyst's
Manual (SECRET) (AD 513 177L); Vol. III: User's Manual (Conf), (AD 513 178L), SAOR
70-11 Oct., Prepared by Tetra Tech.

APSURV MOD 1.4, ASW Programs Surveillance Model (U), Vol. I & II: Abstract/Analyst's
Manual (U) (SECRET) ASW Document 75-103, July, (AD C003 350L), Prepared by E. Dunn.

CONFIDENTIAL

CONFIDENTIAL

B, C, D

Baker, C.L. and Spofford, C.W., "The FACT Model," Vol. II, AESD Tech Note TN-74-04; ONR; Arlington, VA, (1974).

Barbour, D., "Time-Difference and Doppler Difference Errors (C)," NOSC San Diego, CA, CMAP Progress Report No. 77-010, (1977).

Beam, J.P., "Coherence Workshop," *U.S. Navy Journal of Underwater Acoustics*, Vol. 26, No. 3, (1976).

Beyan, M.J. and McCoy, J.J., "Propagation of Radiation from a Finite Beam or Source Through an Anisotropic Random Medium."

Belkin, B., "Analytical Results for the Step Process and Gauss-Markov Process in Passive Detection Problems," *Proceedings of the First Workshop on Operations Research Models of Fluctuations Affecting Passive Sonar Detection*, DTNSRDC, Carderock, MD, (1975).

Bendat, J.S., "Principles and Applications of Random Noise Theory," Wiley, New York, (1958).

Birdsall, T.G., "On Understanding the Matched Filter in the Frequency Domain," *IEEE Trans. Educ.*, 19, 168-169 (1976).

Brock, H.K., "The AESD Parabolic Equation Model," AESD TN-75-07; ONR; Arlington, VA (1975).

Cavanagh, R.C., "Acoustic Fluctuation Modeling and System Performance Estimation," Vol. I & Vol. II (Appendices) SAI-79-737-WA, (1978).

Clay, C.S., "Interference of Arrivals in Continuous Wave Transmission Experiments," Meteorology International Inc., Tech Note Four Project M-153 (1968).

Conover, W.J., "Practical Nonparametric Statistics," J. Wiley & Sons, New York (1971).

Cornyn, J.J., "A Computer Model of an Underwater Acoustics Towed Array," Vol. I, General Description NORDA Report (in press) 1978.

Cramer, H., "Mathematical Methods of Statistics," Princeton University Press, Princeton, NJ, (1946).

Dashen, R., "Path Integrals for Waves in Random Media," JSR-76-1 (SRI, Menlo Park, CA, 1977).

Davenport, W.B. and Root, W.L., "An Introduction to the Theory of Random Signals and Noise," McGraw-Hill, New York, NY, (1958).

Defense Intelligence Agency, "Radiated Noise Levels from Foreign Ships."

CONFIDENTIAL

D, E, F, G

Doles, J.H., III, "A Simple Model of Source Motion Induced Transmission Fluctuations with Application to Beam Noise Fluctuations (U)," Bell Laboratories Report, Contract N00039-76-C-0122, November 1976.

Doob, J.L., "The Brownian Movement and Stochastic Equations," *Annals Math.* 43, 351-369, (1942). Reprinted in: Wax, N. (Ed.), "Noise and Stochastic Processes," Dover, New York, (1954).

Doob, J.L., "Stochastic Processes," Wiley, New York, (1953).

DTNSRDC; "Proceedings of the 1st Workshop on Operations Research Models of Fluctuations Affecting Passive Sensor Detection," Vol. I, C, Vol. II, S, (1976).

Dyer, I., "Statistics of Sound Propagation in the Ocean," *JASA* 48, 337-345 (1970).

Dyer, I., "Statistics of Distant Shipping Noise," *J. Acous. Soc. Amer.* 53, 2, 564-570.

Dyson, F., Munk, W. and Zetler, B., "Interpretation of Multipath Scintillations Eleuthera to Bermuda in Terms of Internal Waves and Tides," *J. Acoust. Soc. Am.*, 59, 1121-33, May 1976.

Feller, W., "An Introduction to Probability Theory and Its Applications," Vol. I, Wiley, New York (1957).

Feller, W., "An Introduction to Probability Theory and Its Applications," Vol. II, Wiley, New York (1966).

Flatte, S.M. and Tappert, F.D., "Calculation of the Effect of Internal Waves on Oceanic Sound Transmission," *JASA* 58, 1151-1159, (1975).

Flatte, S.M., Dashen, R., Munk, W.H. and Zachariasen, F., Stanford Research Institute, "Sound Transmission Through a Fluctuating Ocean," Technical Report JSR-76-39; May 1977.

Floyd, E.R. and Gordon, D.F., "Effects of Propagation on Linear Array Performance," NUC TN 1774, September 1976, (Uncl.)

Flowers, K., "Statistical Models for Acoustic Signals and Noise (U)," NRL Report 8242, 5 July 1978 (C).

Forte, F., McDougall, L.C., Romain, N.E., and Seals, J.D., "Functional Description of PSEUDO," Bell Laboratories Report OSTP-GOFS.

Gasteyer, C.E., "Passive Sonar Detection Processes in the SIM II Model," *Proceedings of the First Workshop on Operations Research Models of Fluctuations Affecting Passive Sonar Detection*, DTNSRDC, Carderock, MD, (1975).

CONFIDENTIAL

C H

Gerlach, A.A., "Correlation Degradation Resulting from Target Motion," NRL Report 7894, July 1975.

Gerlach, A.A., "Motion Induced Coherence Degradation in Passive Systems," *IEEE Trans. ASSP* 26, February 1978.

Gerlach, A.A. and Anderson, W.L., "Limitation on the Coherence of an Acoustic Signal Emanating from a Transiting Submarine," NRL Report 8079, January 1977.

Gerlach, A.A. and Anderson, W.L., "Optimum Coherence Time for the Detection of a Transiting Submarine in Passive Sonar," *JUA (USN)* 27, No. 4, October 1977.

Gerlach, A.A. and Anderson, W.L., "Motional Source Transfer Characteristics of the Ocean with Application to Coherent Interway Processing (U)," NRL Report 8211, May 16, 1978 (S).

Gnedenko, B.V., "The Theory of Probability," Chelsea, New York (1962).

Goldman, J., "A Model of Broadband Ambient Noise Fluctuations Due to Shipping," OSTP-31JG Bell Laboratories, (1974).

Goldman, J., "A Shot Noise Model of the Random Fluctuations in Broadband Ambient Noise Caused by Shipping," Bell Laboratories Report OSTP-57 JG, (1977).

Grace, O.D., "Multipath Recombination (S)," NOSC, San Diego, CA CMAP Progress Report No. 77-001, September 1977.

Gordon, D.F. and Floyd, E.R., "Acoustic Propagation Effects in Beamforming of Long Arrays (U)," presented at the 30th Navy Symposium on Underwater Acoustics, San Diego, CA, October 1976, submitted to *U.S. Navy Journal of Underwater Acoustics*, (Conf.)

Hanish, S., Rollins, C.R. and Cybulski, J., "Acoustic Fluctuations Workshop-Technical Review, Editorial Summary and Papers (U)," NRL Memo Report 3790, August 1978 (C).

Hanna, J.S. and Rost, P.V., "An Analysis of PARKA IIA Data Using the AESD Parabolic Equation Model," AESD Tech Note TN-75-09, ONR, December 1975.

Hardin, R.H. and Tappert, F.D., *SIAM Rev. (Chronicles)* 15, 423 (1973); F.D. Tappert and R.H. Hardin, "Proceedings of the Eighth International Congress on Acoustics," Goldcrest, London, 1974, Vol. II, p. 452.

Heine, J. and Gray, L., "Merchant Ship Radiated Noise Model," BBN Report 3020, Bolt Beranek and Newman, Inc., June 1975.

Heine, J.C., "Recommendations for Modified Statistical Analysis of Ambient Noise Data," Bolt Beranek and Newman Inc., Tech Memo No. 385, November 1977.

CONFIDENTIAL

I, J, L, M

Ianniello, J.P., "Analysis of the Performance Loss of a Towed Array Detection System Due to Random Hydrophone Motion," NUSC Tech Memo 771084, 8 May 1977.

Ianniello, J.P., "The Effort of the Random Sea Surface and a Random Bottom on Multipath Ranging via Autocorrelations at Low Signal to Noise Ratios," NUSC Tech Memo 771099, 31 May 1977.

Ianniello, J.P., "Discussion of the Performance Loss of a Towed Array Detection System due to Random Hydrophone Motions (U)," NUSC Tech Memo 777078, 26 April 1977.

Jobst, W. and Clark, J., "Modulation of Acoustic Phase by Internal-Wave Vertical Velocity," *J. Acoust. Soc. Am.*, 61, 688-93, March 1977.

Jennette, R.L., Sander, E.L. and Pitts, L.E., "The USI Array Noise Model, Version I, Vol. 1, Physics Documentation," USI-APL-R-8, April 1977.

Jennette, R.L., Sander, E.L. and Pitts, L.E., "The USI Array Noise Model, Version I, Vol. 2, Computational Documentation," USI-APL-R-9, April 1977.

Larsen, R.W. and Dunn, E.L., "ASW Programs Surveillance (APSURV Mod II) (U)," Vol. I Executive Summary, Vol. II Technical Description; NOSC Tech Report, September 1978 (S).

Mark, W.D., "Statistics of Multipath Transmission of Finite Bandwidth Signals," *J. Acous. Soc. Am.*, 52, 413-425 (1972).

Marlow, N.A., "A Normal Limit Theorem for Power Sums of Independent Random Variables," *The Bell System Tech. J.*, 2081-2089, November 1967.

Marshall, S.W. and Cornyn, J.J., "Ambient-Noise Prediction, Vol. 1: Model of Low Frequency Ambient Sea Noise," NRL Report 7755, Naval Research Laboratory, June 21, 1974.

Marshall, S.W. and Cornyn, J.J., "Ambient-Noise Prediction, Vol. 2: Model Evaluation with IOMEDEX Data," NRL Report 7756, Naval Research Laboratory, July 1, 1974.

Marshall, S.W., "Acoustic Signal-to-Noise and Azimuthal Noise Directionality in the Mediterranean Sea Using LAMBDA II," NRL Memorandum Report 3050, April 15, 1975.

Marshall, S.W., "Acoustic Performance of LAMBDA II in the Church Opal Experiment", NRL Memorandum Report 3418, December 1976.

(Coordinated at) Mouri Center for Ocean Science, "International Workshop on Low Frequency Propagation on Noise" 14-19, Oct. 1974 (WHOI), Vol. I and II, (1977).

Mohnkern, G.L., "Measurements of Signal Coherence Near Bermuda," NOSC, San Diego, CA, CMAP Progress Report No. 77-005, September 1977.

CONFIDENTIAL

M, N, O, P

Moll, M., Zeskind, R.M. and Sullivan, F.J.M., "Statistical Measurements of Ambient Noise: Algorithms, Program, and Predictions," BBN Report 3390, Bolt Beranek and Newman, Inc., June 1977.

Mollegen, A.T., "Review and Comparison of Step Model and Gaussian-Markov Model," *Proceedings of the First Workshop on Operations Research Models of Fluctuations Affecting Passive Sonar Detection*, DTNSRDC, Carderock, MD, (1975).

Moses, E., Galati, W. and Nicholas, N., "Model Results of the Effects of Internal Waves on Acoustic Propagation," ORI Technical Report 1295, August 3, 1978.

Munk, W.H. and Williams, G.O., "Nature," Vol. 267, No. 5614, pp. 774-778, 30 June 1977.

Munk, W.H. and Zachariasen, F., "Sound Propagation Through a Fluctuating Stratified Ocean: Theory and Observation," *JASA* 59, 818-838, 1976.

Munk, W., "Ocean Acoustic Tomography: Can It Work?" 63, Supplement No. 1, S71A, Spring 1978.

Nakagami, M., "Statistical Characteristics of Short-Wave Fading," *J. Inst. Elec. Commun. Engrs. Japan* 239, (1943). [See, *Statistical Methods in Radio Wave Propagation*, Pergamon Press, New York, (1960)].

National Defense Research Committee Division 6 Summary Technical Reports, "Physics of Sound in the Sea," (1946).

"Planning Summary for Selected Navy Ocean Acoustic Program," Encl (1), to NORDA ltr 200:TM:sgt, Serial S002-78 of 17 Jan. 1978 to OP-095.

Northrop, J. et al., "Environmental Acoustic Predictions for the Northwestern Indian Ocean (U)," NOSC TN 104, May 1977, (Conf).

NOSC, "Bearing Stake Exercise: Preliminary Results (U)," NOSC TR 169, October 31, 1977, (Conf).

"Mathematics of Profile Inversion," NTIS Pub. No. N73-11585, Ed. L. Colin, 1972.

O'Connor, J.C., "Statistics of Sea Noise," MIT Thesis (1973).

Papoulis, A., "Probability, Random Variables, and Stochastic Processes," McGraw-Hill, New York, (1965).

"PARKA IIA — The Acoustic Measurements — Volume I," Maury Center Report 006, August 1971.

Parzen, E., "Stochastic Processes," Holden-Day, San Francisco, CA, (1962).

CONFIDENTIAL

R, S, T, U

Rice, S.O., "The Mathematical Analysis of Random Noise," *Bell System Tech. J.* **23**, 282-332 (1944) and **24**, 46-156 (1945). Reprinted in "Noise and Stochastic Processes," N. Wax, ed. Dover, New York, (1954).

Robertson, G.H., "Computation of the Noncentral Chi-Square Distribution," *Bell System Tech. J.* **48**, 201-207 (1969).

Ross, D. and Alvarez, F.F., "Radiated Underwater Noise of Surface Ships," *U.S. Navy Journal of Underwater Acoustics* **14**, (1964).

SAI, "Review of Models of Beam Noise Statistics," SAI-78-696-WA, November 1977.

Shifrin, Y.S., "Statistical Antenna Theory," The Golem Press 1971.

Sloat, S., "Target Motion Effects on Signal Coherence (C)," NOSC, San Diego, CA, CMAP Progress Report No. 77-011, September 1977.

Smith, P.W., "Statistics of Fluctuations in Measures of Sound Propagated in Shallow Water," Bolt Beranek and Newman Report 2498 (1973).

Smith, P.W., "Fluctuations Caused by Internal Waves in Ocean Sound Transmission Via RSR Paths," Bolt, Beranek and Newman, Report No. 3668.

Smith, P.W., "Spatial Coherence in Multipath or Multimodel Channels," *J. Acous. Soc. Am.* **60**, 305-310 (1976).

Solomon, L.P., Barnes, A. and Jao, J., "Discrete Shipping Model," Planning Systems, Inc. Report (1974).

Spofford, C.W., "The FACT Model Vol. I," Maury Center Report 109, ONR, Arlington, VA, (1974).

Stienberg, J.C. and Birdsall, T.G., *J. of the Acoust. Soc. of Am.*, **39**, 301-315 (1966).

Talham, Robert J., "Ambient-Sea-Noise-Model," *J. Acoust. Soc. Am.*, **36**, 1541-1544 (1964).

Tappert, F.D. and Hardin, R.H., in "A Synopsis of the AESD Workshop on Acoustic Modeling by Non-Ray Techniques, 22-25 May 1973, Washington, D.C.," AESD TN-73-05, ONR, Arlington, VA (November 1973).

Twomey, S., "Introduction to the Mathematics of Inversion in Remote Sensing and Indirect Measurement," Elsevier Pub. New York, 1977.

Urick, R.J., "Signal Excess and Detection Probability of Fluctuating Sonar Signals in Noise," *U.S. Navy Journal of Underwater Acoustics* **27**, 3, 569-585.

CONFIDENTIAL

U, V, W

Urick, R.J., "A Statistical Model for the Fluctuation of Sound Transmission in the Sea," Naval Surface Weapons Center Report TR 75-18, 1975. Also *Proceedings of the First Workshop on Operations Research Models of Fluctuations Affecting Passive Sonar Detection*, DTNSRDC, Carderock, MD, (1975).

Urick, R.J. and Kirklin, R.H., "Fluctuations of Submarine Signals and Narrow Band Noise in a Towed Line Array," Tracor Contract N00019-76-0508, March 1977, (Conf.).

Urick, R.J., "Fluctuation Spectra of Signals Transmitted in the Sea and Their Meaning for Signal Detectability," NOLTR 74-156, Naval Ordnance Lab, (1974).

Van Trees, H.L., "Detection, Estimation, and Modulation Theory" (Three Volumes), Wiley, New York, (1968).

Wagstaff, R.A., "An Ambient Noise Model for the Northeast Pacific Ocean Basin," JUA (USN), July 1977.

Whalen, A.D., "Detection Performance for Fading Signals," (1967).

Whalen, A.D., "Detection of Signals in Noise," Academic Press, New York, (1971).

Worcester, P.F., "Reciprocal Acoustic Transmission in a Midocean Environment," *J. Acoust. Soc. of Am.*, 62, 895-905, (1977).

Williams, R.E. and Wei, C.H., "Spatial and Temporal Fluctuations of Acoustic Signal Propagated Over Long Ocean Paths," JASA 59, 1299-1309 (1976).

UNITED STATES GOVERNMENT

Memorandum

DATE: 7100-031
26 February 2004

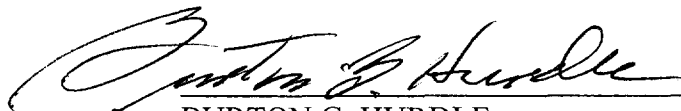
REPLY TO
ATTN OF: Burton G. Hurdle (Code 7103)

SUBJECT: REVIEW OF REF (A) FOR DECLASSIFICATION

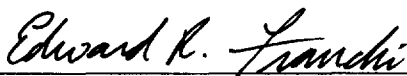
TO: Code 1221.1

REF: (a) "Acoustic Fluctuation Workshop, Feb 22-23 1978" (U), S. Hanish, C.R. Rollins, and J. Cybulski, Acoustics Division, NRL Memo Report 3884, July 2, 1979 (C)

1. Reference (a) is a summary of a Workshop on Acoustic Fluctuation in the Ocean and a copy of papers presented during the Workshop.
2. The technology and equipment of reference (a) have long been superseded. The current value of these papers is historical
3. Based on the above, it is recommended that reference (a) be declassified and released with no restrictions


BURTON G. HURDLE
NRL Code 7103

CONCUR:

 3/1/2004
E.R. Franchi Date
Superintendent, Acoustics Division

CONCUR:

 3/3/04
Tina Smallwood Date
NRL Code 1221.1